Targeting human synovium using homing peptides identified by in vivo phage display

Garrood, Toby

Dedication

In memory of my father

Targeting human synovium using homing peptides identified by *in vivo* phage display

Toby Garrood

Submitted for the degree of Doctor of Philosophy

March 2009

Barts and the London School of Medicine and Dentistry

University of London

Statement of originality

The work described in this thesis was carried out in the laboratories of the Department of Academic Rheumatology, Kings College London and the Centre for Experimental Medicine and Rheumatology, Queen Mary University of London. Unless stated, the author performed the experiments described.

This thesis entitled ‘Targeting human synovium using homing peptides identified from in vivo phage display’ has not been submitted for a degree or any other qualification at any other university.

Toby Garrood
February 2009

Acknowledgements

I would like to thank my supervisor Professor Costantino Pitzalis for the opportunity to undertake this research and his constant support and encouragement during my time working in his group. Thank you also to my second supervisor Dr Sukhi Bansal in the Department of Pharmacy for his support and patience, particularly with the production of so many of the peptides used in this project.

I am very grateful for the support and friendship of all of the members of the rheumatology group at Kings and later at Queen Mary's, particularly Mark Blades for his extensive technical advice and help, especially with the *in vivo* components of the project and histology. Thank you also to Dr Lewis Lee whose original work formed the foundations of this thesis and who was a patient source of advice throughout the project. My thanks must also go to Katherine Segklia who spent many hours working on the synthesis of several of the peptides used herein at the Department of Pharmacy at Kings, and to Dr Val Corrigal particularly for teaching me how to do FACS analyses.

I would also like to extend my particular thanks to Professor Stephen Mather in the Nuclear Medicine Research Laboratory at QMUL for allowing me access to the extensive facilities and expertise in his laboratory, as well as frequent advice. Thanks also to Dave Ellison and Dr Ciara Finucane for their technical help whilst working there, and also Dr Jim Ballinger at Guy's Hospital.

My thanks must also go to Dr John Marshall of the Tumour Biology Laboratory at QMUL for his generous provision of cell lines and advice, and to Professor Dorian Haskard of Imperial College London for allowing us to use the anti-E-selectin antibodies.

My extensive thanks and gratitude also go to the Arthritis Research Campaign for funding this work, without whom it would not have been possible.

Finally, thank you to my wife and sons for their unwavering love and support.

Abstract

Rheumatoid arthritis (RA) is a chronic inflammatory condition affecting diarthrodial synovial joints. Non-random patterns of inflammatory cell recruitment suggest the presence of synovial-specific vascular determinants which enable recruitment of specific inflammatory cell subsets. Using a model whereby human synovial and skin tissue is transplanted into SCID mice, we have previously used *in vivo* peptide phage display to identify novel peptide sequences which confer synovial homing specificity to human synovium. This synovial localisation was blocked by co-administration of free peptide thus confirming its specificity.

In this project the *in vivo* homing properties of the peptide were further explored. The synovial localization of the synovial-specific phage was shown to be specifically increased after intragraft injection of TNFα. Sequence homology was shown between the expressed CKSTHDRLC (3.1) peptide and an extracellular domain of the leucocyte integrin mac-1. The homing properties of the free peptide were investigated by conjugation to the radioisotopes ^{111}In and ^{99m}Tc. No significant differences were found *in vivo* between homing of the 3.1 monomeric peptide to transplanted human skin and synovium. The influence of valency and size of the molecules were investigated through the development of novel techniques: polymerization of the peptide was achieved by conjugation to radiolabelled streptavidin and fluorescent microspheres. *In vivo* experiments found no significant difference between localization of polymerised 3.1 or scrambled control peptide to either transplanted skin or synovium with either construct. Despite the negative results reported here, the techniques described have potential for the investigation of other targeted short-peptide sequences.

Finally, the model was further developed as a tool for the pre-clinical imaging of human synovium i*n vivo* using an ^{111}In- conjugated anti-E-selectin antibody. It was shown that this could be used to resolve specific from non-specific uptake and hence represents, potentially, a powerful new tool for the development of human tissue-specific targeting strategies.

Table of contents

List of Figures

Chapter 1

Chapter 3

Chapter 4

Chapter 5

Chapter 6

Chapter 7

List of tables

Chapter 1

Chapter 2

Chapter 3

Chapter 5

Chapter 6

Chapter 7

Abbreviations

AHA	Aminohexanoic acid
APN	Aminopeptidase N
AU	Absorbance units
BSA	Bovine serum albumin
BLAST	Basic Logic Assignment Search Tool
CAM	Cell adhesion molecule
CCP	Cyclic citrullinated peptide
CIA	Collagen-induced arthritis
CK	Chemokine
CLA	Cutaneous lymphocyte antigen
CT	Computed tomography
DAB	Diaminobenzidine
DMARDs	Disease-modifying anti-rheumatic drugs
DMEM	Dulbecco's Modified Eagles' Medium
DMSO	Dimethylsulphoxide
DTPA	Diethylenetriamine pentaacetic acid
ECM	Extracellular matrix
EDDA	Ethylenediaminediacetic acid
EDTA	Ethylenediaminetetraacetic
EGF	Endothelial growth factor
ELISA	Enzyme-linked immunosorbant assay
EPC	Endothelial progenitor cell
EPR	Enhanced permeability and retention
ESL-1	E-selectin ligand -1
FACS	Fluorescence-assisted cell sorting
FDG	Fluorodeoxyglucose
FGF	Fibroblast growth factor
FITC	Fluorescein isothiocyanate
GAG	Glycosaminoglycan
GlyCAM-1	Glycosaminoglycan cell adhesion molecule-1
HBSS	Hanks balanced salt solution
HEPES	4-(2-hydroxyethyl)-1-piperazineethanesulfonic acid

HEV	High endothelial venule
HIg	Human immunoglobulin
HPLC	High-performance liquid chromatography
HRP	Horse radish peroxidase
HYNIC	6-Hydrazinopyridine-3-carboxylic acid
ICAM	Intercellular adhesion molecule
IL	Interleukin
ITLC	Instant thin-layer chromatography
JAM	Junctional adhesion molecule
LEF	Leflunomide
LFA	Leucocyte functional antigen
LN	Lymph node
mAb	Monoclonal antibody
MAdCAM-1	Mucosal addressin cell adhesion molecule-1
MALDI-TOF	Matrix-assisted laser desorption/ionization time-of-flight
MDP	Methylene diphosphate
MRI	Magnetic resonance imaging
MS	Mass spectrometry
MTX	Methotrexate
mw	Molecular weight
NA	Nicotinic acid
NPAG	4-Nitrophenyl N-acetyl-β-D-glucosaminide
OA	Osteoarthritis
PBM	Perivascular basement membrane
PBS	Phosphate-buffered saline
PDGF	Platelet-derived growth factor
PEG	Polyethylene glycol
PET	Positron emission tomography
pfu	Plaque-forming units
PLN	Peripheral lymph node
PNAd	Peripheral lymph node addressin
PSGL-1	P-selectin glycoprotein ligand-1
RA	Rheumatoid arthritis

ROI	Region of interest
RP-HPLC	Reverse-phase high-performance liquid chromatography
RT	Room temperature
SA	Streptavidin
SCID	Severe combined immunodeficient
SD	Standard deviation
SEM	Standard error of the mean
SPECT	Single photon emission computed tomography
SSZ	Sulphasalazine
TBS	Tris-buffered saline
TEM	Transendothelial migration
TMB	Tetramethylbenzidine Dihydrochloride
TNFα	Tumour necrosis factor-α
TRITC	Tetramethyl Rhodamine Iso-Thiocyanate
UV	Ultraviolet
VCAM	Vascular cell adhesion molecule
VEGF	Vascular endothelial growth factor
VLA	Very late antigen

Chapter 1

Introduction and specific aims of the project

1.1 Rheumatoid arthritis

Rheumatoid arthritis (RA) is a chronic inflammatory condition affecting the synovial joints. Clinically it is characterised by joint inflammation which is usually symmetrical with a predilection for the hands, feet, elbows and knees as well as the cervical spine. It is also associated with variable extra-articular involvement, the presence of which is predictive of poorer prognosis (see later). Presentation can vary substantially between individual patients but standardised classification criteria provide a useful guide in diagnosis (Arnett et al. 1988). The economic cost of RA, both to the individual and to society, is considerable. A review published in 2000 put the annual costs per patient with RA at £3575 with indirect costs (principally due to lost work days) at £3638 (Cooper 2000) and the cost to the British economy of RA in 1992 was estimated at £1.256 billion (McIntosh 1996).

1.1.1 Epidemiology

There are relatively few studies of incidence of RA and of those the sample size has been generally small. This and different sample populations is likely to explain, at least in part, the variability in their findings with estimates ranging from overall incidences of 24-75.3 cases per hundred thousand per year with ranges for women and men of 35.9-98.1 and 12-49.7 respectively (Gabriel 2001). A further problem is that of reliable diagnosis in the early stages of disease: a comparison between incidence derived from symptom reporting up to 12 months and up to 5 years in which cumulative criteria were allowed to meet the conditions for diagnosis, found that incidence for men and women rose from 30.8 to 54 and 12.7 to 24.5 respectively (Wiles et al. 1999). Estimates of disease prevalence are generally more homogeneous, with most studies reporting prevalence for 0.5-1% with around a 2:1 female: male ratio (Gabriel 2001): the disease tends to be more severe in male patients (Weyand et al. 1998).

1.1.2 Genetics

It has been established for some time that there is a considerable genetic component to RA susceptibility. Most estimates of the genetic contribution are

derived from studies of monozygotic and dizygotic twins, from which the relative contribution of genetic and non-genetic factors can be estimated. This is, however, subject to problems such as the heterogeneity of the disease, variations between monozygotic twins in somatic rearrangement and x-chromosome inactivation (Ollier & MacGregor 1995). Estimates of 'heritability', which take into account confounding factors such as disease prevalence within the population, are thought to be more representative of the true genetic liability. A twin heritability study of two separate (UK and Finnish) populations put the genetic contribution at 60% (MacGregor et al. 2000).

The strongest genetic association of RA is that with the human leucocyte antigen (HLA) class II molecule HLA-DR4 and this has been mapped to an area known as the third hypervariable region within the HLA-DRβ1 chain, of which 3 sequences are found in up to 85% of RA patients (Lanchbury 1992). This locus, however, only accounts for a proportion of the genetic contribution to the disease and much research is concentrated on the identification of other associations both within the HLA region and elsewhere in the genome. Rapid advances in sequencing and genetic screening technology, particularly the increasingly dense single nucleotide polymorphism (SNP) map of the human genome, allow for whole-genome screening as well as the investigation of individual candidate genes. These have identified a number of potential susceptibility regions, as well as those which influence disease severity or appear to have protective effects (Oliver, Worthington, & Silman 2006).

1.1.3 Other risk factors for RA

Besides sex and genetic risk factors, several other factors can contribute to RA risk. It has been suggested that exogenous oestrogens may be protective, although there has been significant disagreement between studies (Gabriel 2001) and the jury has yet to return. Similarly, there has long been a suspicion of the contribution of an infective trigger to disease: this is supported by, for instance, evidence of mechanisms of lymphocyte-circulation between the gut and the joint (as will be discussed later) and the genetic association with the antigen-presenting

HLA molecules: supporting evidence of spatial or temporal disease clustering is, however, weak (Gabriel 2001).

The identification of antibodies to cyclic citrullinated peptides (CCPs) and their association with RA has provided a useful new clinical tool for the assessment of patients with inflammatory arthritis. Citrulline is formed by the post-translational modification of arginine residues: antibodies with immunoreactivity against citrulline are present in around 80% of RA patients- a similar value to rheumatoid factor. Their specificity is significantly greater however, with in one study only finding positivity of 1% in healthy controls compared with 10% for rheumatoid factor (Zendman, van Venrooij, & Pruijn 2006). The presence of anti-CCP antibodies can predict the subsequent development of RA in patients presenting with early inflammatory arthritis (van Gaalen et al. 2004) and antibodies have been detected in the serum of patients up to 10 years prior to disease onset (Nielen et al. 2004). A recent meta-analysis has confirmed the enhanced sensitivity of anti-CCP antibodies over rheumatoid factor (Nishimura et al. 2007).

A number of studies have identified significantly increased relative risk of RA in smokers (Gabriel 2001): the risk of smoking has been found in an epidemiological study to be restricted to patients developing anti-CCP antibody-positive RA; furthermore, the risk conferred by HLA-DR4 genes was restricted to anti-CCP positive disease (Klareskog et al. 2006).

1.1.4 Clinical features

The cardinal features of rheumatoid arthritis are pain and swelling of the joints with stiffness, particularly after periods of immobility, often being particularly disabling (Gordon & Hastings 1998). Onset of the disease may take various forms, ranging from acute to gradual onset, as well as atypical presentations such as an acute monoarthritis or initial presentation with polymylagia (not uncommon in the elderly). Joint involvement is typically symmetrical with the most commonly involved joints being the wrists, fingers, knees and feet. Chronic inflammation characteristically results in progressive destruction of the joint with

the appearance of typical erosive features on X-ray, with consequent impairment of function and disability. Other large joints may also be involved, particularly the elbows and shoulders in more severe disease, as well as the cervical spine: erosion of the odontoid peg and consequent subluxation of C1 on C2 can progress to potentially life-threatening spinal cord involvement. Chronic inflammation is associated with progressive joint destruction with resultant loss of use and disability. Tenosynovitis is also common: avulsion of tendons in combination with erosive joint destruction leads to the characteristic deformities which may be seen in the disease: in one long-term series 19% of patients were severely disabled after 20 years and 35% were dead (Scott et al. 1987). Disease activity correlates strongly with disability, with radiographic change correlating with disability in the medium-to-long term (Drossaers-Bakker et al. 1999).

As well as joint involvement, RA is associated with a wide spectrum of extra-articular manifestations involving a range of organs and tissues, with one series showing a 30-year cumulative incidence of 57% (Turesson et al. 2002) (Table 1). Extra-articular manifestations are associated with increased mortality, this being largely due to the presence of the 'severe' features of neuropathy, vasculitis, serositis and Felty's syndrome (Turesson et al. 2002;Turesson et al. 2003): the presence of multiple extra-articular features is also associated with increased mortality (Turesson et al. 2006). Contrary to what is perhaps commonly perceived, studies have not shown a decrease in incidence of extra-articular manifestations over recent decades, at least as far as the mid-1990s (Turesson et al. 2003); it is not yet known whether the introduction of biological agents and more aggressive treatment regimes have had an impact.

Comparative studies have suggested that the disease has become, on average, milder over recent decades, with reductions in both indices of disease activity and disability. This is apparent in series examining patient populations both up to (Bergstrom et al. 1999) and beyond (Pincus, Sokka, & Kautiainen 2005) the introduction of the routine use of TNFα inhibitors. Improvements in the incidence of radiographic damage were also seen in a recent study (Pincus, Sokka, &

Kautiainen 2005). These improvements are associated with significant changes in treatment strategies, with patients in the more recent cohorts more likely to be on any form of treatment and more likely to be on steroid treatment (which in turn was more frequently in combination with other DMARDs): the DMARDs used have also changed with use of methotrexate increasing from 10% in 1985 to 77% in 2000 (Pincus, Sokka, & Kautiainen 2005). The increased understanding of the importance of earlier intervention over the past 20 years is also likely to have had a significant impact: a survey published in 1999 showed a dramatic fall in the time from presentation to the GP to secondary referral, and from the time to DMARD treatment (Irvine, Munro, & Porter 1999): these are likely to have improved further since these data were published. It is probable, therefore, that earlier and more aggressive treatment is largely responsible for these observations, although other non-medical and environmental factors may be relevant. The relationship between improvement in disease activity and functional disability is not, however, always apparent in these studies: another recent series did not see improvements in self-reported function despite better disease control in sequential cohorts of patients (Welsing, Fransen, & van Riel 2005). The authors suggest that this observation may be due to higher patient expectations.

Extra-articular feature	Incidence (%)
Subcutaneous nodules	39.4
Sjögren's syndrome	17.1
Keratoconjunctivitis sicca	15.4
Pericarditis	10.9
Pleuritis	9.4
Pulmonary fibrosis	9.4
Cutaneous vasculitis	5.1
Cervical myelopathy	3.5
Glomerulonephritis	2.9
Neuropathy	2.8
Felty's syndrome	2.7
Bronchiolitis obliterans	1.2
Scleritis	1.0
Amyloidosis	1.0
Xerostomia	1.0
Episcleritis	0.8

Table 1.1: Incidence of extra-articular features in a cohort of 464 U.S. rheumatoid arthritis patients. (Turesson et al. 2002)

1.1.4.1 Prognosis and mortality

The excess mortality in RA is well-established: this is exemplified by a recent study of 1429 patients recruited within 2 years of symptom onset and followed up for up to 18 years (Young et al. 2007). These researchers found a standardised mortality ratio (SMR) of 1.27 in the RA cohort, with excess mortality particularly high within the first 7 years. Their finding indicate that the single biggest cause was cardiovascular disease (in particular ischaemic heart disease) and are in keeping with previous work: other notable increased causes of death were lymphoma (2.3%) and pulmonary fibrosis (6%) - rates of malignancy were not

otherwise raised above expected values. Another recent study of patients initially presenting with inflammatory polyarthritis, 60% of whom subsequently satisfied classification criteria for RA, found that, whilst agreeing with the rates of cancer incidence, survival in patients with malignancy is reduced compared to the population as a whole (Franklin et al. 2007). Significant risk factors for early death in the former study were age, baseline ESR, low haemoglobin, raised serum rheumatoid factor and indices of functional disability. Early functional disability has been found to be predictive of mortality in RA in another recent study: an analysis of a large cohort (1010) of RA patients found a significant correlation between the health assessment questionnaire (HAQ) score and both cardiovascular and all-cause mortality over a 10-year follow-up period (Farragher et al. 2007). One might therefore expect mortality to have improved with the increasing use of disease modifying drugs in recent decades. This, however, at least until recently, does not seem to have been the case with, for instance, a study of 3 successive cohorts of patients between 1965 and 1985 finding no change in mortality with a persistently high SMR (Gabriel, Crowson, & O'Fallon 1999). More recent data suggest that the more pro-active use of disease modifying therapy and the use TNFα blockers may have an impact on mortality. Two prospective studies have shown a decrease in mortality risk with methotrexate and TNFα inhibition in RA, although the latter was only seen in women (Choi et al. 2002;Jacobsson et al. 2007).

1.1.5 Pathology

Normal synovium lines the articular cavity of all diarthrodial joints. The intima, which is in direct contact with the joint cavity, is only one or two cells thick and does not have a true basement membrane (Firestein 1998). The intima is formed of two specialised types of cell, known as synoviocytes: type A synoviocytes, or synovial macrophages, are of myeloid origin and share a number of surface markers with macrophages including CD68 and CD14 as well as major histocompatiblity class II proteins and Fcγ receptors (Tarner et al. 2005). Type B synoviocytes, or synovial fibroblasts, are of mesenchymal origin and express

VCAM-1, complement decay accelerating factor and uridine diphosphoglucose dehydrogenase (UPDG)(Edwards 2000). The synovial sublining consists of a connective tissue matrix with relatively sparse cellularity consisting predominantly of fibroblasts (which appear to be non-specialised and thus distinct from the type B synoviocytes), macrophages, blood vessels and lymphatics, fat and nerve cells.

Macroscopically the inflamed synovium is thickened and villous and can extend onto the articular surface of the joint. This 'front' of inflamed synovium is known and pannus and its invasive and destructive properties are responsible for much of the joint damage that is seen in RA. Histologically the inflamed synovium is hyperplastic and hypercellular. The lining layer is thickened and may be up to 10 cells thick with dramatic increases in type A and B synoviocytes. The sublining also exhibits cellular infiltration by lymphocytes and macrophages as well as florid neoangiogenesis. The components of theses inflammatory changes will be described in more detail in the following sections.

1.1.5.1 T-cells

T-lymphocytes are the largest subgroup of cells present in the inflamed synovium. This, along with other evidence that will be discussed, as well as the previously described association of RA with HLA-DR alleles, suggests a central role for T-cells in RA pathogenesis. As will be described, however, conflicting evidence, notably the failure of T-cell depleting antibodies to control disease (Epstein 1996), suggests that T-cells may not be essential to disease propagation.

Several patterns of T-lymphocyte infiltration have been described in RA synovial tissue described by one group as diffuse, perivascular and lymphoid aggregates (Duke et al. 1982a). The diffuse infiltrates are made up predominantly of CD4+ cells with relatively few CD8+ or B-cells. Perivascular infiltrates also show a paucity of CD8+ cells with some evidence of close association with antigen-presenting interdigitating dendritic cells. Germinal centres, resembling the paracortical region of lymph nodes, can also be seen with clusters of lymphocytes,

the majority of which are CD4 T-cells in close association with B-cells. Large lymphoid aggregates contain a predominance of CD45RA+ (naïve) T-cells, but smaller aggregates and diffuse infiltrates contain a greater proportion of CD45RO+ (memory) cells. Another study identified 2 patterns of cellular aggregation as well as diffuse infiltration: granuloma formation was seen in 24% of patients, and the formation of lymphoid follicles some of which resembled ectopic germinal centre formation, a pattern seen in 24% of patients (Weyand & Goronzy 2003). Examination of T-cell populations from the synovial fluid of patients with RA reveal a significantly higher ratio of CD4 helper to CD4 suppressor cells (despite similar proportions in the peripheral blood) (Lasky, Bauer, & Pope 1988;Pitzalis et al. 1987). Despite the lack of efficacy of T-cell depleting therapies, the role of T-cells in the pathogenesis of RA is supported by the efficacy of T-cell directed therapies, exemplified most recently by the success in clinical trials of the T-cell co-stimulation modifying drug abatacept (Genovese et al. 2005). Although T-cell clonal expansion can be shown in the RA synovium this seems to be somewhat heterogeneous (Kotzin & Kappler 1998): the argument in favour of a common pathogenic antigen remains unresolved.

Pannus encroaching on cartilage consists predominantly of activated macrophages and synovial fibroblasts and these will be discussed in the next sections.

1.1.5.2 Macrophages and synovial fibroblasts

Accumulation of and macrophages as well as lymphocytes is a prominent feature of the inflamed synovium (pannus) where they express a number of activation markers: macrophage density in the synovial sublining has been correlated with clinical and histological findings (Kinne et al. 2006). Activated CD4+ T-cells stimulate macrophages both directly and indirectly via soluble mediators such as interferon γ and IL-17 (Choy & Panayi 2001). This results in the release of effector molecules in including TNFα and IL-1, both of which have increased expression in the synovium and serum of RA patients (Choy & Panayi 2001). TNFα appears to have a dominant role in the pathogenesis of RA and its diverse actions include, along with IL-1, stimulation of matrix metalloproteinase release by synovial fibroblasts, chondrocytes and osteoclasts. Injection of either cytokine

into rabbit knee joints induced inflammatory changes with an apparent synergistic effect when co-injected (Henderson & Pettipher 1989). TNFα transgenic mice develop a chronic inflammatory polyarthritis which is ameliorated by TNFα blockade (Keffer et al. 1991) and, as will be discussed later, the central role of these cytokines has been emphasised by the success of blocking strategies in clinical practice. In addition to these and other pro-inflammatory cytokines, macrophages also secrete a number of chemokines which are chemotactic for inflammatory cells (Szekanecz & Koch 2007). As will also be discussed later, there have been encouraging results with macrophage-targeted therapies in pre-clinical arthritis models.

Synovial fibroblasts are characterised by large pale nuclei and prominent nucleoli indicating active RNA synthesis (Huber et al. 2006). In a SCID mouse model human RA synovial fibroblasts were co-transplanted with cartilage under the renal capsule: the synovial fibroblasts maintained their destructive properties under these conditions indicating that T-cell independent mechanisms may also be important in their activation (Muller-Ladner et al. 1996) and there is considerable evidence that toll-like receptors may have an important role in fibroblast activation in RA (Brentano et al. 2005). It has been suggested that synovial fibroblasts have an aggressive tumour-like phenotype with reduced cell death and up-regulation of anti-apoptotic mediators (Perlman et al. 2000). A comparison of fibroblast-like synoviocytes from normal and RA synovium found increased expression of several integrins in the RA cells with enhanced adhesion *in vitro* to extracellular matrix proteins (Rinaldi et al. 1997a). Activated synovial fibroblasts secrete a number of matrix-degrading enzymes, including matrix metalloproteinases, which are responsible for the joint destruction seen in the disease (Pap et al. 2000). Fibroblasts therefore also represent an attractive target in RA and pre-clinical studies have indicated potential in this approach: methotrexate conjugated to albumin, which is actively taken up by fibroblasts, was significantly more effective than methotrexate alone in a mouse arthritis model (Wunder et al. 2003).

1.1.5.3 B-cells

Rheumatoid factor (usually IgG autoantibodies directed against the constant region of IgG) has long been established as relevant to rheumatoid arthritis, being present in around 80% of patients. More recently the discovery of other autoantibodies, notably those directed against cyclic citrullinated peptides (CCP), have further implicated B-cells in the pathogenesis of RA (Zendman, van Venrooij, & Pruijn 2006). However, the role of these antibodies in disease pathogenesis, or indeed whether they are merely bystanders, remains unclear. Passive transfer of rheumatoid factor does not produce disease, although in RA complement consumption has been shown to be accelerated in seropositive patients (Kaplan et al. 1980). Furthermore, the presence of rheumatoid factor or anti-CCP antibodies have been associated both with increased disease severity and the presence of extra-articular disease (Turesson et al. 2007). Lymphoid aggregates of T- and B-lymphocytes are demonstrable in a subset of patients with RA (Weyand & Goronzy 2003) and oligoclonal B-cell expansion has been demonstrated in RA synovium (Lee et al. 1994). Recent results from the K/BxN murine arthritis model suggest that the formation of circulating immune complexes may be an early trigger of increases in endothelial permeability allowing access of antigen-specific antibodies into joints (Binstadt et al. 2006): whether this is a relevant mechanism in human disease is unknown. Although the precise role of B-cells in the pathogenesis of RA remains unclear, the recent observation that rituximab, a CD20+cell depleting antibody, is efficacious in the treatment of RA points to a central role of B-cells in driving synovial inflammation (Cohen et al. 2006).

1.1.5.4 Neutrophils and mast cells

Neutrophils are key components of the innate immune system and are the predominant cells type in RA synovial fluid as well as being present at the cartilage-pannus junction (Youssef et al. 1996a). As will be discussed later, chemokines chemotactic for neutrophils are over-expressed in the RA joint (Koch et al. 1991;Koch et al. 1995b).

Methylprednisolone has been shown to dramatically inhibit ingress of neutrophils into the joints of patients with RA (Youssef et al. 1996a). Activated neutrophils can release a number of pro-inflammatory cytokines, degradative enzymes and reactive oxygen intermediates which may contribute, directly or indirectly, to joint damage (Edwards & Hallett 1997). Studies in antibody-mediated animal models of arthritis have found that neutrophil depletion can ameliorate disease (Nandakumar, Svensson, & Holmdahl 2003;Wipke et al. 2004).

Mast cells are also present in increased numbers in the RA synovial membrane (Godfrey et al. 1984) and these cells also release a spectrum of pro-inflammatory molecules in activation (Woolley 2003). As with neutrophils, mast cells have been implicated in some animals models of arthritis and, interestingly, have been shown to be essential to the development of arthritis in the K/BxN model where they, along with neutrophils, can act as intermediaries in early immune complex-mediated increases in endothelial permeability (Binstadt et al. 2006). Furthermore, it has recently been shown that mast cell stabilisation can limit joint inflammation in K/BxN serum transfer models of arthritis (Kneilling et al. 2007).

1.1.5.5 Neoangiogenesis

Neoangiogenesis is a normal part of embryonic development and the reproductive cycle: it is also seen in a number of disease states such as wound healing, malignancy, retinopathy and chronic inflammatory conditions such as psoriasis and RA (Pap & Distler 2005). As already mentioned, the inflamed synovial membrane in RA has abundant new vessel formation: this has been shown to correlate with the clinical degree of synovitis (Rooney et al. 1988) and it has been suggested that new vessels formation is the first event in early arthritis (Hirohata & Sakakibara 1999). Markers of endothelial proliferation such as PCNA and Ki67 have been shown to be increased in rheumatoid synovium (Walsh et al. 1998) and endothelial proliferation has itself been found to correlate with clinical activity (FitzGerald et al. 1991). The macroscopic morphology of the vessels also exhibits some variation between patients: the ‘straight’ pattern has been observed more

frequently in RA with ‘tortuous’ more common in spondyloarthropathy, although RA patients may also have a tortuous or mixed pattern. The straight pattern was correlated with the presence of erosive disease in one series (Salvador et al. 2006). Despite this neoangiogenesis, the blood/ synovial volume ratio has been found to be similar or less to that seen in uninflamed tissue (Stevens et al. 1991a;Walsh et al. 1998) thus potentiating the hypoxia within the joint (Stevens et al. 1991b). The vascular endothelial cells, sitting at the interface between the circulation and the inflamed tissue, perform or mediate a number of functions, including leucocyte recruitment, regulation of vessel permeability and dilatation, cytokine production and extracellular matrix synthesis each of which is critical to the inflammatory response (Middleton et al. 2004). In lymphoid tissue endothelium leucocyte adhesion and migration takes place in specialised post-capillary vessels called high endothelial venules (HEVs). The endothelial cells of HEVs have a cuboidal appearance distinguishing them form the more usual flattened endothelial cell morphology. Histologically they also demonstrate high levels of synthetic activity, with a prominent Golgi complex and increased levels of polyribosomes and rough endoplasmic reticulum. Around 25% of lymphocytes circulating through HEV will adhere and transmigrate (Girard & Springer 1995). Histological examination of synovial vascular endothelium has shown morphological changes with the appearance of prominent vessels similar to HEV (FitzGerald et al. 1991), although the binding properties of synovial HEV have shown to be distinct to lymph node HEV (Jalkanen et al. 1986).

A large number of angiogenic mediators can be identified in the RA synovium: many of these are directly pro-angiogenic such as fibroblast growth factor (FGF), platelet-derived endothelial growth factor (PDGF), vascular endothelial growth factor (VEGF), chemokines (particularly IL-8) and angiopoietin (Middleton et al. 2004). Several pro-inflammatory cytokines such as TNFα and IL-1 are also pro-angiogenic, largely via the stimulation of the release of mediators by synovial cells. RA vascular endothelial cells have increased expression of a number of adhesion molecules involved in leucocyte recruitment and these will be discussed later. There is some evidence that two of these, E-selectin and VCAM-1 (both

discussed later) can stimulate angiogenesis: in a rat cornea model, both were found to be pro-angiogenic (Koch et al. 1995a). Rheumatoid synovial fluid was also found to be pro-angiogenic in this model: this was significantly inhibited by the addition of E-selectin or VCAM-1 blocking antibodies (although it is arguable that this may have more to do with the recently discovered phenomenon of vasculogenesis as discussed later).

VEGF is of particular interest: it induces endothelial permeability as well as angiogenesis, it is strongly up-regulated in rheumatoid synovium and synovial fluid (Fava et al. 1994) and is expressed by a number of synovial cells (Nagashima et al. 1995). Serum levels of VEGF have been found to be significantly higher in RA patients compared with controls (Harada et al. 1998;Paleolog et al. 1998) or controls and patients with OA (Lee et al. 2001) and to correlate with serum inflammatory markers and clinical indices of disease activity (Harada et al. 1998;Lee et al. 2001;Paleolog et al. 1998). In another study of 40 patients with RA it was found that those who had evidence of follicular organisation on synovial biopsy had significantly higher levels of serum VEGF than those with diffuse infiltrates (Klimiuk et al. 2002) and VEGF staining in rheumatoid synovium has been found to be predictive of progression in the short (Ballara et al. 2001) and long (Latour et al. 2001) term. *In vitro* culture of synovial cells has shown that VEGF secretion is secreted constitutively by synovial fibroblasts (Jackson et al. 1997) and is stimulated by TNFα and IL-1 as well as under hypoxic conditions (Jackson et al. 1997;Paleolog et al. 1998): furthermore, VEGF polymorphisms have been associated with susceptibility to RA in a case-control study (Han et al. 2004). Treatment with a number of agents has been shown to reduce circulating levels of VEGF, including anti-TNFα antibodies (Paleolog et al. 1998;Strunk, Bundke, & Lange 2006), the IL-6 receptor (Nakahara et al. 2003), glucocorticoids (Strunk, Bundke, & Lange 2006) and DMARDs (Nagashima et al. 2000).

The findings described with VEGF serve to illustrate the central role of neoangiogenesis in RA and as a result there has been considerable interest in

therapeutic blockade of these mechanisms. Such trials have been carried out in oncology for a number of years: recently bevacizumab, a monoclonal anti-VEGF antibody, was shown to prolong survival in patients with metastatic colorectal cancer when added to standard chemotherapy (Hurwitz et al. 2004) and it has now been approved by the FDA. Pre-clinical trials have seen success with a number of inhibitors of angiogenesis: an inhibitor of FGF suppressed arthritis in a rat collagen-induced arthritis (CIA) model (Oliver, Banquerigo, & Brahn 1994) and a receptor tyrosine kinase inhibitor with specific activity against VEGF receptors successfully ameliorated arthritis in two murine arthritis models (Grosios et al. 2004). In a murine CIA model polyclonal anti-VEGF were found to prevent arthritis or to ameliorate it in established disease (Sone et al. 2001): however, in another study in the K/BxN murine arthritis model, antibodies to VEGF were found to only transiently improve arthritis, whereas antibodies to the receptor VEGF-R1 had a profound effect and inhibited bone destruction (De Bandt et al. 2003). In a SCID mouse transplantation model, in which human RA synovium was engrafted, vessel formation was inhibited by subcutaneous administration of the anti-angiogenic agent TNP-470 (Nagashima et al. 2002).

An alternative mechanism for new vessel formation is that of vasculogenesis whereby, as opposed to the formation of new vessels from pre-existing ones, vessels are formed from bone marrow-derived endothelial progenitor cells (EPCs) recruited from the circulation. The hypothesis that this can occur in both RA and OA is supported by the observation of cell clusters in synovial tissue co-expressing stem cell and endothelial cell markers (Ruger et al. 2004). It has been observed that circulating levels of EPCs are reduced in patients with RA and that levels inversely correlate with disease activity (Grisar et al. 2007), suggesting increased recruitment from the circulation to the inflamed synovium. Recent papers have started to define the adhesion mechanisms involved in recruitment of EPCs to inflamed synovial tissue: adhesion of these cells to cultured synovial tissue fibroblasts and frozen tissue sections was inhibited (completely in the case of fibroblasts) by antibodies to VCAM-1 or α_4 integrin (Silverman et al. 2007). In

another study E-selectin was implicated in the recruitment of EPCs in a murine muscle ischaemia model (Oh et al. 2007).

1.1.6 Organ-specific lymphocyte homing

The observation that circulating leucocytes adhere to and migrate across the vascular endothelium was first made seventy years ago; this was noted to occur without breach of the endothelial barrier, suggesting the presence of complex regulatory mechanisms (Clark & Clark 1935). More recently, in a series of classic experiments, Gowans and Knight observed that lymphocytes isolated from the rat thoracic duct homed rapidly back to lymph nodes and secondary lymphoid organs upon re-injection: furthermore, it was noted that this occurred across the distinctly shaped endothelial cells of the post capillary venules (Gowans & Knight 1964). Since then we have learnt much about the molecular basis of leucocyte extravasation and the regulatory mechanisms involved. This understanding of adhesion mechanisms, and the ability of these interactions to enable specific lymphocyte recruitment, has provided a huge and valuable insight into the expression and behaviour of the endothelial molecules involved. Such tissue-specific determinants are potentially of enormous value in the selective targeting of diseased synovium.

1.1.7 Recruitment of leucocytes to inflammatory sites: the multistep model

The ‘multistep’ model of leucocyte migration (Figure 1.1) was originally described over a decade ago as the integration of a number of sequential, apparently discrete, stages beginning with the adhesion of white blood cells to the vascular lumen and culminating in migration through the endothelial cell layer into the extravascular space (Springer 1994). These steps are mediated by multiple molecules, and include: tethering and rolling, activation, firm adhesion and finally transendothelial migration (TEM) (Figure 1.1) Each of these steps, and the molecules involved, will be discussed in detail in the following sections.

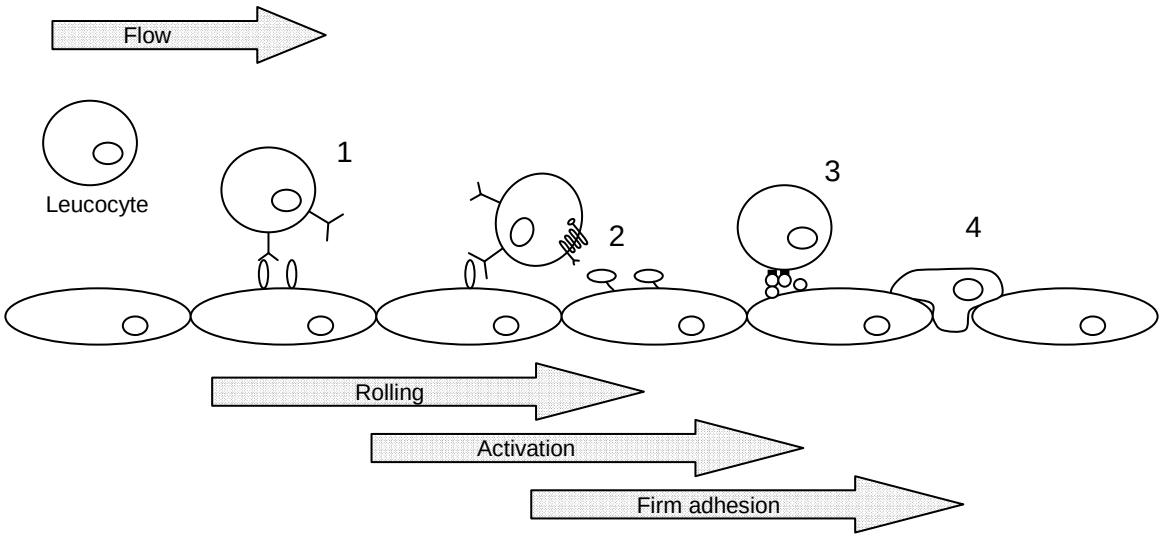

Figure 1.1: The multistep model of leucocyte migration. 1. Interaction between selectins and their carbohydrate ligands results in slowing of the leucocyte as it comes into contact with the vessel wall. 2. Chemokines expressed at the endothelial surface bind their leucocyte receptors resulting in up-regulation of integrin affinity and avidity. 3. Integrin binding to endothelial cell adhesion molecules results in arrest of the leucocyte. 4. Morphological changes and polarisation of adhesion molecules to the leading edge of the leucocyte and followed by transmigration across the endothelial barrier.

1.1.7.1 Selectins and their ligands

Tethering and subsequent rolling represent the 'braking' of leucocytes flowing at speeds of up to 4000 μm/s, resulting from initial contact between the leucocyte, and the luminal endothelium. A series of relatively low-affinity interactions, mediated by several types of adhesion molecules (most importantly the selectins and their carbohydrate ligands) effects slowing of the leucocytes.

The selectins (Table 1.2) are a group of structurally related transmembrane glycoproteins (reviewed in (Crockett-Torabi 1998;Patel, Cuvelier, & Wiehler

2002)) each consisting of an NH_2-terminal calcium-dependent ('c-type') lectin terminal domain followed by an EGF like domain, both of which are likely to be required for ligand binding (Crockett-Torabi 1998), and a variable number of consensus repeats prior to a transmembrane domain and a short cytoplasmic tail (Patel, Cuvelier, & Wiehler 2002). They bind mucin ligands, proteins rich in serine and threonine residues with O-linked sugars, displaying specific carbohydrate epitopes containing sialylated/ fucosylated residues typified by the tetrasaccharide sialyl-Lewis^x (Patel, Cuvelier, & Wiehler 2002). Synthesis of these glycoproteins is mediated by enzymes of the large glycosyltransferase family, the expression of which regulates cellular synthesis of specific glycoprotein structures (Lowe 2002). Three selectins, designated L-, P- and E-selectin, have been described in humans.

L-selectin is constitutively expressed by most circulating leucocytes, although it is down-regulated after lymphocyte activation: the majority of cell-surface L-selectin is expressed on the tips of microvilli (Bruehl, Springer, & Bainton 1996) which has been shown to enhance the initiation of rolling, particularly in larger diameter vessels (Stein et al. 1999). As will be discussed later, it is critical to the rolling of naïve lymphocytes on the HEVs of the secondary lymphoid organs and there is evidence to suggest that the rate of T-cell migration into lymph nodes can be regulated by leucocyte surface-density of L-selectin (Galkina et al. 2007). L-selectin ligands are also expressed at sites of acute inflammation although they are less well characterised than those in the lymphoid tissues: significant reduction of leucocyte infiltration was observed in L-selectin knockout mice in a model of acute inflammation (Tedder, Steeber, & Pizcueta 1995) and reduced levels of leucocyte rolling in inflamed post-capillary venules have been demonstrated in these animals (Arbones et al. 1994). In an *in vivo* model leucocyte rolling was examined in inflamed cremaster endothelium by intravital microscopy: the majority of L-selectin-mediated leucocyte adhesion was mediated by secondary tethering. Furthermore, in PSGL-1 knockout mice L-selectin dependent leucocyte-rolling was abolished- a marked reduction was also seen after treatment of wild-type mice with a blocking anti-PSGL-1 antibody (Sperandio et al. 2003). A more

recent animal study has shown that inactivation of an enzyme critical to the sulfation of heparan sulphate side-chains results in reduced leucocyte rolling in acute inflammation, suggesting a role for heparan sulphate proteoglycans as tissue receptors for L-selectin in this setting (Wang et al. 2005). *In vitro* adhesion assays have demonstrated that L-selectin can bind PSGL-1 and that leucocyte-expressed PSGL-1 can act as a ligand for L-selectin (Tu et al. 1996); such 'secondary tethering' to endothelial-adherent leucocytes enhances subsequent primary P-selectin-mediated capture in these assays. This provides a mechanism of positive feedback whereby adherent leucocytes recruit more leucocytes exponentially; this amplification of recruitment is abolished when L-selectin is blocked (Walcheck et al. 1996). L-selectin ligands can also be expressed by the vascular endothelium at sites of chronic inflammation: ectopic lymphoneogenesis with the formation of lymphoid follicles has been described in a number of diseases, often in association with the adoption of an HEV-like morphology by endothelial cells (Hjelmstrom 2001) which can bind L-selectin (Rosen 2004). Such ectopic lymphoneogenesis is well described in the inflamed rheumatoid synovium (Duke et al. 1982b;FitzGerald et al. 1991;Manzo et al. 2005;Weyand & Goronzy 2003).

Endothelial receptor/ ligand	Leucocyte receptor/ ligand
CD34, podocalyxin, endomucin, GlyCAM-1, MAdCAM-1	L-selectin (CD62L)
E-selectin (CD62E)	CLA
P-selectin (CD62P)	PSGL-1

Abbreviations: GlyCAM-1, glycosaminoglycan cell adhesion molecule-1; CLA, cutaneous lymphocyte antigen; PSGL-1, P-selectin glycoprotein ligand-1; MAdCAM-1, mucosal addressin cell adhesion molecule-1

Table 1.2: Selectins and their ligands

P-selectin is expressed by activated platelets and the endothelial cells of inflamed tissues where it is stored in secretory granules (α-granules in platelets and Weibel-Palade bodies in endothelium) which are translocated to the plasma membrane

upon activation (Patel, Cuvelier, & Wiehler 2002): this allows rapid up-regulation of surface expression in response to an inflammatory stimulus, often mediating early leucocyte recruitment. Its major ligand is the sialylated and fucosylated glycoprotein P-selectin glycoprotein ligand-1 (PSGL-1) which is expressed by circulating myeloid cells and T-cells (Ley & Kansas 2004). As seen with L-selectin, PSGL-1 is expressed on the tips of microvilli of leucocytes (Bruehl et al. 1997).

E-selectin is also expressed by inflamed endothelium but, unlike P-selectin, it is regulated by increased transcription in response to inflammatory stimuli with peak expression occurring at around 4 hours (Bevilacqua et al. 1987). The best characterised ligand for E-selectin is the cutaneous lymphocyte antigen (CLA), so called because it is expressed by up to 90% of T-cells at sites of chronic cutaneous inflammation compared with only 10-25% in the circulation (Berg et al. 1991). CLA is a sialylated carbohydrate epitope originally defined by reactivity with the HECA452 antibody: the precise structure is unknown, although has been shown that PSGL-1 can act as the core molecule (Borges et al. 1997;Fuhlbrigge et al. 1997). As discussed above, E-selectin can also bind L-selectin and *in vivo* evidence suggests that it can contribute to PSGL-1-mediated T_{H1} cell rolling (Hirata et al. 2000). A recent paper elucidated the relative contributions of the E-selectin ligands PSGL-1, E-selectin ligand-1 (ESL-1) and CD44 (discussed further below) in lymphocyte recruitment, with the demonstration of overlapping and sequential roles in leucocyte tethering and arrest (Hidalgo et al. 2007). Of particular interest in this paper was the observation that CD44 ligation (which is involved later in the leucocyte capture process) could influence the expression of PSGL-1 and ESL-1: this might suggest a role in the regulation of secondary tethering of further leucocytes from the circulation. As will be discussed, E-selectin expression is increased in the endothelium in RA synovium: furthermore, T-cells isolated from RA synovium or synovial fluid show significantly enhanced adhesion to E-selectin *in vitro* compared to peripheral blood cells from RA patients or healthy donors (Postigo et al. 1992).

Although selectins are the best characterised mediators of lymphocyte rolling, they are not always required and it may be mediated by other cell adhesion molecules (CAMs). CD44 is a type I transmembrane glycoprotein that is expressed in an activated form by subgroups of activated lymphocytes (reviewed in Ponta, Sherman, & Herrlich 2003)and can mediate selectin-independent lymphocyte rolling on inflamed endothelium (DeGrendele, Estess, & Siegelman 1997). Its principle endothelial ligand is hyaluronic acid, a polysaccharide component of the extracellular matrix, expression of which can be up-regulated by pro-inflammatory stimuli (Mohamadzadeh et al. 1998), although other ligands, including E-selectin, have been described (reviewed in (Naor & Nedvetzki 2003). CD44 expression is up-regulated on lymphocytes isolated from the synovial fluid of RA patients (Kelleher et al. 1995) and there is evidence from animal models of arthritis that CD44 is implicated in its pathogenesis (Mikecz et al. 1999;Sarraj et al. 2006).

Slow lymphocyte rolling can also be mediated by the interaction of the α_4 integrins with their endothelial ligands. It appears, therefore, that a number of molecular interactions can be involved in the progressive slowing of a lymphocyte as it encounters the endothelial surface. In addition to L, P and E-selectins, the α_4-integrins (which are also expressed on the tips of microvilli (Abitorabi et al. 1997)) can support slow rolling (Alon et al. 1995), as can the β_2-integrins in synergy with E- and L-selectin (Jung et al. 1998;Kadono et al. 2002).

Rolling brings leucocytes into contact and allows them to sample the local microenvironment at the endothelial surface. In the absence of stimuli leucocytes detach and remain in the circulation; however, in the presence of luminally expressed activating molecules (principally chemokines) they progress to firm adhesion.

1.1.7.2 Chemokines and leucocyte activation

Chemokines (chemoattractant cytokines) (CKs) are secreted polypeptides of 67-127 amino acids with molecular weights of 8-12 kDa (reviewed in Moser et al.

2004;Rollins 1997;Rossi & Zlotnik 2000). Structurally, in most CKs, the short -NH_2 terminus region precedes 3 anti-parallel β-strands forming a central core, with a COOH-terminal α-helix (Loetscher & Clark-Lewis 2001). Chemokines have been implicated in a variety of functions including angiogenesis, organogenesis and tumour metastasis as well as chemotaxis (Moser et al. 2004). They are classified into families according to the spacing of four highly conserved cysteine residues near the N-terminus: the largest of these are the CC (i.e. with the two cysteine residues adjacent) and CXC (in which they are separated by one amino acid) families. The XC chemokines (XCL1 and XCL2) containing one conserved cysteine only and the CX_3C chemokine CX_3CL1 containing 3 inter-cysteine amino acids have also been described (Moser et al. 2004;Rollins 1997). The original nomenclature, whereby CKs were classified according to their (apparent) primary function has been replaced by a systematic classification by family (Table 1.3) (Zlotnik & Yoshie 2000). Their receptors are serpentine seven-transmembrane G-protein coupled receptors which are classified according the family of their CK ligand(s), i.e. CCR1-9, CXCR1-5, XCR1 and CX_3CR1 (Rossi & Zlotnik 2000). There is considerable overlap between receptor and ligand specificity, with some receptors binding only one CK and others having affinity for several. Equally, CKs may have one or more cognate receptors (Rossi & Zlotnik 2000). Ligation of the leucocyte-expressed CK receptor results in firm adhesion to the vascular lumen, a process mediated predominantly by leucocyte integrins and their endothelial ligands (see next section).

Chemokine expression is up-regulated by a diverse range of stimuli in a large number of cell types. Expression is largely transcriptionally regulated although CKs may also possibly be stored in secretory granules; for instance, storage of CXCL8 (IL-8) in Weibel-Palade bodies has been demonstrated in human endothelial cells after prolonged stimulation (Wolff et al. 1998). CKs can also be broadly divided in to ‘inflammatory’ and ‘homeostatic’ (Table 1.3). Inflammatory CK mediate leucocyte recruitment to sites of inflammation whereas homeostatic CK mediate immunosurveillance of secondary lymphoid organs and the peripheral

tissues (Moser et al. 2004): some CKs do not fall neatly into either category and are referred to as having 'dual-function'.

Inflammatory			Homeostatic		
Systematic name	Functional name	Receptor	Systematic name	Functional name	Receptor
CCL2	MCP-1	CCR2	CCL1*	I-309	CCR8
CCL3	MIP-1α	CCR1,CCR5	CCL17*	TARC	CCR4
CCL4	MIP-1β	CCR5	CCL19	MIP-3β	CCR7
CCL5	RANTES	CCR1 CCR3 CCR5	CCL21	SLC	CCR7
			CCL22	MDC	CCR4
CCL11	Eotaxin	CCR3	CCL25*	TECK	CCR9
CCL27	CTACK	CCR10	CXCL12*	SDF-1α/β	CXCR4
CXCL8	IL-8	CXCR1 CXCR2	CXCL13	BCA-1	CXCR5
CX_3CL1	Fractalkine	CX_3CR1			

Chemokines marked with an asterisk have dual function
Abbreviations: BCA-1, B-cell attracting chemokines-1; CTACK, cutaneous T-cell attracting chemokine; ELC, EBI1 ligand chemokines; MCP-1, monocyte chemotactic protein-1; MDC, macrophage-derived chemokine; MIP-1α, macrophage inflammation protein-1α; RANTES, regulated on activation normal T-cell expressed and secreted; SDF-1α, stromal-cell-derived factor-1α; SLC, secondary lymphoid tissue chemokines TARC, thymus- and activation-regulated chemokine; TECK, thymus-expressed chemokine

Table 1.3: Chemokines and receptors involved in leucocyte homing

CKs expressed by lymph node HEV are not necessarily synthesised locally, as evidenced by the lack of local expression of, for instance, CCL19 mRNA (Baekkevold et al. 2001) and it has been shown that CK synthesised elsewhere within the LN or even arriving in the lymph can be transported to the luminal surface of the HEV (Baekkevold et al. 2001;Gretz et al. 2000); transcytosis of inflammatory CKs to the luminal endothelium from extravascular sources has also been demonstrated (Middleton et al. 1997). After secretion, CKs would simply be washed away by the blood flow if mechanisms for anchoring to the endothelial surface were not present. Glycosaminoglycans (GAGs) are polysaccharides attached to a protein core (proteoglycans); they are expressed by endothelial cells with heparan sulphate being the most abundant (Middleton et al. 2002). They can bind multiple CKs and hence present them to rolling leucocytes: GAGs bind CKs

with variable affinity and therefore provide a framework for the formation of hapotactic gradients (Patel et al. 2001). Furthermore, variations in patterns of GAG expression are demonstrable between the endothelia of normal and diseased tissues suggesting a further mechanism for differential CK expression (Middleton et al. 2002). Although CKs have been shown *in vitro* to be functional in the absence of GAGs, GAG binding significantly enhances their activity (Ali et al. 2000)- this effect is at least in part to GAG-mediated stabilisation of the tertiary structure of CKs or the formation of CK oligomeric complexes in association with GAGs (Goger et al. 2002;Proudfoot et al. 2003). CXCL12 has been shown to bind heparan sulphate proteoglycans on rheumatoid synovial endothelial cells in culture (Santiago et al. 2006).

A large number of human chemokines have now been described and many of these have been shown to activate specific leucocyte subtypes *in vitro* (Laudanna et al. 2002) although definite *in vivo* evidence is only available for a fraction of these (Ley 2003). CK ligation results in up-regulation of integrin-mediated firm adhesion and TEM: this effect is both rapid and transient and is dependent on levels of receptor occupancy although, interestingly, the kinetics of CK-mediated firm adhesion and TEM may differ (Campbell et al. 1996). Clearly the expression of multiple CKRs by particular leucocyte subgroups in combination with variable expression of CKs within tissues has enormous potential for the differential tissue localisation of leucocytes, and it has been suggested that differential endothelial CK expression is responsible for the bulk of homing pattern variability (Hillyer et al. 2003). Furthermore, a number of features of CK/ CKR interaction can further contribute to the diversity of leucocyte response. It has been shown that some CKs can antagonise particular CKRs; agonists for CXCR3, for instance, can antagonise CCR3 (Loetscher & Clark-Lewis 2001). Moreover, ligation of different CKRs in the same cell can initiate different signalling pathways (Gerszten et al. 1999), indeed the same level of occupancy a particular CKR by different CKs can have differing effects (D'Ambrosio et al. 2002).

Apical endothelial chemokines may also directly regulate TEM. In an *in vitro* adhesion assay it was shown that the presence of CCL19 at the endothelial cell surface was required not only for integrin-mediated firm adhesion but also subsequent TEM. This was dependent on the presence of flow and occurred in the absence of a trans-endothelial chemokine gradient. Firm adhesion but not TEM was seen when non-chemokine integrin activators were used (Cinamon, Shinder, & Alon 2001).

Ligation of CK receptors by cognate CK results in cellular activation and progression to firm adhesion to the vascular endothelium with the potential for extravasation into surrounding tissues. The mechanisms by which this is achieved, namely increased affinity, avidity and polarization of cell surface integrins, will be described in more detail below.

1.1.7.3 Integrins and firm adhesion

Integrins (reviewed in Danen & Sonnenberg 2003 and van der Flier & Sonnenberg 2001) are glycosylated transmembrane proteins which exist as non-covalently associated dimers consisting of one α and one β-chain: they have a large extracellular domain consisting of 70-1100 residues and a short cytoplasmic domain of 30-50 residues (with the exception of β_4 which has 1000-residues) (van der Flier & Sonnenberg 2001). To date, 18 α and 8 β subunits have been described in humans which form 24 known heterodimers. The integrins bind to components of the extracellular matrix or specific counter-receptors and have a diverse array of roles in mediating both within the immune system and in tissue organisation and cellular signalling (Danen & Sonnenberg 2003). Five integrins have been identified as being particularly important to leucocyte migration (Table 1.4) (Springer 1994). The endothelial counter-ligands for leucocyte integrins are members of the immunoglobulin superfamily and include ICAMs1-5, VCAM-1 and MAdCAM-1. They are type I transmembrane glycoproteins consisting of a short cytoplasmic tail, a single transmembrane region and a variable number of extracellular immunoglobulin domains (Gahmberg, Tolvanen, & Kotovuori 1997). ICAM-1 and endothelium ICAM-2 are ligands for LFA-1 and Mac-1; ICAM-1

appears to be the dominant ligand in inflammation as it is up-regulated by pro-inflammatory stimuli (Gahmberg, Tolvanen, & Kotovuori 1997), a process that is transcriptionally regulated (Hubbard & Rothlein 2000). Unlike ICAM-1, ICAM-2 is expressed constitutively by the vascular and lymphatic endothelium and is not induced by inflammatory mediators (De Fougerolles et al. 1991;Geijtenbeek et al. 2000). Both ICAM-1 and ICAM-2 are important LFA-1 ligands mediating leucocyte migration into peripheral lymph nodes. There is significant redundancy with both: *in vivo* lymphocyte homing to peripheral lymph nodes (PLNs) was affected little with either ICAM-1 or ICAM-2 blockade, whereas blocking both resulted in significant inhibition of homing (Lehmann et al. 2003). ICAM-2 has been shown to act as an endothelial counter-receptor for DC-SIGN, a C-type lectin expressed by circulating dendritic cell precursors: in an *in vitro* assay this interaction could support rolling under flow conditions and transendothelial migration (Geijtenbeek et al. 2000).

Integrin	Subunits	Expression	Ligands
LFA-1, CD11a/ CD18	$\alpha_L\beta_2$	Monocytes neutrophils T-cells Macrophages Dendritic cells	ICAM-1,-2,-3
Mac-1, CD11b/ CD18	$\alpha_M\beta_2$	Monocytes neutrophils NK cells	ICAM-1 iC3b, Factor X Fibrinogen
p150, 95, CR4 CD11c/ CD18	$\alpha_X\beta_2$	Monocytes NK cells neutrophils, subsets of B- and T-cells	ICAM-1 iC3b fibrinogen
VLA-4, CD 49d/CD29	$\alpha_4\beta_1$	B and T-cells monocytes	VCAM-1 MAdCAM-1 fibronectin
LPAM-1	$\alpha_4\beta_7$	B and T-cells	VCAM-1 MAdCAM-1

Abbreviations: LFA-1, leucocyte functional antigen-1; LPAM-1, lymphocyte Peyer's patch adhesion molecule-1; VLA-4, very late antigen-4

Table 1.4: Lymphocyte integrins and their endothelial ligands

ICAMs also appear to have a signalling function; ligation of ICAM-1 for instance has been shown to activate kinase-dependent signalling pathways with consequent up-regulation of secreted cytokine and membrane-bound protein expression (Hubbard & Rothlein 2000). VCAM-1, like ICAM-1, is expressed at low levels by resting endothelial cells and is up-regulated by pro-inflammatory stimuli: it is the ligand for the $\alpha_4\beta_1$ integrin (VLA-4) which is expressed by most leucocyte subtypes and can also bind $\alpha_4\beta_7$ (Carter & Wicks 2001). As well as supporting firm adhesion, VCAM-1 can also support rolling mediated by VLA-4 and this can progress to firm adhesion in the absence of cytokine stimulation (Alon et al. 1995). VLA-4- mediated T-lymphocyte adhesion to VCAM-1 has been shown to be up-regulated in cells isolated from RA synovium and synovial fluid compared to cells isolated from the peripheral blood of patients and healthy donors (Postigo et al. 1992).

Up-regulation of integrin binding affinity has been shown to occur by two mechanisms, conformational change to a high affinity state and increased lateral mobility leading to cell surface clustering (increased avidity) and polarization. This up-regulation is transient (Campbell et al. 1998) and can be extremely rapid-cell-surface clustering has been shown to occur in less than 0.1s (Grabovsky et al. 2000). These processes are dependent on a 'inside-out' signalling that follow engagement of cell surface receptors by external stimuli that lead to triggering of various intracellular signalling pathways. The same CK can induce up-regulation of the binding affinity of different integrins through separate pathways- in eosinophils conformational changes in Mac-1 and clustering of VLA-4 were both effected by CCL5 and CCL7, although it is unclear whether this is mediated by different CKRs (Weber, Kitayama, & Springer 1996). Interestingly, it was shown that rapid clustering of VLA-4 was stimulated only by localised CKR ligation and not by saturating levels of soluble CK, emphasising the importance of localised signalling for adhesion and subsequent migration (Grabovsky et al. 2000). Moreover, recent work has shown that only immobilised CK can induce LFA-1/ ICAM-1-mediated lymphocyte arrest (Shamri et al. 2005): this report showed that induction of an intermediate affinity state in the integrin was essential to ICAM-1

binding in flow conditions. Binding to ICAM-1 induced a further conformational change to the high affinity state; this process was shown to be very rapid and not to require progressive 'integration' of CK signal (Shamri et al. 2005): this effect also appears to depend on the density of ICAM-1 expression and was not seen with soluble ICAM-1 (Ganpule et al. 1997). Integrins can also initiate internal signalling pathways following external stimuli- so-called 'outside-in' signalling. This follows receptor clustering and formation of the 'focal adhesion plaque' with subsequent signalling dependent upon the GTPase RhoA and the mitogen-activated protein kinase pathway (Jones & Walker 1999). Outside-in signalling has diverse functions in the regulation cell function including proliferation and apoptosis.

Up-regulation of integrin binding results in firm adhesion, bringing the adherent cell to a halt and allowing progression to transendothelial migration.

1.1.7.4 Transendothelial migration

Transendothelial migration (TEM) is complex and the least understood stage of the extravasation process. It is dependent on CK activation of leucocytes and integrin binding to endothelial cell. The transmigrating cell is characterised by structural polarisation with re-organisation of the cytoskeleton and the formation of a lamellipodium at the leading edge of the cell (Springer 1994). TEM generally appears to occur through endothelial cell junctions, although there is some evidence that it can also occur by transcytosis through endothelial cells (Engelhardt & Wolburg 2004). Endothelial cell-cell junctions are formed by the interactions of a number of dedicated adhesion molecules including the junctional adhesion molecules (JAMs), platelet/endothelial cell adhesion molecule (PECAM-1, a member of the immunoglobulin superfamily), occludins, vascular-endothelial (VE)-cadherin, claudins and CD99 (van Buul & Hordijk 2004). The JAMs also act as integrin ligands: JAM-A,B and C bind LFA-1, Mac-1 and VLA-4 respectively (van Buul & Hordijk 2004). TEM is mediated by the binding of leucocyte integrins to PECAM-1 (through homotypic adhesion) and endothelial CAMs to CD99 (which binds VLA-4). It involves the activation of multiple

signalling pathways mediated by the ligation of integrins on the leucocyte and endothelial cell CAMs. Intracellular signalling results in the breakage and formation of leucocyte-endothelial bonds, the opening of the endothelial barrier, as well as mediating the trailing edge retraction and leading edge protrusion of the leucocyte with cell surface polarisation of CKRs (Nieto et al. 1997). It has been demonstrated *in vitro* that leucocytes can migrate through increasing concentration gradients towards the source of a CK (Foxman, Campbell, & Butcher 1997). Diverse patterns of CK are expressed at inflammatory sites: this, coupled with the expression of multiple CKRs by leucocytes, allows precise navigation and localisation of leucocytes. Leucocytes are able to respond to sequential CK gradients thus migrating in a 'step-wise' fashion; this is likely to be due in part to CKR desensitisation at high/ saturating concentrations when the orientation of CKR ligation will also be lost (Foxman, Campbell, & Butcher 1997). Furthermore, it is apparent that some chemoattractants can augment the response to others, whilst for some cross-desensitisation of CKRs occurs in a hierarchical manner providing a potential mechanism for the step-wise response seen (Kitayama et al. 1997). Another mechanism for this effect appears to be the ability of leucocytes to prioritise their response to newly-encountered chemoattractants, i.e. they can 'memorise' previous components of the chemotactic cascade (Foxman, Kunkel, & Butcher 1999).

The final obstacle to the extravasating leucocyte is the perivascular basement membrane (PBM). The mechanisms by which leucocytes cross the PBM remain incompletely defined; recent work has demonstrated a role for the laminin binding integrin $\alpha_6\beta_1$ (Dangerfield et al. 2002a). Laminin is a component of the PBM and it has been shown that its surface expression on neutrophils is up-regulated by the homophilic interaction of leucocyte and endothelial PECAM-1: the passage of neutrophils across the PBM was inhibited by a $\alpha_6\beta_1$-blocking antibody *in vivo* (Dangerfield et al. 2002b). *In vitro* studies have suggested a role for leucocyte proteases in trans-PBM migration (reviewed in (Yadav et al. 2003)) although their role *in vivo* remains unproven.

1.1.8 Tissue–specific lymphocyte homing

Lymphocytes circulate through the peripheral tissues in a non-random manner, allowing optimisation of the immune system's resources. Re-circulation of naïve lymphocytes through lymphoid tissue maximises their chances of encountering antigen, and activation into effector phenotype is accompanied by the acquisition of homing properties for peripheral tissues where antigen may be re-encountered (Mackay 1993). Studies of lymphocyte adhesion to frozen sections of tissue have demonstrated that lymphocytes isolated from peripheral lymph nodes, gut mucosa and synovium exhibit enhanced binding properties to the tissue of origin (Salmi et al. 1992) and it can be shown that lymphocytes isolated from draining lymph at different sites have differential surface adhesion molecule expression (Abitorabi et al. 1996).

1.1.8.1 Addressins and homing receptors

Organ-specific lymphocyte homing is a complex process dependent on the presence of specific ligand/ receptor interactions at each stage of the adhesion process. Although many aspects still remain to be defined, for some tissues at least some of the homing mechanisms have been described. Tissue-specific ligands expressed by vascular endothelial cells are known as 'addressins' which bind homing receptors expressed by subpopulations of leucocytes.

For example, the homing receptor/ addressin pair L-selectin/ peripheral lymph node addressin (PNAd) mediates lymphocyte adhesion to peripheral lymph node HEV (Rosen 2004). PNAd is a complex of sialomucins (defined by reactivity with the MECA-79 antibody) consisting, in humans, of CD34 podocalyxin and endomucin (for an excellent review of L-selectin ligands see Rosen 2004); sulfation by a specific sulfotransferase is required for the recognition of these epitopes (Hemmerich et al. 2001). GlyCAM-1, another component of the PNAd family of ligands, is a secreted molecule (Kikuta & Rosen 1994) and may therefore have a role in regulation of selectin-mediated leucocyte binding (Crockett-Torabi 1998). This observation is supported by studies in knockout mice; in an L-selectin knockout there was no leucocyte adhesion to PLN HEV and

PLNs are smaller in size due to reduced numbers of intra-PLN lymphocytes (Arbones et al. 1994). These homing receptors are, however, neither sufficient nor always necessary for organ-specific homing. Endothelial VAP-1, for instance, may contribute to the adhesion of naïve lymphocytes to PLN HEV; this may be co-dependent on L-selectin or, in some cases, L-selectin independent (Salmi et al. 1997). Another level of homing specificity is conferred by CKs: CCL19 and CCL21, ligands for the CK receptor CCR7, are transcytosed to lymphoid organ HEV and mediate lymphocyte extravasation to these sites (Baekkevold et al. 2001;Gunn et al. 1998). CCR7 is required for homing of naïve lymphocytes to lymphoid tissue: mice expressing a mutant form of CCR7 have disordered PLN architecture (Forster et al. 1999). Furthermore, expression of L-selectin and CCR7 defines a subset of memory T-cells ('central memory' T-cells) which retain homing affinity for lymphoid organs (Sallusto et al. 1999). All PLN naïve cells express CCR7, as do most peripheral tissue T-cells- this may be necessary for re-entry of these cells into the lymphatics also expressing CCL21(Campbell et al. 2001).

Another example of homing receptor/addressin pair is represented by the integrin $\alpha_4\beta_7$ that binds to MadCAM, expressed specifically by gut mucosal venular endothelium, and is critical for lymphocyte recruitment to gut-associated lymphoid tissue (GALT) (Berlin et al. 1993). MAdCAM-1 is expressed by the HEVs of Peyer's patches in the gut : it contains both immunoglobulin and mucin domains (Shyjan et al. 1996) and can also support L-selectin-mediated rolling when decorated by MECA-79 –reactive epitopes (Berg et al. 1993). Antibodies to the $\alpha_4\beta_7$ subunits inhibit lymphocyte recruitment to the gut (Hamann et al. 1994) and mice deficient in α_4 or β_7 integrin subunits have markedly underdeveloped GALT (Arroyo et al. 2000;Wagner et al. 1996). The CK CCL25, which is chemotactic for cells expressing CCR9, is expressed preferentially by regions of the small intestine, where a majority of infiltrating lymphocytes express CCR9, suggesting a further level of homing specificity for the gut (Kunkel et al. 2000;Staton et al. 2006): interestingly, CCL25 was not expressed in the large intestine.

As already discussed, CLA, a glycosylation variant of PSGL-1, is a ligand for E-selectin and is expressed by a majority of infiltrating lymphocytes in inflamed skin (Berg et al. 1991), and in patients with contact dermatitis a proliferative response to antigen is confined to cells expressing CLA (Santamaria Babi et al. 1995). Moreover, infiltrating T-cells from a series of patients with cutaneous T-cell lymphomas were preferentially shown to express CLA (Picker et al. 1990). Further evidence that CLA+ cells have homing specificity for the inflamed skin comes from studies of patients with psoriatic arthritis: despite having inflammatory lesions at both the joints and the skin, CLA+ lymphocytes are confined to the skin (Pitzalis et al. 1996). However, E-selectin is widely expressed in inflammation and, as with gut-homing cells, further components of the 'area code' are necessary for specific recruitment. Most CLA+ skin-infiltrating lymphocytes express high levels of CCR4, the receptor for CCL17, expression of which is up-regulated in inflamed skin (Campbell et al. 1999) (although not exclusively); in this study CCR4 expression by $\alpha_4\beta_7$+ cells was low or negative. An elegant study with an adoptive transfer model has shown that CCL17/ CCR4 are necessary for lymphocyte trafficking to skin (Campbell, O'Connell, & Wurbel 2007). CCL27 is expressed preferentially by resting and inflamed skin and is chemotactic for a subset of CLA+ cells (Morales et al. 1999). In addition, CCR10 is the receptor for CCL27 and is expressed by most infiltrating lymphocytes in inflamed skin (Homey et al. 2002). Furthermore, E-selectin, CCL17 and ICAM-1 co-localise in some dermal vessels from non-inflamed skin, providing a molecular framework enabling immunosurveillance (Chong et al. 2004). It was recently reported that CCR8 is expressed a majority of T-cells in normal skin although rarely in peripheral blood: CCL1, the only ligand for CCR8, is expressed in normal skin; it is therefore likely that this CK has a role in cutaneous immunosurveillance (Schaerli et al. 2004).

Whilst there may be evidence of specific lymphocyte infiltration at other sites, descriptions of specific addressin/ homing receptor pairs for the synovium are lacking. In animal models of arthritis a spectrum of adhesion molecules have been

implicated in pathogenesis including E-and P-selectin, the integrins LFA-1, VLA-4 and mac-1, and the immunoglobulin superfamily molecules ICAM-1 and PECAM-1 (Taylor et al. 1996) (Issekutz, Nakazato, & Issekutz 2003;Watts et al. 2005). Vascular adhesion protein-1 (VAP-1, also known as amine oxidase, copper containing-3) is up-regulated in inflamed human synovium: in an animal model its enzymatic activity has been implicated in leucocyte recruitment and arthritis pathogenesis (Marttila-Ichihara et al. 2006). *In vitro*, distinct endothelial cell recognition systems for the human synovium have been described (Jalkanen et al. 1986) and a number of leucocyte-expressed adhesion molecules have been implicated, including CD44, L-selectin, α_4, β_1 and β_2 integrins on leucocytes and PNAd, VAP-1, P-selectin and E-selectin in the synovium (Fischer, Thiele, & Hamann 1993;Salmi, Rajala, & Jalkanen 1997). Homeostatic chemokines have been associated with the formation of ectopic lymphoid tissue in the rheumatoid synovium and a number of inflammatory chemokines are up-regulated in inflamed RA tissue (Haringman et al. 2006b;Haringman, Ludikhuize, & Tak 2004). Indeed, infusion of CXCL8, the prototypical pro-inflammatory cytokine, into the knee joints of rabbits produces clinical arthritis (Endo et al. 1994). Administration of an anti-IL-8 antibody reduced polymorphonuclear cell infiltration and ameliorated arthritis in LPS and IL-1-induced arthritis in rabbits (Akahoshi et al. 1994).The CK receptors CXCR3, CXCR6 and CCR5 are preferentially expressed by lymphocytes in inflamed synovial tissue (Loetscher & Moser 2002;Norii et al. 2006) and lymphocyte cell-surface density of CCR5 has been correlated with intensity of cell migration to the supernatant of TNFα-transduced synoviocytes *in vitro* (Desmetz et al. 2007); this pattern of expression is associated with the T_{H1} phenotype (Kim et al. 2001). It has also been shown that leucocytes isolated from normal and inflamed gut adhere preferentially to inflamed synovium *in vitro*, suggesting a mechanism for re-circulation of effector cells between the synovium and gut and a possible pathogenic link for the known clinical association between gut and synovial inflammation (Salmi et al. 1995;Salmi & Jalkanen 2001). Specific adhesion molecule expression in the synovium may not be the only explanation for specific leucocyte homing; CS1, a splice variant of fibronectin and a counter receptor for $\alpha_4\beta_1$, is expressed by synovial endothelial cells and up-

regulated in inflammation (Elices et al. 1994). Fibronectin is a well-characterised example of an extracellular matrix protein which acts as a ligand for integrins, and expression of which is differentially regulated. It will therefore be discussed briefly in the following section.

1.1.8.1.1 Fibronectin

Fibronectin is a dimer consisting of 2 polypeptide subunits linked by disulphide bonds, each with a molecular weight of ~250 kDa (Kornblihtt et al. 1996). It exists in a soluble form in the plasma, synthesised by hepatocytes, and an insoluble form in the extracellular matrix synthesised by multiple cell types. It is made up of repeating subunits known as type I-III repeats. The fibronectin gene consists of 50 exons, and alternative splicing results in a number of polypeptide variants of which there are at least 20 in humans (Kornblihtt et al. 1996). The molecule contains at least two regions which mediate cell adhesion: the 10^{th} type III repeat contains an RGD motif which mediates binding to a subset of integrins. Two alternative splice sites, known as extra domains A and B (ED-A and ED-B) are only found in tissue forms of fibronectin (Carsons 2001). Expression of ED-B is up-regulated in the vessels of some types of tumour (Nilsson et al. 2001) and in inflamed synovial tissue (Kriegsmann et al. 2004) and it has been exploited as a ligand for specific targeting of neoplastic tissues (Nilsson et al. 2001). Another alternative splice site is between the 14^{th} and 15^{th} type III repeats and is known as III-CS (connecting sequence). The CS-1 peptide sequence is contained within the III-CS, and includes the LDV motif which mediates binding to the integrin $\alpha_4\beta_1$ (Komoriya et al. 1991). Staining of rheumatoid synovium with antibodies specific to the CS-1 domain has shown expression at the luminal surface of vascular endothelial cells and on lining layer synoviocytes where they meet the joint cavity; minimal staining was seen in normal synovial tissue (Elices et al. 1994;Muller-Ladner et al. 1997). The CS-1 peptide was found to down-regulate *in vitro* lymphocyte adhesion to rheumatoid synovial tissue sections (Elices et al. 1994).

Until recently it was unclear what drove the acquisition of a particular pattern of CAM and CKR expression by lymphocytes. More is now understood about the mechanisms of such 'imprinting' and this will be discussed briefly in the next section.

1.1.8.2 Acquisition of homing properties by lymphocytes

It is well established that differentiation in secondary lymphoid tissues of naïve lymphocytes into the effector/memory cells leads to changes in surface CAM and CKR expression associated with the acquisition of specific homing properties. Experiments utilising adoptive transfer of T-cells have shown that such acquisition of tissue-specific homing properties occurs within 2 days of antigenic stimulation according to the lymphoid tissue in which antigen is encountered (Campbell & Butcher 2002). Furthermore, cytokine-dependent L-selectin and CLA expression during T-cell maturation has also been demonstrated *in vitro* (Picker et al. 1993b;Picker et al. 1993a). More recently it has become clearer that dendritic cells (DCs) are essential for the differentiation of lymphocytes into populations with tissue-homing specificity. For instance, culture of naïve T-cells with antigen loaded DCs from mesenteric lymph nodes induced substantially more expression of $\alpha_4\beta_7$ and CCR9 than was seen with splenic DCs (Johansson-Lindbom et al. 2003). Furthermore, DCs isolated from Peyer's patches have also been shown to induce $\alpha_4\beta_7$ and CCR9 in lymphocytes that could migrate along a CCL25 gradient *in vitro* and demonstrated tropism for the small intestine *in vivo* (Mora et al. 2003). In contrast down-regulation of L-selectin, a typical phenomenon associated with lymphocyte activation, was seen after incubation with DCs from both sites (Johansson-Lindbom et al. 2003). Taken together these data clearly indicate that DCs from different lymphoid stations can induce the repertoire of CAMs and CK-Rs associated with tissue specific homing as well as antigen specificity associated with immunological competence. The importance of the lymphoid tissue local microenvironment for the regulation of homing *in vivo* is further emphasized by the fact that that antigen-primed DCs can induce skin or gut-homing properties when given by intracutaneous or intraperitoneal injection respectively, an effect not seen after iv administration (Dudda, Simon, & Martin

2004). This group also demonstrated differentiation into a skin-homing phenotype of T-cells cultured with Langerhans cells isolated from the skin (Dudda, Simon, & Martin 2004). An important question is whether, once activated, T-cells are permanently committed to a particular homing phenotype or can be 're-educated'. Recent work has shown that T-cells which have acquired skin or gut-homing properties can alter their surface CAM and CKR expression according to their most recent encounter with DCs (Mora et al. 2005b). The mechanisms involved in T-cell imprinting by DCs are unclear, although T-cell activation is a necessary component (Mora et al. 2005a;Siewert et al. 2007). However, as far as the gut is concerned, Vitamin A appears to be a critical moiety in the induction of the gut homing repertoire. In a recent landmark paper, Iwata and colleagues showed that exposure of naïve T-cells to retinoic acid under stimulatory conditions resulted in the expression of the gut-homing phenotype $\alpha_4\beta_7^+$/CCR9$^+$; expression of CLA was suppressed (Iwata et al. 2004). These cells showed chemotaxis to CCL25 and homed preferentially to the gut after adoptive transfer. They also showed that enzymes necessary for the oxidative metabolism of retinol to retinoic acid are expressed by DCs from mesenteric lymph nodes and Peyer's patches as well as the intestinal epithelium, whilst they are only expressed at low levels by DCs from PLNs. Furthermore, it was demonstrated that inhibition of these enzymes suppressed $\alpha_4\beta_7$ and CCR9 expression, as did blockade of the nuclear retinoic acid receptor. A wider understanding of these processes with particular reference to the joint could have significant therapeutic implications for the manipulation of the immune response and for targeting specific treatments to rheumatic diseases (for a more detailed review of this topic see Dudda & Martin 2004).

1.1.9 Therapeutic targeting of adhesion molecules

Adhesion molecules are crucial to the orchestration of the immune response, and are therefore attractive therapeutic targets. Levels of soluble adhesion molecules can be correlated with disease activity in a number of inflammatory conditions, including RA (Klimiuk et al. 2002;Nassonov et al. 2000), although it is often debatable whether this confers any advantage over conventional inflammatory

markers (Marshall & Haskard 2002). There has also been some success reported with the targeting of adhesion molecules for imaging- a radiolabelled anti-E-selectin antibody in RA was particularly promising (Jamar et al. 2002). The therapeutic targeting of a number of adhesion molecules have been investigated in animal models and, despite disappointing results with some agents, there have been encouraging results in some human studies. Perhaps the most successful to date are the glycoprotein IIb/IIIa ($\alpha_{IIb}\beta_3$) antagonists which inhibit platelet aggregation and are used clinically in acute coronary syndromes and following angioplasty (Hamm 2003). There is also encouraging data from human studies for α_4-antagonists in multiple sclerosis and Crohn's disease although natalizumab, a humanised monoclonal antibody against the α_4 subunit, has recently been associated with progressive multifocal leucoencephalopathy secondary to reactivation of latent JC polyomavirus (Berger & Koralnik 2005). Blockade of CXCL8 (Marshall & Haskard 2002) and the α_L integrin subunit (Gordon et al. 2003) have been effective in cutaneous psoriasis. In a phase I/II trial, RA patients given a single iv dose of an anti-ICAM-1 monoclonal antibody sustained a clinical improvement (Kavanaugh et al. 1996) and a preliminary study with an oral CCR1 (the ligand for the inflammatory CKs CCL3 and CCL5) antagonist showed a reduction in infiltrating macrophages and lymphocytes in the synovium of RA patients and a trend towards clinical improvement (Haringman et al. 2003). Another therapeutic trial of an antibody directed against CCL2 in RA patients failed to produce clinical improvement (Haringman et al. 2006a). A general concern regarding non-selective targeting of adhesion mechanisms may be the iatrogenic development of some of the clinical problems highlighted by the lecucoyte antigen deficiency syndromes. Therefore, as mentioned above, better understanding of the mechanisms involved in tissue specific lymphocyte recirculation is likely to bring more fruitful results.

1.1.10 Treatment of rheumatoid arthritis

Until relatively recently the management of RA was, generally, to gradually increase analgesic and conventional anti-inflammatory therapy, culminating in the use of disease-modifying anti-inflammatory drugs (DMARDs) until symptomatic

control was achieved. Over the last 15 years, however, there has been an inversion of this treatment 'pyramid' with the emphasis now on early intervention with disease modifying therapy. Firstly, it is now evident that the rate of progression of radiological damage is most rapid in the early stages of the disease: in one cohort of 181 patients with early RA followed up for 10 years it was found that radiographic progression was most rapid in the first 2 years with 75% of erosions occurring in the first 5 years (Lindqvist et al. 2003). Secondly, it has been consistently shown that earlier use of disease-modifying therapy has a better longer-term outcome, with better results seen with more aggressive treatment regimes (Goekoop-Ruiterman et al. 2005). These DMARDs and corticosteroids are discussed in more detail below.

1.1.10.1 Corticosteroids

It is now almost 60 years since the original reports of the efficacy of steroids on the clinical symptoms of RA (Hench et al. 1950). The original optimism has long-since been superseded by the serious side-effects of the long-term use of systemic steroids, although recent trials have suggested that the early limited use of steroids may significantly impact longer-term disease outcome (Landewe et al. 2002). Despite this, their application is largely restricted to short-term use in disease flares either systemically or by intra-articular injection. However, recent evidence that low-dose systemic steroids retard disease progression may lead to their more widespread use (Wassenberg et al. 2005). Corticosteroids therefore provide the archetypical example of a treatment whose use is curtailed by toxicity: the potential advantages of tissue-specific targeting are clear and will be discussed later. Furthermore, concerns about the use of corticosteroids in RA, a condition already characterised by increased cardiovascular risk, have been underscored by a recent study showing significantly increased risk of cardiovascular risk in rheumatoid factor-positive patients who had received steroid treatment (Davis 2007).

1.1.10.2 Disease-modifying anti-rheumatic drugs

By definition, a disease modifying drug in RA is one which slows radiographic progression of joint disease. Regular monitoring of the progression of joint

damage in RA is particularly important in light of the well-established observation that progression is common despite improvement in other indices of disease activity (Molenaar et al. 2004). The correlation of joint damage with disability (Scott et al. 2000) emphasises the importance of this as a therapeutic goal. A number of drugs have been shown clinically to influence disease progression: several of these such as intramuscular gold and penicillamine have largely fallen into disuse, principally due to adverse side-effect profiles. Methotrexate (MTX), a folic acid analogue, is the most commonly used first-line DMARD in the UK, with sulphasalazine (SSZ) and leflunomide (LEF) most commonly second line, either as monotherapy or in combinations. Methotrexate has been shown to consistently improve clinical and laboratory disease markers as well as functional outcome in clinical studies (Weinblatt et al. 1994). Furthermore, a study of 1240 RA patients over a mean follow-up period of 6 years found that methotrexate use was associated with reduced mortality although this was significant only for cardiovascular causes (Choi et al. 2002). Sulphasalazine is also widely used: its mechanism of action is unclear with its effects most likely to be mediated by its metabolite suplfapyridine. Its efficacy in RA has been proven in several randomised controlled trials, both with placebo and active treatment control groups (Weinblatt et al. 1999). Leflunomide was the first disease-modifying drug for RA which was designed specifically for treatment of the disease. Its dominant mode of action is the blocking of pyrimidine synthesis by inhibition of the enzyme dihydrooratate dehydrogenase, with resultant inhibition of the cell cycle in activated lymphocytes. One large randomised study of 402 RA patients found significantly better improvement in clinical and laboratory parameters compared with placebo with an equivalent response to that seen with methotrexate (Strand et al. 1999). Each of these drugs is associated with a significant side-effect profile which can be dose-limiting: the most significant of these are myelosuppression and hepatotoxicity which can, in rare instances, be fatal, particularly if compliance with recommended blood monitoring is poor. Side-effects are a significant causes of longer-term treatment failure (Capell 2002), as is lack of efficacy in the short term or loss of efficacy over longer periods. Resistance to DMARDs are not yet fully understood although a variety of mechanisms have been suggested which

may be inherent or acquired with exposure to treatment (Van der Heijden et al. 2007).

All of the above-mentioned drugs appear to have disease-modifying activity radiographically. Since the efficacy of this group of drugs became apparent it has become ethically impossible to conduct placebo-controlled trials (Stein & Pincus 1999), and therefore most trials now compare different therapeutic regimens. Most studies which have compared MTX, SSZ and LEF have found equivalent disease-modifying effects for all 3, although progression of disease is still seen in most studies (Pincus et al. 2002). The failure of DMARDs to fully control disease activity or progression in a majority of patients has led to widespread interest and increasingly routine clinical use of other approaches to treatment. These include the so-called biological agents which will be discussed in section 1.1.10.4, and the use of combinations of DMARDs as will be discussed in the next section.

1.1.10.3 Combination therapy

The failure of disease control by many patients in the short and longer term by many patients on DMARD monotherapy has precipitated a large number of trials in which various combinations of drugs are tried. A number of strategies may be used, often either increasing the number of drugs until control is achieved or starting with a particular combination before cutting down once the disease is under control. Contrary to what might be expected, some combinations have been shown to offer significantly better control without an increase in the frequency or severity of side effects (Garrood & Scott 2001). In particular, it has been noted that early aggressive management of the disease with a regime including steroids resulted not only in more rapid disease control but also a significant inhibition of radiological progression. Importantly, despite the withdrawal of steroids over the first few months of therapy this benefit was maintained over several years thus suggesting that aggressive therapy earlier in disease has sustained benefits at least into the medium term (Boers et al. 1997;Landewe et al. 2002). Another recent study randomised patients with early RA to one of four treatment groups: sequential monotherapy, step-up therapy with the addition of another DMARD if

required, initial combination therapy including MTX, SSZ and high-dose prednisolone, or initial combination therapy with MTX and infliximab (Goekoop-Ruiterman et al. 2005). Initial disease control was better in the latter two groups receiving initial combination therapy and functional improvement remained significant at 1 year. By 2 years, however, disease activity was similar across all 4 groups: despite this, there was a sustained difference in radiographic progression with the initial combination therapies continuing to confer an advantage at this stage (Goekoop-Ruiterman et al. 2007).

It seems clear, therefore, that at least in a subgroup of patients with early RA, that aggressive treatment with combination therapy can have a sustained benefit on disease progression. What remains unclear is exactly which patients will benefit the most: the trials in early RA support the hypothesis that there is a window of opportunity earlier in the disease during which aggressive treatment can have a significant effect on longer-term prognosis. Stratification of patients according to sub-classifications based on disease phenotype (clinical or histological) or genotype will, it is hoped, eventually enable treatment to be targeted more effectively. An example of recent success in this respect was the association of gene polymorphisms of enzymes associated with adenosine release with clinical response to methotrexate (Wessels et al. 2006). Research in this area is ongoing.

1.1.10.4 Biological therapy

A number of biological agents are now licensed for use for the treatment of RA in the UK. The most popular of these are the anti-TNFα group of compounds, with drugs targeting other molecules such as interleukin-1, interleukin-6 and CTLA-4 also in stage 3 clinical trials or expected to be licensed imminently. These will be reviewed briefly here.

1.1.10.4.1 Anti-TNFα drugs and other ‘biologics’

Infliximab is a chimeric (human/murine) monoclonal antibody to TNFα which is administered intravenously and was the first of this group of drugs to be licensed in the UK. A number of randomised controlled trials have confirmed its efficacy in RA: as it is a chimeric antibody it is associated in some patients with the

formation of human anti-chimeric antibodies and therefore is frequently given in combination with methotrexate or another DMARD (Scott & Kingsley 2006). The ATTRACT study randomised 428 patients with active RA despite MTX treatment to concomitant therapy with infliximab in 2 dose groups or placebo. Significant clinical improvement was seen in the infliximab group which was sustained over 54 weeks with subsequent extension of the trial showing persistent efficacy at 102 weeks (Lipsky et al. 2000;Maini et al. 2004). Adalimumab is a fully humanised recombinant antibody to TNFα which is administered by subcutaneous injection. In a trial of RA patients with a partial response to methotrexate, 619 were randomised to one of two adalimumab treatment groups or placebo, with significantly more patients achieving clinical improvement at 24 and 48 weeks (Keystone et al. 2004). Etanercept is the third UK-licensed anti-TNFα therapy. It is a soluble p75 TNF-receptor fusion protein which is administered subcutaneously. In a trial of patients with early RA, 632 were randomised to placebo-controlled treatment in one of 2 etanercept groups or oral methotrexate (Bathon et al. 2000). Reponses to treatment were similar at 52 weeks, although response was significantly more rapid in those patients receiving etanercept. A striking feature of these trials is the response seen in terms of radiological progression. In all the trials quoted above there was significantly less radiographic progression than in the control groups, with some groups exhibiting virtual arrest of radiographic progression. These observations, particularly as clinical remission was only achieved in a minority of patients, lend further weight to the hypothesis that there is, at least to some degree, a dissociation between the disease processes responsible for clinical inflammation and radiological damage (Kirwan 2004).

Despite the obvious promise of the anti-TNFα group of drugs, they have not been the panacea that perhaps was hoped. A significant proportion of patients fail to respond to treatment and they are also associated with a number of potentially serious adverse effects, including reactivation of tuberculosis, infection, demyelination, interstitial lungs disease, aplastic anaemia and worsening of heart failure (Scott & Kingsley 2006). A recent large retrospective cohort study confirmed the increased risk of infection with TNFα blockade (Curtis et al. 2007).

Despite this, another recent study, the first to specifically address mortality in patients treated with TNFα blockers, found reduced mortality in women treated with this group of drugs although this was not seen in men: the reasons for this are yet to be defined (Jacobbson 2007). Furthermore there is an unresolved debate about the possible association of TNFα blockade with lymphoma: an increased risk has been reported, but it is difficult to determine whether this is genuine in light of the known background increased risk of lymphoma with RA (Scott & Kingsley 2006). A recent study of almost 20,000 patients over up to 7 years of follow-up, more than half of whom received anti-TNFα therapy, found no increased risk of lymphoma associated with treatment (Wolfe & Michaud 2007).

Recombinant protein technology and the increasingly widespread use of therapeutic monoclonal antibodies have led to an explosion in the possibilities for specific therapeutic intervention in RA. A number of these other than the TNFα inhibitors discussed above are either licensed or approaching licensing in the UK and will be discussed briefly. Anakinra is a recombinant human interleukin-1 receptor antagonist (IL-1ra) which has produced significant clinical response either in combination with MTX or alone in placebo-controlled trials: it also impedes radiographic progression (Bresnihan & Cobby 2003). Despite this, its relatively modest effects in comparison with anti-TNFα-blockers (although no head-to-head studies have been done) have meant that it has not come into widespread use.

Rituximab is a monoclonal antibody directed against the CD20 antigen with administration resulting in the depletion of CD20+ cells. It is well-established as an effective agent in the treatment of non-Hodgkins lymphoma and recent randomised controlled trials have shown it to be effective in the treatment of sero-positive rheumatoid arthritis (Emery et al. 2006). Open-label studies have shown its effectiveness in patients who are resistant to anti-TNFα treatment (Jois et al. 2007) and the results of one large study suggest that rituximab may be more effective than alternative TNFα-blocking agents after failure of the first (Finckh et al. 2007). Synovial biopsies taken before and 1 month after rituximab treatment

have shown B-cell depletion in some, but not all patients, despite profound drops in circulating levels of CD20+ cells (Vos et al. 2007). This observation could reflect local variations, for instance, in B-cell survival factors- elucidating this further could enable better targeting of B-cell depleting therapy. Unfortunately this study did not report correlations between local synovial B-cell depletion and clinical outcome.

Abatacept is a recombinant fusion protein consisting of the extra-cellular domain of human CTLA-4 and a human IgG1 Fc fragment. It interferes with the interaction of CTLA-4 with CD80 and CD86 on the surface of antigen presenting cells with CD28 on T-cells, thus inhibiting the co-stimulatory signal. It has been shown to be effective in patients in whom MTX or anti-TNFα therapy has been ineffective (Genovese et al. 2005;Kremer et al. 2003) and is likely to find a place as a second-line biological agent in RA. A humanised antibody to the interleukin-6 receptor has also been shown to be effective in a trial of 164 patients refractory to at least one previous DMARD (Nishimoto et al. 2004).

1.1.10.5 Gene therapy

The identification of individual molecular components of RA pathogenic pathways and the success of biological therapies has emphasised the potential of gene therapy in the disease. A number of approaches in animal models have been successful, both with *in vivo* and *ex vivo* transfection techniques. Much of these have used adenoviral vectors, limitations of which include immunogenicity and limited transfected gene expression (reviewed in (Adriaansen, Vervoordeldonk, & Tak 2006)). Administration can be systemic or intra-articular: systemically administered vehicles will only accumulate at low concentrations in joints and there is therefore considerable interest in the specific targeting of adenovirus and other vectors. An example of this is the successful approach of modifying adenovirus by the addition of an RGD sequence to a coat protein which results in significantly enhanced expression of a luciferase gene by synoviocytes *in vitro* (Bakker et al. 2001). Similarly enhanced expression was seen after intra-articular injection of RGD-modified and non-modified vectors in mice in both inflamed

and non-inflamed joints: when used to transfect a IL-1ra gene intra-articular injection of the RGD-adenovirus resulted in significantly better amelioration of arthritis. The identification of specific targeting strategies therefore would have particular relevance to this area of RA therapy.

The importance of early diagnosis of RA is clear from the increasing evidence that early intervention has long-term prognostic implications as has been discussed. These observations beg the question of whether earlier diagnosis is achievable. The increasing knowledge of RA epidemiology including risk factors, including demographic and genetic, may in the future enable identification of groups of patients at high risk of developing disease. The availability of diagnostic tools to identify patients with early disease is therefore crucial; furthermore sensitive detection of pathology could be invaluable in clarifying the diagnosis in patients who present with undifferentiated inflammatory arthritis, many of whom will eventually satisfy the criteria for RA. The presence of inflammatory changes in clinically unaffected joints in patients with RA and the detection of such changes before the onset of clinical arthritis (Kraan et al. 1998) underlines the potential of sensitive imaging both for diagnosis and for the monitoring of response to treatment. This will be discussed in the next section.

1.1.11 Diagnostic imaging of rheumatoid arthritis

A number of modalities are used for the imaging of inflammatory joint disease: of these X-ray is the most accessible. The relative advantages of each of these will be discussed in this section.

1.1.11.1 X-ray

For decades plain x-rays have been a standard investigation in the diagnosis, assessment and monitoring of patients with rheumatoid arthritis (Brower 1990). X-rays have a number of obvious advantages over other imaging modalities which justify their widespread use: they are cheap and widely available with most hospitals having appropriate facilities. Furthermore the radiation dose is small compared to some other imaging modalities such as computed tomography (CT) and radionuclide scans.

A minimum radiological evaluation of patient with new-onset RA would include x-rays of the hands and feet, both in postero-anterior (PA) and oblique (e.g. Norgard) views. A number of abnormalities may be visible including soft tissue swelling, peri-articular osteoporosis, loss of joint space, the presence of bony erosions and, in the later stages of disease, joint destruction and deformity. The presence of erosions is one of the classification criteria of RA (Arnett et al. 1988) and indicative of a poorer prognosis. One study found that 35% of patients presenting within 3 months of symptom onset had erosions at presentation, rising to 73% in those presenting beyond 12 months (Irvine, Munro, & Porter 1999). Their presence is predictive of the development of further erosions (Boers et al. 2001;Jansen et al. 2001;Scott 2000) and radiological bony damage correlates with long-term disability (Scott et al. 2000). One of the primary aims of RA therapy is, therefore, to retard the progression of radiological damage: disease modifying anti-rheumatic drugs (DMARDs) are so-defined by their ability to impede such changes.

Despite their routine use, X-rays remains far from ideal as a tool for imaging RA, particularly in monitoring response to therapy. Firstly, the development of erosions is an indicator of 'end-organ' damage and is therefore a relatively late event in the disease. Although other changes may be seen as noted above, these do not necessarily correlate with or predict bone damage. Secondly, their sensitivity to change is limited to periods of at least six months or more limiting their use as a tool in optimisation of therapy in the short term. This is particularly important for several reasons: it is now understood that development of erosions can occur most rapidly in the early stages of disease and therefore, ideally, more sensitive means of predicting bone damage are required during this crucial period. The importance of this is compounded by clinical data suggesting that a therapeutic 'window' exists early in the disease in which aggressive treatment can modify long-term outcome. Furthermore, the availability of drugs which can modify disease progression make it ethically dubious for a placebo or no-treatment arm to be used in clinical trials: the resultant loss of relative effect size of drugs under

investigation necessitates the development of more sensitive tools to monitor response in terms of progression. Moreover, MRI and ultrasound studies (discussed below) have indicated that XR is insensitive to early erosions. Finally, X-rays can give virtually no information about soft tissue pathology such as synovial proliferation (Ostergaard & Szkudlarek 2003): as more is understood about the pathology of RA the role of imaging modalities which can give information about the soft tissues is increasingly relevant. The importance of this is exemplified by data suggesting that there is a poor correlation between clinical disease activity and radiological progression (McQueen et al. 2003) with some patients continuing to progress radiologically despite clinical remission (McQueen et al. 1999;Molenaar et al. 2004). Despite this, the ready availability of X-rays means that they will continue to be a routine tool in the routine management of RA. Scoring systems (such as the Sharp and Larsen scores (Larsen, Dale, & Eek 1977;Sharp et al. 1985)) have been extensively validated for use in clinical trials and have been shown to have inter-observer reliability.

A number of alternative imaging modalities are being investigated for use in RA with some of these becoming routine clinically. These will be discussed further below.

1.1.11.2 Magnetic resonance imaging

The ability of magnetic resonance imaging (MRI) to image in multiple planes lends it the potential to image erosions with greater sensitivity, and hence earlier, than plain X-ray. MRI can also image the soft tissues and therefore, for instance, synovial effusions and tenosynovitis as well as the synovium (Backhaus et al. 1999) and the use of contrast enables the differentiation between active and inactive synovial hypertrophy (Cimmino et al. 2003). MRI therefore has a number of potential advantages which, along with the absence of ionising radiation, has made it the subject of intense study over recent years.

A number of studies have compared the sensitivity of MRI and X-ray for the detection of erosions and found enhanced sensitivity compared with x-ray

(Backhaus et al. 1999;Backhaus et al. 2002;Klarlund et al. 2000;Ostergaard et al. 1999). Studies have confirmed that erosions detectable by MRI are the same lesions as those which are (or become) visible on X-ray (Backhaus et al. 2002;Dohn et al. 2006) with such lesions often becoming visible on X-ray at follow-up, although ones study has put this figure at only 25% at 1 year (McQueen et al. 2001). A recent study showed that significantly more loss of bone volume was required for an erosion detected by MRI to be visible on plain X-ray (Ejbjerg et al. 2006). It is clear, therefore, that MRI-detected erosions can be predictive of X-ray erosions, but a key question is whether other changes imaged by MRI can be predictive of future damage. Bone oedema is a feature uniquely identifiable by MRI and has been shown to be predictive of subsequent erosive changes at the wrist in a site-specific manner, suggesting that bone oedema is a pre-erosive lesion (McQueen et al. 1999). Recently a study has, for the first time, looked at the correlation between MRI changes and bone histology in patients undergoing joint replacement (Jimenez-Boj et al. 2007). Bony erosions seen on MRI were found to be associated with infiltrating synovial tissue and lymphocytic infiltration at the interface between synovium and bone marrow fat confirming the presence of bone marrow-associated inflammation in these lesions. Quantification of synovial membrane volume is possible and, at the wrist, has been shown to be sensitive to treatment-induced change at 3 and 6 months (Ostergaard et al. 1999). Furthermore, this study showed that baseline synovial membrane volume correlated with development of erosions over 1 year.

Despite the obvious attractiveness of MRI, there are several disadvantages. Firstly it is costly: this and limitations in access to routine scanning make it largely impractical for routine use, although dedicated coils for imaging peripheral joints may improve this situation. Secondly, due to acquisition times, it is only practical to image a limited number of joints, such as the MCPJs and thus information about non-imaged joints will be limited. Studies have shown that the rate of progression of erosive changes can progress at different rates in different joints (Scott, Coulton, & Popert 1986). This is important as it has been suggested that the predictive value of MRI may be most powerful at the individual joint level

(Boers et al. 2001). A further problem is that of inter-observer variability in MRI scoring, an inevitable problem with the enhanced quantity of information available from MRI, although recent reports have claimed good inter-observer agreement. Although results to date with MRI support its use for the detection of inflammatory joint lesions, its role as a predictive tool is less clear as such longer-term follow-up data is currently unavailable. The relative availability and economy of ultrasound has, in light of these drawbacks, become increasingly attractive and will be discussed in the next section.

1.1.11.3 Ultrasound

Recent advances in ultrasound technology, particularly the availability of higher frequency machines which enable increased image resolution, have increased the popularity of ultrasound as a tool for routine joint assessment. It's obvious advantages are as described above, although these have to be counterbalanced by limited depth penetration compared with MRI, limitation of multi-planar imaging in some joints (such as the 3rd and 4th metacarpophalangeal joints), and potential problems with inter-observer agreement.

Ultrasound can detect synovial thickening and can be even more sensitive than MRI for the detection of synovial effusions and tenosynovitis (Backhaus et al. 1999), and is more sensitive than X-ray for erosions (Backhaus et al. 2002;Szkudlarek et al. 2006;Wakefield et al. 2000). Its inability to penetrate bone and limited planar access in some joints can limit this and MRI, particularly with techniques such as 3D MRI, remains more sensitive for bony lesions (Backhaus et al. 2002).

The use of power Doppler, which can detect blood flow in synovial vessels, in conjunction with conventional ultrasound enables quantification of the synovial vascularisation: this technique has been shown to be effective at the finger joints (Qvistgaard et al. 2001) and at the knee joint where the power Doppler signal has been shown to correlate with the histological score of vascularity in synovial biopsies (Walther et al. 2001). A recent randomised placebo-controlled trial

looked at ultrasound outcomes in a group of patients with early RA treated with methotrexate with or without infliximab (Taylor et al. 2004). A strong correlation was found between the ultrasound score of synovial thickening and vascularity and subsequent deterioration in radiographic joint scores: this was abolished in those patients treated with infliximab. These findings suggest that ultrasound may have a role in directing treatment in individual patients. Another recent study has shown a significant association between synovial vascularity and synovial hypertrophy, as assessed by ultrasound, with subsequent structural damage: this effect could be seen even in joints that were clinically asymptomatic (Brown et al. 2008).

In summary, MRI and ultrasound have provided valuable advances in the imaging of the inflammatory joint lesions of RA and may have an important role in predicting outcomes and response to therapy. The observation that progression of radiological damage occurs in the absence of clinically-detectable synovitis is well-established (as already discussed), and a recent study has underscored previous observations that synovitis can be detected both by MRI and ultrasound in such patients (Brown et al. 2006). However, as discussed, each of these has its own disadvantages. Furthermore, the practical limitation of both techniques to imaging a few joints at a time limit their use in extrapolating results to the patient as a whole. There is therefore continued interest in techniques which allow imaging of multiple groups of joints using tracers which take advantages of disease physiology or variations in molecular expression within diseased tissue. The most developed of these is nuclear scintigraphy, and will be discussed in the next section.

1.1.11.4 Nuclear imaging

Nuclear scintigraphy uses radioisotopes to label molecules, distribution of which can be assessed with a scintigraphic camera after administration to a patient. 2D imaging is the most commonly used, although 3D imaging is possible with single photon emission tomography (SPECT) or positron emission tomography (PET).

These can be combined with computed tomography (CT) or MRI to produce detailed composite images.

The most frequently used reagent for imaging of bones and inflamed joints is methylene diphosphate (MDP) labelled with ^{99m}Tc. Uptake of this molecule is increased in areas of increased bone blood flow and turnover (which is seen adjacent to inflamed joints). Prospective studies have demonstrated the sensitivity of MDP scintigraphy for inflamed joints (Backhaus et al. 1999), with negative uptake at a joint having strong negative predictive value for the development of erosions (Mottonen et al. 1988). However, specificity for joints which will develop erosions is poor (Backhaus et al. 2002) and although sensitive to changes in disease activity over 1-2 years (Backhaus et al. 2002;Klarlund et al. 2000) it is unclear whether it has suitable sensitivity in the shorter term.

The prognostic limitations of MDP scintigraphy along with its limited value in detecting short-term response treatment have resulted in the investigation of alternative agents. These can be divided into those which are non-specific, i.e. exploit local physiological changes, and those which target specific molecules up-regulated in the inflamed synovium. These, and strategies for the specific targeting of therapeutic compounds will be discussed in detail in section 1.4. A limitation of conventional 2D nuclear scintigraphy is that of resolution. PET allows the capture of 3D images and hence enhanced resolution and spatial localisation of pathology: this will be discussed in the next section.

1.1.11.5 Positron emission tomography

PET imaging uses tracers containing radioisotopes whose decay causes the emission of two antiparallel photons resulting from the collision of a positron with an electron (reviewed in (Marsden & Sutcliffe-Goulden 2000). Simultaneous detection of these photons allows the origin to be plotted along a line between the detectors: an array of detectors can therefore produce high resolution 3D images. A further advantage of PET is that the radioisotopes used, such as ^{15}O, ^{11}C and ^{18}F can be incorporated into biologically active molecules or closely-related

analogues such as ^{18}fluorodeoxyglucose (^{18}FDG). However, these isotopes have short half-lives (e.g. 20 minutes for ^{11}C and 110 minutes for ^{18}F): a cyclotron is required for their production and their use is therefore limited to a facility with a cyclotron on site or nearby. The cost of radionuclide production and the scanning equipment limits the use of PET to specialist centres.

Clinically PET is used most frequently for diagnosis, staging and treatment monitoring in oncology. Many tumour cell types have up-regulated glucose uptake and metabolism and hence will exhibit increased uptake of ^{18}FDG: once phosphorylated within the cell little further metabolism takes place and hence the radioisotope is trapped providing the opportunity for imaging (O'Doherty 2000). FDG uptake is also increased in inflammatory lesions with increased expression of glucoses transporters (Mochizuki et al. 2001); furthermore, TNFα has been shown to increase glucose uptake in fibroblasts and macrophages (Beckers et al. 2004) and there is therefore obvious potential for its use in RA. The first published study consisted of a small series of RA patients and observed a correlation between MRI-derived synovial volume and ^{18}FDG uptake at the wrist (Polisson et al. 1995) both before and after treatment although correlation with clinical outcome was limited. Recently another study in RA patients found strong correlation between synovial thickening measured by ultrasound and PET standardized uptake volume (Beckers et al. 2004). Globally, there was significant correlation with clinical parameters and disease markers, although PET did not appear to be more sensitive than clinical examination. Another study found good correlation between clinical evidence of inflammation and ^{18}FDG uptake in the small joints of the hands of patients with RA, although PET seemed to confer little advantages over clinical examination (Elzinga et al. 2007). One report has described whole-body ^{18}FDG PET imaging in RA which found correlation with clinical findings, including uptake in extra-articular sites (Goerres et al. 2006). Another recent paper described correlation between PET imaging using a ^{11}C-conjugated tracer targeting peripheral benzodiazepine receptors expressed by macrophages, clinical findings and immunohistochemical staining for these receptors (van der Laken et al. 2008).

PET imaging of RA, although in its infancy, is promising and, in combination with advances with molecular targeting has significant potential. Availability of the technique, however, and cost are likely to limit its use to the research setting for some time to come.

1.1.11.6 Emerging technologies

The targeting of tissue or pathology-specific molecules lends itself most readily to use in nuclear imaging techniques: there is, however, increasing interest in its application to MRI and ultrasound. The use of contrast agents is routine is a means of enhancing delineation between tissues: contrast agents are generally non-specific, examples including gadolinium-DTPA as already mentioned in MRI and microbubbles to enhance the Doppler signal for in ultrasonography. The conjugation of standard or novel contrast agents to targeting molecules, such as antibodies or peptides, has the potential to enhance the imaging of diseased tissues and there has been success with a number of agents in pre-clinical models. Examples of this include the use of RGD peptides and proteins to target liposomes for MRI imaging (Mulder et al. 2005) and echistatin-conjugated microbubbles for use in ultrasound (Ellegala et al. 2003) in tumour models.

Optical imaging using near-infrared fluorescent probes relies on the relatively high transparency of biological tissues to light in the wavelength region 600-1000nm. Illumination from one or more sources allows the creation of 2D or 3D images. In a murine arthritis model cy5.5, a near-infrared fluorescent dye which binds serum albumin, was successfully used to image arthritic joints (Hansch et al. 2004); in another study cy5.5 conjugated to an RGD-containing peptide could image tumours expressing $\alpha_v\beta_3$ in a xenograft model (Cheng et al. 2005).

1.2 Peptides as agents for tissue and receptor-specific targeting

In the previous sections the molecular and immunological basis for endothelial diversity was discussed with implicit opportunities for tissue-specific targeting. In this project a short peptide sequence was identified and developed as a tool for the targeting of synovium: in this section I will discuss some of the developments already made in this area, with particular reference to the short amino-acid motif RGD.

1.2.1 Somatostatin and other regulatory peptide analogues

Analogues of the regulatory peptide somatostatin are now well-established for the clinical imaging of neuroendocrine and other tumours and were the first group of peptide reagents to be used clinically for nuclear imaging. Somatostatin is a widely-expressed neuroendocrine peptide and expression of its receptor is up-regulated on a variety of tumours arising from neuroendocrine tissues (Heppeler et al. 2000). Somatostatin is unstable *in vivo* and is subject to rapid degradation by serum and tissues proteases: modification was therefore required to produce a compound suitable for therapeutic use. The most widely used of these is octreotide which consists of a hexapeptide disulphide-constrained sequence consisting of substituted D-amino acids and a C-terminal amino-alcohol group (Pless 1992). Octreotide (and other somatostatin analogues) has enhanced plasma stability and is widely use clinically: its uptake and internalisation by subtypes of somatostatin receptor have also enabled its widespread use in imaging of a number of tumours. These structural differences illustrate how the substitution of unnatural amino acids can render enhanced metabolic stability to a peptide, and also how biological activity can be retained with the use of short amino-acid sequences. The first use of octreotide for imaging used a modified sequence with a substituted tyrosine for phenylalanine at position 3 which enabled labelling with ^{123}I. As a 'non-residualising' label ^{123}I-tyrosine is rapidly removed from the cell after lysosomal degradation. ^{111}In- DTPA and other bifunctional chelating agents, which can be conjugated to proteins and peptides via terminal amino groups and the ε-amino groups of lysine residues,prior to conjugation to a radiometal, are

'residualising'- their retention in cells is longer due to the absence of a pathway for excretion from the cell and therefore they remain 'trapped'. Results with ^{111}In-DTPA-octreotide gave better tumour-to-background ratios than with ^{123}I-Tyr$_3$-octreotide due to lower circulating levels of degradation products than that seen with the former: tumour uptake was also probably enhanced by the longer circulating half-life of ^{111}In-DTPA-octreotide (Krenning et al. 1992). ^{111}In remains the most widespread isotope for use in somatostatin receptor imaging, although a ^{99m}Tc-labelled somatostatin analogue is licensed in the US for the assessment of pulmonary nodules (Gotthardt et al. 2004) and there have recently been encouraging results with ^{99m}Tc-labelled octreotide (Gabriel et al. 2003). Recently a ^{18}F-labelled octreotide analogue (with carbohydrate modification) has shown promising results for PET imaging (Meisetschlager et al. 2006). A number of other regulatory peptides, including gastrin, VIP substance P and bombesin are at various stage of pre-clinical and clinical development as imaging agents (Gotthardt et al. 2004).

1.2.2 RGD-sequence containing peptides

The integrin $\alpha_v\beta_3$ (also known as the vitronectin receptor) is expressed in health at low levels on vascular and uterine and intestinal smooth muscle cells; it is also expressed on a minority of neutrophils and on activated macrophages and osteoclasts (Eliceiri & Cheresh 1999;Wilder 2002). In angiogenesis its expression is markedly upregulated on endothelial cells and, in adult humans, this is seen in wound healing, chronic inflammatory lesions and placental tissue. It is also upregulated within some tumours, such as melanoma, glioma, ovarian and breast cancer (Wilder 2002). $\alpha_v\beta_3$ binds a number of components of the extracellular matrix, including vitronectin and fibronectin. Studies in animal models have shown that therapeutic blockade of $\alpha_v\beta_3$ can induce endothelial cell apoptosis, inhibit angiogenesis and can cause tumour regression (Brooks et al. 1995). $\alpha_v\beta_3$ is upregulated on the vascular endothelial cells of rheumatoid synovium and its expression can also be demonstrated in the synovial lining layer (Baeten et al. 2000;Walsh et al. 1998). In RA synovium, endothelial $\alpha_v\beta_3$ expression correlates with serum CRP (Baeten et al. 2000). Interestingly, differential $\alpha_v\beta_3$ expression

has been demonstrated between RA and spondyloarthropathy synovium, with decreased expression in the synovial lining in RA compared with SpA (Baeten et al. 2000). A comparison of normal, OA and RA synovial tissue found that synovial lining cell β_3 expression was seen in 2/15 samples and limited to a minority of cells, 7/17 RA sections were positive (Rinaldi et al. 1997b). Despite this, trials of Vitaxin, a humanized version of the murine antibody LM609, in RA have been discontinued due to lack of efficacy[*], although trials are ongoing in oncology.

It is well established that short peptide motifs can act as ligands for integrins. The best, and first, described is the arginine-glycine-aspartic acid (RGD) sequence which is present in a number of proteins. Its original description was within the fibronectin molecule: in a series of experiments a series of peptide fragments from the fibronectin sequence were tested in order to determine the minimal sequence which was necessary for cell attachment; this resulted in the description of the RGDS motif as sufficient to support cell binding (Pierschbacher & Ruoslahti 1984a). Initial experiments found that the substitution of any of the RGD residues resulted in loss of activity, although some amino acid substitutions of the serine were compatible with function (Pierschbacher & Ruoslahti 1984b). Further experiments testing peptide inhibition of fibronectin binding to the fibronectin receptor (later identified as $\alpha_v\beta_1$) found that inhibitory activity was affected by the amino acid 'X' in the RGDX sequence, as well as the flanking amino acid sequences (Hautanen et al. 1989). This finding was underscored by the observation that the peptide GRGDSP, whilst substantially less active than a large 110 kDa fibronectin fragment, was significantly more active than an 11.5 kDa fragment containing the same sequence; this suggests the importance of protein conformation and/ or surrounding sequences on the affinity of RGD-dependent ligand binding (Hautanen et al. 1989). These sequence variations also affect ligand specificity- for instance vitronectin, another RGD containing protein was inactive in these experiments. Some amino acid substitutions in the RGD

[*] Medimmune press release 30/08/2004, available at http://phx.corporate-ir.net/phoenix.zhtml?c=83037&p=irol-investornewsArticle&ID=607978&highlight=

sequence were compatible with retained, although markedly reduced, activity; the reversed DGR sequence also had markedly reduced potency. Stereochemistry is also important: substitution of the L-aspartic acid with the D-isomer in a fibronectin-derived peptide fragment resulted in loss of activity (Pierschbacher & Ruoslahti 1987).

Since the original description of the fibronectin sequence a number of extracellular matrix proteins have been shown to contain the RGD motif, including vitronectin, fibrinogen, thrombospondin, von Willebrand factor and osteopontin; collagen also contains an RGD sequence which is exposed only after proteolysis (Eliceiri & Cheresh 1999): a number of these are upregulated in RA synovium (Nikkari et al. 1995). Interestingly, a splice variant of fibronectin containing the non-RGD containing CS-1 polypeptide sequence, which is a ligand for the integrin $\alpha_4\beta_1$ is preferentially expressed in rheumatoid synovium (Elices et al. 1994). 8 of the known 24 human integrins are known to bind the RGD sequence in proteins (Ruoslahti 1996) and these are summarized in Figure 1.2. As well as affecting the affinity of the RGD peptide for its ligands, the flanking sequence can also affect its specificity for different ligands. For instance, substitution of D-serine for L-serine in the linear peptide Gly-Srg-Gly-Asp-Ser-Pro-Cys resulted in loss of the peptides ability to inhibit cell binding to vitronectin whilst inhibition of fibronectin-mediated binding was little changed (Pierschbacher & Ruoslahti 1987). This study also demonstrated the dramatic effect of stabilisation of the conformation of the peptide by cyclisation: a cyclic peptide containing the same sequence had a log reduction in IC50 in the same vitronectin-based adhesion assay although, unexpectedly, inhibition of binding to fibronectin was lost. Peptide conformation results in significant loss of 'conformational freedom' in solution; as conformation in solution may not reflect that seen bound to a receptor, it has been theorised that such restriction, when it includes the biologically active tertiary structure, will increase receptor affinity (Gurrath et al. 1992). NMR studies of cyclic peptide confirmation have suggested that confirmation is critical to integrin specificity with the distance between the Arg and Asp side chain carbon atoms being particularly important to specificity

for $\alpha_v\beta_3$ (Pfaff et al. 1994). This is in keeping with data suggesting that $\alpha_v\beta_3$ has a narrower and hence more restrictive RGD biding site (Pfaff et al. 1994 and references therein). Previous studies have shown that cyclic peptides are also more stable to degradation *in vivo* (Veber & Freidinger 1985). Studies *in vitro* have shown greater stability of cyclic peptides containing a disulphide bond at acidic and neutral pH compared with their linear equivalents; although under more basic conditions peptide deterioration was more pronounced, largely due to degradation of the disulphide bond (Bogdanowich-Knipp et al. 1999).

Several other short peptide sequences have been identified as having specificity for sub-groups of integrins, such as the LDV motif present in the CS-1 fibronectin sequence (related sequences are also found in MAdCAM-1 and ICAM-1) which binds $\alpha_4\beta_1$, $\alpha_4\beta_7$ and $\alpha_9\beta_1$ (Humphries, Byron, & Humphries 2006). The crystal structure of $\alpha_v\beta_3$ in association with RGD peptide ligand has been determined (Xiong et al. 2002): divalent cation-dependent binding occurs in the cleft between the α and β-subunits with the arginine and aspartic acid residues in close association with residues on the α and β chains respectively.

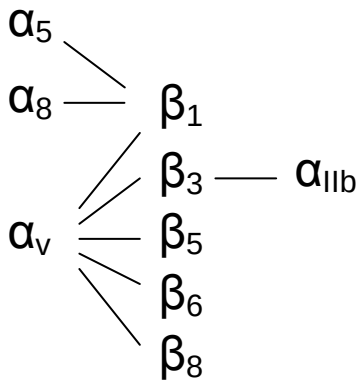

Figure 1.2: The known associations of integrin α and β subunits to form RGD-containing protein-binding dimmers.

The identification of this short sequence has clear potential applications for the imaging and delivery of therapeutic compounds to tissues, such as tumours, which over-express RGD-binding integrins. Short peptide sequences have a number of potential advantages as pharmacological agents over longer polypeptides and

proteins: potentially cheaper production of synthetic vs. recombinant molecules, greater activity as a ratio to molecular weight, enhanced stability in storage, less tendency to immunogenicity and better penetration to the extravascular space (Ladner et al. 2004).

The upregulated expression of $\alpha_v\beta_3$ in many pathological states and the versatility and relatively easy production of RGD-based peptides makes this an attractive tool for imaging and drug delivery. The most extensively investigated synthetic RGD peptides are derived from the cyclic pentapeptide Arginine-Glycine-Aspartic acid-Phenylalanine-Valine (RGDFV) which has been shown to have high affinity and specificity for $\alpha_v\beta_3$ (Aumailley et al. 1991). ^{125}I-labelled peptides derived from the lead peptide cited above, in which F or V has been substituted by a tyrosine residue, were shown to have around 30x the inhibitory capacity of a linear peptide on vitronectin/ $\alpha_v\beta_3$ binding *in vitro* (Haubner et al. 1999). Biodistribution studies in a xenograft model, in which human $\alpha_v\beta_3$-expressing melanoma cells were grown in athymic mice, found that the radioiodinated peptide homed specifically to tumours, with a maximum tumour: blood ratio of 7.7 at 60 minutes. Similar results were seen with osteosarcoma xenografts, with specific uptake still seen at 4 hours (Haubner et al. 1999). These experiments found that clearance of the peptide was predominantly hepatic or intestinal with consequent accumulation of activity in the abdominal area- clearly this presents problems for tracer studies.

Substitution of the valine residue for a lysine allows further derivitisation of the peptide via the ε-NH_2 group of the lysine: conjugation of DTPA, a bifunctional chelating agent, to the lysine group allows subsequent radiolabelling with ^{111}In. Investigations into the effect of metal chelation on RGD affinity have found that binding remains unaffected with DOTA- and HYNIC-conjugated small cyclic RGD peptides (Liu 2006). Studies with this agent in a tumour xenograft model found specific tumour uptake with predominantly renal accumulation (van Hagen et al. 2000). ^{111}In-DTPA also has the advantage that it is a residualising radionuclide with consequent longer retention times by cells following uptake,

whereas amino acids are rapidly excreted form cell following lysosomal degradation of the peptide (Gotthardt et al. 2004): specific uptake by tumour cells was demonstrated *in vitro* (van Hagen et al. 2000). Further modification of the peptide structure has been employed to favourably alter the pharmacokinetics. Glycosylation of the c(RGDyK) peptide via the lysine residue resulted in minimal alteration of inhibitory IC50 *in vitro*. *In vivo* there was reduced hepatic uptake, longer circulation half life and improved tumour uptake, probably due to increased hydrophilicity (Haubner et al. 2001). Radio-iodinated c(RGDyK) which had been conjugated to PEG via the lysine ε-amino group showed faster blood clearance, lower renal accumulation and improved tumour uptake compared to the non-PEGylated peptide (Chen et al. 2004b).

Peptide phage display has provided a powerful tool for the discovery of novel RGD-sequences: screening RGD-binding integrins with phage libraries containing variable numbers of disulphide-constrained sequences found that both ring size and flanking sequences were important in defining specificity (Koivunen, Wang, & Ruoslahti 1995). One particular peptide, ACDCRGDCFCG (RGD-4C) containing four cysteine residues with two disulphide bonds had 20-fold greater inhibitory capacity for $\alpha_v\beta_3$ or $\alpha_v\beta_5$ binding to vitronectin than single disulphide-bond peptides. More recently a peptide with a single disulphide bond was identified by phage display which had similar inhibitory capacity for phage expressing this sequence as the free RGD-4C peptide (Holig et al. 2004). A ^{99m}Tc-RGD4C peptide was tested in human renal adenocarcinoma and colon carcinoma xenografts: no significant uptake was seen between the test and control sequence peptides (Su et al. 2002). Modification of the labelling method (using EDDA rather than tricine as the co-ligand) reduced peptide protein binding but had no effect on uptake by human endothelial cells *in vitro* (Su et al. 2003).Although $\alpha_v\beta_3$ expression was not assessed in the tumours, *in vitro* assays suggested low cell surface expression. It is difficult to draw conclusions about the relative efficacy of these peptides when tested in different models, but on the evidence available the cyclic pentapeptides appear to be the most promising, although as discussed in the

next paragraph there has been some success with the use of the RGD4C peptide as a delivery vector for a pro-apoptotic peptide.

As well as applications as imaging agents, RGD peptides have also been used successfully as delivery agents for therapeutic molecules in several pre-clinical models. Doxorubicin was conjugated to the RGD-4C sequence discussed above and used to treat mice xenografted with human breast carcinoma tissue: mice treated weekly the RGD-doxorubicin had prolonged survival times compared with control groups of mice treated with doxorubicin coupled to a control peptide, doxorubicin alone or vehicle alone (Arap, Pasqualini, & Ruoslahti 1998). Furthermore, reduced vascular toxicity was seen in the heart and liver in those animals treated with the peptide-conjugated drug. In a similar model, mice treated weekly with the RGD-4C conjugated to a pro-apoptotic peptide ($(KLAKLAK)_2$) had smaller tumours at 90 days than those treated with unconjugated RGD-4C and KLAKLAK peptides (Ellerby et al. 1999). Conjugation of paclitaxel, an anti-tumour agent used in metastatic breast cancer, to a dimeric RGD peptide produced a molecule with slightly reduced pro-apoptotic activity on carcinoma cells *in vitro* but with specific *in vivo* homing to xenografted tumour tissue (Chen et al. 2005).

1.3 Selective targeting of the synovium

Selective or specific targeting of the synovium can be broadly divided into two categories: approaches used for the targeting of radioisotopes and those used to deliver therapeutic compounds. Within each of these groups both non-specific (selective) and specific localisation techniques have been investigated, and these will be discussed separately.

1.3.1.1 Non-specific strategies

A number of approaches are available to alter the pharmacokinetics of systemically administered compounds in order to favourably improve their biodistribution and therapeutic index. Perhaps the simplest of these is conjugation to a larger molecule such as polyethylene glycol (PEG). By increasing the molecular weight (mw) of a polypeptide or other compound by 60 kDa or more, PEGylation has a number of effects: these are further affected by the binding of

water molecules increasing the effective mw. PEGylation can have a dramatic effect on the circulating half-life, with increases seen from minutes to hours or days, it reduces renal clearance, protects the drug from degradation and reduces immunogenicity (reviewed in (Harris & Chess 2003)). Although biological activity may also be reduced, this can be largely off-set by the increased half-life. Examples of currently available drugs include PEGylated forms of interferon-α doxorubicin for the treatment of hepatitis C and breast cancer respectively (Harris & Chess 2003). In addition a PEGylated anti-TNFα antibody fragment has undergone a successful phase II trial in RA patients (Choy et al. 2002).

Human polyclonal IgG labelled with ^{99m}Tc has been shown to be superior to MDP-^{99m}Tc for the imaging of inflamed joints: in one study differences in uptake were seen in erosive and non-erosive disease, and between RA and OA which were not seen with MDP-^{99m}Tc (de Bois et al. 1994). Although increased vascular permeability is the likely dominant factor in immunoglobulin accumulation, it is also possible that Fc receptors expressed by cells within the synovium play a role. In a recent comparative study, IgG-^{99m}Tc was shown to be superior to MDP-^{99m}Tc in assessing the efficacy of radiation synovectomy at the knee (Arzu et al. 2003). Moreover, IgG-^{99m}Tc has been shown to better distinguish between active and inactive joints in chronic RA (Berna et al. 1992). Other agents which have been used with some success in RA in include ^{99m}Tc-dextran (Kaya et al. 2004) and ^{99m}Tc-ciprofloxacin (Appelboom et al. 2003): the latter study lacked a control tracer group, and the uptake seen was likely to have, again, been non-specific.

The conjugation of drugs to large carrier molecules has also been successfully employed in pre-clinical models. Methotrexate has a relatively short plasma half-life, largely due to rapid renal excretion: radiolabelled albumin accumulates in inflamed joints (Wunder et al. 2003) and conjugation of albumin to methotrexate has been shown to prolong its circulation time and to improve the pharmacokinetics in animal tumour and arthritis models (Stehle et al. 1997;Wunder et al. 2003). An albumin/ MTX conjugate has been shown to be significantly more effective than unconjugated methotrexate for both the treatment

and prophylaxis of collagen-induced arthritis: increased uptake by synovial fibroblasts was demonstrated thus suggesting a second mechanism for enhanced synovial uptake (Fiehn et al. 2004b;Fiehn et al. 2004a).

Another technique for the improvement of tissue drug delivery is encapsulation in liposomes. Liposomes are vesicles consisting of a phospholipid bi-layer encapsulating an aqueous core and they have been successfully used for the delivery of a variety of therapeutic compounds (Torchilin 2005). Early work with liposomes was hampered by their high clearance rate by the reticuloendothelial system largely limiting their use to the targeting of these organs; PEGylation and other modifications can reduce opsonisation in the circulation and dramatically increase their circulating half-life. Examples of liposome formulations now in routine clinical use include doxorubicin and daunorubicin for the treatment of metastatic breast cancer and Kaposi's sarcoma, and amphotericin B for the management of systemic fungal infection in immunocompromised patients (Torchilin & Lukyanov 2003). Other formulations being studied include those intended for use in nuclear imaging and the delivery of cytotoxic drugs, cytokines and gene therapy. Construction of liposomes from pH-sensitive polymers can allow fusion with the endovacuolar membrane after endocytosis and thus release of the payload into the cytoplasm. Application of liposome technology to the imaging and treatment of RA has been attempted for some time. Intra-articular injection of liposome-encapsulated corticosteroids resulted in a therapeutic response in a small group of patients with RA (de Silva et al. 1979). Encouraging results have been reported after injection of liposomal drug formulations in animal models: both liposomal MTX and clodronate had enhanced efficacy over the free drug when injected intravenously in a rat arthritis model with a reduction in the hematopoietic toxicity of MTX (Richards et al. 1999;Williams, Camilleri, & Williams 1994). The efficacy of MTX-liposomes was reduced when PEG-liposomes were used, probably due to reduced synovial macrophage uptake (Williams et al. 2000). More recently it was shown that liposomal prednisolone was significantly more efficacious than the same dose of the free drug in two murine arthritis models (Metselaar et al. 2003;Metselaar et al. 2004). It was shown

in these studies that the intravenously-administered PEG-liposomes homed to inflamed joints and that there was an associated reduction in cartilage damage. Histologically, liposomes were shown to accumulate mainly in the lining layer. Impressively, the same therapeutic effect could only be achieved by repeated pulsed treatment with 10-fold higher doses of free prednisolone. ^{99m}Tc-liposomes have been shown to accumulate in inflamed joints in an animal model (Boerman et al. 1997) and uptake was shown to be as good as ^{111}In-IgG in a small clinical study of inflammatory lesions including arthritis (Dams et al. 2000).

Despite the favourable effects of the above delivery strategies, they are non-specific and the use of techniques to target specific tissue or cells, particularly when combined with those detailed above, have the potential to further refine tissue-specific targeting. This will be discussed in the next section.

1.3.1.2 Specific approaches

A number of molecules have been investigated as potential targets for radionuclide imaging in inflammatory arthritis. The success of biological agents targeted at cytokines involved in the inflammatory cascade has led to their investigation as imaging agents. ^{123}I-labelled interleukin-1 receptor antagonist (IL1-ra) was shown to accumulate in inflamed joints in patients with RA, but similar uptake was seen with radiolabelled albumin suggesting that the effect was non-specific (Barrera et al. 2000). In another study ^{99m}Tc-labelled anti-TNFα antibody was shown to accumulate in inflamed joints and this uptake was sensitive to short term change after treatment with corticosteroid (Barrera et al. 2003). However, pre-treatment with blocking antibody showed that much of this effect was non-specific, but 25% of tracer accumulation could be attributed to specific uptake. The difficulty of substantial non-specific uptake was also highlighted by another study with a radiolabelled monoclonal antibody to rat CD4 which did not show increased uptake over isotype control in an experimental model (Kinne et al. 1993).

A more successful approach has been targeting of E-selectin, an adhesion molecule which is up-regulated in the vascular endothelium in inflammation but is virtually absent in uninflamed tissues. It is upregulated on the endothelium of RA synovium (Smith et al. 2001) and levels of soluble E-selectin are raised in the serum of RA patients (Klimiuk et al. 2002). A comparison between ^{99m}Tc-human immunoglobulin (HIg) and ^{111}In-Fab (from the 1.2B6 murine IgG1 anti-human E-selectin clone) in RA patients found that E-selectin targeting offered enhanced sensitivity and probably specificity at 24 hours (Jamar et al. 1997). A more recent study found that this ^{111}In-Fab had enhanced specificity over conventional ^{99m}-oxidronate bone scanning (Jamar et al. 2002). *In vitro* evidence that E-selectin is internalised by activated endothelial cells upon ligation with specific antibody (von Asmuth et al. 1992) adds to its attractiveness as a target.

Another encouraging approach has been the targeting of folic acid receptors (Turk et al. 2002): these are up-regulated on the cell membrane of RA macrophages. In a rat arthritis model specific uptake of ^{99m}Tc-folic acid was seen in inflamed joints: specificity was confirmed by significant reduction of uptake when co-administered with a saturating dose of unlabelled folic acid; reduction in uptake was also seen after macrophage depletion.

Despite the aforementioned disappointment with anti-$\alpha_v\beta_3$ antibody in the treatment of RA, results so far with RGD peptides as treatment or drug delivery agent in animal models of arthritis are encouraging. Weekly intra-articular administration of the RGD peptide c(RGDfV) in rabbits with antigen-induced arthritis resulted in reduced joint swelling, neovascularisation, inflammatory cell infiltrate, pannus formation and cartilage erosions compared with animals treated with a control peptide (Storgard et al. 1999). In mice with collagen-induced arthritis, phage expressing an RGD peptide containing 2 disulphide bonds (RGD4C) which has selectivity for $\alpha_v\beta_3$ and $\alpha_v\beta_5$ was shown to accumulate specifically in the synovium of inflamed joints: this homing was inhibited by co-injection of the free RGD4C peptide (Gerlag et al. 2001). Administration of the peptide conjugated to the pro-apoptotic domain D(KLAKLAK)$_2$ reduced clinical arthritis with an increase in apoptosis in synovial endothelial cells.

There has also been success in pre-clinical models with the targeted delivery of liposomes. As well as improving regional homing, the use of internalizing antibodies can further enhance cellular delivery (Andresen, Jensen, & Jorgensen 2005). A recent paper described the use of liposomes conjugated to a cyclic RGD peptide to deliver dexamethasone to inflamed joints in a rat adjuvant-induced arthritis model (Koning et al. 2006). Animals treated with RGD-conjugated liposomes had a significantly greater improvement in arthritis scores than those treated with unconjugated liposomes. A peptide (identified by screening of a phage library) with binding affinity for the VEGF receptor has been shown to target liposomes to cells expressing the receptor *in vitro* (Janssen et al. 2003) and this may have future potential as a strategy for targeting in inflammatory arthritis.

1.4 Platform technologies used in the project and previous work

1.4.1 The SCID mouse chimeric transplantation model

The SCID (severe combined immunodeficiency) autosomal recessive mutation was first described in mice in 1983 (Bosma, Custer, & Bosma 1983). Affected animals have a defect in V(D)J recombination and have no functional B- or T-cells: the mutation, on chromosome 16, also results in defects in DNA repair (Fulop & Phillips 1990). Beige-SCID mice have, in addition, reduced NK cell function and therefore may be more suitable recipients of xenografted tissue (MacDougall et al. 1990). Furthermore, beige-SCID mice have a substantially reduced incidence of 'leakiness'- this spontaneous production of T-cells and immunoglobulin can affect up to 25% of mice bearing the SCID mutation alone (Mosier et al. 1993).

The first description of the xenografting of human synovial tissue cells into immunodeficient (nude) mice was in 1981 when it was shown that synovial cells derived from human rheumatoid synovial tissue could survive after subcutaneous injection for up to 30 days (Brinckerhoff & Harris, Jr. 1981). Another successful cell-based approach has been the co-transplantation of RA fibroblasts and cartilage under the renal capsule of SCID mice, in which invasion into the

cartilage was shown (Muller-Ladner et al. 1996;Pap et al. 2001). Several techniques have been adopted for the transplantation of human synovial tissue into SCID mice; tissue used for these studies is generally obtained from patients undergoing joint replacement. The first description was of transplantation of small volumes of synovium under the renal capsule which had impressive (96%) graft survival up to 66 days. The most common approach is of subcutaneous transplantation: graft survival can be seen for several weeks with a high frequency of graft survival: human endothelial cells can be seen in tissues stained for human-specific vascular markers and transplanted tissue retains its morphology although there is a reduction in mononuclear cell density with time (Proudman et al. 1999). The formation of anastomoses between the human and murine circulation can be demonstrated by immunohistochemical or immunofluorescent co-staining for human and murine-specific vascular markers (Lee et al. 2002;Wahid et al. 2000). Furthermore, these anastomoses can be shown to be functional, as demonstrated by the co-localisation of a biotinylated anti-ICAM-1 with human vessels within the grafts after intravenous injection of a human specific antibody (Wahid et al. 2000). Four weeks after transplantation there is also down-regulation of the inflammatory phenotype, with reduced expression of the adhesion molecules VCAM-1, ICAM-1 and E-selectin in RA synovial grafts compared with the fresh tissue (Proudman et al. 1999). Notably, however, intragraft injection of pro-inflammatory cytokines TNFα or IL-1β can up-regulate the expression of E-selectin, VCAM-1 and ICAM-1 in the grafts. E-selectin expression returns to baseline by 24 hours whilst VCAM-1 and ICAM-1 expression can persist up to 48 hours post-stimulation (Proudman, Cleland, & Mayrhofer 1999;Wahid et al. 2000). Our group and others have reported that TNFα stimulation has also been shown to enhance the homing of human peripheral blood lymphocytes to engrafted tissue after intravenous or intraperitoneal injection of ^{111}In-labelled cells (Jorgensen et al. 1996;Wahid et al. 2000).

1.4.2 Peptide phage display

The exploitation of filamentous phage as an expression vector for peptide sequences was first described in 1985. Wild-type M13 phage consists of a single

6408 nucleotide strand of DNA encapsulated by a protein coat: this is made up of 2700 copies of the major coat protein PVIII (Rodi & Makowski 1999). Additional proteins are expressed at each end of the phage: at one end five copies each of PVII and PIX, and five copies each of PIII and PVI at the other (Figure 1.3). M13 phage replicates by infecting its intermediate host *Escherichiae coli* (*E.coli*). The PIII protein attaches to the F pilus of the bacteria which is followed by internalisation. Double-stranded DNA (dsDNA) is produced which enables synthesis of the phage proteins and replication of the ssDNA: after assembly the phage particle is extruded form the bacterium (Kehoe & Kay 2005). Fusion of randomly synthesised (degenerate) oligonucleotide sequences into the phage genome allows the expression of peptides with the phage on the phage coat as fusion proteins (Devlin, Panganiban, & Devlin 1990). Of the phage coat proteins PIII, PVIII and PVI have been utilised but by far the most frequently used is PIII. Libraries of phage expressing randomly-generated peptide sequences can be screened against target ligands: elution of unbound phage and amplification of the bound phage pool results in the enrichment of phage clones expressing specific peptide binding sequences (Devlin, Panganiban, & Devlin 1990). The incorporation of flanking cysteine residues allows the formation of disulphide bonds between the –SH side-chains with resulting cyclic peptides: when linear and cyclic libraries were used to select peptides binding streptavidin similar peptide sequences were identified with greater affinity shown by the cyclic peptides (Giebel et al. 1995;McLafferty et al. 1993).

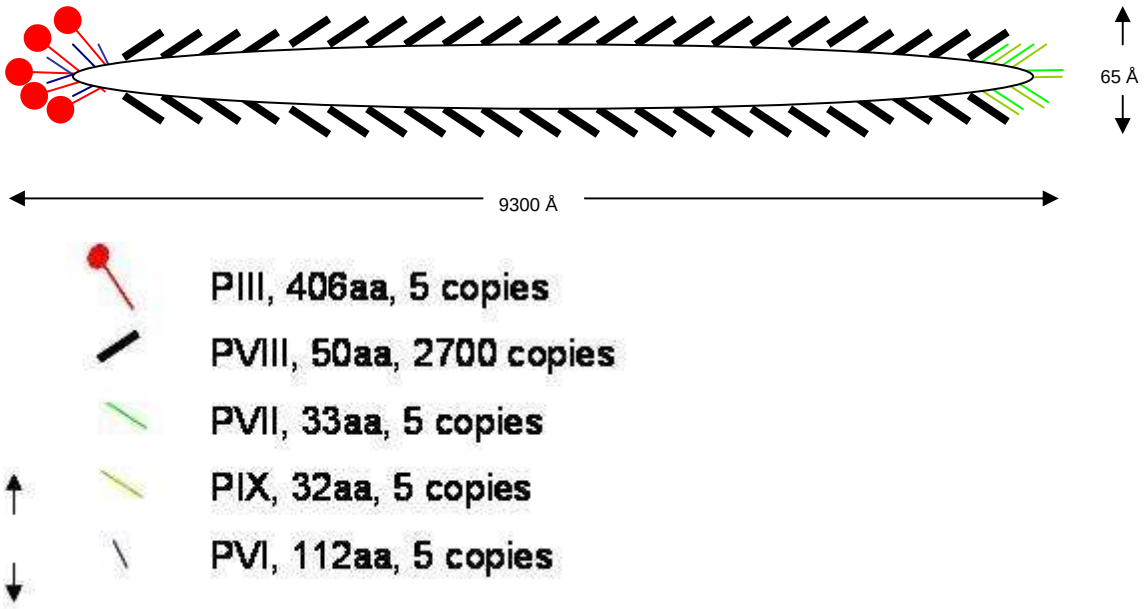

Figure 1.3: M13 phage structure. The coat protein PVIII encases a single strand of DNA with the various minor coat proteins expressed at either end of the virion (adapted from (Kehoe & Kay 2005)).

1.4.2.1 *In vivo* phage display for the selection of novel peptides to vascular luminal epitopes

The versatility of phage display technology places it in a unique position in its application to the identification of novel peptide or antibody sequence for the targeting of tissue. The injection of phage libraries into animals can, using the same principles used for *in vitro* phage selection, be used to identify clones with binding specificity to an organ or tissue of interest. One of the most attractive features of this technique is that no prior knowledge is needed of the ligand to which the phage will bind, and hence phage can be isolated by screening on a particular cell line or tissue with the subsequent identification of clones which bind to what may be previously unidentified ligands. *In vivo* screening has a number of advantages over *in vitro* strategies. A significant problem with

endothelial cells in culture is that they may progressively de-differentiate with loss of phenotypic expression of membrane-bound molecules and altered adhesive characteristics (Borsum et al. 1982;de Bono & Green 1984): this could include the loss of tissue-specific molecular determinants. Reasons for this are likely to include loss of the chemical and cellular microenvironment- for instance, regulation of expression of endothelin expression by myocardial endothelial cells was shown to be dependent on the close proximity of cardiac myocytes in co-culture (Nishida et al. 1993). A study in which human endothelial cells were co-cultured with RA fibroblasts derived from patients with RA found that ECs co-cultured with the synovial, but not skin, fibroblasts were capable of supporting neutrophil recruitment (Lally et al. 2005). Furthermore, the selection of phage from libraries injected intravenously enables isolation of clones binding specifically to *endothelial* ligands- this is clearly of critical importance for the selection of novel sequences intended for development as mediators for the targeting intravenously-administered compounds. Finally, this selection occurs under conditions of physiological flow and hence will restrict clones to those with greater binding affinities. There are clear ethical barriers to the screening of human subjects (although there have been a small number if such studies as will be described later) and the transplantation of human tissue into immunocompromised animals provides a unique platform for the *in vivo* screening of human vascular endothelia. Heterogeneity of surface molecule expression is extensive throughout the circulation and variation in expression of endothelial-specific genes is widespread (Aird 2003). As already discussed in section 1.2.2.1 the description of tissue-specific addressins (either identified or implied) provides a good example of this diversity. Further evidence comes from studies of phage library screening *in vivo*. Screening of a phage-displayed peptide library in mice produced, after 3 rounds of selection, phage with homing selectivity for a variety of tissues (indeed, selective phage were isolated for all tissues analysed): sequencing of clones showed that binding motifs differed for each organ (Rajotte et al. 1998). Limited studies in human patients have produced similar results. Arap *et al* screened a seven amino-acid disulphide-constrained phage-displayed peptide library in a patient who had been declared brain-dead

(Arap et al. 2002b). Biopsies were taken from multiple tissues 15 minutes after intravenous injection of the library and high-throughput screening was used to analyse large numbers of isolated clones. Comparison of peptide motifs from phage isolated from the various tissues demonstrated that phage were distributed in a non-random manner and that certain motifs could be shown to occur significantly more frequently in particular organs. In another study, in which a phage library was injected into patients with end-stage malignancy, phage clones were again shown to accumulate non-randomly in tumour tissue- in some of these patients repeat screening rounds were possible (Krag et al. 2006). Several studies have translated the identification of tissue-specific peptides identified from phage display into conjugates for the delivery of therapeutic agents. As already discussed, *in vivo* screening of a human breast carcinoma cell line transplanted into SCID mice identified the integrin-binding RGD motif: conjugation of the peptide to doxorubicin was shown to improve the therapeutic index when compared to the free drug (Arap, Pasqualini, & Ruoslahti 1998). In this study another peptide motif, NGR, was also identified which, when conjugated to doxorubicin, had similar results. Although the NGR peptide motif had some binding affinity for the $\alpha_v\beta_3$ integrin this was weaker that seen with RGD and was not inhibited by the RGD peptide. Its ligand was subsequently identified as aminopeptidase N (APN), and this was found to be up-regulated in the vasculature of human and murine tumours (Pasqualini et al. 2000). Furthermore, antibodies to APN were found to have anti-angiogenic activity Screening of a cyclic nonapeptide phage-displayed library identified a murine breast-homing sequence, CPEGPGAGC, for which was identified as being membrane dipeptidase (Essler & Ruoslahti 2002) and a 13 amino acid murine lung-homing sequence was found to bind to membrane dipeptidase (Rajotte & Ruoslahti 1999). Arap *et al* identified a peptide sequence, SMSIARL, with homing specificity for the prostate after screening a phage library in mice. Conjugation of this peptide sequence to the pro-apoptotic sequence $D(KLAKLAK)_2$ followed by intravenous injection resulted in damage specifically to prostate cells: the conjugate also significantly prolonged survival in mice genetically susceptible to prostate cancer (Arap et al. 2002a). Phage expressing a disulphide-constrained prostate-homing sequence,

CRRAGGSC, were found to co-localise with the interleukin-11 receptor IL11-Rα and that this is up-regulated in prostatic malignancy (Zurita et al. 2004). In another study illustrating the potential diversity of peptide phage-display applications, screening of a phage library in genetically obese mice identified a sequence, CKGGRAKDC, which targets adipose tissue. Intravenous injection of D(KLAKLAK)$_2$-conjugated peptide could reverse obesity in mice fed a high-calorie diet. The peptide was found to bind to prohibitin, a membrane associated protein, which is thought to have a role in the regulation of cell survival (Kolonin et al. 2004).

The above examples demonstrate the diversity of protein ligands which have been found to act as vascular receptors for tissue-specific phage. Whilst the best described peptide homing motif, RGD, binds an endothelial integrin, there are many instances of the receptor being of another class of proteins which may not be classic adhesion molecules, examples of which are given above. It is even possible that tissue-specific determinants may not be protein-based, for instance considerable variation in tissue distribution of heparan sulphates have been demonstrated using antibodies developed from phage display (Dennissen et al. 2002). This serves to underline the diversity of endothelial molecular expression. There is widespread heterogeneity both between and within tissue in patterns of endothelial protein expression reflecting the diversity in function of these cells. As already discussed, variation is also seen in the expression of extracellular matrix proteins such as that seen with fibronectin.

1.4.3 Previous work

In our laboratory we have adapted the aforementioned chimeric synovium transplantation models for the *in vivo* panning of phage display libraries and investigation of targeting strategies. In our model, human OA or RA synovial tissue obtained from patients undergoing joint replacement is co-transplanted with human skin as a human control tissue. The successful engraftment of human skin into SCID mice is well-established: in one study engraftment was 90% successful

with preservation of normal histology 4 weeks after transplantation and retention of human vascular endothelial determinants (Yan et al. 1993). As with synovial grafts, low levels of VCAM-1 and E-selectin expression were present in the grafts with somewhat higher levels of ICAM-1; all three were up-regulated by intragraft injection of TNFα (Yan et al. 1993). In this model TNFα stimulation induced ingress of murine leucocytes into the transplanted tissue and this was inhibited by prior intravenous administration of anti-E-selectin antibody (Yan et al. 1994). In agreement with previous researchers, we found successful engraftment of both skin and synovial tissues with the majority of transplants surviving; vascularisation was found to be similar for both tissues (Lee et al. 2002). The scheme for biopanning and enrichment of phage was as detailed in Figure 1.4. A M13 phage library, in which seven amino-acid, disulphide-constrained peptides were expressed by the PIII protein were obtained from a commercial source (New England Biolabs, Hitchin, UK), was first validated by biopanning against streptavidin *in vitro*. The phage clones isolated, expressing a peptide containing the expected HPQ motif, were subsequently used as controls. 10^{11} plaque-forming units (pfu) of phage were injected intravenously into SCID mice double-transplanted with 2 synovial and 2 skin transplants. After 15 minutes incubation the thoracic cavity was exposed under terminal anaesthesia and the circulation perfused via the left ventricle with saline. The grafts were extracted and homogenised prior to elution of bound phage form the tissue: this pool of phage was amplified by co-culture with the *E.coli* host before re-injection into transplanted mice. After 4 rounds of selection homing of the synovium-selected phage pool was increased 600-fold over the control phage clone. This specific homing was seen with both OA and RA grafts and co-localisation of the phage with human vascular endothelium was seen on immunofluorescent staining of the grafts, with minimal staining in the skin tissue. One clone from the final round of selection which exhibited 10-fold selectivity for synovium over the control was selected for further study. Homing of this clone, expressing the sequence CKSTHDRLC, was inhibited in a dose-dependent manner by co-injection of the free biotinylated synthetic peptide (not seen with the control peptide). Co-

localisation of the peptide was also seen with human vascular endothelium within the synovial grafts.

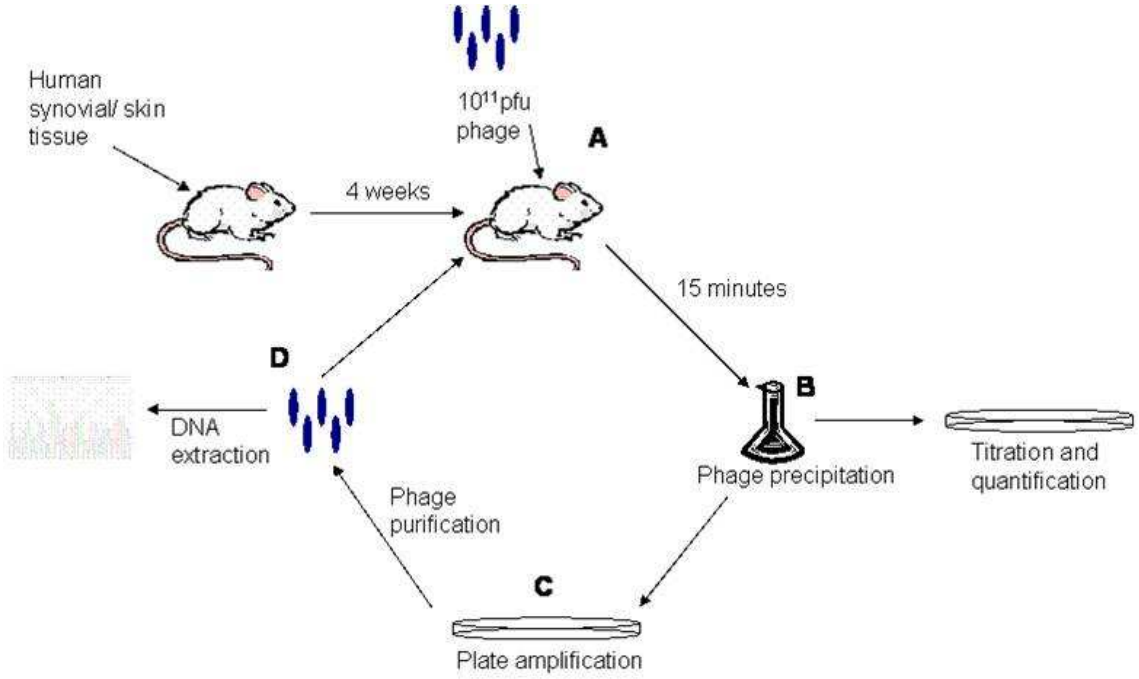

Figure 1.4: Outline of technique for *in vivo* phage selection. A Phage library expressing random peptide sequences is injected into SCID mice transplanted with human skin and synovium. After 15 minutes incubation the transplanted tissues are retrieved, homogenised and phage eluted (**B**). Phage concentration can then be determined in the tissue or phage can be re-amplified in plate culture (**C**), purified (**D**) and re-injected into transplanted mice. Successive enrichment rounds result in the identification of phage expressing peptide sequences which confer homing specificity for the tissue of interest.

1.5 Aims and outline of thesis

The primary purpose of this thesis was to develop the synovial-homing peptide as a vector for the targeting of diagnostic and therapeutic agents to human synovium. In particular the aims were as follows:

1. To further develop and characterise the synovial homing phage and the human SCID mouse transplantation model as a platform for the validation of novel targeting agents.
2. To develop monomeric synthetic synovial homing peptides to deliver radioisotope imaging agents specifically to human synovium in *in vivo* biodistribution studies in the SCID mouse chimera model.
3. To develop novel polymeric peptide constructs in order to increase specific affinity and tissue delivery.

Firstly, in Chapter 3, I demonstrate that the synovial homing (3.1) phage clone localises reproducibly to transplanted human synovium. Notably synovial localisation was found to be increased by up-regulation of the inflammatory phenotype of the transplanted tissue. In particular adhesion molecule expression in stimulated tissue was examined to confirm up-regulation of endothelial inflammatory markers. Finally, in this Chapter, I examined sequence homology between the peptide and candidate molecular mediators of tissue-specific homing and investigated the potential of such candidates in ligand binding assays.

In Chapter 4 the transplantation model was developed as a tool for the investigation of novel agents using SPECT-based imaging of synovial tissue. The SPECT/CT imaging system was validated specifically with the SCID mouse chimera model, as was the quantification of uptake of radioactivity within transplanted tissues. This system was used to demonstrate that specific uptake of a radiolabelled anti-E-selectin antibody could be differentiated form the non-specific uptake of an isotype control, thereby demonstrating the potential of this model as a platform for testing novel tissue/inflammation specific agents.

In Chapter 5 the synovial homing peptide was labelled with the radioisotopes ^{111}In or ^{99m}Tc and tested for homing specificity in the transplantation model. *In vitro* stability and protein binding of the ^{99m}Tc-labelled peptides were investigated and the effect of alternative labelling chemistries explored. The potential contribution of increased permeability of the vascular endothelium of the transplanted human synovium and skin was also investigated.

In Chapter 6 a novel method was developed for the rapid tetramerisation and radiolabelling of peptide by conjugation to ^{111}In-labelled streptavidin. The constructs were validated extensively *in vitro* using RGD peptides of similar length and identical linkers prior to the testing *in vivo* of synovial-homing specificity in transplanted SCID mice.

Finally, in Chapter 7, a novel method is described for the coating of fluorescent microspheres with peptide. These were tested *in vivo* with RGD peptides before injection of synovial-homing peptide into transplanted mice in order to determine homing to transplanted tissues.

In Chapter 8 the findings from the experimental work is discussed in detail and the thesis finishes with a discussion of future work which may be of benefit in this area.

Chapter 2: Materials and methods

2.1 The SCID mouse transplantation model

The animal work described in this project is based on the human synovium chimeric transplantation model which has previously been described extensively. Human skin was co-transplanted when indicated as a human control tissue.

2.1.1 Ethical approval

Tissue collection was carried out at the time of operation in patients undergoing knee replacement surgery. Ethical approval was obtained from the local ethics committee (Local Research Ethics Committee number 05/Q0703/198). Informed written consent was obtained from patients at the time of surgery.

A project license for all the animal work carried out was obtained from the Home Office.

2.1.2 Tissue collection and processing

Tissue removed during surgery was obtained from patients undergoing surgery at Guy's Hospital. Tissue was collected in sterile containers and washed in sterile Hank's balanced salt solution (HBSS). Synovium was dissected from the tissues in a class II laminar flow hood and cut into pieces of a suitable size for transplant (~5mm^3). Freezing media was prepared by diluting 20% dimethyl sulphoxide (DMSO) (Sigma) in heat-inactivated fetal calf serum (Sigma) and mixing 1:1 with RPMI medium. Tissue in ~1 ml of freezing media was placed into cryovials (Nunc, Roskilde, Denmark) and put in an isopropanol cell freezing chamber which was transferred to a -80 ^{0}C freezer. Once frozen the vials were stored long-term under liquid nitrogen. Tissues were prepared for histology by snap freezing in OCT embedding matrix (CellPath, Newtown, UK) in liquid nitrogen-cooled isopentane. Tissues were stored at -70 ^{0}C until needed. Tissue sections were cut at a thickness of 6 μm in a manual cryostat (Leica Microsystems, Milton Keynes, UK) and placed onto glass slides (Superfrost+, VWR, Poole, UK) and air dried overnight before storing at -70^0 C.

2.1.3 Animals

Breeding pairs of severe combined immunodeficient (SCID) mice were maintained in sterile conditions in an isolator under positive pressure in the Biological Services Unit, St Thomas' Hospital or at the William Harvey Institute, Queen Mary University of London. Mice were transplanted at 4-6 weeks old.

2.1.4 Tissue processing for transplantation

Prior to transplantation frozen tissue was defrosted at 37^0C in a SW20 circulatory water bath (Julabo, Peterborough, UK) and washed in sterile HBSS. The tissues were wrapped in sterile gauze moistened with HBSS and placed in sterile 50 ml centrifuge tubes (Corning, Artington, UK) for transport.

Anaesthetic was prepared by mixing Hypnorm (0.315 mg/ml fentanyl citrate, 10 mg/ml fluanisone; Vetapharma, Leeds, UK), Hypnoval (midazolam 5 mg/ml, Roche) and sterile water in a 1:1:6 ratio. Mice were anaesthetised by intraperitoneal injection of 100-120 μg of anaesthetic. One or two incisions (depending on whether the mice were to be transplanted with synovium and skin or synovium alone) either side of the midline were made in the dorsal skin and the tissue inserted and secured with insoluble sutures (Ethicon, Ohio, USA). Mice were used for experiments 2-4 weeks after tissue transplantation.

2.1.5 Stimulation of grafts with TNFα

For intragraft injection of TNFα mice were anaesthetised with 1.2 L/minute O_2 + Halothane (induction concentration 4%, maintenance concentration 2%) using Boyle's apparatus. Grafts were injected with 50 μL 0.9% saline containing 200 ng recombinant human TNFα (R and D Systems, Abingdon, UK) or 50 μL 0.9% saline control with a 1 ml insulin syringe (Becton Dickinson, Oxford, UK).

2.1.6 Evans blue vascular permeability assay

In order to assess the permeability of the transplanted tissues to macromolecules the Evans Blue permeability assay was used. SCID mice transplanted with human tissues were injected via the tail vein with 200 μL Evans Blue (Sigma) diluted to 0.5 mg/ml in sterile PBS (~50 mg/kg). After an hour the thoracic cavity was

exposed under terminal anaesthesia and the circulation perfused with 50 ml 0.9% saline as described for the phage studies. Tissues were retrieved and frozen in 1.5 ml centrifuge tubes until analysis.

To quantify dye uptake in the tissues the tissues were defrosted, washed twice in PBS and weighed in clean 1.5 ml centrifuge tubes. 1 ml formamide (Sigma) was added and the tubes were incubated at room temperature for 6 days. At the end of the incubation period the samples were centrifuged in a microcentrifuge for 10 minutes at 10,000 rpm: the formamide was then carefully pipetted into 1 ml plastic cuvettes and the absorbance at 620 nm read in a spectrophotometer (Ultrospec 2100 pro, Amersham Biosciences, Amersham, UK).

2.2 Amplification, sequencing and titering of phage clones.

In this project two phage clones were used for *in vivo* biodistribution and *in vitro* candidate ligand adhesion assay. The synovial-homing phage expressing the disulphide-constrained peptide sequence CKSTHDRLC (hereafter known as clone 3.1) and a phage clone expressing the disulphide-constrained streptavidin-binding sequence CGTWSHPQC (SC1) (as a negative control), both of which were isolated in the course of the work described in the introduction, were used for the *in vivo* and *in vitro* experiments.

2.2.1 Preparation of materials

2.2.1.1 LB media

10 g Bacto-tryptone

5 g yeast extract

5 g sodium chloride

Reagents were dissolved in 1 L distilled water and autoclaved

2.2.1.2 Xgal/IPTG Agar plates

The phage used in this project were derived from a library created with the cloning vector M13mp19 which contains the lacZα gene. 5-Bromo-4-chloro-3-indolyl-beta-D-galactopyranoside (X-Gal) is a substrate for β-galactosidase,

which is encoded for by the lacZα gene: phage plaques therefore appear blue allowing for easy identification. isopropyl β-D-thiogalactoside (IPTG) binds and inhibits the lac repressor and hence acts as an inducer for the enzyme.

A solution was prepared by dissolving 1g of X-gal (Cambio, Cambridge, UK) and 1.25 g of IPTG (Cambio) in 20 ml of dimethyl formamide. The solution was stored in the dark at -20^0 C. Agar was prepared by dissolving 14 g of agar in 1 L LB media and autoclaving: once the solution had cooled to <70 ^{0}C 1 ml of X-gal/IPTG solution was added and the agar poured into triple-vented Petri dishes. The agar was allowed to harden overnight and stored in the dark at 4-8^0 C.

2.2.1.3 Agar top

7 g agar and 1 g $MgCl_2.6H_2O$ were dissolved in 1 L LB media and autoclaved. The solution was decanted into sterile 50 ml tubes and stored at RT.

2.2.1.4 TBS

Tris-buffered saline (TBS) was prepared by dissolving 50 mM Trizma base and 150 mM NaCl in 1 L distilled water. The pH was adjusted to 7.5 with HCl and the solution autoclaved.

2.2.1.5 Minimal media agar plates

2xM9 salt was prepared by dissolving 12 g Na_2HPO_4, 6 g KH_2PO_4, 1 g NaCl and 2 g NH_4Cl in 1 L distilled water.

2.2.1.6 Maintenance of *E.coli* host

In order to positively select for *E.coli* expressing the bacterial F-pilus, bacteria were streaked from -70^{0}C glycerol stocks onto minimal media agar plates and incubated overnight at 37^{0}C. Bacteria were amplified for use in phage experiments by seeding a single colony from the plate into a sterile cell culture flask containing 50 ml of LB media. The flask was incubated in a shaking incubator overnight at 37 ^{0}C and then stored at 4 ^{0}C.

2.2.2 Amplification

Phage clones (from the library of M13 phage expressing seven-amino acid disulphide-constrained cyclic peptides (Ph.D.C7C system, New England Biolabs, Hitchin, UK) used to select for synovial-homing sequences *in vivo* as previously described) were amplified by adding 5 μL phage stock and *Escherichia coli* host (New England Biolabs) to 3 ml agar top and incubating on IPTG/XGAL plates (agar (14g/L agar in LB media containing 1ml/L IPTG/XGAL (25 ml dimethyl formamide containing 1.25 g isopropyl β-D-thiogalactoside and 1 g 5-bromo-4-chloro-3-indolyl-β-D-galactoside (Cambio)) overnight at 37^0 C. The phage layer was then homogenized in 25ml LB media and centrifuged for 1 hour at 2,400 g in 50 ml centrifuge tubes in an ALC PK131R centrifuge (ALC, Italy). Phage was precipitated by the 1:6 addition of 20% PEG-8000 with 2.5 M NaCl and incubating in ice for 1 hour. The tubes were centrifuged again for 1 hour at 2,400 g and the supernatant discarded. The pellet was re-suspended in 1 ml TBS (50 mM Tris-HCl pH 7.5, 150 mM NaCl), transferred to 1.5 ml centrifuge tubes and centrifuged for 10 minutes at 13,000 rpm in a microcentrifuge (MSE Microcentaur, Sanyo, Watford, UK). The supernatant was transferred to 50 ml centrifuge tubes, diluted to 5 ml in TBS and 1:6 PEG/NaCl added before incubating for 1 hour on ice. The tubes were centrifuged for 30 minutes at 2,400 g and the phage pellet resuspended in 1ml TBS which was diluted 1:1glycine for storage at -20^0 C.

2.2.3 Quantification by titration

Phage concentrations were determined by diluting the stocks in 10^8-10^9 in LB media and adding 10 μL to 200 μL of amplified *E.coli* diluted 1:50 in LB media. 3 ml agar top (melted and allow to cool to $<50^0$C) was added and the agar was poured onto IPTG/Xgal plates in triplicate and incubated overnight at 37^0 C. Blue plaques representing individual plaque-forming units (pfu) were counted: dilutions were carried out in order to ensure that the minimum number of counts per plate was 100 in order to maximize accuracy.

2.2.4 Confirmation of PIII displayed peptide sequences

DNA was extracted from the phage stocks as follows. 100 μL of phage stock was diluted 1:10 in TBS in 1.5 ml centrifuge tubes and centrifuged for 10 minutes at 13,000 rpm in a microcentrifuge. The supernatant was transferred to a clean 1.5 ml centrifuge tube, diluted 2:5 with PEG/NaCl and incubated on ice for 10 minutes. The tubes were centrifuged at 13,000 rpm for 10 minutes and the supernatant discarded. The pellet was re-suspended in 200 μL iodide buffer (10 mM Tris pH 8.0 + 4 M NaI), 500 μL ethanol was added and the tubes incubated for 10 minutes at RT. The supernatant was discarded and the pellet washed in 70% ethanol before re-suspension in TBS pH 8.0. The DNA concentration of the sample was confirmed with a Nanodrop spectrophotometer reading absorbance at 260 nm. 8.8 μL of the DNA solution was added to thin walled PCT tubes (Greiner, Stonehouse, UK). 3.2 μL of -96 III primer (5´- ^{HO}CCC TCA TAG TTA GCG TAA CG –3', New England Biolabs) at a concentration of 1 pmol/L in distilled water was added to the tubes. Finally, 8 μL of BigDye terminator ready reaction mix (Applied Biosystems, Warrington, UK) was added and the PCR performed in a GeneAmp 9600 PCR cycler (Applied Biosystems). At the end of the cycle unincorporated dye terminators were removed by ispropanol precipitation: 20 μL of distilled water and 60 μL of isopropanol was added to each tube, mixed and incubated at RT for 15 minutes. The tubes were centrifuged for 20 minutes at 13,000 rpm and the supernatant removed. The DNA pellet was washed with 75% isopropanol and re-centrifuged. The supernatant was removed and the tubes stored at -20 ^{0}C until use.

The sequencing gel was prepared by adding 35 μL of N,N,N'N'-tetramethylethylenediamine and 250 μL of ammonium persulphate to 30 ml gel solution (5% polyacrylamide, 6 M urea) and pouring into a 36 cm glass plate cassette. A 36-lane comb was placed at the top of the gel after polymerisation and the cassette loaded into an ABI Prism 377 sequencer. The buffer tanks were filled with a tris-borate/ EDTA buffer (National diagnostics, Hessel, UK) and the pre-run sequence (preSeq Run 36E-1200) initiated. The sequencer, controlled remotely by a Macintosh power PC, was set for a 1200 scans/hour using the run

module, Seq Run 36E-1200, and dye set/primer (mobility) file, DT [BD Set Any-Primer], configured for the Filter Set E data collection.

The loading buffer was prepared by adding 400 µL of formamide and 100 µL of blue dextran (25 mM EDTA (pH8.0) with blue dextran (50 mg/mL), Perkin-Elmer). Once the plates had reached the optimal temperature the DNA samples were reconstituted in 3 µL of loading buffer and denatured by heating to 95°C for 2 minutes on a PCR cycler. The samples were kept on ice whilst the samples were loaded onto the gel. For each of the samples, 2 µL were loaded into the wells according to the corresponding description on the sample sheet. The 7-hour run module program (Seq Run 36E-1200) was initiated for the electrophoresis of the PCR products. The data generated for the laser scanned gel image was analysed by ABI Prism software and the complementary insert sequence was derived. For later studies the sequencing system was unavailable and the primer and DNA were therefore sent for sequencing by a third party (Cogenics, Takeley, Essex, UK).

The DNA sequence was then decoded for peptides using a website based translation utility (http:bio.lundberg.gu.se/edu/translat.html). The algorithm for translating the encoding DNA to the peptide sequence is described in Table 2.1.

	Clone 3.1
3'5' antisense sequence	GCA CAG ACG ATC ATG AGT CGA CTT ACA
Translated sequence	Cys Lys Ser Thr His Asp Arg Leu Cys

	Clone SC1
3'5' antisense sequence	GCA CTG CGG ATG AGA CCA CGT ACC ACA
Translated sequence	Cys Gly Thr Trp Ser His Pro Gln Cys

Table 2.1: PIII gene inserted sequences obtained by sequencing of phage clone DNA. The 3'5' antisense sequence was translated using the web-based translation tool at http://www.expasy.ch/tools/dna.html

2.2.5 ELISA of phage binding to candidate ligands

This method was used to determine the binding of phage to immobilised candidate ligands. Divalent cations were added to all buffers used in the ELISA experiments.

Buffers were made up for the ELISAs as follows

Binding buffer: 20 mM Tris-buffered saline pH 7.4 (20 mM Tris Base, 150 mM NaCl) containing 0.5 mM $MgCl_2$, 1 mM $MnCl_2$ and 1 mM $CaCl_2$

Wash buffer: Binding buffer + 0.1% Tween-20

Blocking buffer: Binding buffer + 2% bovine serum albumin (BSA) (VWR, Poole, UK)

Conjugate buffer: Wash buffer + 1% BSA

Recombinant ICAM-1 (R and D Systems), plasma fibronectin (Sigma) or streptavidin (Sigma) were dissolved to the required concentrations binding buffer and added to 96-well plates (Maxisorb, Nunc) and incubated overnight at 4^0 C. The plates were washed 4 times in wash buffer and then blocked with 200 μL blocking buffer for 2 hours at room temperature (RT). The plates were washed again 4 times and incubated with 50 μL phage at the required concentrations in conjugate buffer for 1 hour at RT. The plates were washed again 4 times in wash buffer and incubated with 50 μL HRP-conjugated anti-M13 antibody (Amersham

Biosciences, Amersham, UK) diluted 1:5,000 in conjugate buffer for 1 hour at RT. The substrate buffer was prepared by dissolving 1 tablet of 3,3',5,5'– Tetramethylbenzidine Dihydrochloride (TMB) (Sigma) in 10 ml 0.05 M phosphate-citrate buffer pH 5.0 with the addition of 2 μL of 30% H_2O_2 (Sigma) immediately prior to use. 50 μL of the substrate was added to each well and the colour allowed to develop. The reaction was stopped by the addition of 12.5 μL of 2 M H_2SO_4 and the absorbance at 450 nm read in an automated plate reader (Anthos Scientific Instruments, Salzburg, Austria).

2.2.6 In vivo distribution of phage

Phage were diluted from stocks titrated as above to 10^{11} pfu/ 200 μL 0.9% saline and kept on ice until use. SCID mice transplanted with human synovium and skin injected intragraft 6 or 18 hours previously with TNFα or 0.9% saline were injected intravenously via the tail vein with 10^{11}pfu of 3.1 or control phage and incubated for 15 minutes. Under terminal anaesthesia the chest cavity was exposed by an incision in the midline of the anterior chest wall and retracted with a clamp. The heart was cannulated via the left ventricle, an incision was made in the right atrium and the circulation perfused with 50 ml 0.9% saline. The transplanted tissues were retrieved and washed in sterile PBS before placing in sterile 7 mL plastic vials and storing at -20^0C. Tissues to be used for histology were immediately snap frozen in OCT in liquid nitrogen-cooled isopentane.

Extracted grafts were defrosted to room temperature, washed 3 times in TBS and weighed before homogenization in TBS containing protease inhibitor cocktail. 100 μL of homogenate was placed in a clean vial and the phage eluted by the addition of 200 μL 0.1 M glycine pH 2.0. After 2 minutes incubation the solution was neutralized by the addition of 12 μL 2 M tris base after which the solution was then diluted 1:10 or 1:100 in TBS containing 10 μL protease inhibitor cocktail/ 10mL and titrated onto IPTG/Xgal plates with *E.coli* host as detailed above. The plates were incubated overnight at 37 ^{0}C and individual plaques counted the following morning as detailed above.

At the end of experiments in which the transplants were required to be analysed histologically the transplants were placed in OCT and snap-frozen in liquid nitrogen-cooled isopentane and stored at -70 ^{0}C until needed

2.2.7 BLAST search for protein sequence matches with the synovial-homing peptide

In order to investigate whether the constrained peptide sequence expressed by the synovial-homing phage has any homology with known human proteins the peptide sequence was entered into the basic logic assignment search tool (BLAST) available at http://130.14.29.110/BLAST/. This tool searches for areas of sequence similarity between the reference sequence and registered protein sequences. The search was restricted to human proteins and modified to search for short sequences.

2.3 Immunohistochemistry and immunofluorescence staining

2.3.1 Immunohistochemistry protocols

Fresh human synovium or skin, murine tissues, *ex vivo* transplants of tissues transplanted into SCID mice and *ex vivo* tumour tissue were prepared for histology by embedding in OCT media and snap-freezing in liquid-nitrogen cooled isopentane. Frozen tissues were stored at -80 ^{0}C until required. OCT-embedded tissue was cut into 5 μm sections in a cryostat (Leica) and placed onto glass slides (Superfrost Plus, VWR, Poole, UK). Slides were dried overnight and frozen at -80^{0}C until required.

2.3.1.1 Anti-E-selectin/ CEA

For staining the slides were fixed in acetone at 4 ^{0}C for 10 minutes and blocked with serum-free protein block (Dako, Ely, UK) for 30 minutes at room temperature (RT). Slides were incubated in primary antibody (anti-CEA diluted 1:100 (from 1 mg/ml stock), anti-E-selectin diluted 1:200 (from 2 mg/ml stock) in antibody diluent (Dako)) for 1 hour at RT. The slides were washed in TBS pH 7.4

3 times and incubated with Envision HRP-conjugated anti-mouse/ rabbit polymer (Dako) for 30 minutes at RT. After a further 3 washes the HRP substrate DAB was added for 3 minutes and rinsed off. The slides were washed in TBS for 5 minutes and immersed in haematoxylin for 20 seconds before washing in distilled water for 3 minutes and tap water for a further 10 seconds. The sections were dehydrated and cleared by incubation for 2 minutes twice each in ethanol and xylene and mounted with Depex mounting medium (VWR).

2.3.1.2 Staining for human von Willebrand factor and murine CD31

For quantification of total vascularisation of transplanted human skin and synovium and murine organs tissues were double-stained for the species-specific vascular endothelial markers human von Willebrand Factor (vWF) and murine CD31.

Slides were defrosted and fixed in acetone for 10 minutes at 4^0 C. After air-drying the slides were rehydrated in TBS and blocked with biotin block (Dako) according to the manufacturer's instructions. The slides were then washed twice in TBS for 5 minutes each and blocked with serum-free protein block (Dako) for 30 minutes at RT. The slides were blotted dry and incubated with the primary antibodies-anti-human vWF (Dako, clone F8/86) 1:300 and biotinylated anti-murine CD31 (clone MEC 13.3, BD Pharmingen, Oxford, UK) 1:400, diluted in antibody diluent (Dako) for 1 hour at RT. At the end of the incubation the slides were jet-washed with TBS and washed twice in TBS as before. The slides were incubated with biotinylated rabbit anti-mouse antibody (Dako, clone E0464) diluted 1:300 in antibody diluent for a further 30 minutes at RT followed by horseradish peroxidase-conjugated avidin-biotin complex (Dako) for 30 minutes. The slides were washed again and incubated with the HRP substrate diaminobenzidine (DAB) (Dako) for 3 minutes. After washing the slides were counterstained by immersion in haematoxylin for 20 seconds and washed for 3 minutes in distilled water and 10 seconds in tap water. The slides were dehydrated by incubation for 5

minutes in 2 changes of ethanol and cleared by incubation in 2 changes of xylene, followed by immediate mounting in DePEX.

2.3.1.3 Staining of *ex vivo* A375P tumours for murine CD31 and $\alpha_v\beta_3$

Tissue sections were prepared for staining as above. Slides were removed from storage and allowed to come to room temperature after which they were fixed in acetone at 4 ^{0}C and blocked with biotin blocking solutions followed by protein block as in the previous sections. The slides were incubated with the primary antibodies biotinylated anti-murine CD31 (as above), anti- human $\alpha_v\beta_3$ (Chemicon, clone LM609) diluted 1:200 or murine IgG_1 isotype control. After washing the anti-$\alpha_v\beta_3$ treated sections were incubated with the secondary antibody biotinylated rabbit anti-mouse immunoglobulins (Dako, clone E0464) diluted 1:300 for 30 minutes. After washing the sections were incubated with alkaline phosphate-conjugated avidin biotin complex (Dako) for 30 minutes followed by the alkaline phosphatase reagent Vector Red (Vector Laboratories, Peterborough, UK) for 20 minutes, made up in Tris-HCl pH 8.2 according to the manufacturers instructions, to which was added 50mg/ml levamisole (Sigma). After a further wash the slides were counterstained as previously and mounted with VectaMount (Vector Laboratories).

2.3.2 Immunofluorescence

2.3.2.1 Preparation of MOWIOL mounting media

6 g glycerol (Sigma) was added to 2.4 g Mowiol 4-88 (Calbiochem, Darmstadt, Germany) in 6 ml double-distilled water with 12 ml 0.2M Tris buffer pH 8.5. (Calbiochem, Darmstadt, Germany) and mixed for 24 hours at RT on a magnetic stirrer. The solution was heated to and held at 50 ^{0}C for 10 minutes after which it was centrifuged for 15 minutes at 5,000 g. The supernatant was decanted and stored in aliquots at -20 ^{0}C until needed.

2.3.2.2 Immunofluorescent staining for M13 phage

Transplant sections from mice injected intravenously with phage were stained for M13 phage with counterstaining for human vessels as follows:

Tissue sections were prepared as for previous experiments and fixed in acetone at 4^0C for 10 minutes. After air drying the slides were blocked with serum-free protein block (Dako) for 30 minutes at RT and then incubated with the primary murine anti-M13 antibody (Serotec, clone MCA1858R) diluted 1:400 for 1 hour at RT. The slides were washed 3 times in TBS and then incubated with biotinylated rabbit anti-mouse (Dako, as above) diluted 1:300 for 30 minutes. After washing the slides were incubated with Alexa Fluor 555-conjugated streptavidin (Molecular Probes, Invitrogen, Paisley, UK) 10 μg/ml for 30 minutes and washed. The sections were counterstained for human vWF by incubation with FITC-conjugated sheep anti-human vWF (Serotec, AHPO62F) diluted 1:100 for 30 minutes. After a final wash the slides were mounted with MOWIOL mounting media supplemented with 90 mg/ml diazobicyclo-octane (DABCO) (Sigma).

2.3.2.3 Immunofluorescent staining for ICAM-1and E-selectin

Ex vivo transplants +/- TNFα pre-stimulation were stained for the adhesion molecules ICAM-1 and E-selectin using the primary antibodies synthesized from hybridoma supernatants as described above. The dilutions used were 0.2 μg/ml and 1 μg/ml for the anti-ICAM-1 anti E-selectin antibodies respectively. The protocol was otherwise as for M13 staining.

For the quantification of the endothelial expression of E-selectin representative sections of grafts treated with TNFα or saline control were examined. 2 tissue sections from each experimental condition were examined at 3 different cutting levels: a minimum of 150 human vessels were identified from each tissue sample and the number with positive vessels staining for E-selectin determined. Expression of ICAM-1, which after TNFα stimulation is expressed widely in transplanted synovial tissue, was determined by examining tissue from 2-3 cutting levels in 2 tissue sections from each condition: a minimum of 35 fields were examined from each tissue and scored on an arbitrary scale from 0 (no expression)

to 3 (widespread expression). Representative sections were scored independently by a second blinded observer: inter-observer error was found to be <5%.

2.3.2.4 Immunofluorescent staining for human and murine vascular endothelium

In order to visualize anastomoses between the human and murine circulations immunofluorescent staining was carried out as follows (unless specified all incubation were carried out at room temperature). Frozen 5 μm sections of *ex vivo* synovium and skin grafts were allowed to defrost before fixing in acetone at 4^0C for 10 minutes. The slides were allowed to air dry and the sections encircled with a wax pen in order to prevent spillage of the staining reagents. The sections were blocked by incubation with 100 μl serum-free protein block for 30 minutes after which the slides were blotted dry. The sections were stained for murine CD31 by incubation with 50 μl biotinylated anti-murine CD31 antibody (clone MEC13.3, BD Pharmingen) diluted 1:100 in Dako antibody diluent for 1 hour. The slides were jet washed with TBS and washed twice more for 5 minutes each and incubated with 50μL streptavidin-conjugated Alexa 555 (Invitrogen) diluted 1:200 for 1 hour. After washing as before 50 μl of sheep antihuman vWF (Serotec) diluted 1:100 was added and incubated for 30 minutes at RT. After a final wash the slides were mounted in MOWIOL media as before.

2.4 Recombinant antibody production from hybridoma cell culture and purification

Anti ICAM-1 (6.5B6) and E-selectin (1.2B6) antibodies for use in immunohistochemical staining and, with anti-E-selectin, for *in vivo* imaging experiments were produced from hybridoma cell cultures as detailed below.

2.4.1 Preparation of cell culture media

Media for hybridoma cells was prepared by adding 4.5 mg/ml L-glutamine and penicillin/ streptomycin to 10% FCS in RPMI medium.

2.4.2 Maintenance of hybridoma cells

Hybridoma cells were defrosted from liquid nitrogen-stored stocks and added to cell-culture media as above. Initially 6.5B6 cells were grown in smaller volume 25 cm^2 culture flasks (Corning) before transfer on reaching sufficient density to 75 cm^2 and 150 cm^2 flasks. The cells were split on reaching sufficient density by centrifugation and re-suspension in twice the original volume before decanting into 2 new flasks. Prior to antibody purification the cells were incubated and grown to maximum density prior to termination of the incubation.

1.2B6 hybridomas were grown using a different method using a Bioreactor as follows: the Bioreactor hybridoma incubation system (Celline, Integra Biosciences, Switzerland) consists of two chambers- a small lower chamber in which the cell suspension is placed with a larger (1L) upper compartment for cell culture media. Their compartments are separated by a 10 kDa cutoff semi-permeable membrane: this allows the diffusion of smaller molecules between compartments with the retention of larger molecules and particles, including secreted immunoglobulin and cells, in the lower compartment. The lower compartment is lined by a silicon membrane which allows diffusion of O_2 and CO_2. The upper compartment was pre-equilibrated with 50ml of culture media for 10 minutes after which 15ml of media containing $>1.5x10^6$ hybridoma cells/ml. The upper compartment was filled with 1 L of media. After 7 days the media was decanted from the upper compartment and the cell suspension aspirated from the lower compartment: 3 ml of this was diluted to 15 ml and returned to the chamber fresh media placed in the upper compartment. The retained cell suspension was immediately centrifuged as above and the supernatant frozen until required.

2.4.3 Purification of antibody from hybridoma supernatant

Two methods were used for the purification of antibody from the hybridoma supernatants, depending on the original supernatant volume.

2.4.3.1 Purification of 6.5B6 (anti ICAM-1) antibody

The cell culture medium containing hybridoma cells suspension was poured into 50 ml centrifuge tubes and centrifuged at 600 g for 10 minutes. A saturated

solution of ammonium sulphate was made up by adding ammonium sulphate to de-ionised water in a glass flask on a heated magnetic stirrer. The saturated solution was filtered by passing through filter paper (Whatman No. 1, Whatman, Maidstone, UK) and was then added 1:1 to the supernatant in 50 ml centrifuge tubes and incubated overnight at 4^0 C. The tubes were centrifuged for 30 minutes at 1850 g and the supernatant discarded. The pellet of precipitated protein containing the immunoglobulin fraction was resuspended in 20 mM PBS pH 7.0 and transferred to prepared 12-14,000 mw cut-off dialysis tubing (VWR). The solution was dialysed against three changes of PBS, the last overnight at 4^0C. The antibody was purified from the dialysed solution by affinity chromatography using a protein G column (Hi-Trap, Amersham Biosciences), protein G having high affinity for murine IgG_1. The 5 ml column was prepared by washing with 10 column-volumes of 20 mM PBS pH 7.0 followed by the dialyte containing the antibody. The column was washed with a further 10 column volumes of PBS and the bound antibody then eluted with 0.1 M glycine-HCl pH 2.7. 2.5 ml fractions were collected in sterile tubes containing 0.25 ml 1 M Tris-HCl pH 9.0 to neutralize the acid. The antibody concentration was measured by spectrophotometric absorbance at 280 nm and the aliquots were then frozen at -20 ^{0}C until required.

2.4.3.2 Purification of 1.2B6 (anti E-selectin) antibody

As the 1.2B6 (anti-E-selectin) hybridomas were cultured in bioreactors the volume of the supernatant was smaller and hence the following method was used to purify antibody: hybridoma supernatant was centrifuged at 2,400 g for 10 minutes in 50 ml centrifuge tubes and the supernatant was decanted, passed through a 0.2 μm filter and transferred to a 15 ml ultracentrifuge unit with a 10,000 Da molecular weight cut-off filter. The solution was centrifuged from an initial volume of 15 ml until reduced to1-2 ml, diluted up to 15 ml with 20 mM sodium phosphate buffer pH 7.0 (loading buffer) and repeated. The final purification step using the Protein G affinity column was as described above.

2.4.4 Radiolabelling of antibodies and in vivo imaging with NanoSPECT/CT

The aim of these experiments was to determine whether the NanoSPECT/CT system could be used to image specific uptake of radiolabelled anti E-selectin (1.2B6) antibody into transplanted human synovial tissue. Anti-human chorioembryonic antigen (CEA) for use as an isotype control was obtained from the Biotherapeutics Development Laboratory at Cancer Research UK.

2.4.5 Conjugation of antibodies to DTPA

In order to enable labelling of the antibodies with ^{111}In the antibodies were conjugated to the bifunctional chelating agent diethylenetriaminepentaacetic acid (DTPA) using the method of Cooper *et al* (Cooper, Sabbah, & Mather 2006). The isocyanatobenzyl group of isocyanatobenzyl-DTPA (Macrocyclics, Dallas, TX) reacts with amino side chains within the protein to form a covalent bond. The product is stable for prolonged periods when stored at -20^0 C. 5 mg of antibody in was diluted to 5-10 ml in ultrapure H_2O and pipetted into an ultrafiltration tube with a molecular weight cut-off of 10,000 Daltons (Amicon, Millipore, Watford, UK). In order to remove contaminating metal ions 50 μL of 0.1 M ammonium acetate buffer pH 6.0 (containing 300 μL/L acetic acid) + 50 mM EDTA was added per 10 mg of antibody and the solution incubated for 30 minutes at RT. The tube was centrifuged at 1360 g until the volume had reduced by 2-3-fold and the solution was then diluted to 15 ml with 0.1 M HEPES buffer pH 8.5. This was repeated 3 times and the solution was then transferred to a metal-free plastic tube (Cryovial, Nunc) after the pH had been checked to be 8.5. SCN-Bn-DTPA was prepared by dissolving 50 mg/ml in absolute ethanol: the absorbance of the antibody solution was read at 280 nm in a spectrophotometer and the antibody concentration derived. SCN-Bn-DTPA was added to give a 50-fold molar excess over the antibody and the reaction mixture was incubated at 4 ^{0}C overnight. The following day the retained ultrafiltration tube was rinsed with 0.1 M ammonium acetate pH 6.0 and the reaction mixture added, following which it was diluted to 15 ml with ammonium acetate buffer. The tube was centrifuged until the volume had reduced ~3-fold: this step was repeated until the spectrophotometric absorbance of the ultrafiltrate was zero indicating removal of unconjugated SCN-

Bn-DTPA. The absorbance of the protein solution was read at 280 nm in order to determine the concentration; the solution was sterile filtered using a 0.2 μm syringe filter and the final solution stored in aliquots at -20^0 C.

2.4.5.1 Determination of antibody immunoreactivity by ELISA

In order to confirm the specificity of purified antibody for ligand (E-selectin or ICAM-1) the binding affinity was tested by ELISA. The ligand was dissolved in PBS pH 7.4 at the specified concentrations, 50 μL was added per well of a 96-well plate (Maxisorb, Nunc) and the plate incubated overnight at 4^0 C. The following day the plate was washed 4 times with PBS containing 0.05% Tween-20 (Sigma) and blocked by incubating for 2 hours at RT with 2% bovine serum albumin (BSA) (VWR, Poole, UK) in PBS. The purified antibody and control antibodies were diluted 1:1,000 in PBS+1% BSA and 50 μL added to wells with a further 1 hour incubation at RT. The plate was washed again and the wells incubated with 50 μL HRP-conjugated goat anti-mouse antibody (Dako) diluted 1:10,000 in PBSA + 1% BSA for 1 hour at RT and washed again 4 times before being allowed to air-dry. The substrate buffer was prepared by dissolving 1 tablet of 3,3',5,5'–Tetramethylbenzidine Dihydrochloride (TMB) in 10 ml 0.05 M phosphate-citrate buffer pH 5.0 with the addition of 2 μL of 30% H_2O_2 immediately prior to use. 50 μL of the substrate was added to each well and the colour allowed to develop. The reaction was stopped by the addition of 12.5 μL of 2 M H_2SO_4 and the absorbance at 450 nm read in an automated plate reader (Anthos Scientific Instruments, Salzburg, Austria).

2.4.6 Radiolabelling of antibodies

DTPA-conjugated protein was diluted from the concentrated stock to the desired concentration in ammonium acetate buffer pH 6.0. A volume of $^{111}InCl_3$ in 0.05 M HCl of known activity was added in a volume not exceeding 20% of the total reaction volume. After incubation for 30 minutes at RT free ^{111}In was chelated by the addition of 10% volume 50 mM EDTA in 0.1M ammonium acetate pH6.0. The reaction mixture was incubated for a further 5 minutes at RT following which the labelling efficiency was determined by size-exclusion high-performance liquid chromatography (SE-HPLC) or instant thin-layer chromatography (ITLC) with

ammonium acetate buffer pH 6.0 as the solvent as detailed previously. If required, the antibody was purified with 0.5 ml Zeba spin columns (Pierce, Cramlington, UK) pre-equilibrated with sterile PBS according to the manufacturer's instructions. If the product was to be used for further experiments it was stored at 4-8 ^{0}C until use.

2.4.7 NanoSPECT/CT imaging of transplanted SCID mice

Single photon emission computed tomography (SPECT) is a scanning technique which uses mobile gamma camera to acquire images from multiple degrees of rotation around the subject. The use of multi-pinhole collimators allows much greater resolution images to be obtained; simultaneous computed tomography (CT) scanning allows the acquisition of matched CT and SPECT images which can then be fused to from 3D reconstructed images showing areas of uptake of an administered radiotracer. For these experiments a NanoSPECT/CT small animal imaging system was used (Bioscan, Washington, DC); this system employs an array of 4 multi-pinhole collimators in parallel with CT scanning in order to produce high resolution images of excellent quality. Proprietary software is used to construct 3-dimensional CT/SPECT fusion images which allow quantification of radioactivity within defined regions of interest (ROI).

Prior to scanning mice were anaesthetised in an anaesthetic chamber with an in-flow of 4% halothane, 1.5 L/min O_2 and 0.8 L/min N_2O_2 from a Boyle's apparatus. After induction anaesthesia was maintained with 2% halothane. The mouse was transferred to a bed kept at 37 ^{0}C on a gantry for imaging: gas anaesthesia was maintained for the duration of the scan. After acquisition of a CT topogram the region for scanning acquisition was defined (typically full body or the region of the transplants only). The full scanning protocol was commenced with CT scan followed by in-line SPECT with a minimum acquisition of 30,000 counts per projection. At the end of the scan mice were allowed to recover: for the final scan of the series the mice were killed by intra-peritoneal injection of Sagatal prior to the scan. At the end of the study tissues and transplants were retrieved for weighing and measurement of radioactivity in a gamma counter. At the end of the

study tissues and transplants were retrieved for weighing and measurement of radioactivity in a gamma counter (LKB Wallac Compugamma 1282, Perkin Elmer, Beaconsfield, UK). The absolute activity was corrected for the graft weight and injected dose and the results expressed as the % of injected activity per gram of tissue.

2.5 Radiolabelling and biodistribution of synthetic peptides

Peptides of the same structure as those expressed by synovial-homing (3.1) phage and streptavidin-binding phage (as a negative control) were synthesized with the addition of various tags for visualisation by fluorescent microscopy or to enable radiolabelling. The sequences of the peptides used in this project are shown in Table 2.2.

Peptide name	Sequence
3.1 (synovial homing peptide)	CKSTHDRLC
s3.1 (scrambled 3.1)	CLTKRSHDC
RGD2C	CSPRGDHPC
sRGD2C (scrambled RGD2C)	CDPRPHSGC
SC7 (streptavidin-binding sequence)	CGRYDHPQC

Table 2.2: The sequence of phage-derived peptides used in this project. For translation of the single-letter amino acid code see appendix 1

2.5.1 Solid-phase peptide synthesis

Some (FITC, DTPA and HYNIC-conjugated peptides) were synthesized in-house in the Department of Pharmacy, others (HYNIC and biotin-conjugated) were obtained according to our specifications from Genscript (Piscataway, NJ) and Peptide Protein Research (Wixkham, Hampshire, UK). When synthesized in-house, the majority of this work was done by Dr Sukhi Bansal, Miss Katherine Segklia and Dr Lewis Lee. Peptides were produced by solid-phase synthesis using an automated synthesizer or manually using 9-fluorenylmethyloxycarbonyl

(fMOC) for temporary amino side-chain protection. The synthesis was carried out in 1000 Å pore sized control glass pore columns using O-Benzotriazole-N,N,N',N'-tetramethyl-uronium-hexafluoro-phosphate (HBTU, Applied Biosystems) as the coupling reagent. A 6-carbon spacer (6-aminohexanoic acid) was conjugated to the N-terminus prior to the addition of the labelling group. Except for DTPA, other groups (FITC, biotin and HYNIC) were conjugated to the peptide whilst on the solid phase. The peptides were cleaved off the column using a mixture of 90% trifluoroacetic acid/water, precipitated in ice-cold diethylether and then filtered through a sintered glass funnel under vacuum. The peptide precipitate was dissolved in 10% acetic acid/water and purified to >90% by reverse phase high performance liquid chromatography (HPLC, Gilson, Wien, Austria) using a 300 Å pore sized C18 column (Vydac, Hesperia, USA) and eluted with 0.05% trifluoroacetic acid (BDH) and 60% acetonitrile (BDH). The final product was freeze-dried for long-term stability. Purity was confirmed as >95% for all peptides by reverse-phase high-performance liquid chromatography and the expected molecular weight confirmed by mass spectrometry as detailed below.

2.5.2 Mass spectrometry

Peptides produced in-house were analysed by matrix-assisted laser desorption/ionization time-of-flight (MALDI-TOF) mass spectrometry to quantify molecular weight. The sample was prepared by adding 1 µl of peptide to 1 µl of a saturated solution of α-cyano-4-hydroxycinnamic acid in 50% acetonitrile + 50% m0.1% TFA and analysed with a Bruker Autoflex MALDI-TOF MS system (Bruker Daltonics, Coventry, UK).

2.5.2.1 Staining of synovial tissue sections with fluorochrome-conjugated peptides

In these experiments peptides conjugated to the fluorochromes FITC or carboxyfluorescein were assessed for binding to synovial tissue sections from patients with OA or RA. The control sequence used was the streptavidin-binding sequence described in Table 2.1. Peptides were diluted in TBS to the indicated

concentration. Fluorescence of the peptide solution was quantified by pipetting 10 μL into a haemocytometer and measuring the fluorescence intensity with the fluorescence microscope at 10x magnification. If required, adjustments were made to the stock dilution to ensure equal fluorescence intensity for the test and control peptides. Tissues were fixed in ice-cold acetone or 2.5% paraformaldehyde in PBS at RT for 10 minutes. Tissues fixed in paraformaldehyde were then incubated in 0.1% sodium borohydride on PBS in a fume hood for 20 minutes at RT to minimize background autofluorescence: these slides were then washed twice for 5 minutes each in TBS. The slides were blocked for non-specific protein binding by incubation with 0.1% bovine serum albumin for 30 minutes at RT. The blocking solution was tapped off and the peptide solutions at various concentrations were added to the tissue sections and incubated for 1 hour at RT. The slides were jet washed with TBS and washed 2 further times in TBS. The sections were counterstained for human vessels by incubation with murine anti-human von Willebrand factor monoclonal antibody (Dako clone F8/86) diluted 1:80 in TBS + 0.1% BSA for 1 hour at RT followed by washing as before. The TRITC-conjugated secondary antibody goat anti-mouse immunoglobulins (Dako) was diluted 1:50 in TBS and incubated on the slides for 30 minutes before further washing. Finally the slides were mounted with MOWIOL mounting media containing 90 mg/ml DABCO. The slides were examined on an Olympus fluorescence microscope: human vessels were identified by staining for von Willebrand Factor and assessed visually for intensity of peptide staining.

Fluorescence intensity of vessel staining was also quantified by digital analysis. Using proprietary software (Cell-P, Olympus) a digital mask was created to exclude areas of tissue not staining for vWF. Fluorescence intensity of these areas in the FITC spectrum was measured on an arbitrary scale. Multiple tissue fields were examined at 20x magnification.

2.5.3 Radiolabelling of peptide with ^{111}In

Lyophilised DTPA-conjugated peptide stored at 20 ^{0}C was allowed to equilibrate to room temperature and dissolved to 1 mg/ml in double-distilled water. $^{111}InCl_3$

in 0.05 M HCl (Mallinckrodt Medical, Gosport, Hampshire, UK) was diluted 1:1 with 1 M sodium acetate solution to which was added the required volume of peptide solution. The labelling reaction was allowed to proceed at room temperature for 15 minutes. Labelling efficiency was assessed by instant thin-layer chromatography (ITLC) was follows: a sample (~1 μl) of the labelling solution was spotted onto a 10 cm silica gel strip (Pall Life Sciences, Ann Arbor, MI) at a point 1.5 cm from one end and placed in a glass beaker containing a small volume of acid citrate dextrose (4 g citric acid, 12.8 g trisodium citrate dehydrate and 6 g dextrose in 500 ml H_2O) and allowed to run until the solvent had reached the upper border of the strip. With this technique unbound indium migrates with the solvent front (Rf=1.0) whilst indium bound to peptide remains at the solvent front (Rf= 0). Strips were allowed to dry, cut into sections and the activity counted in a well-type gamma counter (LKB Wallac Compugamma 1282, Perkin Elmer, Beaconsfield, UK).

For *in vivo* biodistribution studies SCID mice were double-transplanted with human synovium and skin as previously described and the experiments were performed 2-4 weeks post-transplantation. The DTPA-peptide was radiolabelled as detailed above with ITLC performed prior to use to confirm acceptable radiolabelling and the radiolabelling solution was diluted with 0.9% saline to a final injection volume of 200 μl. Mice were injected with the radiolabelled peptide via the tail vein and incubated for 15 minutes. Under terminal anaesthesia the thoracic cavity was exposed and the circulation perfused with 50 ml 0.9% saline as previously described. Organs and transplanted tissues were removed and placed into pre-weighed plastic vials: these were weighed again in order to determine the tissue weight and the radioactivity measured in a gamma counter. Samples of the injected dose were also counted in triplicate.

For the preliminary study animals were injected with test peptide or unconjugated indium; for subsequent studies the SC7 peptide was used as control. In two experiments grafts were pre-stimulated by the intragraft injection of rhTNFα or

saline control; this was carried out as detailed previously. The biodistribution experiments were carried out 6 hours post-intragraft injection.

2.5.4 Radiolabelling of peptide with ^{99m}Tc

Peptide conjugated to the bifunctional chelating agent HYNIC was conjugated to technetium using different co-ligands as detailed below

2.5.4.1 Tricine as co-ligand

Method 1: HYNIC-peptide was equilibrated to room temperature and dissolved to a concentration of 1 mg/ml in double-distilled H_2O. In a screw-top cryovial (Corning) 10 µl peptide was added to 0.5 ml tricine (100 mg/ml in 25 mM succinic acid buffer) with ~50µl $^{99m}TcO_4^-$ (~10 MBq) and 25 µL $SnCl_2$ (10 mg in 10 ml 0.1 M HCl) and incubated for 45 minutes at room temperature. ITLC was run as described in section 2.6.5 with three different solvents: PBS was used to separate free from bound $^{99m}TcO_4^-$, 2-butanone to separate ^{99m}Tc-tricine and 50% acetonitrile to determine the amount of insoluble ^{99m}Tc colloid (Decristoforo & Mather 1999b).

Method 2: 5 µg of peptide (1 mg/ml in water) was added to 0.25 ml of tricine (100 mg/ml in water). 100 µl of $^{99m}TcO_4^-$ (~100MBq) was added followed by 5 µl $SnCl_2$ (3mg/ml in absolute ethanol). The reaction was incubated for 30 minutes at room temperature.

2.5.4.2 Ethylenediaminediacetic acid (EDDA) as co-ligand

5µl of peptide (1mg/ml in H_2O) was incubated with 0.125 ml 0.3 M Na_2HPO_4 and 0.125 ml EDDA solution (10 mg/ml in 0.1 M NaOH), 100 µl of $^{99m}TcO_4^-$ (~100 MBq) and 5 µl $SnCl_2$ (3 mg/ml in absolute ethanol). The reaction mixture was incubated for 30 minutes at 95 ^{0}C on a dry heating block.

2.5.4.3 EDDA + tricine as co-ligands

5 µl of peptide (1 mg/ml in H_2O) was incubated with 0.125 ml tricine solution (20 mg/ml in 0.3 M Na_2HPO_4), 0.125 ml EDDA solution (10 mg/ml in 0.1 M NaOH),

100 µl of $^{99m}TcO_4^-$ (~100 MBq) and 5 µl $SnCl_2$ (3 mg/ml in absolute ethanol). The reaction mixture was incubated for 30 minutes at 95 ^{0}C on a dry heating block.

2.5.4.4 Tricine + nicotinic acid as co-ligands

5 µl of peptide (1 mg/ml in H_2O) was incubated with 0.2 ml tricine solution (100 mg/ml in H_2O), 0.05 ml nicotinic acid solution (90 mg/ml in H_2O), 100 µl of $^{99m}TcO_4^-$ (~100 MBq) and 5 µl $SnCl_2$ (3 mg/ml in absolute ethanol). The reaction mixture was incubated for 30 minutes at 95 ^{0}C on a dry heating block.

2.5.5 Instant thin-layer chromatography

For indium-labelled antibodies ITLC was run on silica-gel ITLC strips (Pall Life Sciences, Ann Arbor, MI) with 0.1 M ammonium acetate pH 6.0 + 50 mM EDTA as solvent: strips were imaged using a Cyclone storage phosphor system (Perkin Elmer, Beaconsfield, UK) and the proportion of ^{111}In at the origin (bound) and at the solvent front (unbound) determined using proprietary software. As an alternative to imaging the strips were cut in half and the activity on the pieces containing the origin or solvent front counted in a gamma counter. For ^{99m}Tc-labelled peptides the solvents used were saline, 2-butanone and 50% acetonitrile for separation of free ^{99m}Tc/ chelator, $^{99m}TcO_4^-$ and ^{99m}Tc colloid respectively.

2.5.6 High-performance liquid chromatography (HPLC)

2.5.6.1 Reverse-phase HPLC

Analysis of radiolabelled peptides was performed using RP-HPLC using a Beckman System Gold (Beckman Coulter, High Wycombe, UK) running proprietary 24 Karat software with an in-line UV detector (Beckman 168) and GABI radioactivity monitor (Raytest, Straubenhart, Germany) with a 250x4.6 mm 5 micron C18 column (Phenemonex, Macclesfield, UK). The solvents used were 0.1% trifluoroacetic acid (TFA) and 0.1% TFA acetonitrile: the method used a gradient of 0-60% acetonitrile over 20 minutes after a 5 minute run-in time with a flow rate of 1 ml/min.

2.5.6.2 Size-exclusion HPLC

Radiolabelling of antibodies and proteins was performed with size-exclusion chromatography: the pump and detector systems were identical to those for RP-HPLC. A Biosep-sec-s 2000 column was used (Phenomenex) with isocratic 0.1 M phosphate buffer pH 7 + 2 mM EDTA with or without 10% ethanol as the running solvent.

2.5.7 Serum stability

Serum stability and protein binding were analysed using previously published methods (King et al. 2007). Serum was prepared by obtaining blood by cardiac puncture from SCID mice under terminal anaesthesia, allowing it to clot and centrifuging. To assess the stability of ^{99m}Tc-labelled peptides in serum 50 µl of ^{99m}Tc-peptide was added to 200 µl of serum and incubated at 37 ^{0}C. At 1 and 4 hours 40 µl of the sample was removed and mixed with 100 µl acetonitrile in a 1.5 ml centrifuge tube to precipitate the serum proteins. The tube was centrifuged for 5 minutes at 6,500 rpm in a microcentrifuge and the supernatant, containing non-protein bound peptide and free ^{99m}Tc, analysed by RP-HPLC.

2.5.8 Protein binding

Binding of peptide to serum proteins was assessed by filtration in sephadex size-exclusion spin columns. G-50 columns (Amersham Healthcare, Amersham, UK) were prepared by centrifuging at 2,000 g for 1 minute. 10 µl of serum was added to the top of the resin and the column spun at 2,000 g for a further 2 minutes. The activity of the retentate and filtrate, representing non-protein bound and protein bound fractions respectively, were measured in a gamma counter.

2.5.9 Peptide biodistribution studies

Peptide was radiolabelled as described. 2-4 weeks after transplantation with synovium and skin (2 transplants of each) mice were injected via the tail vein with radiolabelled peptide in 100-200 µl buffer. Mice were incubated for the indicated periods. At the end of the incubation period sodium pentobarbitone (Euthatal, Rhoen Merieux, Toulouse, France) was injected into the peritoneum: once under

terminal anaesthesia, if the circulation was to be perfused, the thoracic cavity was exposed and the circulation perfused via the left ventricle with 50 ml of 0.9% saline. Transplants, blood and tissues were removed and placed in pre-weighed vials. The vials were weighed again to determine the weight of the tissues and the activity measured in a gamma counter (Compugamma). When indicated, mice were co-injected with a 1000-fold excess of cold peptide as a block.

2.6 *In vitro* cell adhesion assays and growth of melanoma cells *in vivo*

For experiments in which binding of peptide or protein ligands to $\alpha_v\beta_3$ was tested cell lines expressing $\alpha_v\beta_3$ were used. The MCF7 β3 cell line is a human breast carcinoma cell line that has been stably transfected with the β_3 integrin subunit and hence expresses $\alpha_v\beta_3$ on the cell surface (Pereira et al. 2004). These cells were used to validate the initial assays. However, they do not form xenograft tumours and therefore for later experiments the alternative A375P cell line was used. These are immortalised melanoma cells which express $\alpha_v\beta_3$ in their native form and form tumours when injected into immunodeficient mice. Both cell lines were kind gifts from Dr John Marshall (Cancer Research UK).

2.6.1 Preparation of cell culture media

Cell culture media was prepared as follows

2.6.1.1 MCF7 cells

Dulbecco's Modified Eagles' Medium (DMEM)(Sigma) containing 10% Fetal Calf Serum (Sigma), 5 ml penicillin and streptomycin (10,000 units Penicillin V and 5 mg streptomycin/ml) (Sigma), 4.5 g/L L-glutamine (Sigma) and 1 ml 10 mg/ml insulin (Sigma) in 1% acetic acid.

2.6.1.2 A375P cells

DMEM containing 10% FCS, 5 ml penicillin and streptomycin (10,000 units Penicillin V and 5 mg streptomycin/ml), 4.5 g/L L-glutamine.

2.6.2 Maintenance of MCF7 and melanoma cell lines

Cell lines were defrosted from frozen stocks (in 10% DMSO, 10% fetal calf serum in Dulbecco Modified Eagles Medium (DMEM) (Sigma)). The defrosted cell suspension was washed in cell culture medium in a 50 ml centrifuge tube followed by centrifugation at 220 g for 5 minutes. The cells were re-suspended in fresh media and 20 ml was poured into 75 cm^2 culture flasks (Corning). Flasks were incubated at 37 ^{0}C with 5% CO_2 in humidified incubator at 37 ^{0}C. When the cells reached ~90 % confluency they were split as follows: media was decanted from the flasks which were then washed twice with sterile PBS (Cambrex). 3 ml 0.05% EDTA (Sigma) was poured into the flasks and incubated for 5 minutes at 37 ^{0}C. The flasks were tapped several times in order to ensure maximal cell detachment: the cell suspension was transferred to a sterile 50 ml centrifuge tube containing PBS and centrifuged as above. The supernatant was discarded and the cells re-suspended in 20 ml of fresh media before transfer into fresh culture flasks.

2.6.3 FACS analysis of $\alpha_v\beta_3$ expression

Sub-confluent cells were washed and detached from flasks as described in section 2.2.2. The cells were washed three times in sterile PBS and re-suspended in FACS buffer (10 mM PBS or 20 mM TBS + 0.1% azide + 1% BSA) at a concentration of 10^6/ml. 100 μl of the cell suspension was transferred to FACS tubes and centrifuged at 250 g for 3 minutes: the cells were re-suspended in FACS buffer and washed again. After washing the supernatant was discarded from the tubes and the cells re-suspended in the remaining FACS buffer (~100 μL). 100 μL of anti-$\alpha_v\beta_3$ antibody clone LM609 (Chemicon, Chandler's Ford, Hampshire) diluted to 10 μg/ml was added and mixed before incubating on ice for 40 minutes. At the end of the incubation the cells were washed twice in FACS buffer. 100 μL of Alexa Fluor 488-conjugated goat $F(ab')_2$ anti-murine IgG_1 (Molecular Probes) diluted to 5 μg/ml was added and the cells incubated for a further 30 minutes on ice. The cells were then washed again twice and re-suspended in 300 μL of 1% paraformaldehyde in PBS. FACS analysis was performed using a FACSCalibur system (Becton Dickinson) controlled by an Apple Macintosh PC running CellQuest software (Becton Dickinson).

2.6.4 Tumour growth *in vivo*

To assess the capacity of RGD-coated microspheres to home to cells expressing $\alpha_v\beta_3$ *in vivo* a tumour model was utilised. The A375P cell is an immortalised human melanoma cell line which constitutively expresses $\alpha_v\beta_3$. Initial experiments were performed in which the cells were suspended in Matrigel (BD Biosciences): tumours grew well reaching 0.5-1 cm after 3 weeks and $\alpha_v\beta_3$ expression was confirmed by histological analysis. Supplies of Matrigel, however, became problematic due to a recall by the manufacturer and therefore the model was adapted as follows.

A375P cells were grown to sub-confluence in 75cm^2 flasks and detached by incubation with 0.05% EDTA for 5 minutes. The cells were washed 3 times in serum-free media and resuspended in media at a concentration of 1-2 x 10^6 cells in 200 µl. 200 µl of cells were injected subcutaneously into the dorsum of SCID mice. The mice were used for further experiments when the tumours had reached 0.5-1 cm diameter.

2.7 Development of tetrameric peptide-streptavidin conjugate

2.7.1 Biotinylation of cRGDyK peptide

For some of the experiments in this section a commercially available cRGDyK peptide (Peptides International, Louisville, Kentucky) was used due to its proven efficacy as a $\alpha_v\beta_3$ ligand. The peptide was biotinylated via the ε-amino side chain of the lysine residue as follows. Peptide was dissolved in 0.2 M $NaHCO_3$ buffer to which was added a 10-fold molar excess of the biotinylation reagent sulfo-NHS-LC-biotin (Pierce). The reaction solution was incubated for 30 minutes at room temperature and terminated by the addition of 0.1% TFA. RP-HPLC analysis showed a shift of the retention time of the peptide confirming biotinylation. The peptide was purified by loading onto a preparative HPLC column run with a 0-60% acetonitrile gradient over 60 minutes. Individual peaks were collected each of which was again analysed by HPLC to confirm that the expected fraction

contained the purified biotinylated peptide. The peptide was freeze dried and analysed by MALDI-TOF MS as described elsewhere.

2.7.2 Optimisation of peptide binding to streptavidin

In order to determine the optimal peptide concentration needed to maximize the valency of the peptide-streptavidin conjugates, streptavidin was incubated with varying concentrations of peptide and the concentration of unoccupied biotin binding sites determined. Relative concentrations of unoccupied binding sites, free biotin groups and streptavidin were determined by the use of streptavidin-conjugated HRP, biotinylated HRP and anti-streptavidin antibodies respectively.

Biotinylated peptides were dissolved in ultrapure water at a concentration of 1mg/ml and stored at -20 ^{0}C until required. Streptavidin purified from *Streptomyces avidinii* (Sigma) was dissolved in ultrapure water at a concentration of 1 mg/ml. The stated biotin binding activity of streptavidin was 14 U/mg of protein (one unit will bind 1 μg biotin) which gives a theoretical molecular weight of 70,000 Da. As one molecule of streptavidin has 4 biotin-binding sites, peptide was added to streptavidin in a 4:1 molar ratio and multiples thereof in 0.5 ml centrifuge tubes. The reaction volume was diluted to 60 μg streptavidin/ml in TBS pH 7.4, vortexed and incubated for 1 hour at room temperature. The solution was diluted sequentially 1:4, 50 μL added to wells on duplicate on a 96-well plate (Maxisorb, Nunc) and incubated overnight at 4 ^{0}C. The plates were washed 4 times in a plate washer with PBS containing 0.05% Tween-20 (Sigma) and each well incubated with 50 μL biotin-HRP diluted 1:12500 (from Dako ABC-HRP kit) in TBS, streptavidin-conjugated HRP (Sigma) 2 μg/ml in TBS or anti-streptavidin antibody (AbCAM, ab10020). Wells incubated with anti-streptavidin antibody were incubated, after washing, with the secondary antibody HRP-conjugated goat anti-mouse (Dako, P0447) diluted 1:5000 for a further hour. The HRP substrate was prepared by dissolving one tablet of 3,3',5,5' tetramethylbenzidine dihydrochloride (TMB)(Sigma) in 10ml 0.05 M phosphate-citrate buffer with the addition of 2 μL 30% H_2O_2 immediately prior to use. The colour was allowed to develop and the reaction was then stopped by the addition

of 12.5 μL 2 M H_2SO_4 which produced a yellow colour. Absorbance was read at 450 nm in an automated plate reader. The results of this experiment allowed, the biotin-binding capacity and hence the degree of saturation of the streptavidin to be determined after incubation with biotinylated peptide. This method was also used to determine the efficiency of the spin column purification described in the next section.

2.7.3 Purification of streptavidin-peptide

In order to remove unbound peptide following incubation of streptavidin with saturating concentrations, size-exclusion filtration was used. This has the advantage that it could also be used to purify radiolabelled streptavidin-DTPA from unbound ^{111}In. 2 ml Zeba filtration columns (Pierce) were prepared by centrifugation for 1 minute at 1,000 g. Following this 1ml of PBS was added and the centrifugation repeated. This was repeated 3 times in order to equilibrate the column. A minimum volume of 200 μL of streptavidin/ peptide solution was added to the column followed by 40 μL of ultrapure water as a 'stacker'. The column was centrifuged again for 1 minute at 1,000 g

2.7.4 Conjugation of streptavidin to DTPA

Diethylenetriaminepentaacetic acid (DTPA) is a chelating agent for trivalent metal cations commonly used in radiolabelling. DTPA was conjugated to streptavidin using the method described by Cooper *et al* (Cooper, Sabbah, & Mather 2006). Antibody or streptavidin was dissolved in double-distilled water (Egastat Maxima, Elga, Marlow, UK) to 1mg/ml and transferred to a 15ml ultrafiltration unit with a 10,000 molecular weight cut-off filter (Amicon Ultra, Millipore, Watford, UK). In order to remove contaminating metal cations 50 μL of 50mM ethylenediaminetetraacetic acid (EDTA) in 0.1M acetate buffer pH 6.0 (prepared by dissolving 0.1 M sodium acetate in 1 L double-distilled water and adding 300 μL acetic acid) was added per 10 mg of protein. The mixture was incubated for 30 minutes at RT and then centrifuged at 1360 g until the volume had reduced 2-3 fold. The solution was topped up to 15 ml with 0.1 M HEPES pH 8.5 and this was repeated 3 times, after which the pH was checked to be at 8.5. For the final centrifugation the volume was reduced to a protein concentration of ~10 mg/ml:

50 μL of the solution was removed and diluted in acetate buffer in order to determine the absorbance at 280nm. From this the protein concentration was derived and the solution was pipetted into a cryovial. The chelating agent with a reactive isothiocyanate group p-2-(4-isothiocyanatobenzyl)-DTPA (Macrocyclics, Dallas, TX) was dissolved at a concentration of 50 mg/ml in 100% ethanol (VWR, Lutterworth, UK) and added in 20-fold molar excess to the streptavidin solution. The vial was vortexed and incubated overnight at 4 ^{0}C. The ultrafiltration tube was rinsed with 0.1 M acetate buffer pH 6.0 and the streptavidin-DTPA solution was pipetted into the tube and diluted to 15 ml. The tube was centrifuged until the volume had reduced by >3x. The absorbance of the filtrate was read at 280 nm in order to assess the concentration of free DTPA and the washing step was repeated until the filtrate absorbance had stopped falling. The streptavidin or antibody-DTPA solution was removed from the tube and sterile filtered using a 0.22 μM syringe filter and frozen in aliquots after a sample was removed to measure absorbance.

2.7.4.1 Determination of streptavidin-DTPA concentration by ELISA

It is possible that the conjugation of DTPA to streptavidin alters the UV absorbance and that trace concentration of free DTPA could also interfere with spectrophotometric results. An ELISA was therefore developed to determine streptavidin-DTPA concentrations. Monoclonal antibody to streptavidin (AbCam, clone ab10020) was diluted to 0.2 μg/ml in PBS pH 7.4 and 50 μl was added to wells of a 96-well plate. After overnight incubation at 4 ^{0}C the plate was washed 4 times with was buffer (PBS + 0.1% Tween-20) and blocked with 2% BSA in PBS for 2 hours at RT. The plate was washed 4 times and incubated with sequential dilutions of streptavidin in PBS for 1 hour at RT. After a further 4 washes the plates was incubated with HRP-conjugated polyclonal rabbit anti-streptavidin antibody diluted 1:10,000 in PBS + 1% BSA and incubated for 1 hour at RT. After a final 4 washes the plate was developed with TMB substrate and the absorbance read as detailed for previous ELISA experiments.

2.7.5 Radiolabelling of streptavidin-peptide

Streptavidin-DTPA was diluted to the required concentration in a total volume of 50 μL acetate buffer pH 6.0 in a 1.5 ml centrifuge tube: 10 μL of $^{111}InCl_3$ in 0.05 M HCl (~5 MBq) was added and the solution was incubated for 30 minutes at RT. 6 μL of 50 mM EDTA in acetate buffer was added in order to chelate unbound indium and incubated for a further 5 minutes. Radiolabelling efficiency was measured by instant thin layer chromatography (ITLC) with acetate buffer as the mobile phase and size-exclusion high-performance liquid chromatography (SE-HPLC) as described in section 2.5.6.2.

To radiolabel streptavidin-bound peptides, streptavidin was pre-incubated with peptide solutions in 4-fold excess for 1 hour in acetate buffer prior to the radiolabelling reaction. The solution was then added to a 0.5 ml Zeba spin-column pre-equilibrated with PBS according to the manufacturer's instructions and centrifuged at 1,500 g for 2 minutes. Measurement of the radiochemical purity before and after filtration and measurement of activity of the purified sample allowed the concentration of radiolabelled streptavidin-peptide to be determined.

2.7.6 RGD peptide binding assays

A number of ELISA-based assays were used to examine binding of monovalent and tetravalent peptide to $\alpha_v\beta_3$, either directly or indirectly as in the binding inhibition assays.

2.7.6.1 Fibronectin binding to $\alpha_v\beta_3$

To optimize the binding assays of fibronectin to $\alpha_v\beta_3$ was examined under varying cation conditions using buffer as described in section 2.2.5 as follows. Purified $\alpha_v\beta_3$ (Chemicon) was dissolved in 20 mM Tris-buffered saline pH 7.4 at a concentration of 0.5 μg/ml (or variable concentration as indicated) with cation concentrations as indicated in the results section (binding buffer) and 50 μL per well added to 96-well plates. After overnight incubation or incubation for 1 hour at 37 ^{0}C the plate was washed 6 times in wash buffer. 50 μL of purified fibronectin (Sigma) at a dilution of 2 μg/ml in conjugate buffer was added to the

wells and incubated for a further 1 hour at RT. After 4 washes the 50 μL of the secondary antibody HRP-conjugated anti-fibronectin (AbCam, Cambridge, UK, clone ab25467) diluted 1:2000 was added to the wells and incubated for one hour. After a final wash TMB substrate was added and the ELISA completed as previously described (section 2.2.5).

2.7.6.2 Competitive binding assays

For competitive binding assays the above protocol was used with the addition of 25 μL of the competing peptide or streptavidin-conjugated peptide in conjugate buffer prior to the addition of 2 5μL of fibronectin 4 μg/ml in conjugate buffer (i.e. twice the concentration used for non-competitive binding assays to give the same final concentration). The assay was carried out otherwise as in the previous section.

2.7.6.3 Binding of tetravalent peptide to $\alpha_v\beta_3$

$\alpha_v\beta_3$ plates were prepared as above. Tetravalent peptide was prepared by incubation of peptide with streptavidin as before, with subsequent dilution in conjugate buffer. 50 μL of dilutions were added to wells and incubated for 1 hour at RT. The plates were washed 4x with wash buffer and incubated with anti-streptavidin antibody and completed as in section 2.7.1.

2.7.6.4 Cell adhesion assays

Adhesion of cells to immobilized ligand was assessed using a previously described colourimetric adhesion assay (Hapke et al. 2001) as follows. Ligand was diluted in PBS pH 7.4 and coated onto 96-well maxisorb plates by the addition of 50 μl per well followed by overnight incubation at 4 ^{0}C. The following day the plates were washed 4x in PBS containing 0.05% Tween-20 and blocked with 2% BSA in PBS for 2 hours at RT. Subconfluent adherent cells were detached from 75cm^2 flasks as follows: the media was decanted and the cells rinsed twice with PBS pH 7.4. 3 ml 0.02% EDTA was added to the flasks which were then incubated for 10 minutes at 37 ^{0}C. The cells were detached by tapping the flasks and transferred to a 50 ml centrifuge tube with a sterile 3 ml pipette. The cells were suspended in serum-free RPMI medium and centrifuged for 5

minutes at 220 g: the supernatant was decanted and the cells washed twice more. The cell concentration was measured using a Trypan blue exclusion assay: the cell suspension was mixed 1:1 with 0.4% solution of Trypan blue (Sigma) and the cells counted in a Neubauer Improved haemocytometer under a light microscope. The cell suspension was diluted with serum-free RPMI medium to the required concentration for use in the assay.

After the blocking step the plates were washed and 50 µl of cell suspension added to each well. For competition assays the wells were pre-incubated with 25 µl of competitor solution prior to addition of 25 µL of cells at twice the required final concentration. Cell adhesion was allowed to take place over 1 hour at 37 ^{0}C. The plates were washed twice by gentle immersion in PBS pH 7.4 followed by the addition of 50 µl 4-Nitrophenyl N-acetyl-β-D-glucosaminide (NPAG, 7.5 mM in 0.1 M sodium citrate pH 5.0 mixed 1:1 with 0.1% Triton X-100). NPAG is cleaved by the intracellular enzyme β-N-Acetylglucosaminidase releasing 4-nitrophenol. The colour was allowed to develop by overnight incubation at 37 ^{0}C and the reaction stopped by the addition of 75 µl stop buffer (50 mM glycine pH 10.5 containing 5 mM EDTA). Absorbance was read in a plate reader at 650 nm.

2.7.7 *In vitro* RGD-streptavidin cell-binding assay

To determine binding of ^{111}In-labelled RGD-peptide to $\alpha_v\beta_3$-expressing cells a radioligand binding assay was performed as follows. MCF7β3 and A375P cells were grown to confluence as previously described, detached and washed twice in serum-free media prior to re-suspension in internalization buffer (RPMI medium containing 20mM HEPES + 1% BSA) at a concentration of $2x10^6$ cells/ml. Various concentrations of ^{111}In-labelled RGD2C-, cRGDyK- or scrambled RGD2C-streptavidin were added to 0.5 ml of cells in a 1.5 ml centrifuge tube, gently vortexed and incubated at 37 ^{0}C for 1 hour. The cell suspension was washed twice in ice-cold PBS and the radioactivity of the pellets read in a gamma counter.

2.7.8 Binding of ^{111}In-streptavidin to biotinylated HRP in solution

To confirm the binding of ^{111}In-labelled streptavidin to biotin a 16-fold molar excess of biotinylated HRP (Pierce) was added to an aliquot of ^{111}In-streptavidin in a 1.5 ml centrifuge tube. After 30 minutes a sample of the reaction solution was analysed by size-exclusion HPLC as were a samples of biotinylated HRP alone and ^{111}In-labelled streptavidin alone.

2.7.9 Binding of ^{111}In-streptavidin- peptide to $\alpha_v\beta_3$ in solution

Binding of the radiolabelled streptavidin-RGD2C peptide to $\alpha_v\beta_3$ in solution was examined in order to ensure that the radiolabelling did not abrogate binding to the ligand. The following experiment was therefore performed to see whether binding could be demonstrated in solution.

^{111}In-labelled streptavidin- cRGDyK or sRGD2C peptide was prepared as described previously and equilibrated in binding buffer and added to $\alpha_v\beta_3$ (original concentration 200 μl/ml) in a microcentrifuge tube to give a reaction volume of 31.9 μl containing $4.5x10^{-7}$ mmol/ml ^{111}In-streptavidin-peptide and $4.5x10^{-7}$ mmol/ml. The solution was incubated for 1 hour at room temperature after which the solutions and ^{111}In-streptavidin peptide alone were analysed by SE-HPLC.

2.7.10 *In vivo* studies with streptavidin-synovial homing peptide

^{111}In-streptavidin-peptide was prepared as described and purified by spin column filtration into sterile PBS for injection into mice. Mice double transplanted with human skin and synovium or carrying $\alpha_v\beta_3$-positive tumours were injected intravenously with the solution at the doses indicated in the results sections. At the indicated time points the mice were killed by intra-peritoneal injection of Sagatal and the transplanted organs retrieved for weighing and measurement of radioactivity as for previous biodistribution experiments.

2.8 Polymerisation of peptide with fluorescent microspheres

2.8.1 Conjugation to Neutravidin

Neutravidin is a proprietary deglycosylated form of avidin which has lower non-specific binding activity. It is also considerably cheaper than streptavidin and was therefore used for this part of the project. It was conjugated to fluorescent microspheres as follows.

5 ml of a 2% aqueous suspension of 1 μm aldehyde-sulphate fluorescent microspheres with optimal excitation/ emission wavelengths of 496/506 nm and surface (Fluospheres, Invitrogen, Paisley, UK) were added to 4 mg of Neutravidin in 2 ml of 50 mM phosphate buffer pH 6.5 in a 15 ml plastic centrifuge tube. This conjugates the Neutravidin to the microspheres by the formation of Schiff bases between the aldehyde surface groups and the ε-amino group of lysine residues in the protein molecule. The vial was protected from light and agitated at RT overnight. The microspheres were washed 4 times by centrifugation at 2,400 g for 15 minutes followed by re-suspension on PBS pH 7.4 before final re-suspension in PBS containing 0.1% azide and 1% BSA. 1 ml of supernatant was retained from each centrifugation; this was centrifuged again at 13,000 rpm for 15 minutes in a microcentrifuge and the absorbance read at 280 nm in order to ensure removal of unbound Neutravidin.

2.8.1.1 Confirmation of microsphere labelling with Neutravidin

In order to confirm the presence of Neutravidin on the surface of the microspheres radio-labelled biotin was used: binding of the biotin would confirm the presence of conjugated Neutravidin.

2.8.1.1.1 Radiolabelling of biotin

Diethylenetriaminepentaacetic acid α,ω-bis(biocytinamide) (Sigma D1534, mw 1102) (hereafter referred to as DTPA-$(biotin)_2$) consists of 2 DTPA and 2 biotin groups per molecule. The compound was radiolabelled was follows: DTPA-$(biotin)_2$ was diluted to 1 μg in 50 μL acetate buffer pH 6.0 to which was added 10

μL of $^{111}InCl_3$ stock and incubated for 30 minutes at RT. At the end of the incubation period 6 μL of acetate buffer containing 50 mM EDTA was added and the reaction mixture incubated for a further 5 minutes. To confirm radiolabelling of the biotin a previously published method was used (Rusckowski et al. 1995): a sample of the radiolabelled biotin-DTPA was incubated with a ten-fold excess of streptavidin in the radiolabelling buffer for 1 hour. A G-50 size-exclusion column (Amersham Biosciences) was prepared by centrifuging at 5,000 rpm in a microcentrifuge for 1 minute. 20-25 μL of the streptavidin solution was added to the column which was centrifuged again. Radioactivity of the column and the filtrate were measured in a gamma counter: protein-bound ^{111}In-DTPA-biotin would be in the filtrate whilst unbound ^{111}In is retained in the column. There are no published reports of the separation of unbound ^{111}In from ^{111}In-DTPA-biotin and therefore ITLC as described for ^{111}In-labelled antibodies and streptavidin was carried out and compared with from SE-HPLC which was carried out in parallel as previously described.

2.8.1.2 Confirmation of Neutravidin binding to microspheres by competitive binding assay

Neutravidin-conjugated microspheres were incubated with a fixed concentration of ^{111}In-biotin-DTPA in the presence of increasing concentration of cold biotin-DTPA: these were mixed together prior to the addition to microspheres. The biotin-DTPA was added to 100 μL aliquots of Neutravidin-conjugated or unconjugated microspheres in 1.5 ml centrifuge tubes and incubated for 1 hour at RT with regular mixing. At the end of this period the microspheres were washed twice by diluting to 1 ml with PBS and centrifuging in a microcentrifuge at 5,000 rpm for 10 minutes. After the second wash the supernatant was carefully aspirated and the radioactivity of the microsphere pellets read in a gamma counter.

2.8.2 Conjugation of microspheres to RGD peptide

To assess the capacity of peptide-conjugated microspheres to bind to a cell-expressed ligand the RGD peptide as used in the previous chapter was employed. This would enable optimization the surface coating of the microspheres with peptide, binding affinity of which could then be assessed by FACS. The data from the previous experiment provided the concentration of peptide at which the

microspheres would be saturated. Peptide was added at a saturating concentration to a microsphere suspension in a 1.5 ml centrifuge tube and incubated for 1 hour at RT with regular mixing. The microspheres were washed by re-suspension in PBS and centrifuging in a microcentrifuge for 10 minutes at 5,000 rpm. After 3 washes the microspheres were re-suspended in FACS buffer (TBS+100 mM $MgCl_2$, 200 mM $CaCl_2$ and 200 mM $MnCl_2$ + 0.1% azide + 1% BSA) and stored at 4 ^{0}C.

MCF7 β3 or A375P cells were grown to sub-confluence and detached as detailed previously. The cells were washed twice in PBS and twice in FACS buffer and 10^5 cells were added in 0.5 ml FACS buffer to 1.5 ml centrifuge tubes. The tubes were centrifuged in a microcentrifuge for 3 minutes at 3,000 rpm and the supernatant discarded by pouring off- this left around 100 µl in the tube. The cells were re-suspended by gently vortexing and the required concentration of microspheres added. The tubes were incubated on ice for 1 hour with regular vortexing after which the cells were washed twice in FACS buffer. If FACS analysis was not to be carried out immediately the cells were fixed by re-suspension in 1% paraformaldehyde in PBS.

Radiolabelling of the microspheres was to be achieved by the substitution of biotinylated peptide with DTPA-$(biotin)_2$. The effect of differing ratios of peptide: DTPA-$(biotin)_2$ were determined as follows. 50 µl of Neutravidin-conjugated microspheres were added to 0.5 ml centrifuge tubes containing various ratios of biotinylated cRGDyK to DTPA-$(biotin)_2$: the total molar concentration was equal in all tubes. After mixing the microspheres were incubated for 1 hour at RT and washed four times in FACS buffer. A375P cells were detached as detailed above and 10^5 cells in 100 µl FACS buffer added to 1.5 ml centrifuge tubes; microspheres were then added to the tubes in duplicate and the experiment completed as previously.

FACS analysis was carried out with a FACSCalibur system (Beckton Dickinson) and analysed by CellQuest software run on an Apple Mac PC. Regions of interest

were defined of labelled and unlabelled cells and the results expressed as % cells labelled.

2.8.3 Labelling of microspheres with peptide and ^{111}In- DTPA-(biotin)$_2$ and peptide and *in vivo* biodistribution experiments

A 2% solution of Neutravidin-conjugated fluorescent microspheres was added to a 4:1 solution of biotinylated peptide: ^{111}In—biotin-DTPA in 1.5 ml centrifuge tubes to give a final biotinylated peptide/^{111}In—biotin-DTPA concentration of $2x10^{-5}$ mmol/ml (previously determined to be a saturating concentration). The solution was incubated for 1 hour at room temperature and washed 4 times in PBS containing 1% BSA before final re-suspension to give a 2% solution of microspheres.

200 μL (~3 MBq) of RGDyC or sRGD2C peptide-labelled microspheres were injected into mice bearing A375P tumours via the tail vein. After 15 minutes the animals were killed and the tumours and murine organs retrieved, weighed and the activity measured in the gamma counter. Diluted triplicate reference samples of the injected solution were measured in the gamma counter in parallel with the tissues.

For the 3.1 and scrambled 3.1 peptides, 6 hours after intragraft injection of 200ng TNFα, SCID mice transplanted with human skin and synovium were injected via the tail vein with 200 μl (~3 MBq) of the 3.1 peptide or scrambled 3.1 peptide-labelled microsphere suspension. After 15 minutes, 1 hour or 24 hours the animals were killed and the transplants and organs retrieved as above.

2.9 Statistical analysis

All statistical analysis was performed using Prism 3.0 software (Graphpad, San Diego, Ca). Groups were compared using a 2-tailed unpaired t-test; multiple groups were analysed using one-way analysis of variance (ANOVA) with Bonferroni's post test to pairs of columns of interest. Linear regression analysis was performed where indicated after log-transformation of the data.

Chapter 3

Validation of the synovial homing phage in the SCID mouse transplantation model as a platform for testing *in vivo* localisation of novel targeting agents

3.1 Introduction

The first stage of this project was to ensure the reproducibility of the SCID mouse transplantation model. This involved confirmation of transplant engraftment and vascularisation as well as confirmation of the specificity of 3.1 phage specificity for human synovium as described in the original phage work. As discussed in the introduction some preliminary data had shown that 3.1 phage homing to transplanted synovium could be up-regulated by intragraft injection of TNFα in a small number of animals. I therefore repeated this experiment with larger numbers of animals. Secondly, grafts from transplanted animals were also examined for the presence of murine/ human vascular anastomoses and the effect on adhesion molecule expression of TNFα stimulation. Finally, I investigated sequence homology between the 3.1 peptide sequence and potential candidates. I describe the identification of a striking sequence homology with the mac-1 leucocyte integrin and the experiments to test 3.1 phage binding affinity. I conclude discussing alternative potential candidate ligands for the 3.1 phage sequence.

3.2 Validation of SCID mouse model and specific phage homing

3.2.1 Confirmation of vascularisation of grafts

Synovial tissue and skin were obtained from patients undergoing joint replacement surgery and transplanted under the dorsal skin of SCID mice at 3-6 weeks of age. After 2-4 weeks tissues were retrieved and processed for histology as detailed in the methods section.

Macroscopically grafts were well-vascularised after 2-4 weeks with >95% graft survival. In order to confirm the formation of anastomoses between the human and murine circulations the tissues were stained by immunofluorescence for the endothelial markers von Willebrand Factor (human) and CD31 (murine). Von Willebrand Factor is a glycoprotein involved in haemostasis which is expressed exclusively by endothelial cells, megakaryocytes and platelets (Ruggeri & Ware 1993) and is therefore suitable as a specific marker for human endothelial cells in

this model. CD31 (also known as platelet-endothelial cell adhesion molecule-1/ PECAM-1) is expressed by a number of circulating cells including platelets, neutrophils, monocytes and some T-cell subsets, and by endothelial cells where it is a critical component of endothelial cell junctions (Newman 1997). Both *ex vivo* synovial and skin grafts were stained and representative sections are shown in Figure 3.1. Human vessels, indicated by green staining for vWF, and murine vessels, indicated by red CD31 staining are represented in both skin and synovium confirming the presence of both human and murine vessels within the grafts and, importantly, preservation of a human-specific phenotype. In addition, the formation of human-murine vessel anastomoses in clearly demonstrated and is indicated in the diagrams with arrows. This, therefore, supports the capacity of the model to enable delivery of systemically-administered compounds to the human vascular endothelium.

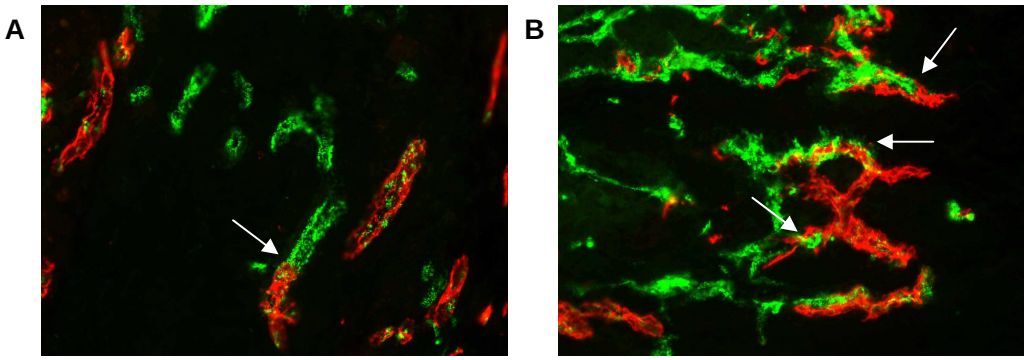

Figure 3.1: **The formation of anastomoses between human and murine vessels within transplanted human tissues**. Frozen tissue sections of synovial (A) and skin (B) *ex vivo* transplants were stained by immunofluorescence for the vascular endothelial-specific markers human von Willebrand Factor (green) and murine CD31 (red). The presence of both human and murine vessels was confirmed in the grafts with anastomoses between the human and murine vessels clearly visible (arrows). Original magnification x40

3.2.2 Sequencing of PIII gene confirms retention of the expected inserted oligonucleotide sequences

One of the enormous advantages of peptide phage display technology is the predictable link between phenotype and genotype. Transfection of oligonucleotide sequences into the phage surface protein PIII gene results in the expression of fusion proteins which, in the case of the 3.1 phage, confers homing specificity for human synovium *in vivo*. Prior to the use of the phage clones for *in vivo* or *in vitro* experiments, phage were amplified from frozen stocks as detailed in the methods and expression of the expected peptide sequences was confirmed by DNA sequencing. For the *in vivo* experiments a phage clone previously selected from the same library as the 3.1 clone for binding specificity to streptavidin was used. This clone, known as streptavidin clone 1 (SC1), expressed a peptide containing the expected HPQ sequence (discussed in more detail later). Both of these clones were isolated by Dr Lewis Lee during as part of the phage library validation experiments prior to the *in vivo* selection of the 3.1 phage.

DNA was extracted from the phage stocks as detailed in the methods: a specific primer was used to amplify the DNA by PCR and the sequencing was carried out on an in-house automated sequencing system. For later experiments, due to the loss of the sequencing facility, the DNA and primers were sent to an external resource for PCR and sequencing. The phage were sequenced each time fresh stocks were produced by amplification and this consistently confirmed the presence of the expected DNA sequences.

Representative sequencing chromatograms are shown in Figure 3.2: The oligonucleotide sequence was translated using an on-line tool and this confirmed the coding for the expected peptide sequence (Table 3.1).

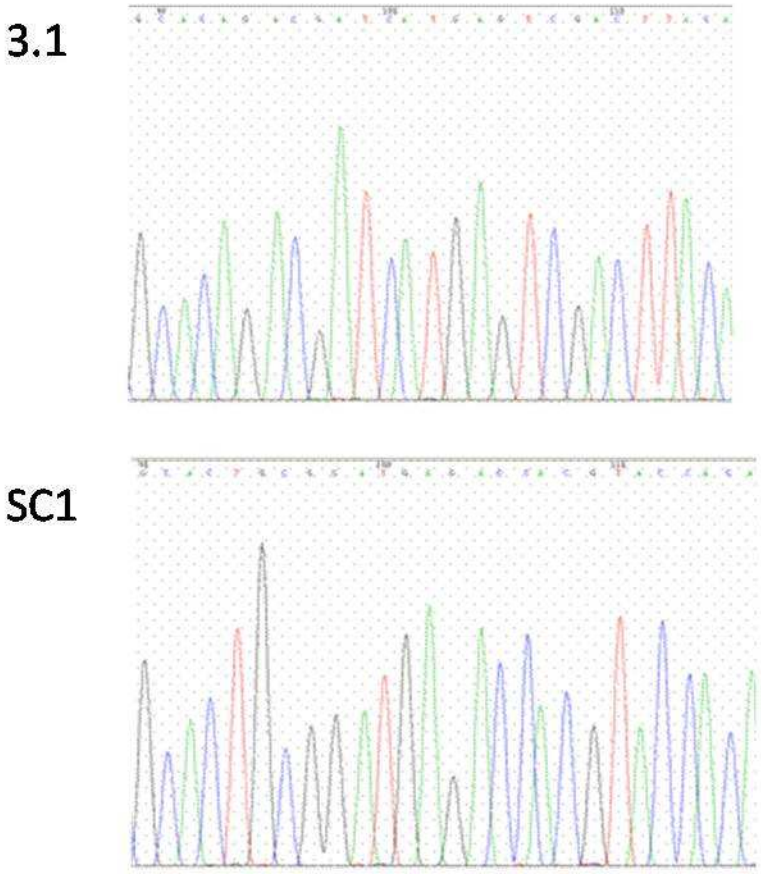

Figure 3.2: **Representative sequence chromatograms of the phage clones used in this project.** DNA was extracted by PEG precipitation of phage from stock solutions followed by incubation with NaI/ ethanol to strip the phage proteins and precipitate DNA. After washing, DNA was amplified by PCR with a specific primer prior to sequencing. The chromatograms confirm the expected inserted DNA sequences: sequencing was performed each time phage were re-amplified from stocks.

	Clone 3.1
3’5’ antisense sequence	GCA CAG ACG ATC ATG AGT CGA CTT ACA
Translated sequence	Cys Lys Ser Thr His Asp Arg Leu Cys

	Clone RGD
3’5’ antisense sequence	GCA AGG ATG ATC ACC ACG AGG AGA ACA
Translated sequence	Cys Ser Pro Arg Gly Asp His Pro Cys

	Clone SC1
3’5’ antisense sequence	GCA CTG CGG ATG AGA CCA CGT ACC ACA
Translated sequence	Cys Gly Thr Trp Ser His Pro Gln Cys

Table 3.1: Translation of fusion peptide sequence from sequencing data. After each phage amplification expression of the expected peptide sequence was confirmed by amplification of the DNA with specific primers and sequencing. The 3’5’ antisense sequence obtained was converted into the peptide sequence using an on-line DNA translation tool.

3.2.3 TNFα up-regulates tissue localization of the synovial-homing phage specifically to synovial but not skin grafts maximally 6 hours post- injection.

Preliminary experiments, as discussed in the introduction, had shown that intragraft injection of recombinant human TNFα increased synovial-specific phage homing at 6 hours. TNFα is a dominant pro-inflammatory cytokine with a critical role in the pathogenesis of rheumatoid arthritis and part of its effects are mediated through its ability to modulate adhesion and migration: the use TNFα-blocking therapies has now becoming routine in clinical practice (Feldmann & Maini 2001). Some of effects are mediated through its ability to modulate adhesion and migration: an early observation with the use of TNFα-blocking therapies was an increase in the number of circulating peripheral blood lymphocytes- this was associated with a reduction in synovial cellularity and

expression of E-selectin and VCAM-1 (Tak et al. 1996) The observation that synovial adhesion molecules are down-regulated following anti-TNFα therapy has been confirmed by other studies (Paleolog et al. 1996) underlining the key role of this cytokine in regulating adhesion and migration phenomena. Previously we have shown *in vivo* that injection of human TNFα into human synovial grafts results in up-regulation of human CAM expression by the graft vasculature (Wahid et al. 2000) and that this correlates with an increased migration of human cells into stimulated grafts.

To determine whether recombinant human TNFα modulates expression of the synovial MVE receptor recognized by the CKSTHDRLC-expressing 3.1 phage, synovial and skin grafts were pre-stimulated by intragraft injection of 200 ng TNFα or 0.9% saline control. 6 or 18 hours after TNFα injection, the mice were injected intravenously with 200 pfu of the CKSTHDRLC-expressing 3.1 phage or SC1 control sequence phage. Transplanted tissues were harvested after 15 minutes circulation time following perfusion of the systemic circulation via the left ventricle with 50 mls 0.9% saline to wash out unbound phage. The results of this experiment are shown in Figure 3.3. At baseline (no TNFα stimulation), CKSTHDRLC phage recovery from synovial grafts is significantly higher than that seen in skin grafts ($p=<0.001$) and that of the control phage to both synovial and skin grafts ($p=<0.001$), an observation consistent with our previous findings (Lee et al. 2002). 6 hours after TNFα intragraft injection phage homing to the synovial transplants issignificantly up-regulated compared with baseline, with approximately two-fold increase in synovial localization ($p=<0.001$). Importantly, no significant up-regulation of homing to the skin grafts is seen for either phage clone at 6 hours. At 18 hours post TNFα stimulation CKSTHDRLC phage localization to synovial grafts returned to levels similar to those seen at baseline ($p=>0.05$ compared with baseline). No significant changes were seen in the levels of control phage localization at 6 hours. Homing of both phage clones to the murine kidneys is similar at all time points indicating similar levels of injected phage.

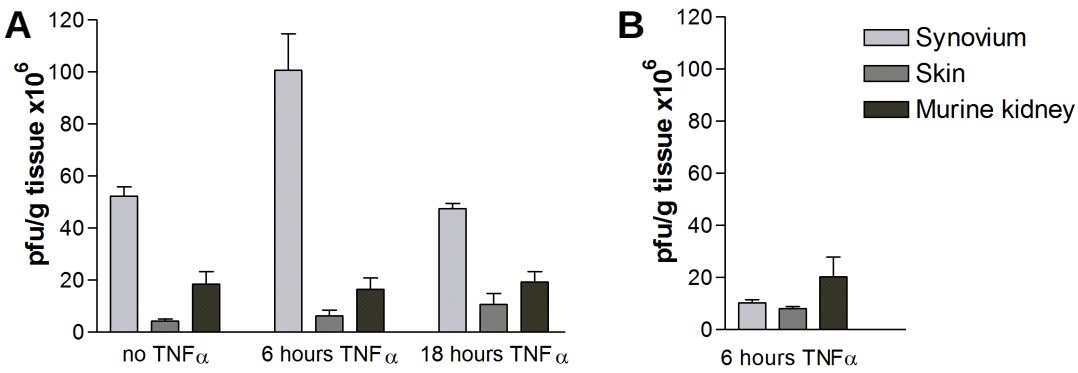

Figure 3.3: **Homing of CKSTHDRLC phage (A) and control phage (B) to transplanted human tissues in SCID mice.** Four weeks post-transplantation human synovium and skin into SCID mice, the grafts were injected with 200 ng of rhTNFα or saline control. After 6 or 18 hours, the mice were injected intravenously with 1 $x10^{11}$ pfu of 3.1 or strep clone 1 phage. The mice were culled, the transplanted tissues and murine kidney removed, and numbers of phage in each tissue determined as detailed in the materials and methods. The results are shown as the mean $\pm$ S.E.M. of triplicate plate readings. At 6 hours, 3.1 phage binding in human synovium is significantly greater than at baseline ($p=<0.001$, unpaired, two tailed t-test). No significant effect is seen at 18 hours. No significant effects were seen on 3.1 phage binding in human skin or murine kidney; similarly, no significant effects were seen in any tissue on strep clone 1 at 6 hours. The differences between phage homing to synovium and skin were significant at all time points. n=14-16 transplants per condition.

3.2.4 Visualisation of phage homing and up-regulation with TNFα by immunofluorescence

In order to examine the localization of the phage within the tissues transplants from double-transplanted mice injected with 3.1 phage after intragraft rhTNFα or saline injection, grafts were extracted and stained by immunofluorescence for the major phage coat protein M13. Human vessels were counterstained for von Willebrand Factor as previously. Representative sections are shown in Figure 3.4: in the saline-treated tissues co-localisation of the phage with human vessels isseen in the synovial grafts, low levels of phage are also seen in the skin. After TNFα

stimulation increased co-localisation of phage with the human vasculature is seen in the synovial tissue with no observable change in levels of localization in the skin.

These data suggest that the ligand for the CKSTHDRLC (3.1) phage is up-regulated by TNFα as well as being present under basal conditions in these tissues. Furthermore, no significant differences were seen in the control tissue (skin), this is despite there being a clearly demonstrable pro-inflammatory effect as evidenced by up-regulation of both E-selectin and ICAM-1 expression at 6 hours. These observations suggest that the phage are binding a synovium-specific TNFα–responsive ligand and raise the possibility that it may be a synovial homing-receptor. Although tissue-specific homing receptor/ addressin pairs have not been identified for human synovium there is substantial indirect evidence that such interactions may exist, such as the observation of non-random accumulation of lymphocyte subsets in the inflamed synovium (Pitzalis et al. 1987) and the selective adhesion of lymphocytes isolated from inflamed human synovium to synovial tissue sections (Salmi et al. 1992).

The time course of up-regulation of phage homing to synovium may provide some insight into the nature of the ligand. The relatively short-term time frame, with down-regulation by 18 hours suggests cell membrane expression (as opposed to extracellular matrix). E-selectin expression peaks *in vitro* after TNFα-stimulation at 4-6 hours, although expression can remain up-regulated for 24-48 hours (To et al. 1996). However, the lack of an increase in homing of the 3.1 phage to skin despite up-regulation of E-selectin expression in our study makes this an unlikely candidate ligand although a tissue-specific post-translational modification is possible. Similarly, up-regulation of ICAM-1 expression is seen in both skin and synovium and is therefore less likely to be the target: furthermore the dynamics of ICAM-1 expression as already discussed are not in its favour and lack of binding of the phage to ICAM-1 was confirmed by ELISA (see next section). Although TNFα is known to synergise with VEGF in the stimulation of neoangiogenesis the short time frame of the effect on phage homing rules this out as an explanation for

the phenomenon. Our findings therefore raise the possibility that the synovial endothelial ligand may be a novel tissue homing receptor; the observation that phage homing is seen in the resting as well as the inflammatory state suggests that it may have roles in cell recruitment in diseases states as well, possibly, as in routine immuno-surveillance. The demonstration that the synovial-homing of the phage is up-regulated by TNFα adds significantly to the utility of the specific peptide sequence as targeting tool. Potentially, reagents bearing this specific sequence would be not only be selective for synovial tissue and but also preferentially accumulate in actively inflamed synovial tissues. This has obvious implications for imaging and optimal delivery of therapeutic molecules for rheumatoid arthritis.

These findings confirm the potential of this peptide for the targeting of therapeutic agents to the synovium. Experiments to investigate the *in vivo* tissue specificity of the monomeric peptide will be discussed in Chapter 5.

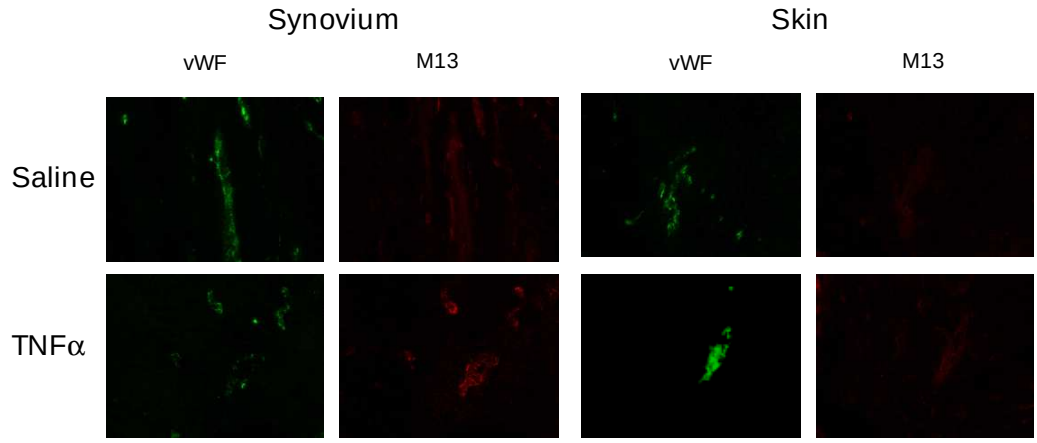

Figure 3.4: Representative sections of grafts pre-stimulated 6 hours previously with TNFα or saline control from mice injected with the synovial-specific phage. Grafts were stained by immunofluorescence for the phage coat protein M13 (red) and counterstained for the human endothelial-specific marker von Willebrand factor (green). Low levels of phage co-localisation with vascular endothelium are seen in saline-treated synovium and, to a lesser degree, skin. There is increased phage localization and intensity in the TNFα-treated synovium with a minimal increase in the skin. These findings are consistent with that from the phage titration data shown in Figure 3.3. Original magnification x40.

3.2.5 TNFα up-regulates human adhesion molecule expression in both synovial and skin transplanted tissues 6 hours after injection

We have shown in previously published work that adhesion molecule expression in transplanted human synovial tissue is significantly down-regulated 2-4 weeks post-transplant, suggesting that in the absence of continuing pro-inflammatory stimuli the transplants revert to a 'resting state' phenotype (Wahid et al. 2000). Despite this, the 3.1 phage clone was selected under these conditions thus suggesting the presence of the synovial ligand in uninflamed tissue. As discussed in the introduction, 24-48 hours post-injection intragraft of TNFα, ICAM-1 and VCAM1 are up-regulated in synovial grafts. Other groups have reported the up-regulation of E-selectin in transplanted synovium at 6 hours indicating that TNFα up-regulates the inflammatory phenotype of the transplanted synovium at least as early as this time point. The results presented in the previous two sections describe the tissue-specific upregulation by TNFα of 3.1 phage homing to human synovial tissue. Although we and others have previously reported up-regulation of cell adhesion molecule expression in transplanted synovium after intragraft injection of TNFα, the conclusion that the 3.1 phage ligand is synovial-specific, and more critically that it is specifically up-regulated in inflamed synovium, is contingent on the demonstration of a comparable stimulatory effect of TNFα on both tissues at this time point. *Ex vivo* tissues injected with TNFα or vehicle-only control 6-hours prior to retrieval were therefore examined for the expression of the adhesion molecules E-selectin and ICAM-1. Briefly, SCID mice were double-transplanted with human skin and synovium: after 2-4 weeks the grafts were injected with 200 ng rhTNFα or saline vehicle control. After 6 hours the animals were killed and the transplanted tissues processed for histological staining as detailed and stained by immunofluorescence for the adhesion molecules ICAM-1 and E-selectin with counterstaining for the human-specific vascular endothelial marker von Willebrand Factor (vWF). Representative sections are shown in Figure 3.5. Low levels of staining were seen for both E-selectin and ICAM-1 in the unstimulated tissues. There is clear up-regulation of both E-selectin and ICAM-1 expression in TNFα-treated grafts at this 6-hour time point with a

positive effect apparent in both skin and synovial transplants- it can be seen that both adhesion molecules co-localise with the counterstain for human vessels. Low levels of ICAM-1 expression were seen in both the skin and synovium in untreated tissues, and widespread extravascular expression of ICAM-1 could be seen particularly in the synovial grafts after TNFα stimulation. Expression of both ICAM-1 and E-selectin have been described in normal synovial tissue (Fairburn et al. 1993), although in our unstimulated transplants it was virtually undetectable.

An arbitrary scale (0-3) was used to grade the extent and intensity of ICAM-1 expression in synovial tissue before and after TNFα injection. The results shown in Figure 2 A show a significant increase in ICAM-1 expression in the synovial tissue after TNFα stimulation ($p=<0.05$).

It can be seen in Figure 3.5 that both adhesion molecules co-localise with the counterstain for human vessels. E-selectin expression is restricted to the vascular endothelium whilst, in synovium particularly after TNFα expression, ICAM-1 expression can be seen both in the vessels and, as expected, by other synovial cell types. This restriction of E-selectin expression to vascular endothelial cells and both skin and synovium enabled the effect of TNFα stimulation to be compared. Human vessels were identified by vWF staining and the number counterstaining for E-selectin counted. The results, shown in Figure 2 B, demonstrate a significant up-regulation of E-selectin at 6 hours in both the synovial and skin transplants ($p=<0.05$). Notably, there is no significant difference in E-selectin expression in the TNFα-treated skin and synovial grafts. Thus we were able to show that TNFα upregulated the inflammatory phenotype of the transplanted human synovial and skin vascular endothelium, and that this upregulation is similar for the two tissues.

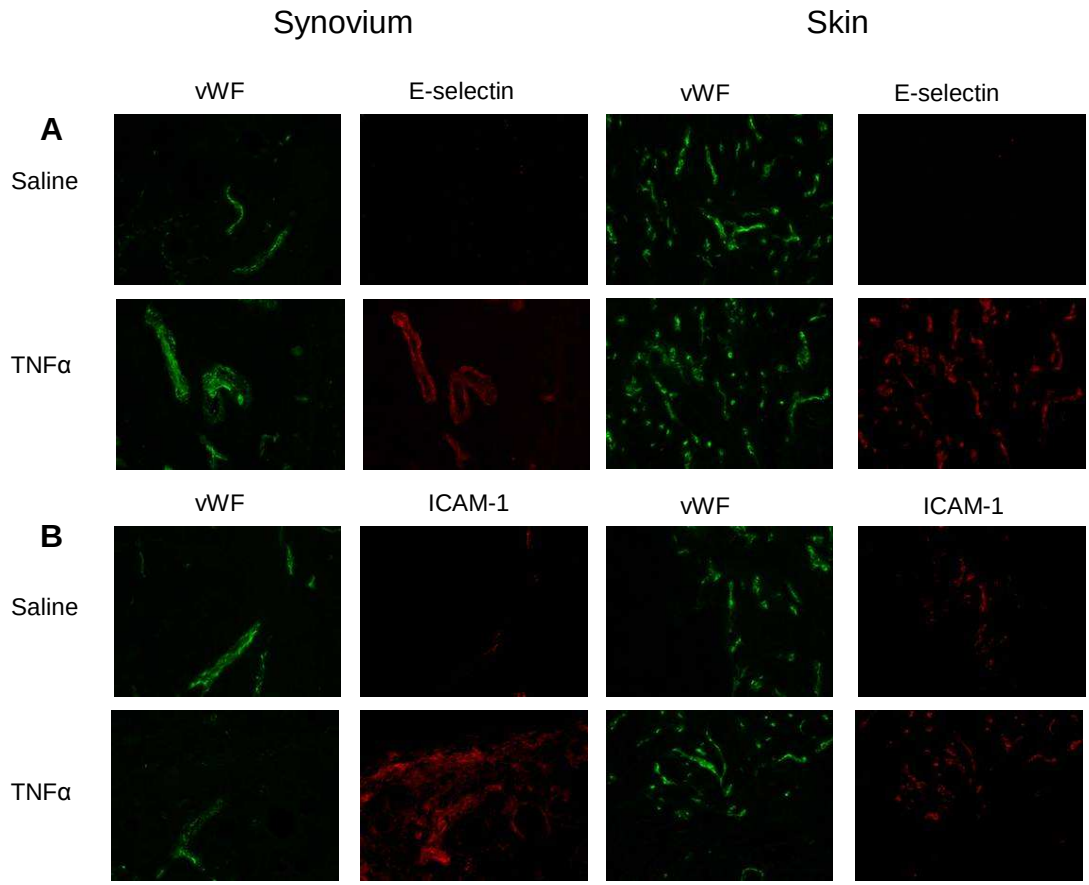

Figure 3.5: Representative sections from transplants 6 hours post-intragraft injection of TNFα or saline. Immunofluorescent staining was used to detect human von Willebrand factor (green) or ICAM-1/ E-selectin (red). There is clear up-regulation of both ICAM-1 and E-selectin expression; E-selectin expression is restricted to the vessels in both the skin and synovium. After TNFα stimulation there is up-regulation of expression in the vessels of both skin and synovium as well as more extensive extravascular expression in the synovium. Original magnification x40.

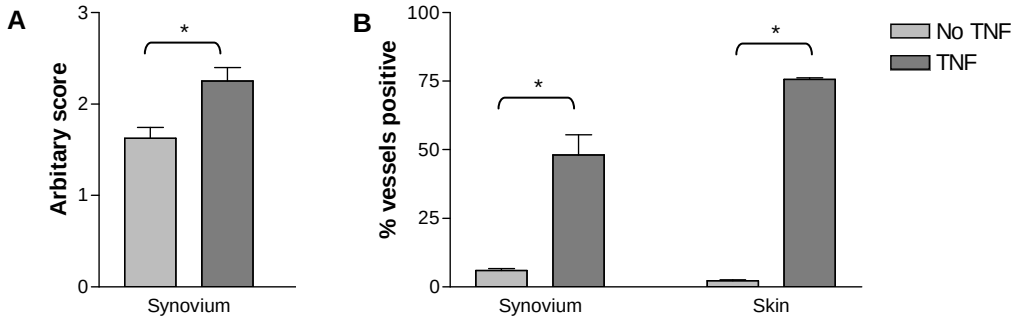

Figure 3.6: Quantification of ICAM-1 (A) and E-selectin (B) in transplanted tissues 6 hours post-intragraft injection of 200ng TNFα. A 2 synovial transplants were examined from each group and a minimum of 35 fields from 2-3 cutting levels were examined. Regions of human tissue were identified by the vWF counterstain. The extent of staining for ICAM-1 was graded on an arbitrary scale from 0-3. Significantly more staining is seen after intragraft injection of TNFα ($p=<0.05$) **B** 2 transplants were examined from each group, each at 3 different levels; human vessels were identified by staining for vWF and assessed for positive or negative staining for E-selectin: 150-350 vessels were examined per transplant. Differences were significant for TNFα-treated vs. saline-treated tissue (* $p=<0.05$, unpaired 2-tailed T-test). There is a non-significant difference in E-selectin expression in the TNFα-treated tissues in favour of skin. Results shown are mean +/- S.D.

3.3 Identification of candidate phage/ peptide ligands

As discussed in the introduction, there is significant indirect evidence for the existence of a synovial-specific 'addressin' as evidenced by the apparent non-random circulation of inflammatory cells. The observation that synovial-specific phage homing is up-regulated in inflamed tissue supports the possibility that one such addressin may be the receptor for the phage. Previously, however, several groups have reported receptors for tissue specific peptide-displaying phage as being non-classical adhesion molecules. Work is ongoing in our laboratory to identify the phage receptor by affinity chromatography; however a search of

protein sequence databases produced a striking match as discussed in the next section.

3.3.1 BLAST search of the KSTHDRL sequence reveals sequence homology with an extracellular region of the human mac-1 integrin.

In order to investigate whether the constrained peptide sequence expressed by the synovial-homing phage has any homology with known human proteins the peptide sequence was entered into the Basic Logic Assignment Search Tool (BLAST) available at http://130.14.29.110/BLAST/. This tool searches for areas of sequence similarity between the reference sequence and registered protein sequences. The search was restricted to human proteins and modified to search for short sequences. A number of matches were obtained of 5-7 residues and these are summarized in Table 3.2. A number of the matched sequences are with proteins which are of unknown function; of the remainder the majority are intracellular and therefore unlikely to be relevant: as the phage is introduced to the tissues via the circulation the synovial ligand is likely to be encountered on the vascular luminal endothelium cells or the extracellular matrix. The most striking match is with an extracellular region at position 660-665 of the human integrin α_m-integrin subunit. α_m (CD11b) associates with β_2 (CD18) to form the mac-1 integrin. The 7 residue sequence has 85% homology with the KSTHDRL sequence: the arginine/ histidine substitution at position 4 can be regarded as a 'conservative' substitution as both of these are basic residues. Of the remaining sequence matches, chemokine-like factor superfamily 6 is a protein with similarity to the chemokine family and although widely expressed it is of unknown function (Han et al. 2003). Regulator of G-protein signaling 3 (RGS3) is predominantly intracellular, although translocation to the plasma membrane can occur on G-protein activation (Dulin et al. 1999) and thus role in inflammatory synovitis can therefore not be excluded.

Mac-1 ($\alpha_m\beta_2$) is part of the integrin family of heterodimeric receptors and is expressed predominantly by myeloid and natural killer cells, although it can also be expressed by lymphocytes (Li 1999). It has been implicated in adhesive

interactions with a number of endothelial cell-expressed molecules and extracellular matrix proteins including ICAM-1(Diamond et al. 1991), ICAM-2 (Xie et al. 1995), fibrinogen (Lishko et al. 2004) and fibronectin (Lishko, Yakubenko, & Ugarova 2003) as well as non-protein ligands such as glycosaminoglycans (Diamond et al. 1995) and plastic (Yakubenko et al. 2002). Of these, fibronectin and ICAM-1 are the most interesting potential targets in RA tissue and the interaction of phage with these ligands was investigated further in the next section.

Peptide Sequence	Database match
KSTHDRL	
KSTRDRL	Integrin alpha-m
STHNRL	Wnt-8a precursor
KSSHDR	Thymopoietin
SAHDRL	RING finger protein 150
STQDRL	Bromodomain containing 7 Protein geranylgeranyl transferase type I
KSTQDR	KIAA 1244 (hypothetical protein)
STHDKL	strawberry notch homolog 1
THDRL	RAD54-like PHLDB1 v-akt murine thymoma viral oncogene homolog
_STHDR	chemokine-like superfamily 6
KSTHD	Regulator of G-protein signaling 3 Pyrophosphatase (inorganic) 1

Table 3.2: Results of a BLAST search of the synovial-homing peptide sequence. Matches spanning 5 or more residues are shown. Residues in red match residues in the reference sequence whereas residues in black are substitutions

3.3.2 Optimisation of phage ligand binding assay

As discussed above, the identification of sequence homology of the peptide sequence and of mac-1 integrin suggested a number of candidate ligands, 2 of which- ICAM-1 and fibronectin- were felt warrant further investigation. An ELISA-based assay would enable relatively quick screening of candidate ligands. For these assays the phage selected against streptavidin was to be used as a positive control.

The candidate ligand was bound to a 96-well plate overnight and, after washing and blocking, was incubated with varying concentrations of phage. After a further wash bound phage was detected with an HRP-conjugated anti-M13 antibody and developed with TMB before reading absorbance at 450 nm. In preliminary experiments background binding of phage was found to be significant, therefore the experiments were repeated without the ligand on order to investigate different blocking agents. The blocking step was carried out with 1% casein, 5% BSA or 2% milk, each made up in PBS. Phage were incubated on the plates in PBS + 0.1% Tween-20 and the assay completed as detailed above. The results, shown in Figure 3.7, show a clear reduction in binding if BSA or milk are used instead of casein. There is a small difference between milk and BSA with lower binding on the milk-blocked plates. However, as milk contains biotin, BSA was used in order to allow the streptavidin-binding page to be used as a positive control in these assays.

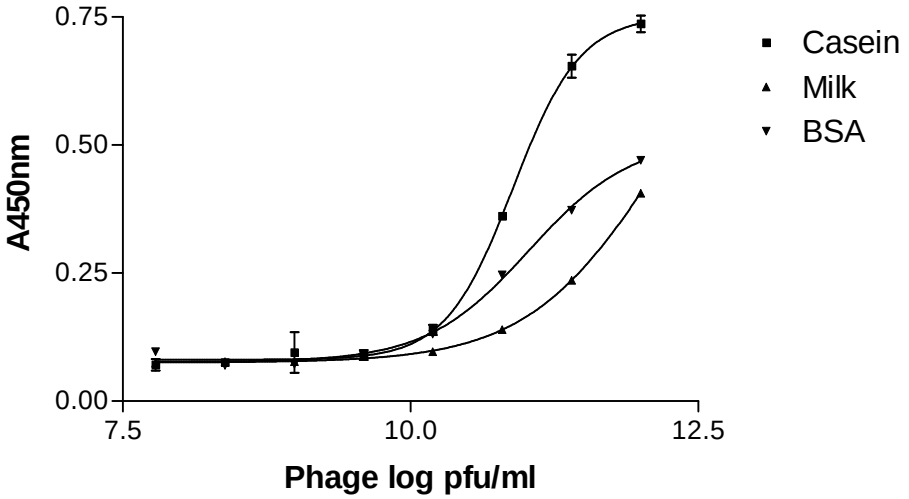

Figure 3.7: **Background binding of 3.1 phage clone in ELISA.** 96-well plates were blocked with 5% BSA, 2% milk or 1% casein and incubated with various concentration of phage for 1 hour. The plates were washed and incubated with HRP-conjugated anti-M13 antibody and developed with TMB. There is considerably higher background binding with casein with a smaller difference between BSA and milk. Means of duplicate wells +/- SD

3.3.3 Binding of phage to candidate ligands

For these experiments the same streptavidin-binding HPQ motif phage clone was used as a control. This phage was isolated from the same library as the synovial-homing phage and the peptide has the same seven amino acid, disulphide-constrained structure. The sequence, CGTWHPQC, contains the HPQ motif which has been found to be the most frequently-occurring motif in previous panning experiments against streptavidin - indeed, one group found that all isolated sequences contained HPQ (Giebel et al. 1995). Crystal structure analysis of the peptide-streptavidin complex has shown that the HPQ motif occupies the biotin binding site of streptavidin (Weber, Pantoliano, & Thompson 1992). Previous studies have shown that cyclic HPQ-containing peptides have significantly enhanced binding affinity over linear peptides, with K_d values in the range 0.23-78 μM (Giebel et al. 1995). This is several orders of magnitude higher

than the K_d of the biotin for streptavidin (10^{-15} M) and is therefore ideal as a positive control.

The assay detailed in the previous section was repeated with candidate ligands. Both ICAM-1 and fibronectin are up-regulated in rheumatoid synovium and are implicated in adhesion and the recruitment of leucocytes to the inflamed tissue. Fibronectin (isolated from human serum), recombinant human ICAM-1 or streptavidin (positive control) were coated to the plates overnight and blocked with BSA. Phage (3.1 or strep. clone 1) in conjugate buffer containing Tween-20 and BSA were incubated on the plates in decreasing dilutions and the ELISA was completed as above. Binding of the ICAM-1 and fibronectin to the plates was confirmed by incubation with specific antibodies followed by HRP-conjugated anti-mouse immunoglobulin antibody. A separate plate was coated with anti-M13 antibodies prior to incubation with phage and completed as for the other plates: this allowed confirmation and correction if necessary of the phage concentrations. Divalent cations were added to all the ELISA buffers as a number of integrin/ ligand interactions have been shown to be cation-dependent (Shimizu & Mobley 1993).

The results of the fibronectin and ICAM-1 plates are shown in Figure 3.8. The SC1 phage clone was used both as a positive control for binding to streptavidin and a negative control for binding to the candidate ligands. It can be seen that no specific binding is seen for the CKSTHDRLC-expressing 3.1 phage clone to either fibronectin or ICAM-1 or to streptavidin as negative control ligand. On the other hand, as expected, the HPQ SC1 phage clone clearly binds specifically to streptavidin but not to ICAM-1 or fibronectin. These results confirm that the 3.1 phage does not bind ICAM-1 or fibronectin indicating the synovial endothelial receptor(s) represents represent an as yet unknown tissue determinant.

This experiment, therefore, failed to demonstrate any specificity for the 3.1 phage to either of these antigens. Other than there genuinely being no specificity of the phage for the antigens there are two alternative explanations for these results. The

first is the sensitivity of the assays to detect low levels/ low affinity binding. As shown, the background binding of the phage in the first assay could obscure specific binding. With ICAM-1 it is theoretically possible that the monoclonal antibody used for detection and the phage recognise the same binding site on the molecule although this is unlikely. The second explanation is that the expression of the antigens differs in synovial tissue: as already discussed, splice variants of fibronectin are expressed selectively in inflamed synovium. Post-translational modification of ICAM-1 has been described with differential glycosylation demonstrated between cell types *in vitro* (Champagne et al. 1998). There are alternative means, potentially, of investigating phage binding to candidate ligands; however it was decided at this stage to concentrate on identification of the ligand by affinity chromatography which is being pursued as a separate project.

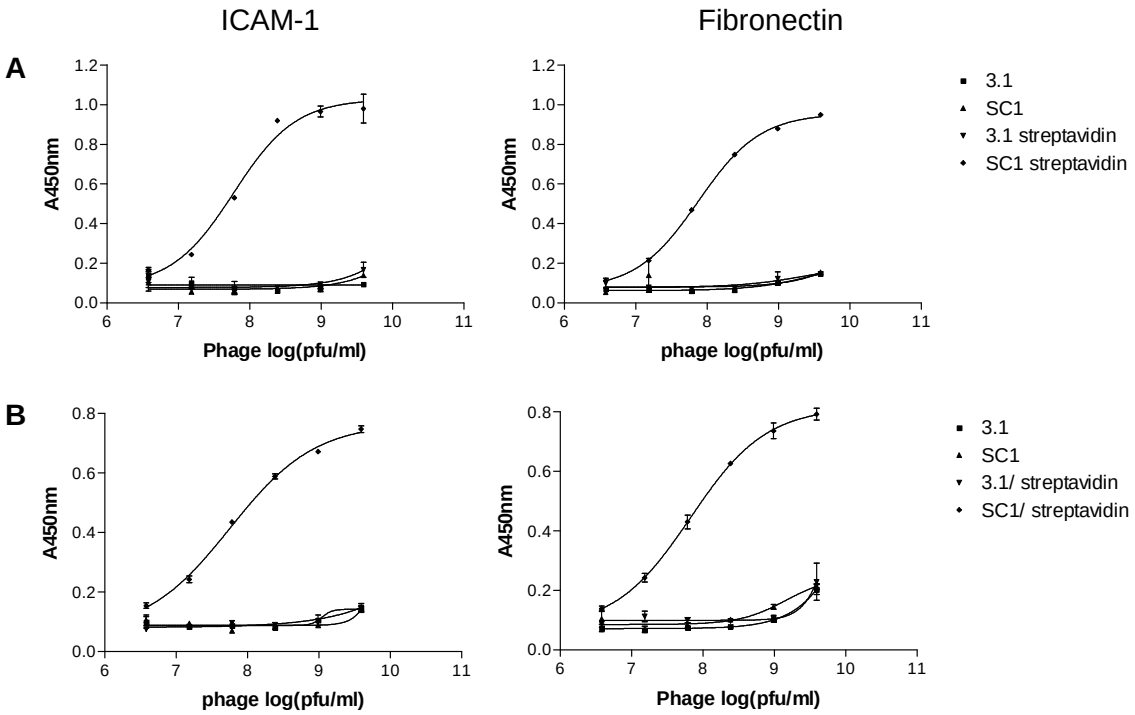

Figure 3.8: **Binding of phage to candidate ligands.** ICAM-1or fibronectin were incubated on 96-well plates overnight at concentrations of 10 μg/ml (**A**) or 1 μg/ml (**B**) with streptavidin as positive control. The plates were incubated with various concentrations of 3.1 or SC1 phage: bound phage were detected with HRP-conjugated anti-M13 antibodies followed by DAB substrate. Mean of duplicate wells +/- SD.

3.4 Summary

In this chapter, importantly, the reproducibility of the model and the specificity of phage clone 3.1 homing to transplanted human synovium compared with control skin tissue was confirmed. In addition it has been shown that intragraft injection of TNFα results in specific upregulation of synovial-specific phage homing at 6 hours post-stimulation and that this reverts to baseline levels after 18 hours. If the synovial ligand is, as hypothesised, a synovial-specific addressin, i.e. a homing receptor for tissue-specific lymphocyte homing, these data suggest a role for the molecule in both routine immunosurveillance as well as in the inflamed states seen in disease. This further emphasises the potential of the synovial receptor as a target, as the enhanced ability to concentrate a targeted compound at a diseased site could further minimise drug toxicity at non-inflamed loci. The observation that similar up-regulation of tissue markers of TNFα-induced stimulation is seen in both skin and synovial transplants confirms the tissue-specificity of the phage-homing response.

Despite the match of the peptide sequence with a sequence contained within the mac-1 integrin binding of phage clone 3.1 to purified recombinant ICAM-1 or purified fibronectin was not seen *in vitro*. Although there may have been limitations in the assay, or alternatively that the phage may be binding to tissue-specific variants of these molecules, these data in association with the demonstrated kinetics of homing up-regulation following TNFα stimulation suggest that these are not the synovial ligands. However, what is known about the ligand profile of mac-1 make it the most promiscuous of the integrins and this would add weight to the possibility that the ligand is an as yet unidentified mac-1 target. Further working is in progress to identify the synovial target for the phage-expressed peptides.

Chapter 4

Development of the SCID mouse chimera model as a tool for imaging transplanted human synovium

4.1 Introduction

A major focus of the work contained in this project was the identification and development of a peptide-based molecule that could be used as an agent for the imaging of inflamed synovial tissue. We therefore took the opportunity to examine whether the SCID mouse model could be further developed as a tool for the assessment of imaging agents. The availability of a SPECT-based imaging technique would not only advance the model in this respect, but could also have further advantages in the assessment of tissue-specific peptide homing. Of these the most obvious would be to enable uptake to be measured in transplanted tissues at sequential time points within the same animal. This would have clear advantages both experimentally in minimising variation between tissue at each of the observed time points, and in limiting the quantities of human tissue ad experimental animals needed for studies.

Over recent years the development of increasingly sensitive small animal imaging systems has enabled closer approximation, in terms of resolution, to human imaging techniques. One of these, the Bioscan NanoSPECT/CT imaging system became available to us towards the end of this project and provided a unique opportunity for the imaging of transplanted human tissue in the SCID mouse model. A further advantage to the use of this system is that it enables quantification of localisation of exogenous radiolabelled molecules at multiple time points in the same animal. This has clear advantages for the assessment of the synovial specificity of peptide-based radiolabelled constructs such as those detailed in chapter 5.

Single-photon emission tomography (SPECT) is a radionuclide-based imaging technique which utilises a pinhole collimator to focus the emitted gamma rays on a detector. The collimator can thus restrict image acquisition to one gamma ray per projection, magnifying the image with resultant enhancement in resolution (King et al. 2002). The use of multiple pin-holes produces multiple projections on a detector maximising use of the detector surface and optimisation of resolution. The NanoSPECT/CT imaging system consists of in-line SPECT and X-ray-based

helical computed tomography (CT) scanners. This enables the construction of 3D images derived from tissue-distribution of radioactivity and conventional CT which can be overlayed: these images can then be used to view and quantify accumulation of activity within specific organs. The SPECT component of the system uses helical scanning in conjunction with four cameras each with multi-pinhole collimators. The resultant available resolution is down to 0.8mm which, for the purpose of our study, is excellent for the imaging of the transplanted human tissues.

The aim of this part of the project was, therefore, to determine whether the tissues could be visualised after administration of an imaging agent, and to see whether differences between specific and non-specific uptake could be detected, with the ultimate intention of using this to evaluate the synovial-homing peptide as a tool for imaging. For this purpose, a murine antibody to human E-selectin, derived from the 1.2B6 hybridoma, was used. This antibody cross-reacts with porcine E-selectin, but not murine and so is suitable for use in this model. The antibody and a scFv fragment have been successfully used to image inflammatory synovitis in human subjects as discussed in the introduction. The antibody was purified from the hybridoma (a generous gift from Professor D.Haskard, Imperial College London) supernatant and modified for radiolabelling. Radiolabelled 1.2B6 or isotype control antibodies were then injected into SCID mice transplanted with human synovium after intragraft injection of TNFα and imaged. The scans were used to quantify the intragraft accumulation of radioactivity and to determine whether specific from non-specific uptake could be resolved.

4.2 Purification of and radiolabelling of antibodies to human vascular endothelial inflammatory markers

4.2.1 DTPA-conjugated antibodies retain affinity for E-selectin

Anti E-selectin antibodies were purified from 1.2B6 hybridoma culture supernatant as detailed in the methods and were the same as those used for the immunofluorescence staining in section 3. 1.2B6 and isotype control antibodies

were derivatised by conjugation to DTPA to allow radiolabelling with ^{111}In and washed in ultrafiltration columns until absorbance at 280nm of the filtrate was zero indicating removal of unbound DTPA: concentration of the final product was determined by spectrophotometry. It was important to confirm that immunoreactivity of the conjugated antibody was retained after DTPA conjugation: the affinity of the conjugated and unconjugated antibodies for immobilised E-selectin were therefore compared by ELISA. The results of this experiment are shown in Figure 4.1a. A clear dose-response curve is seen for both DTPA-conjugated and unconjugated antibodies with similar binding curves. Non-linear regression analysis of the data allowed the EC50 of each antibody to be compared; these were 0.142 and 0.1408 μg/ml for the unconjugated and conjugated antibodies respectively and were not significantly different. No significant immunoreactivity was seen with an isotype control antibody. These data confirm that DTPA conjugation has no effect on immunoaffinity of 1.2B6 mAb for E-selectin.

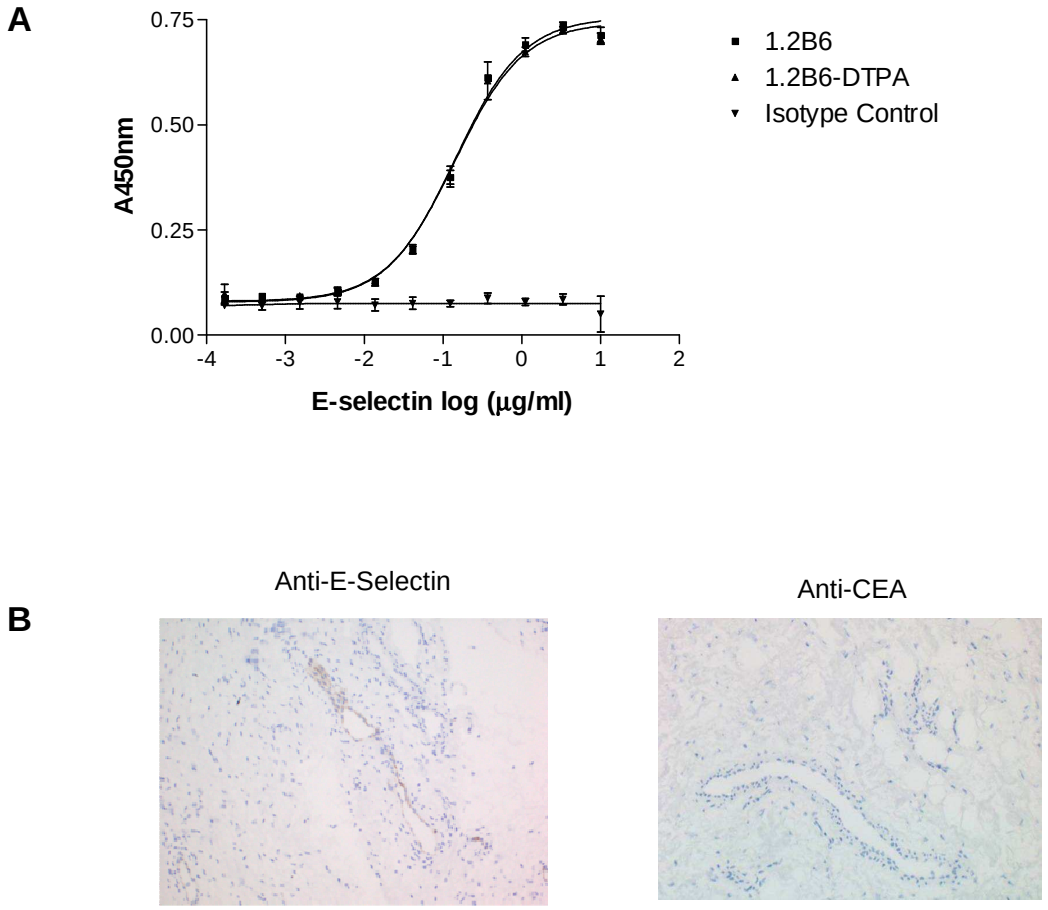

Figure 4.1: **A Immunoaffinity of antibody before and after conjugation to DTPA.** An ELISA plate was coated with E-selectin in reducing concentrations and incubated with purified anti-E-selectin (1.2B6) antibody before and after DTPA conjugation or an IgG_1 isotype control. No difference is seen between the binding curves of the anti-E-selectin antibodies and non-linear regression analysis confirmed identical EC50 values. No specific immunoreactivity was seen with an isotype control antibody. Mean of duplicate wells +/- SD.

B Immunohistochemical staining of human RA synovial tissue with anti E-selectin and control antibodies. RA tissues sections were incubated with the same concentration (5 µg/ml) of anti-E-selectin or anti-CEA antibodies. A HRP-conjugated anti-mouse immunoglobulin secondary antibody was used and developed with DAB substrate. No specific binding was seen on the anti-CEA section, specific staining of vessels is seen with anti-E-selectin. Original magnification x20.

4.2.2 Anti-CEA antibodies do not bind synovial tissue sections

In order to confirm immunoreactivity on inflamed synovial tissue, frozen RA tissue sections were stained with equal concentrations of anti E-selectin or isotype-matched anti-CEA antibodies which were to be used as controls. E-selectin expression by vascular endothelial cells is up-regulated in the synovium of patients with RA and RA tissue was therefore used to examine binding of anti-E-selectin antibodies to activated synovial endothelial cells. Representative sections are shown in Figure 4.1B. As expected, specific staining of vessels is seen for E-selectin: expression is restricted to the vascular endothelium which is in keeping with the known expression pattern of E-selectin. No specific staining could be seen with the anti-CEA antibodies either on endothelial cells or elsewhere within the synovial tissue section thus confirming its suitability as a negative control.

4.2.3 Radiolabelling and purification of ^{111}In-antibodies

The conjugation of DTPA to the antibody allows easy labelling with ^{111}In by incubation with $^{111}InCl_3$ at pH 6.0 for 30 minutes. In human studies the injected dose was around 35μg of DTPA-F(ab')$_2$ and therefore in mice we wanted to inject the minimum that the specific activity would allow. To investigate the maximal specific activity reducing concentrations of DTPA-1.2B6 were labelled with ~5 MBq of ^{111}In. The proportion of free ^{111}In was then determined by instant thin-layer chromatography (ITLC) with or without reverse-phase high-performance liquid chromatography. The results, shown in Figure 4.2, show that 5 μg could be labelled with efficiency approaching 100%, below this there was a substantial loss of specific labelling. It was found that the radiochemical purity following the labelling reaction was somewhat variable. As we were trying to achieve maximum specific activity the process was sensitive to the quality of the radiochemical stock- labelling efficiency did tend to deteriorate during the week, probably due to a combination of decay and trace metal contamination of the stock. Therefore, as much as possible, labelling was done at the beginning of the week. If labelling fell below 95% a size-exclusion spin column purification step was used after which purity was >99%. Representative RP-HPLC chromatograms are shown in Figure

4.2. The large single peak seen with 280 nm absorbance confirms purity of the antibody (Figure 4.2A). A single peak of radioactivity is also seen confirming >99% conjugation of ^{111}In to the antibody.

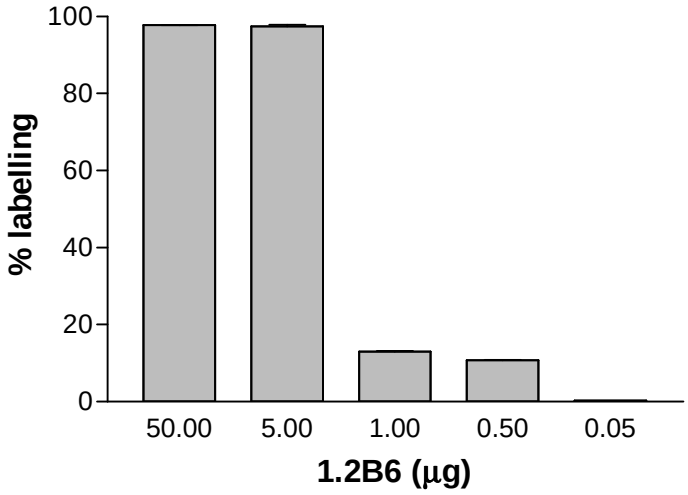

Figure 4.2: **Radiolabelling efficiency of 1.2B6 (anti-E-selectin) antibodies**. 1.2B6 antibody was diluted as indicated in 50 µl 0.1 M ammonium acetate buffer and incubated with 5 MBq ^{111}In for 30 minutes at room temperature. The reaction was stopped by the addition of 10% volume 50 mM EDTA and radiochemical purity determined by instant thin layer chromatography in duplicate. % labelling indicates the proportion of ^{111}In bound to antibody. The optimum specific activity achieve was 1 MBq/µg. Mean +/- SD.

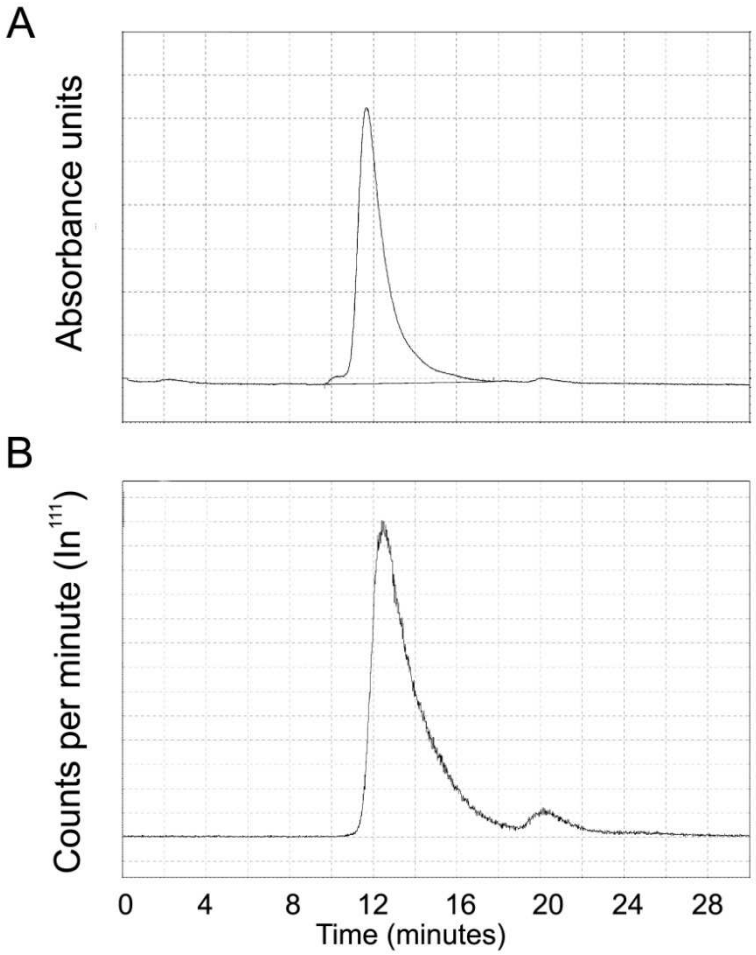

Figure 4.3: **Radiolabelling of DTPA-conjugated antibodies.** Size-exclusion high-performance liquid chromatograms of 1.2B6 antibody after purification and conjugation to DTPA (**A**, absorbance at 280nm) and after radiolabelling with ^{111}In (**B**, radioactivity in counts per minute).

4.3 Synovial tissue grafts are visible on SPECT scan after intravenous administration of ^{111}In-antibodies

The aim of imaging experiments was to determine whether the NanoSPECT/CT imaging system could be used to visualise uptake of a systemically administered radiolabelled compound and, furthermore, to discriminate specific from non-specific uptake. As discussed in the introduction, the neoangiogenic vessels of inflamed synovium are hyperpermeable: this has been successfully exploited for the purposes of imaging with non-specific agents, but has also hampered the search for more specific imaging agents.

SCID mice were double-transplanted with human synovial tissue. Two-three weeks after transplantation, the synovial grafts were injected with rhTNFα to stimulate expression of E-selectin by human endothelial cells. After 5 hours the mice were injected intravenously with 2-4 MBq ^{111}In-labelled 1.2B6 (2-5 μg) or isotype control mAb (3.5-6.5 μg), with a slightly higher quantity of control antibody due to lower specific activity. After 1 hour and at 4, 24 and 48 hours mice were anaesthetised and imaged by in the NanoSPECT/CT imaging system. At the end of the experiment the transplanted organs were retrieved for weighing and measurement of radioactivity in a gamma counter.

Fusion images of the CT and SPECT scans clearly identified the transplanted tissues: this enabled quantification of uptake at all time points. Representative SPECT/CT fusion images of ^{111}In-1.2B6 injected animals are shown in Figure 4.4: there is clear definition of the transplants with respect to background allowing acceptable delineation of the transplants for quantification. The 3D reconstruction (Figure 4.4A) shows uptake of the ^{111}In-labelled 1.2B6 mAb clearly visible in the transplants at 24 hours. Saggital and transverse sections (Figure 4.4B) taken at 1 and 24 hours show a clear increase in uptake of the radiolabelled antibody between the two time points. This indicates that the SCID mouse transplantation model is suitable for visualisation of antibody localisation *in vivo* to RA synovium at multiple time points.

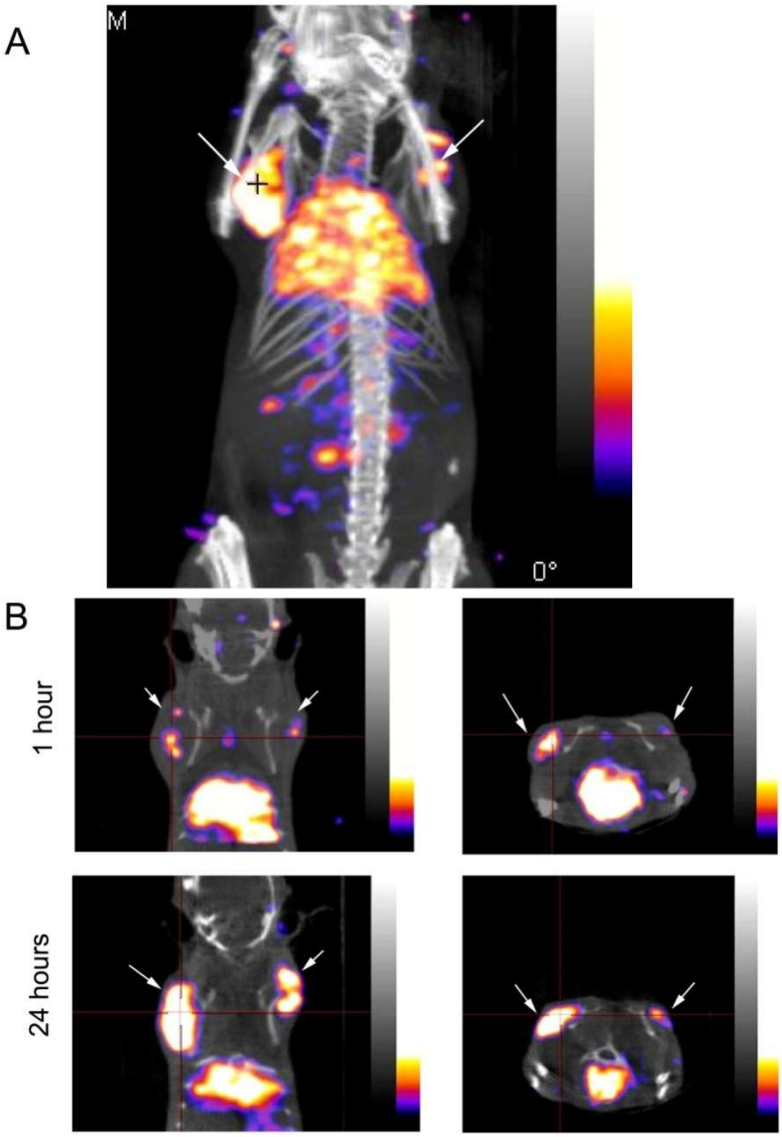

Figure 4.4: **Visualisation of transplanted synovial tissue by CT/ SPECT imaging** .CT/SPECT images of a double-transplanted mouse injected with ^{111}In 5 hours post-intragraft injection of rhTNFα. Images shown are full body 3D reconstruction at 24 hours (**A**) coronal and saggital projections at 1 and 24 hours (**B**). The CT image is in greyscale and the colours represent radioactivity from low (dark) to high (white).The transplanted tissues are indicated by the white arrows.

4.4 Significant correlation between synovial graft activity on SPECT and *ex vivo*

The NanoSPECT/CT system allows, following image reconstruction, for the quantification of activity in defined regions. This has the substantial advantage of enabling assessment of uptake in a transplant at multiple time points in the same animal. However, the small animals SPECT/CT imaging technology is relatively new and relatively little has been published to date. The accuracy of the NanoSPECT/CT for the quantification of tissue uptake of radioactivity has been published in abstract form (Gershman et al. 2007). This study used standards of known activity: there are to date no publications examining the correlation between activity of tissues as measured by NanoSPECT and activity *ex vivo*. I therefore wanted to validate the quantification of graft uptake of an injected dose of radioactivity by comparing uptake as quantified from the SPECT scan with that of the *ex vivo* grafts as measured in a gamma counter. For the quantification experiment grafts were injected with TNFα five hours prior to the administration of ^{111}In-1.2B6 or control antibody in order to up-regulate E-selectin expression by the microvascular endothelium. NanoSPECT/CT images were acquired at 1, 4, 24, and 48 hours: at the end of the experiment the transplanted tissues were retrieved were weighed and the SPECT-quantified activity plotted against that measured in the gamma counter. The results of the linear regression analysis are shown in Figure 4.5: highly significant correlation is significant with an r^2 of 0.982. This validates the data acquired from this experiment for the quantification of the graft uptake activity at multiple time points in single animals.

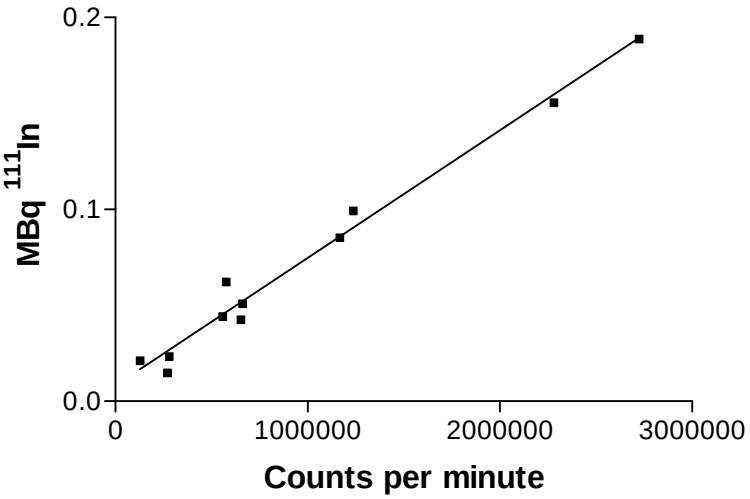

Figure 4.5: **Correlation between SPECT-determined graft activity and *ex vivo* activity measured in the gamma counter**. Synovial transplant activity derived from *in vivo* SPECT imaging was plotted against counts per minute measured of *ex vivo* transplants in a gamma counter. There is significant correlation (r^2 of 0.982) between the gamma counter and SPECT data: this confirms the suitability of imaging under these conditions for the quantification of graft uptake of radioactivity.

4.5 Significantly greater uptake of anti-E-selectin antibody vs. anti-CEA is seen 24 hours post-injection

Uptake of radioactivity in each of the two synovial grafts was measured at 1, 4, 24, and 48 hours in each animal. CT/SPECT fusion images were produced using the proprietary software and a region of interest drawn around the transplants. The activity within the area was corrected for the weight of the grafts, which were retrieved after the animals were killed at 48 hours, and for the injected dose. Finally, the results were corrected for the decay factor for the time between injection of the radioisotope and acquisition of the images. The results (shown as % of the injected dose per gram of tissue plotted against time) are shown in Figure 4.6 and it can be seen that there are significant differences in graft uptake between the anti-E-selectin and isotype control antibodies at 4 and 24 hours ($p=<0.05$). The difference did not quite reach significance at 1 hour ($p=0.054$) and there was a non-significant trend in favour of E-selectin at 48 hours ($p=0.14$). Altogether, these experiments validate this model for the testing of ‘discovery’ reagents as imaging or delivery systems to human tissues.

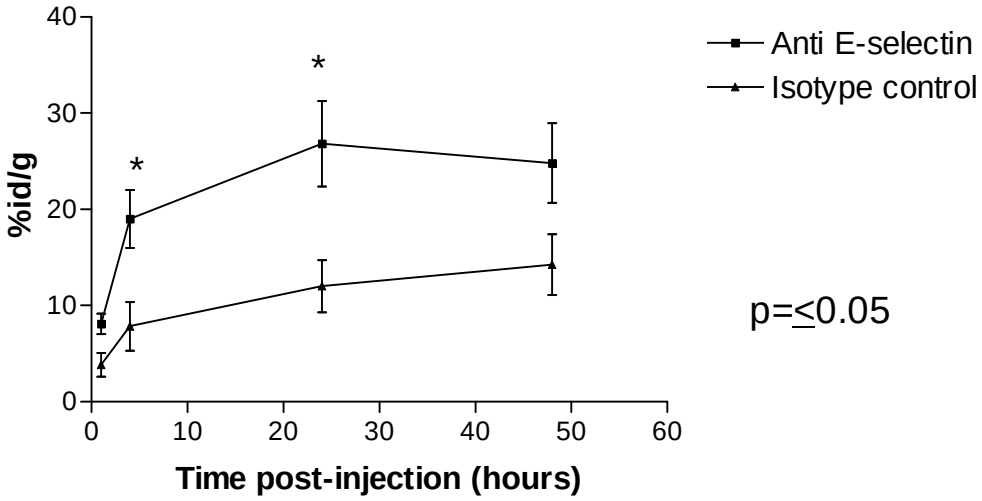

Figure 4.6: **Uptake of injected ^{111}In-labelled anti-E-selectin or control antibodies into transplants after intravenous injection.** SPECT quantification of graft uptake of ^{111}In-labelled anti-E-selectin (1.2B6) and isotype control antibodies at 1, 4, 24 and 48 hours. Human synovial tissue grafts transplanted into SCID mice were injected with TNFα 5 hours prior to intravenous administration of radiolabelled antibody. Mice were scanned at the indicated time points and the transplanted tissues retrieved at the end of the study. 3 mice per group, n=6 transplants (1.2B6), 5 transplants (control). Results are shown as % injected dose per gram of tissue. Mean +/- SEM.

4.6 Summary

The results presented in this section demonstrate that the SCID mouse transplantation is a powerful novel tool for the imaging of human synovium in a pre-clinical model. Although there are published reports of the imaging of arthritis models in animals their application to the testing of human-specific reagents may be limited by species-specific restriction of the reagent. This is exemplified by the anti E-selectin antibody used in this study which, although cross reactive with porcine E-selectin, is not immunoreactive with the murine epitope. A further significant advantage of the model is the capacity to quantify graft uptake at multiple time-points in the same animals, minimising variation in results arising due to differences between individual transplants and donors. This also enables the maximisation of resources of human tissue which are finite, and increases the total number of samples per study.

Purified 1.2B6 antibody was shown to be immunoreactive with vessels in RA synovial frozen tissue sections and with immobilised E-selectin by ELISA. Furthermore, no difference in immunoreactivity between unconjugated and DTPA-conjugated antibodies: DTPA is conjugated via the ε-amino group of lysine residues within the protein and thus could potentially affect reactivity by binding critical lysine residues within the ligand binding domain.

Uptake of both the 1.2B6 and isotype control antibodies was seen at all time points in the TNFα-treated transplants. The substantial uptake seen of the control antibody underlines the difficulties with achieving specific uptake on a background of graft hyperpermeability. Several imaging agents have been used which successfully exploit vascular hyperpermeability in inflammatory synovitis including non-specific immunoglobulin (Berna et al. 1992). As discussed in the introduction, the use of specific agents have been met with variable success, enhanced uptake being often found to be due to non-specific mechanisms: only 25% of joint uptake after administration of a ^{99m}Tc-labelled anti-TNFα antibody was found to be specific (Barrera et al. 2003). A recent case report suggested the

use of radiolabelled anti-TNFα for the monitoring of response to intra-articular anti-TNFα (Conti et al. 2005): it is not clear how much of an advantage this might be over a non-specific agent, or whether it is a sensitive tool for the assessment of intra-articular levels of TNFα.

Larger particles such as liposomes (Dams et al. 2000) have also been used with some success in a limited number of patients. ^{99m}Tc-labelled nanocolloid, a denatured human albumin which forms particles of up to 80nm, has been investigated as a tool for the imaging of joint inflammation. In a series of 59 patients with arthralgia ^{99m}Tc-nanocolloid scintigraphy detected 82% of clinically involved joints, positive uptake was also seen in the joints of 3 clinically negative patients (Adams 2001). More recently, Palosaari *et al* compared ^{99m}Tc-nanocolloid scintigraphy and MRI at the wrist joint in patients with early RA (Palosaari et al. 2006). Scintigraphic uptake at the joint was associated with the development of erosions at 2 years, although the predictive value, or whether this was more sensitive than clinical scoring, was unclear. Furthermore the correlation between MRI and scintigraphic progression was not explored.

It remains unclear, therefore, whether the use of non-specific radioisotope imaging modalities offer any real advantages over clinical measures. Hence there remains considerable potential for more specific imaging agents which may have greater sensitivity and predictive utility. Imaging E-selectin expression is therefore of considerable interest, and has been shown in a small number of patients to have greater sensitivity over non-specific immunoglobulin. This may be in part due the internalisation of antibody after ligation of E-selectin: evidence from *in vitro* internalisation studies has shown that ligation of E-selectin by antibody results in internalisation of the complex, an effect not seen with ligation of ICAM-1 by antibody (von Asmuth et al. 1992). E-selectin therefore has significant potential as an agent as an imaging for inflammatory arthritis: such specific imaging has the possible advantages of offering more sensitive prognostic assessments of patients with early arthritis.

Of particular relevance to this project is the demonstration that despite the clear levels of non-specific uptake of antibody demonstrated here, the SCID mouse transplantation model has the power to detect differences in specific versus non-specific uptake. Furthermore it has been shown here that targeted molecules can offer higher selectivity in the targeted delivery of radioisotopes: these findings are pre-requisite for the application of small peptides to this, which are discussed in the next chapter.

Chapter 5

Investigation of tissue specificity of the synovium-homing monomeric peptide *in vitro* and *in vivo*

5.1 Introduction

The identification of a small peptide sequence which confers synovial specificity for the 3.1 phage has two major potential applications. Firstly, conjugation to radionuclides could enable its use as an imaging agent: as discussed in the introduction, molecular imaging has several possible advantages over conventional modalities in inflammatory arthritis. Principal of these is the visualisation of the disease process itself as opposed to surrogate markers such as bone erosions, synovial fluid and oedema. This could therefore have the advantages of enhanced specificity for synovial inflammation with consequent earlier diagnosis and the significant prognostic advantages that this may offer. Furthermore, imaging of molecules implicated in the disease process could enable earlier detection of response to therapy: again, in view of what is now understood about the benefits of early aggressive treatment, this could be crucial in ascertaining the efficacy of a particular therapeutic regimen. Second is the application of the peptide as a targeting molecule for therapeutic compounds, either in the form of directly conjugated molecules or for larger particles, such as liposomes, which can deliver a larger payload. Conventional (non-biological) disease-modifying therapy is still limited in its use by substantial systemic toxicity: specific targeting of these drugs could widen the therapeutic index by concentrating the drug at the site of action, with implications for efficacy and, by extension, cost. Although the synovial receptor for the peptide is unknown it was shown in Chapter 3 that its expression is likely to be upregulated by TNFα, and that this effect was specific to the synovium as it was not seen in human skin. This suggests that the receptor may be up-regulated in inflamed synovium further enhancing the selectivity of the peptide.

The aims of this chapter were to investigate whether the peptide retains its specificity for synovial tissue in its monomeric form independently of the phage. For this several strategies were adopted: binding to synovial tissue sections was tested with peptide conjugated to fluorochromes and analysed by microscopic techniques. For *in vivo* homing the peptide was conjugated to radionuclides by a

variety of means: radioisotope labelling has the greatest sensitivity of *in vivo* techniques and has the advantage of allowing the injection of sub-micromolar quantities of peptide. These conjugates were tested *in vivo* against control peptides or human skin transplant controls: the *in vitro* stability and protein binding of the ^{99m}Tc-conjugated peptides were tested and the effect of alternative labelling chemistries determined. Finally, as it was noted that uptake of peptide to both transplanted tissues was generally high, the permeability of the vascular endothelium of the transplanted human tissues was explored.

5.2 Binding of fluorochrome-conjugated peptide to human synovial tissue sections

Fluorochrome-conjugated cyclic peptides CKSTHDRLC synovial-binding sequence (hereafter referred to as 3.1 peptide) and CGRYDHPQC control streptavidin binding sequence (hereafter referred to as SC7) were incubated on RA or OA synovial tissue sections and counterstained for human vessels by staining for human vWF. Human vessels counterstained for von Willebrand factor were identified under fluorescence microscopy and assessed for peptide binding in the FITC spectrum. No difference was seen between the 3.1 or control peptides at any of the concentrations; at the higher concentrations widespread non-specific binding was seen and, as seen in the digital fluorescence analysis, at 10 μg/ml fluorescence approached saturation. These findings were supported by results from digital image analysis in which, again, no consistent significant differences were seen (Figure 5.1). The findings were similar for both RA and OA tissue sections with no consistent differences seen at any peptide concentration: at the lower concentrations fluorescence approached background levels (shown as 'control' sections imaged with no peptide stain) with a linear increase with increasing concentration. Thus no specific binding of the 3.1 peptide was seen in these experiments.

There are several potential explanations for the failure of these experiments to demonstrate specific binding. Firstly is the sensitivity of the assay: direct visualisation of fluorochrome-conjugated peptide may be insufficient to detect

specific binding at lower concentrations; the increase in both test and control peptide vessel fluorescence at higher levels suggests that under these conditions the binding seen is non-specific. Secondly, the optimal conditions for peptide binding are not known: these experiments were repeated with and without protein-blocking steps, and with different fixative techniques with no difference noted in the results- the possibility that the tissue ligands denatured in the fixing process cannot be excluded. Furthermore, as is discussed in more detail later in this thesis, the physiological conditions required for binding, such as the presence of divalent cations, may not be optimal. Thirdly, as already discussed, the phage are likely to be identifying ligands expressed at the luminal surface of the synovial vessels: this, therefore, does not exclude the possibility that the ligand is expressed in the extravascular space- if this were so identification of contrast between vessels and extravascular difficult may be difficult if specific binding were achieved. Fourthly, the charges of the peptides at pH 7.4 differ and this may affect the non-specific binding properties seen on tissue sections, possibly favouring the control peptide. The control peptide sequence was originally selected as it was a streptavidin-binding peptide sequence that was used in the original phage experiments; in later experiments detailed in Chapters 6 and 7 a scrambled sequence was used with the same charge as the 3.1 peptide sequence. Finally the possibility remains that the monomeric peptide has lost the some or all of its binding affinity when expressed by phage- this concept will be returned to later.

For these reasons experiments with the monomeric peptide were concentrated on the *in vivo* model as described in the remainder of this chapter.

Figure 5.1 (next page): Digital fluorescence analysis of human vessels in RA synovial tissue sections stained with FITC-peptide. Tissue sections were incubated with FITC-conjugated 3.1 or control peptide and counterstained for the human endothelial cell marker vWF. The vWF staining was used to create a mask to exclude non-endothelial cell tissue in which the FITC fluorescence levels were quantified. **A** Fluorescence levels for a variety of peptide concentrations: no significant differences were seen between the 3.1 and control peptide (3-5 fields per condition). **B** Further analysis at peptide concentrations of 5 and 2.5μg/ml on sections from a different donor. There was a small but significant difference in favour of the control peptide at the lower concentration. After correction of each field for background fluorescence this difference disappears (**C**). (6-12 fields per condition). Mean +/- SEM

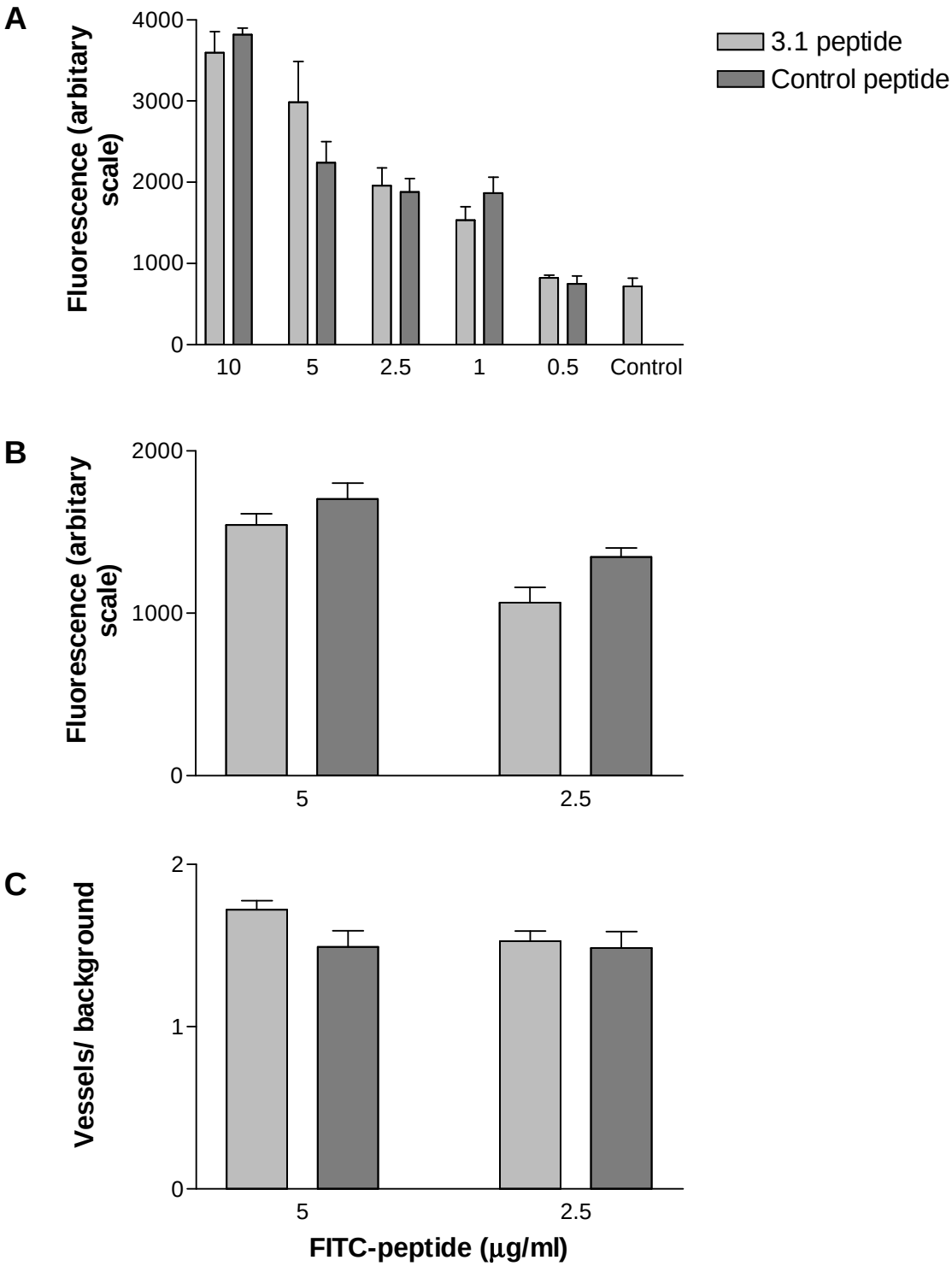
A
Fluorescence (arbitary scale)
4000
3000
2000
1000
0
10
5
2.5
1
0.5
Control
3.1 peptide
Control peptide
B
Fluorescence (arbitary scale)
2000
1000
0
5
2.5
C
Vessels/ background
2
1
0
5
2.5
FITC-peptide (µg/ml)

5.3 Conjugation of monomeric peptides to radioisotopes and investigation of *in vivo* homing specificity

5.3.1 Labelling of DTPA-conjugated monomeric synthetic peptides with ^{111}In

Diethyltriaminepentaacetic acid (DTPA) is a bifunctional chelating agent which is routinely used in clinical practice to label small peptides for imaging; the most frequently used of these is DTPA-octreotide. Its polydentate chemistry ensures stability of the conjugated radiolabel under physiological conditions making it suitable for *in vivo* use (Liu & Edwards 2001). The structure of the ^{111}In-DTPA complex is illustrated in Figure 5.2**A**. DTPA-3.1 and DTPA-control (streptavidin-binding) peptides were labelled with ^{111}In as described in the methods. Instant thin-layer chromatography (ITLC) allows fast assessment of the efficiency of the radiolabelling reactions and was used in all the experiments described here prior to *in vivo* experiments.

In a preliminary experiment 4 MBq of ^{111}In was added to 0.8 mg peptide or to solution containing no peptide. The results shown in Table 5.1 show, as expected, that ^{111}In chelated to the DTPA-peptide remains at the origin whilst unbound ^{111}In migrates with the solvent front, thus confirming the validity of the ITLC method.

	Peptide	No peptide
Origin	58984	1667
Solvent front	555	27833
% at origin	99.07	5.65

Table 5.1: ITLC results of 0.8 mg DTPA-3.1 peptide or control solution after incubation with 4 MBq ^{111}In.

In a further experiment, 0.1 mg of DTPA-3.1 peptide was labelled with 3 MBq or 9 Mbq of ^{111}In. ITLC was performed immediately and after 6 hours of incubation at room temperature in order to confirm stability of the ^{111}In conjugation over time. The results are shown in Table 5.2: >90% labelling is still present after 6 hours at RT. Extension of this experiment to 24 hours showed significant loss of labelling beyond this point: these results are shown in Figure 5.2**B**.

	Activity	
Hours	3MBq	9MBq
0	98.4%	92.9%
6	98.3%	93.0%

Table 5.2: Percentage of ^{111}In bound to DTPA-3.1 pep as quantified by instant thin layer chromatography.

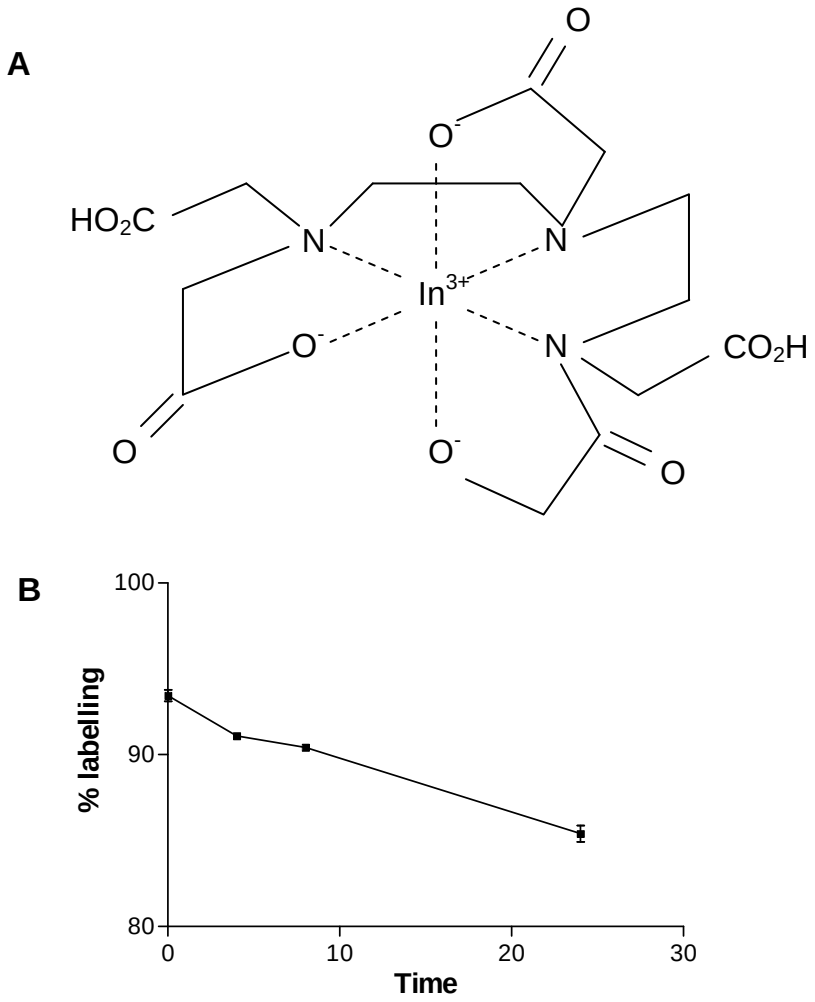

Figure 5.2 Radiolabelling and stability of ^{111}In-labelled peptide A The DTPA co-ordination complex with In^{3+}. **B** Stability of ^{111}In-labelled DTPA-peptide at room temperature over 24 hours: peptide was labelled with ^{111}In and the proportion of free ^{111}In determined at each time point by ITLC with acid citrate dextrose as solvent.

5.3.2 In vivo studies with ^{111}In-labelled 3.1peptide

5.3.2.1 ^{111}In DTPA-3.1 peptide versus free indium

As a preliminary experiment the *in vivo* biodistribution of radiolabelled 3.1-peptide was compared with free indium, as at this stage of the project only the 3.1 peptide was available for use. 200 µl of peptide was labelled with 0.2 MBq of ^{111}In for injection into each animal. For this and all subsequent experiments animals were injected within 2 hours of radiolabelling, with initial radiolabelling efficiency being >98%. The control animals were injected with the same activity of ^{111}In in vehicle. Two animals were used for each condition, each of which was transplanted with 2 synovial grafts. After injection of the peptide the animals were incubated for 15 minutes prior to perfusion of the circulation and retrieval of organs and transplanted tissues.

The results of the biodistribution study are shown in Figure 5.4**A**. There are clear differences between the organ distribution of the peptide-conjugated and unconjugated ^{111}In, with significant differences as indicated and significantly greater homing of the peptide-conjugated ^{111}In to synovium. This obviously does not imply specificity as the size and charge of the molecule can have major influences on behaviour *in vivo.* The experiment was therefore repeated with a control-sequence peptide.

5.3.2.2 ^{111}In test vs. control peptide

For these experiments the streptavidin-binding SC7 peptide was conjugated to DTPA and used as an irrelevant control. Labelling of DTPA-peptide was carried out as before by the addition of 0.2 MBq ^{111}In/ 200 µg peptide. Radiolabelling efficiency of the peptides for this experiment as determined by ITLC is detailed in Table 5.3. Labelling of the SC7 peptide was a little less efficient, although at >90% this was felt sufficient for the *in vivo* study.

Peptide	Radiolabelling
3.1	96.8%
SC7	93.6%

Table 5.3: **Radiolabelling efficiency of peptide as measured by ITLC for use in second *in vivo* experiment.** Results shown are the mean of duplicate tests.

For the biodistribution experiment double-transplanted mice (5 injected with 3.1 peptide and 4 with SC7 peptide) were injected as before with 200 μg peptide with, after 15 minutes incubation, perfusion of the systemic circulation and retrieval of tissues. The results are shown in Figure 5.4**B**. No significant difference is seen between the test and control peptides, or between skin and synovium for either peptide, or between synovium and skin. There are a number of potential explanations for the failure of this experiment to demonstrate selective homing of the 3.1 peptide. The first of these lies with the conjugation of the peptide to DTPA. Although HPLC suggested the presence of a pure product, MS analysis showed the presence of unconjugated peptide (Figure 5.3). It is possible, therefore, that if DTPA conjugation reduces the affinity of the peptide for its receptor that the unconjugated peptide competitively inhibited ^{111}In, and hence detectable, binding. Secondly, the injected dose may have been saturating specific receptors: as illustrated in Figure 5.5, once the saturating dose is exceeded non-specific binding is responsible for a linear increase in the total tissue concentration with consequent diminishment of the sensitivity of the assay to detect specific uptake. Although the injected dose (200 μg) of peptide was the same as that needed to maximally inhibit phage homing in previously described experiments (Lee et al. 2002) the affinity of the phage for the receptor may well be significantly in excess of that of the peptide, at least in part due to the polyvalent presentation of peptide on the phage. Both of these issues were addressed by the use of ^{99m}Tc in the labelling of peptides for subsequent experiments.

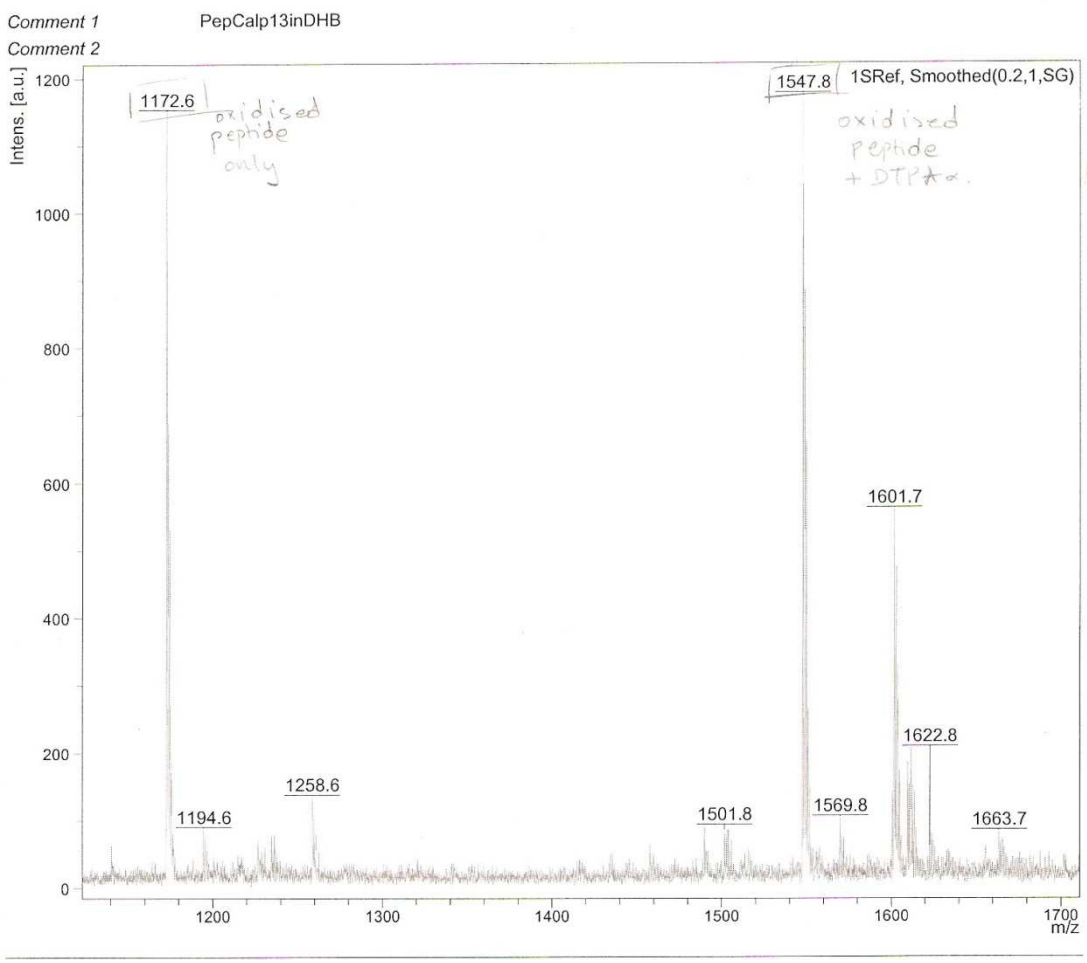

Figure 5.3: MALDI-TOF MS analysis of DTPA-peptide. The two major peaks correspond to the synovial-homing peptide with and without conjugated DTPA, confirming the presence of unconjugated peptide in the final product.

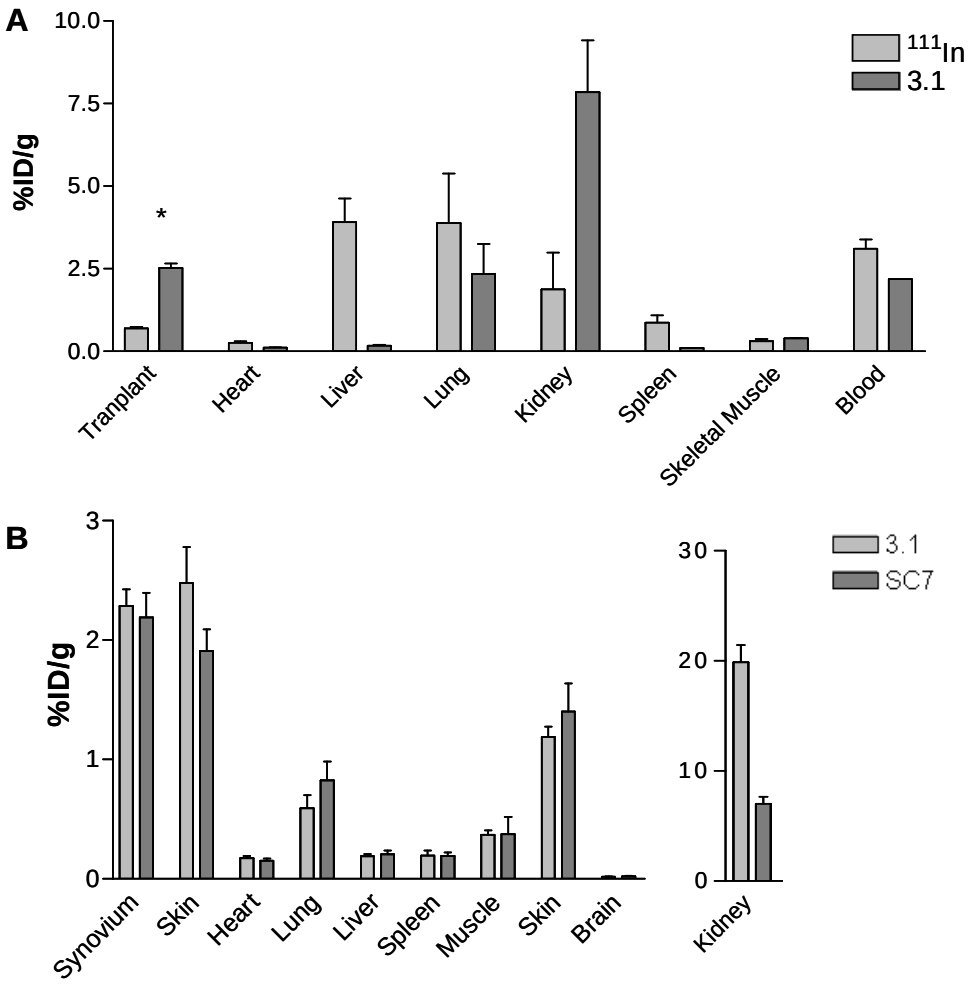

Figure 5.4: *In vivo* biodistribution of ^{111}In-labelled peptides. A SCID mice transplanted with human synovium were injected with ^{111}In-labelled 3.1 peptide or free ^{111}In. After 15 minutes the circulation was perfused with 0.9% saline and the transplants and murine organs retrieved: a significant difference ($p=<0.05$) was seen in homing to the transplants between peptide and ^{111}In (n=8 transplants per group). There are clear differences in the biodistribution of the 2 agents. **B** SCID mice transplanted with human synovium and skin were injected with ^{111}-labelled $^{3.1}$ peptide or SC7 peptide and perfused after 15 minutes incubation as above. No significant difference is seen between homing of the peptides to skin or synovium. Differing uptake by the kidney is likely to represent differences in charge between the peptides. n=4 animals/ 8 transplants per group.

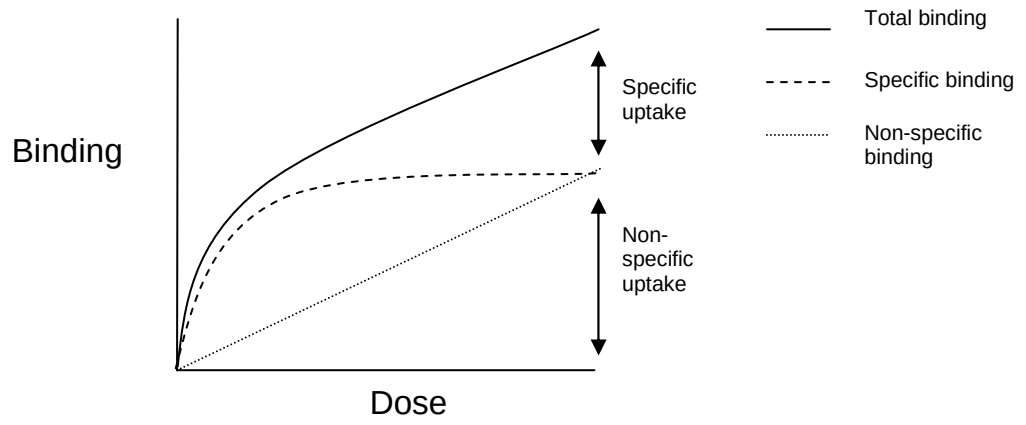

Figure 5.5: Graphical illustration of the contribution of specific and non-specific binding to tissue concentration of peptide. Non-specific binding increases in a linear fashion: as specific binding becomes saturated the proportion of tissue uptake attributable to specific binding diminishes as the administered dose is increased with progressive reduction in the sensitivity of the assay to detect specific uptake.

5.4 Labelling of synovial homing peptides with ^{99m}Tc

Although labelling of the DTPA-peptides was simple and efficient, the isotope had to be obtained commercially: as it has half-life of 2.6 days it was expensive to do repeat experiments. For the studies detailed in the previous section mice were injected with 20 0µg peptide: this was because at this dose it has previously been shown that homing of phage to the synovial transplants can be inhibited. However, it is possible that at this injected dose specific binding is saturated and specific uptake is not detected due to the level of non-specific homing of both peptides. Two alternative labelling strategies were attempted. First of these was the labelling of tyrosine residues with ^{125}I: this has the advantage that as it labels native tyrosine residues large artificial chelating molecules need not be conjugated to the peptides with, theoretically, minimal disruption to the overall structure of the peptide. The control sequence already contains a tyrosine residue; as the 3.1 peptide does not, a tyrosine residue was conjugated to the N-terminus of the peptide after a 6-aminohexanoic acid spacing group. The peptides were labelled using the Iodogen method (Butler, Lam, & Fisher 1984) and labelling assessed, as previously, with RP-HPLC. The *in vivo* experiments did not demonstrate any

significant difference between homing of the test or control peptides to skin or synovium: however, following the labelling reaction several species were seen on the chromatograms, with the largest peak responsible for <90% of the total radioactivity. It was therefore felt that these results were difficult to interpret and the use of ^{125}I labelling was abandoned (data not shown). A further disadvantage of radioiodination for imaging studies is that following internalisation and lysosomal degradation, iodinated tyrosine may be rapidly removed from cells and subsequently de-iodinated in the liver. Thus the use of 'residualising' labels, such as ^{111}In-DTPA or ^{99m}Tc-HYNIC can result in longer retention of the tracer by the target tissue and hence better target-to-background ratios (Gotthardt et al. 2004). For future experiments it was decided to switch to ^{99m}Tc. This isotope is the most commonly used in clinical practice: it is usually produced on-site and is therefore freely available at low cost. ^{99m}Tc is the metastable nuclear isomer of the ^{99}Tc ground state: it emits monochromatic 140keV photons which enable excellent spatial resolution for imaging. The 6-hour half-life enables relatively large activities to me administered more safely than with other isotopes. It is produced from the parent radionuclide ^{99}Mo in a ^{99m}Tc-^{99}Mo generator: ^{99m}Tc is eluted with saline in the form ^{99m}Tc pertechnetate (Liu, Edwards, & Barrett 1997).

6-Hydrazinopyridine 3-carboxylic acid (HYNIC) is a bifunctional chelating agent frequently used for the radiolabelling of proteins and peptides with ^{99m}Tc. For the labelling reaction TcO_4^- is added to solution of peptide, $SnCl_2$ and a co-ligand. The $SnCl_2$ acts as a reducing agent, reducing the $^{99m}Tc^{7+}$ to the oxidation state $^{99m}Tc^{4+}$. As HYNIC only contains one co-ordination site a co-ligand, such as tricine, is necessary to form the stable octahedral complex.

5.4.1 Labelling with ^{99m}Tc

HYNIC-peptide was labelled with ^{99m}Tc and tricine as co-ligand as detailed in the methods. There are several potential impurities following the labelling reaction, these being free $^{99m}TcO_4^-$, ^{99m}Tc-tricine and insoluble ^{99m}Tc colloid. Three ITLC conditions were used to resolve these, 2-butanone to separate $^{99m}TcO_4^-$, PBS to separate ^{99m}Tc-tricine and 50% acetonitrile for ^{99m}Tc colloid.

Results with 2-butanone and PBS were satisfactory, and showed that the majority of unbound ^{99m}Tc was in the form ^{99m}Tc-tricine. However, most of the activity remained at the origin of the strips with 50% acetonitrile with the 3.1 peptide, with increasing the concentration to 80% making little difference. The possible reasons for this were two-fold: firstly it was possible that all the ^{99m}Tc was in the form of the insoluble colloid or alternatively there was little motility of the peptide with the solvent. To resolve this, the labelled peptide was analysed by reverse-phase high-performance liquid chromatography (RP-HPLC). A representative trace is shown in Figure 5.6. This shows a single peak with which is associated 100% of the eluted activity. As ^{99m}Tc-colloid could be retained entirely by the column the RP-HPLC was repeated with collection of the fraction containing the eluted peak. This was compared with a reference sample and found to contain the same activity: this was therefore taken as conformation that the peak seen represented all the ^{99m}Tc in the sample which was conjugated to the peptide.

To determine the maximum specific activity obtainable with this method the reaction was performed with reducing concentrations of peptide in parallel. For the *in vivo* experiments I wanted to try a range of injected doses: previous work with ^{111}In-pentreotide in rats has found that the lowest possible dose may not produce the most sensitive results, with specific uptake in receptor-positive organs exhibiting a bell-shaped curve (Breeman et al. 1995). Earlier experiments had found that the majority of unbound ^{99m}Tc was in the form ^{99m}Tc-tricine, and PBS was therefore used as the solvent for this study. The results, seen in Figure 5.7, show that good labelling was achievable at a specific activity of 10 MBq/μg and that this was stable in the medium at room temperature over 24 hours. There was significant loss of labelling efficiency at peptide concentrations lower than this.

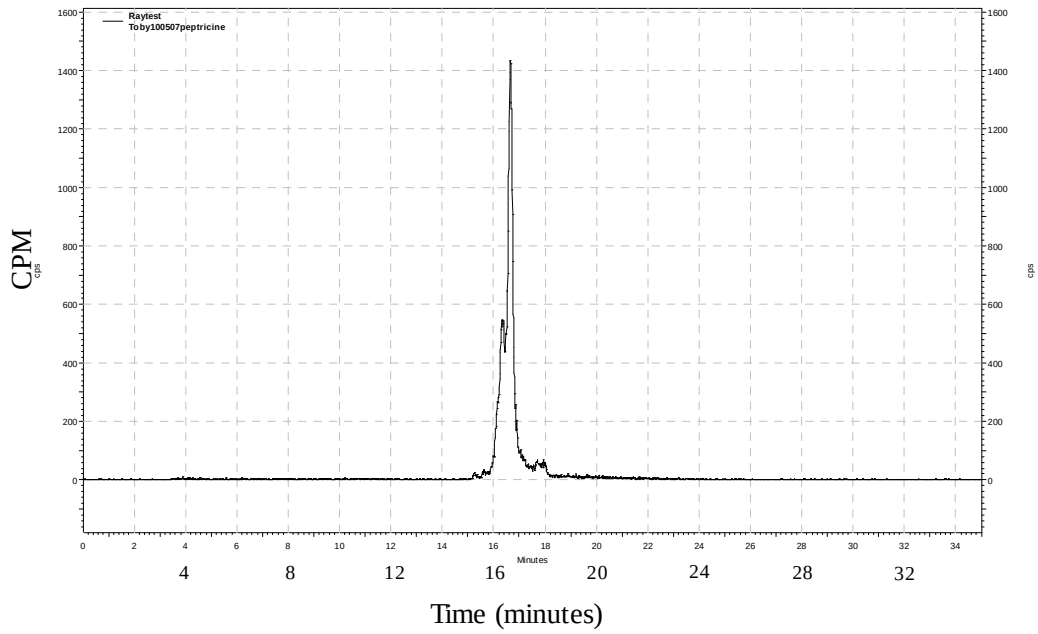

Figure 5.6: Labelling of HYNIC-peptide with 99mTc. Representative radiochromatogram of ^{99m}Tc-HYNIC-3.1peptide with tricine as co-ligand. 100% of activity is eluted in the peak at 16.5 minutes indicating excellent radiochemical yield. The double peak is likely to be due to isomerism within the labelling complex (Decristoforo & Mather 1999a).

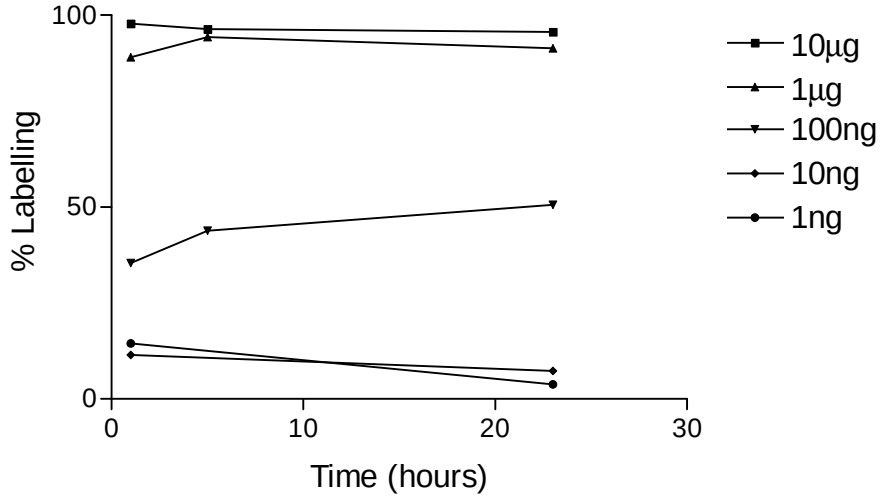

Figure 5.7: Radiolabelling yield and stability of ^{99m}Tc-HYNIC-3.1 peptide. HYNIC peptide was radiolabelled with 10 MBq ^{99m}Tc and tricine as co-ligand at the indicated concentrations and assessed by ITLC. Good radiolabelling efficiency was achieved at 10 MBq/µg with excellent stability in solution over 24 hours.

5.4.2 In vivo biodistribution studies with ^{99m}Tc-labelled peptides

5.4.2.1 Tissue localisation of ^{99m}Tc-peptide with and without systemic perfusion

Prior to carrying out full-scale biodistribution studies I wanted to assess whether perfusion of the murine circulation was necessary prior to extraction of the tissues. This was necessary for the *in vivo* phage experiments, particularly for selection of phage as it would, theoretically, clear low-affinity and non-specifically bound phage. However, it was not clear whether this was necessary for the peptide experiments. The low molecular weight of the peptides could lead to rapid tissue penetration as well as clearance from the circulation by the kidneys, with relatively little circulating peptide remaining in the blood proportionately to that in the tissues. As a preliminary experiment 4 double-transplanted mice were injected with 1 μg or 0.1 μg (~1 MBq) of ^{99m}Tc-peptide: after 15 minutes the circulation was perfused as before and the transplants removed. A further 2 animals were injected but not perused at the end of the incubation period. The results of this are shown in Figure 5.8B. There are small non-significant differences between the synovium and skin at this time point with no differences between the perfused and unperfused animals.

5.4.2.2 Half life of radiolabelled peptide *in vivo*

In order to estimate the serum half-life of the ^{99m}Tc-3.1 peptide untransplanted SCID mice were injected with 1 μg (~1 MBq) of radiolabelled peptide and killed at various time points for measurement of radioactivity in the blood. The results are shown in Figure 5.8**A**. The fitting of a single-phase exponential curve to the graph allows an estimate of the half-life at 3 minutes, which is likely to be due to rapid renal excretion of the peptide. Although clearance from the circulation appears to be rapid, if there is significant non-specific extravasation of peptide into the grafts clearance of unbound peptide may be slower and therefore an incubation time of 1 hour was selected for the following biodistribution experiments.

5.4.2.3 *In vivo* biodistribution of ^{99m}Tc-HYNIC-peptide at 1 hour

For the reasons discussed above the mice used in these experiments were incubated for 1 hour prior to retrieval of the transplants and murine organs. SCID mice double-transplanted with human skin and synovium were injected intravenously with the indicated dose of ^{99m}Tc-labelled 3.1 peptide. After incubation the mice were killed and the tissues retrieved for measurement of radioactivity. Various injected doses were used and the results are shown in Figure 5.9. As with previous experiments, no significant differences were seen between peptide localisation to transplanted human skin or synovium at any of the injected doses. The tissue uptake was generally lower for the 1 μg dose than for the lowered injected doses although this was non-significant. It is not clear why this is seen: it could be argued that the larger injected dose results in inhibition of specific binding, although the lower tissue uptake is seen in both synovium and skin. 3.1 phage has previously been shown to home preferentially to synovium in animals transplanted with both tissues and therefore it seems improbable that we are seeing inhibition of specific uptake.

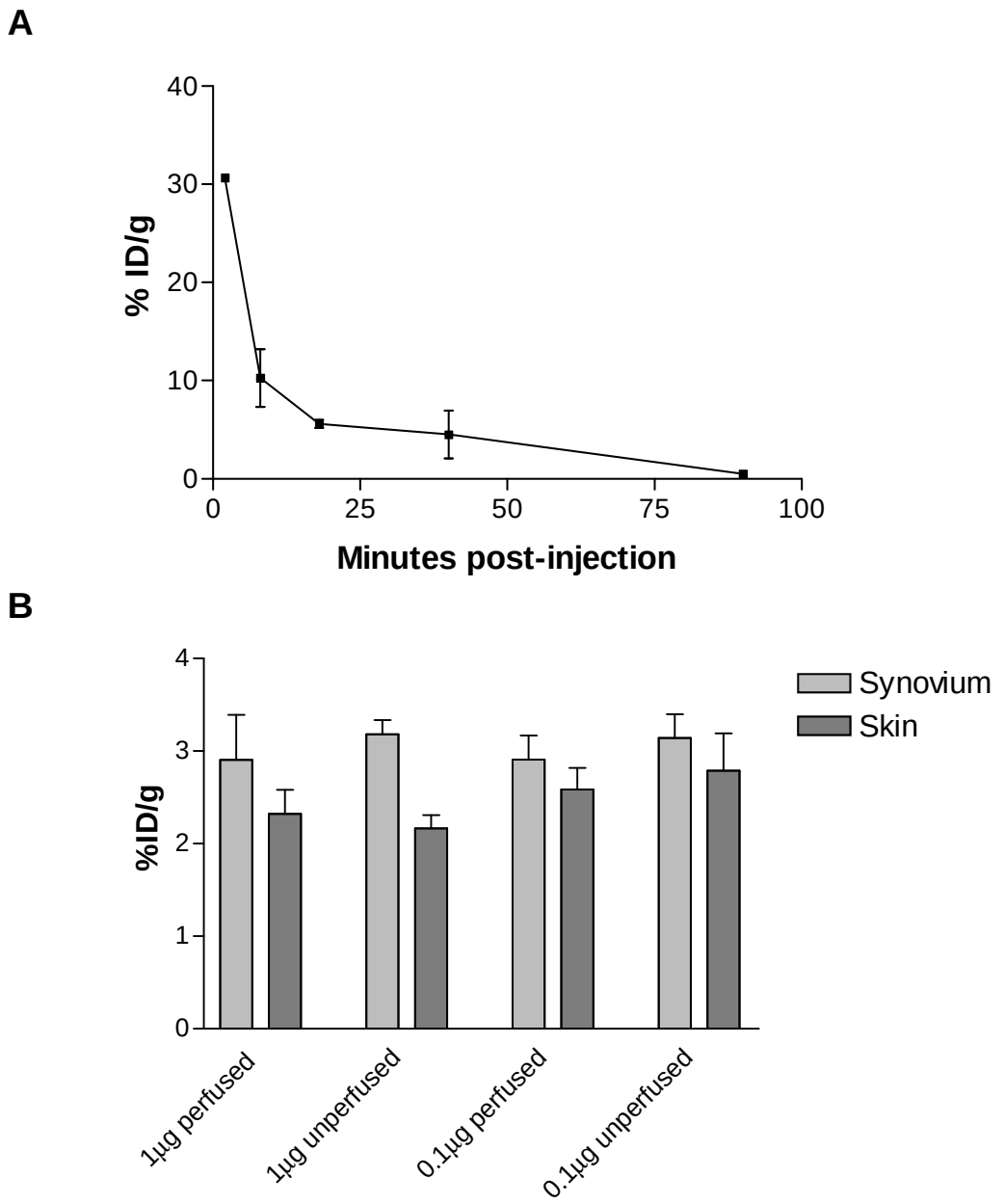

Figure 5.8: *In vivo* clearance and biodistribution of ^{99m}Tc-peptide. A Mice were injected with 1 µg ^{99m}Tc-3.1 peptide and killed at various time points for the collection of blood and measurement of radioactivity. Non-linear regression analysis of the data gives an estimated serum half-life of 3 minutes. n=1 mouse (1st and final time points), 2-3 mice (intermediate time-points). **B** SCID mice double-transplanted with human skin and synovium were injected with ^{99m}Tc-3.1 peptide and killed after 15 minutes with or without perfusion. No differences were

seen between the perfused and un-perfused animals. n= 4 transplants per condition perfused/ 2 transplants per condition unperfused. Mean +/- SEM

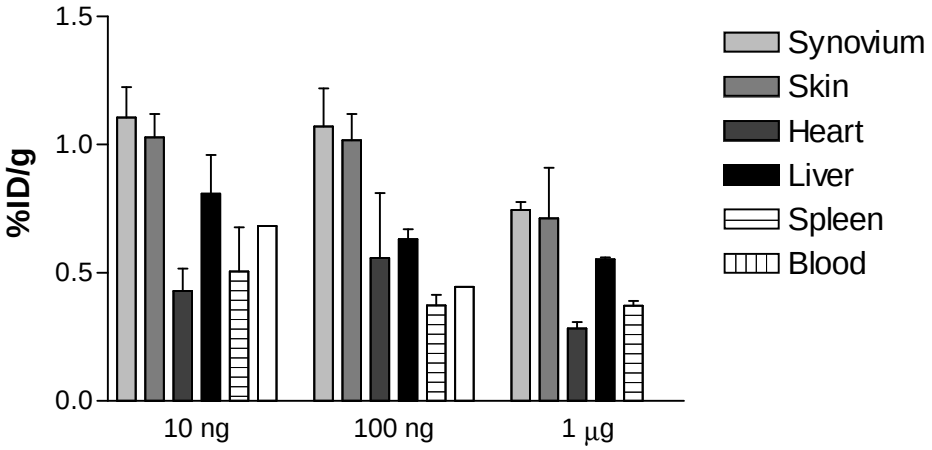

Figure 5.9: Biodistribution of ^{99m}Tc-peptides. SCID mice were double-transplanted with human skin and synovium and injected intravenously with the indicated doses of ^{99m}Tc-3.1 peptide. After incubation for 1 hour the tissues were retrieved, weighed and the radioactivity measured. No significant difference was seen between the skin and synovium at any of these time points; tissue uptake was lower at the injected dose of 1 μg although this was non-significant. n=4 transplants per condition (10 ng and 1 μg), 6 transplants (100 ng). Mean +/- SEM.

5.4.3 Labelling of HYNIC peptide with ^{99m}Tc in the presence of various co-ligands

Although tricine is the best-established co-ligand used for stabilisation of the HYNIC/ tricine/ ^{99m}Tc complex, there is increasing use of alternative co-ligands in view of the findings that this can have significant effects on the properties of the labelled peptide with effects on lipophilicity (associated with altered RP-HPLC retention times) and serum protein binding: consequent effects on non-specific binding can be seen *in vivo* (Decristoforo et al. 2006;Decristoforo & Mather 1999a). These *in vitro* properties are associated with altered biodistribution *in vivo*: increased lipophilicity can result in enhanced uptake by liver and gut which

can have particular consequences for imaging. Higher protein binding can result in prolonged retention in the circulation with consequently lower tumour to background ratios. Later in the project I therefore returned to the HYNIC peptide, at which stage I also had better access to HPLC facilities, and assessed the efficiency labelling with different co-ligands and the serum stability as well as protein binding of the labelled peptide.

The HYNIC-peptide was labelled with ^{99m}Tc in the presence of various co-ligands as detailed in the methods. Representative reverse-phase HPLC radiochromatograms are shown in Figure 5.10. The best labelling was achieved with tricine or nicotinic acid (NA)/ tricine as co-ligands. Labelling with EDDA or with tricine/ EDDA exchange did not produce a clean product and were therefore not pursued. Both tricine and NA/tricine labelling produced peaks that appeared to contain more than a single species which is most likely to be due to isomerism within the complexes (Decristoforo & Mather 1999a).

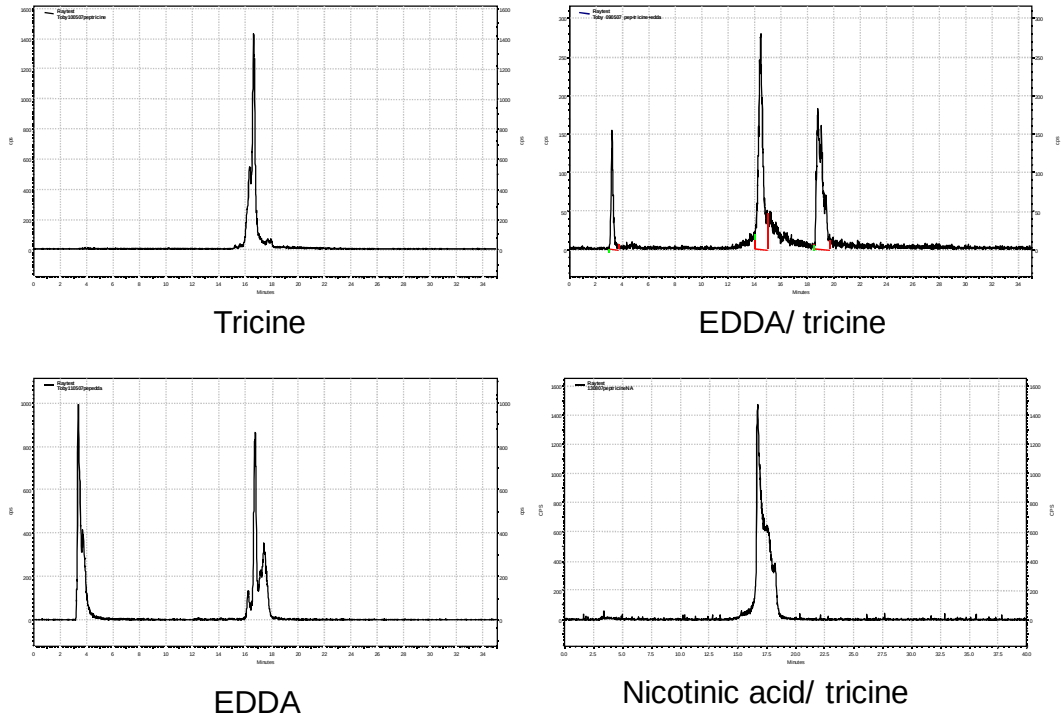

Figure 5.10: Variation in ^{99m}Tc labelling chemistry. HYNIC-peptide was labelled with ^{99m}Tc in the presence of various co-ligands as detailed in the methods. Purity of the radiolabelled product was determined by RP-HPLC. Labelling with tricine or nicotinic acid/ tricine as co-ligands produced pure products, whereas EDDA/ tricine and EDDA produced multiple species with significant free ^{99m}Tc. Scales are counts per minute (cpm) on the y-axis, time (minutes) on the x-axis.

5.4.4 Serum stability and protein binding of ^{99m}Tc-HYNIC-peptide

With a view to repetition of the biodistribution experiments with ^{99m}Tc-labelled peptide with the alternative NA/tricine co-ligand chemistry serum stability and protein binding of the two labelling complexes were compared.

Serum stability and protein binding were assessed using a previously published method (King et al. 2007). Briefly, the HYNIC-peptide was labelled with ^{99m}Tc

with tricine or nicotinic acid and tricine as co-ligands. The peptide was incubated in murine serum at 37^0C and samples removed for analysis after 1 and 4 hours. RP-HPLC was performed after removal of serum proteins by acetonitrile precipitation and centrifugation; protein binding was assessed by retention of the radiolabel in size-exclusion spin columns.

The results of the serum stability experiment are shown in Figure 5.11 and Table 5.4. The peak at the earlier retention time seen in the 1 and 4 hours time points represents loss of the radiolabel from the peptide. At 1 hour both peptides are largely intact with 98% of the activity of the tricine/HYNIC peptide and 87% of the nicotinic acid/ tricine/ HYNIC peptide remaining at the later retention time corresponding to that seen at 0 hours. At 1 hour although there is some loss of radiolabelling the integrity of the peptide peaks is preserved indicating minimal breakdown of the peptides in serum. At 4 hours one peak is again seen for the ^{99m}Tc-tricine –HYNIC peptide: however, at this time point a second peak has emerged with the ^{99m}Tc-NA/tricine-HYNIC-peptide suggesting that some degradation of the peptide has taken place. However, the rapid elimination of peptide from the circulation shown with the tricine/ HYNIC peptide makes the reduced serum stability at 4 hours less relevant: if the peptide were specifically internalised by cells rapidly this should be seen in the biodistribution experiments as unbound peptide is cleared from the tissues.

The results of the protein binding experiments are shown in Table 5.5. The differences in serum protein binding between the two co-ligand complexes are significant at both time points with there being less protein binding with NA/tricine as the co-ligands. This would results in significantly enhanced bio-availability of the peptide and, therefore, could significantly impact tissue-specific uptake. This labelling chemistry was therefore used in a further biodistribution experiment.

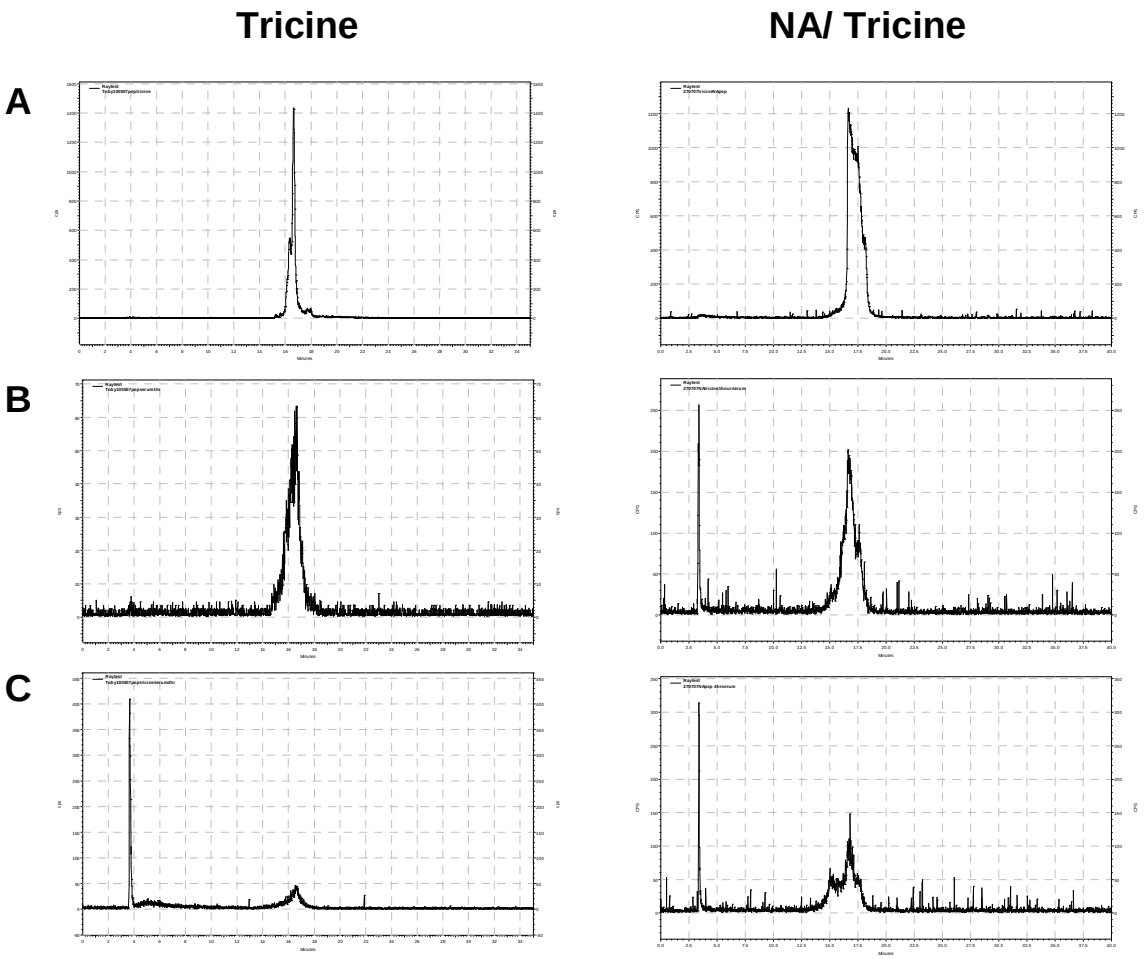

Figure 5.11: Serum stability of ^{99m}Tc-HYNIC peptides. The HYNIC peptide was radiolabelled with tricine or nicotinic acid/ tricine as co-ligands and incubated in murine serum at 37 ^{0}C. At 0 (A), 1 (B) and 4 (C) hours samples of serum were removed and analysed by RP-HPLC after precipitation of serum proteins. Scales are counts per minute (cpm) on the y-axis, time (minutes) on the x-axis.

	Co-ligand % labelling	
Time (hours)	**Tricine**	**Nicotinic acid/ tricine**
0	**100**	**100**
1	**97.6**	**86.9**
4	**60.3**	**84.2**

Table 5.4: Stability of ^{99m}Tc-labelled 3.1 HYNIC-peptide in murine serum. Radiolabelled peptide was incubated in murine serum at 37^{0}C. At the indicated time points samples were removed and analysed by RP-HPLC after acetonitrile precipitation of serum proteins. Integration of the peaks allowed quantification of ^{99m}Tc remaining bound to the peptide.

	Co-ligand	
Time (hours)	**Tricine**	**Nicotinic acid/ tricine**
1	**9.6**	**2.3**
4	**18.1**	**6.4**

Table 5.5: % binding of ^{99m}Tc-labelled 3.1 HYNIC-peptide to murine serum proteins. Radiolabelled peptide was incubated in murine serum at 37^{0}C. At the indicated time points samples were removed and added to size-exclusion filtration spin columns. Eluted (protein bound) peptide is shown as a percentage of the total activity added. Mean results of duplicate columns.

5.4.5 Biodistribution of ^{99m}Tc-HYNIC-3.1 peptide with nicotinic acid/ tricine as co-ligands

HYNIC-3.1 peptide was radiolabelled with ^{99m}Tc with nicotinic acid and tricine as ternary ligands. 0.1 μg (~2.4 MBq) of the radiolabelled peptide was injected into 3 SCID mice double-transplanted with human skin and synovium. After 1 or 4 hours the mice were killed and the transplants and murine tissues retrieved, weighed and the radioactivity measured. An additional 3 mice were co-injected with an excess of cold peptide to determine whether this resulted in any significant inhibition of tissue uptake of peptide which would indicate specific localisation. The results of this experiment are shown in Figure 5.12: the differences between synovium and skin uptake of peptide are not significantly different at 1 or 4 hours, and the co-injection of excess free peptide did not result in significant down-regulation of peptide homing in either tissue. The levels detected in the tissue after 1 hour were similar to those seen with the ^{99m}Tc-tricine-HYNIC-peptide. The lack of a significant difference between homing to human skin and synovium suggests that this is non-specific. The biodistribution results including murine organs are shown in Table 5.6.

Although uptake in transplanted human skin and synovium are similar, these are generally high compared to some of the murine organs. Similar observations were made with the previous biodistribution experiments: this suggested that although uptake was non-specific, it was increased in the transplanted tissues. The reason for this was unclear but, bearing in mind the known hyperpermeability of inflamed synovial tissue, it was decided to further investigate tissue permeability to large molecules.

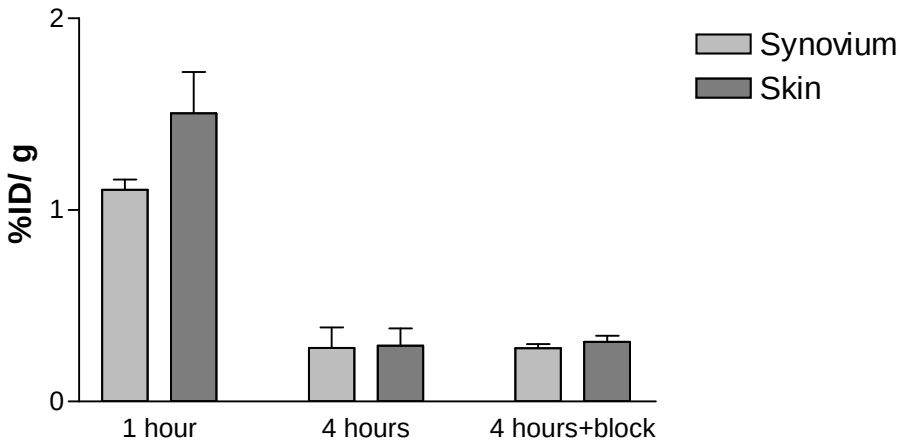

Figure 5.12: Biodistribution of ^{99m}Tc-HYNIC peptide with nicotinic acid/ tricine as co-ligands. SCID mice double –transplanted with human skin and synovium injected with 0.1µg of ^{99m}Tc-labelled HYNIC-peptide. After 1 or 4 hours incubation the animals were killed and the transplants removed, weighed and radioactivity measured. An additional group was co-injected with an excess of unlabelled peptide to block specific binding. 6 transplants per condition. Results shown are % injected dose/ gram of tissue. Mean+/- SEM.

Tissue	1 hour	4 hours
Synovium (T)	1.11 ± 0.05	0.28 ± 0.11
Skin (T)	1.51 ± 0.21	0.29 ± 0.03
Heart	0.19 ± 0.01	0.056 ± 0.006
Lung	0.62 ± 0.03	0.23 ± 0.05
Liver	1.42 ± 1.06	0.19 ± 0.03
Kidney	17.57 ± 1.85	3.99 ± 0.73
Spleen	0.22 ± 0.02	0.13 ± 0.06
Gut	1.64 ± 1.25	0.42 ± 0.26
Muscle	0.14 ± 0.01	0.58 ± 0.13
Blood	0.53 ± 0.11	0.204 ± 0.83

Table 5.6: Results of the biodistribution experiment detailed in section 5.4.6. Double transplanted SCID mice were injected with ^{99m}Tc-HYNIC-3.1 peptide. At the indicated time points the mice were killed, transplanted tissues and organs retrieved and radioactivity measured. Results shown are % injected dose/ gram of tissue. Mean +/- SEM. ((T) = transplant)

5.5 Permeability of graft vascular endothelium to macromolecules

The results from the biodistribution experiments detailed in the previous sections show that specific uptake was not seen in transplanted human synovium compared with human skin. However, uptake in the human tissue was somewhat higher compared to that seen in some murine organs and therefore it was postulated that the transplant vessels might be hyperpermeable. This was investigated using a 2-step method. Firstly, the vascularisation of the human and murine vessels was determined using immunohistochemistry and a point-counting method; and secondly the permeability of the tissues was determined using a dye based assay. Correction of the permeability experiments for vessel density would provide a estimate of relative vessel permeability between the tissues.

5.5.1 Quantification of graft vascularisation

The Evans Blue permeability assay detailed in the next section is dependent on the extravasation of albumin from the tissue vessels. This is obviously a function of vessel density in the tissue; as there is substantial variation between tissues it was decided to correct the results for vascularity. Tissues were stained as detailed in Chapter 2 and representative micrographs are shown in Figure 5.13A-D. A point counting method was used to determine the volume fraction of vascular endothelial cells: for this a number of fields were counted. In order to ensure that the mean obtained was representative of the vessel density the progressive mean was plotted and successive fields counted until the mean count stabilised: a representative plot is shown in Figure 5.13E. For the human synovium and skin it was expected that there might be significant variation between and within tissues, and therefore multiple representative grafts were assessed, with three levels cut from each. The results are shown in Figure 5.14**A**. The vessel density was similar in human skin and synovium with higher vessels counts in most of the sampled murine tissues, most markedly in the kidney.

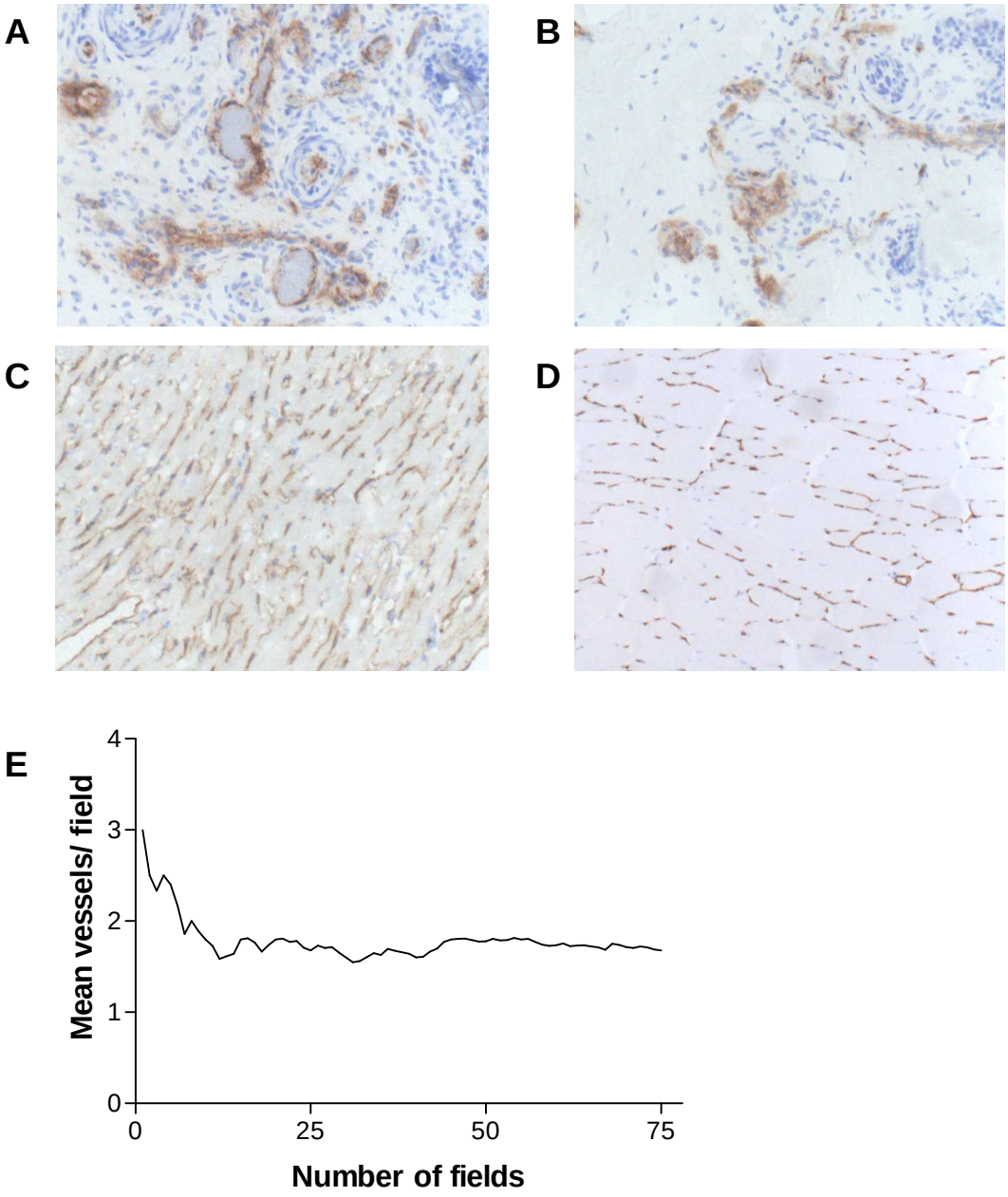

Figure 5.13: Determination of the density of vascular endothelium in tissues. Representative micrographs of tissues stained for vascular endothelial specific markers A-B Representative micrographs of *ex vivo* human synovium (A) and skin transplants (B) stained for human vWF. C murine heart, D murine muscle. Original magnification x40 (A+B), x20 (C+D). E: Determination of the progressive mean of number of vessels/ field.

5.6 Evans Blue permeability assay

Evans blue is a diazo dye that binds rapidly and with high affinity to serum albumin (Freedman & Johnson 1969). The stable interaction with albumin makes it very suitable as a means of tracking albumin extravasation and tissue permeability and hence is widely used for this purpose. The permeability assay was carried out using a previously published method (Lacolley et al. 1998). Mice transplanted with synovium or both synovium and skin were injected with 50 mg/kg Evans Blue via the tail vein. After 1 hour under terminal anaesthesia the thoracic cavity was exposed and the circulation perused with 50 ml 0.9% saline. The transplanted tissues and organs of interest were removed and frozen. To quantify the dye the tissues were defrosted, washed twice and weighed before incubation for 6 days in formamide at RT. At the end of the incubation period the tubes were centrifuged briefly to sediment any debris and the absorbance measured at 620 nm. Serial absorbance measurement showed that by 6 days dye extraction had plateaued. The results were corrected for vessel density from the data presented in the previous section. The bar chart in Figure 5.14**B** shows the dye extraction corrected for tissue density and weight and expressed as a ratio of tissue to heart uptake: there are no significant differences between uptake in the murine control tissues indicating similar uptake of albumin in each of these. Both human skin and synovium have significantly greater uptake than each of the murine tissues ($p=<0.05$) with no significant differences between skin and synovium, indicating enhanced vessel permeability within the transplants to albumin (mw~60,000 Da). As already discussed, the vessels of hyperplastic synovial tissue are hyperpermeable to macromolecules and so this result is not unexpected. The cause of the high permeability in the skin is less clear: it is possible that damage occurs during the processing and freezing of the tissues prior to transplantation; it is also very possible that the vascular interfaces at the human/ murine anastomoses and associated neoangiogenic vessels are hyperpermeable, although more specific investigation of this hypothesis was not pursued.

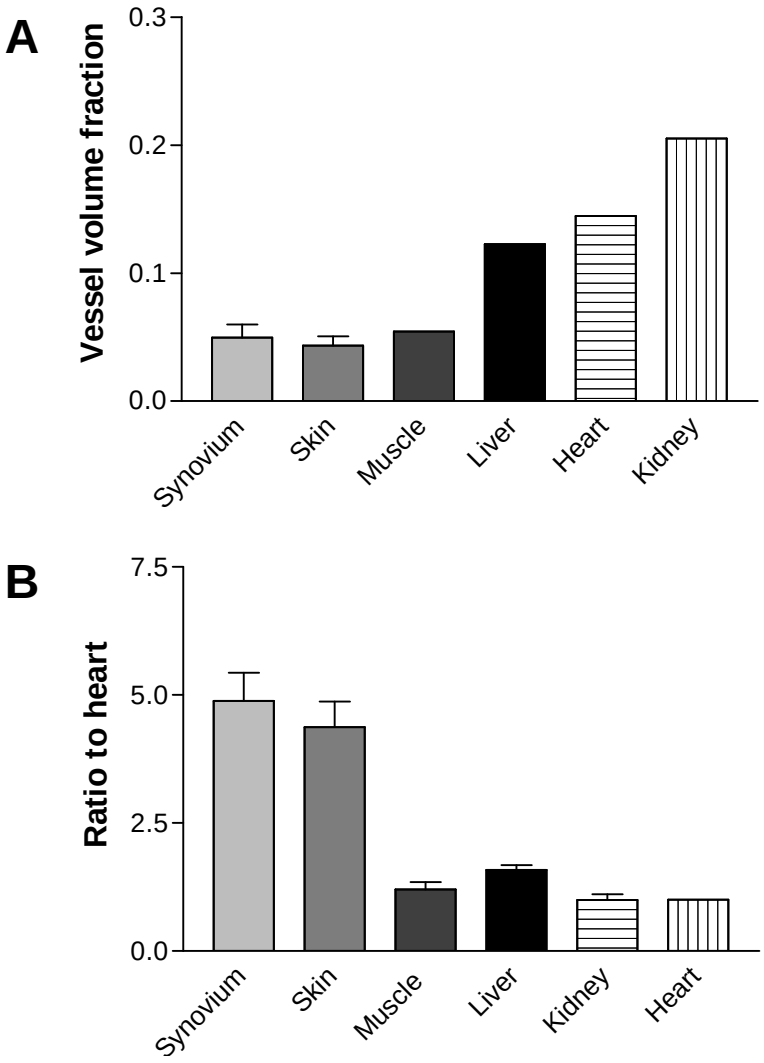

Figure 5.14: Relative permeability of transplanted tissues and murine organs *in vivo*. **A** Volume fraction of vascular endothelial cells in transplants and murine tissues. Tissue sections were stained for the human and murine vascular endothelial cell-specific markers vWF and CD31 respectively. The volume fraction of endothelial cells was quantified by a point counting technique. **B** The albumin-binding dye Evan's Blue was injected into transplanted SCID mice: after 1 hour incubation the systemic circulation was perfused and the dye extracted from the tissues by incubation in formamide: after 6 days the absorbance was read at 620nm. There is significantly greater albumin extravasation in the transplanted tissue compared to the control murine tissues ($p=<0.05$). No significant differences are seen between the murine organs. Mean +/- SEM. n=7 animals/ 14 transplants.

5.7 Summary

Previous work has shown that the 3.1 peptide, when expressed by phage, homes selectively to transplanted human skin and it was shown in chapter 3 that this was selectively up-regulated in tissues pre-stimulated with TNFα. In this chapter the monomeric synthetic peptide was tested for its capacity to adhere in human synovial tissue sections or to home to transplanted human synovium *in vivo*. Although a linear increase was seen in vessel fluorescence with increasing concentrations of fluorochrome-conjugated peptide, no differences were seen between the test and control peptides suggesting that most or all of the binding seen was non-specific. There are a number of potential explanations for this finding which may have been the result of experimental conditions, in particular the effect of the fixation process on the tissue ligand, the differing amino acid components and hence charge of the peptides and the absence of potentially essential co-factors for binding such as divalent cations. A further possible limitation was the sensitivity of the assay to detect specific binding which may have been undetectable due to the background interference of non-specific binding and tissue autofluorescence. For these reasons the peptide was tested further *in vivo* in the SCID mouse transplantation model with radiolabelled peptide which offers the most sensitive detection of tissue localisation.

The first experiments with ^{111}In-conjugated peptide failed to show any differences between localisation of the test or control peptides to transplanted human skin or synovium. These findings may have been due to the relatively high, and therefore possibly saturating, doses used; furthermore, there was contamination of DTPA-peptide with unconjugated peptide and impairment of ligand affinity by DTPA conjugation may have resulted in competitive inhibition of binding by the unconjugated peptide. This latter complication does seem less likely: the DTPA was separated from the cyclic peptide by the relatively rigid 6-carbon spacer 6-aminoheaxanoic acid. However, for this combination of reasons, the relative expense of ^{111}In and difficulties with ^{125}I labelling, further experiments were conducted with ^{99m}Tc as the radiotracer.

A number of labelling chemistries were investigated, of which the co-ligands tricine or nicotinic acid/ tricine gave the best results with excellent radiochemical yield. Both had good stability in serum at 1 hour although at 4 hours there was significant loss of the radiolabel and, with the nicotinic acid/ tricine co-ligands, possibly deterioration of the HYNIC-peptide structure. Furthermore there were significant differences in serum protein binding *in vitro* with co-ligand variation. At 1 hour no significant differences were seen in the localisation of the peptides to human skin or synovium; a further experiment with a 4-hour incubation with the ^{99m}Tc-nicotinic acid/ tricine-HYNIC-3.1 peptide again found no significant difference. The *in vivo* conditions for this experiment were, physiologically, identical to those for the phage selection and tissue homing experiments. Differences between the structure and behaviour of the monomeric peptides and the phage have to be considered, therefore, to explain the defences between the *in vivo* phage and monomeric peptide experiments. Of these, three stand out as of most likely significance. The first of these is size: bacteriophage are large particles and, therefore, are likely to extravasate much more slowly from the circulation, if at all. Tissue localisation therefore reflects phage that are still in the circulation (although this was minimised by systemic perfusion) or adhering, specifically or otherwise, to the luminal surface of the tissue vasculature. The peptide molecules are, conversely, much more likely to enter the extravascular space by passive diffusion, particularly in the hyperpermeable vessels of inflamed synovium. Longer incubation times would be expected to allow clearance of unbound peptide: however, at 1 and 4 hours no differences were seen between synovium and the human control tissue. This suggests that the peptide binding to receptors, if occurring at all, is low affinity and that little in any internalisation is taking place. Internalisation would be the ideal property of a tissue-specific targeting peptide and retention would be enhanced with the use of the 'residualising' bifunctional chelating agent complexes used in these experiments. The phage experiments do, of course, tell us nothing about whether the ligand/ receptor complex might be internalised and this therefore can only be hoped for rather than expected. Secondly is valency: the phage are polyvalent, with each expressing 5

copies of the PIII surface protein-conjugated peptide. *In vivo* and *in vitro* studies have shown that increasing the valency of targeted peptides can significantly enhance binding affinity, sometimes dramatically (Chen et al. 2005;Kok et al. 2002;Molenaar et al. 2002): polyvalency may therefore be critical to peptide homing in our model. A third possibility is that the PIII protein may be essential to the specific phage homing: there is at least one published report of tissue-specific phage binding being conferred by the PIII protein rather than the expressed peptide sequence (Clement et al. 2003), although our experiments have shown the peptide is at least necessary to synovial homing: whether it is sufficient will be discussed in the final chapter.

The final experiment in this chapter was to determine whether permeability of the transplanted tissue was increased compared to murine tissue. It was shown that there was significantly increased permeability to albumin in both transplanted skin and synovium compared to murine heart, liver, muscle and kidney. This experiment highlights a disadvantage of this model in assessing specific tissue localisation of short peptides, which reflects the disadvantage of the targeting of inflamed synovium generally. As previously discussed, enhanced permeability of the vessels of inflamed synovium to large molecules is likely to have been a significant impediment to the assessment of specific localisation of targeted molecules. For the reasons discussed above, a means of experimentally increasing both the size and valency of the peptide conjugates was sought and this is the subject of the next chapter.

Chapter 6

Development of a tetravalent radiolabelled peptide molecule and investigation of *in vivo* synovial targeting

6.1 Introduction

As discussed in the previous chapter, there are a number of potential reasons for the failure to show specificity of the peptide for transplanted human synovial tissue *in vivo.* Perhaps the most compelling of these is valency: peptide presentation of the phage particles is polyvalent, with 5 copies of the PIII fusion protein per phage, and hence this may be critical to the binding affinity. This effect may also be reflected in our previous observations of inhibition of phage homing by monovalent peptide: high concentrations were required in order to achieve maximal inhibition of phage homing (500 μg/ animal). This represents a huge molar excess of free peptide; much of this is likely to be lost by rapid renal excretion but to a certain degree the differences in valency between the free and phage-expressed peptide may be significant.

Polyvalency is central to many biological interactions of which there are numerous examples; increasing the number of receptor/ ligand interactions at the site of an interaction between cells or proteins can not only increase the strength of that interaction but can also precipitate or enhance activation of a receptor (Mammen, Choi, & Whitesides 1998). Many examples of such polyvalent interactions are seen in the adhesion pathways discussed in the introduction, indeed integrin activation is frequently achieved via cell-surface clustering. In order to address this problem we investigated means of polymerising the peptide. The simplest means of achieving this was to use streptavidin (SA) to bind biotinylated peptide to form a tetravalent molecule. Streptavidin is a ~60,000 Da molecular weight protein which is isolated from the bacterium *streptomyces avidinii*: it consists of 4 identical subunits each consisting of 159 amino acid residues, each of which can bind one molecule of d-biotin. The dissociation constant of this interaction is around 10^{-15} M making one of the strongest non-covalent molecular interactions known to occur naturally (Weber et al. 1989): the consequent stability of the tetravalent molecule makes streptavidin ideal as a tool for use in the delivery of biotinylated compounds. Of particular interest in recent years has been the use of streptavidin in the ‘pretargeting’ of radioisotopes to

tumours. This technique was borne out of the problems associated with direct labelling of tumour-targeting antibodies with radioisotopes for imaging or therapy, particularly with slow clearance and consequent high background radiation doses. A number of approaches have been successful in pre-clinical models, including the use of antibodies conjugated to streptavidin. Following administration of the conjugate a clearing agent can be administered to remove unbound conjugate from the circulation, followed by a low molecular-weight biotin-radioisotope conjugate which is cleared rapidly unless bound by streptavidin (Chang et al. 2002). This has been successful in a number of animal models and early clinical studies (Goldenberg et al. 2006).

The polymerisation of biotinylated antibodies with streptavidin has been successfully employed to increase the binding avidity over monomeric antibodies as was found, for instance, in an investigation of the avidity of a polymerised scFv to CEA identified by phage display compared to the monomer (Cloutier et al. 2000). Polymerisation of antibody molecules with multiple biotins can result in multimers of varying sizes which can influence cell binding and stimulate internalisation of antibodies, uptake of which is poor in the monomeric form. This has been shown with antibodies to ICAM- and PECAM *in vitro* (Muro et al. 2003;Wiewrodt et al. 2002) the latter of which was successfully used to deliver an antioxidant enzyme to rat lungs in an H_2O_2-injury model (Muzykantov et al. 1999). This approach has also been successful with peptides: Molennar *et al* showed that the avidity of a P-selectin binding peptide identified by phage display was increased 200-fold increase in avidity in an ELISA-based assay (Molenaar et al. 2002). Conjugation of the peptide to streptavidin would also have the effect of prolonging the circulating half-life of the peptide. A study of the biodistribution of ^{125}I-labelled streptavidin in Balb/c mice found a circulating half-life of around 24 hours, with the highest tissue uptake seen in the kidney (Schechter et al. 1990). Pre-incubation with biotin had little effect on the biodistribution.

To develop this as a tool for polymerising the CKSTHDRLC peptide streptavidin was first used to polymerise an RGD peptide previously identified using the same

seven amino acid residue disulphide-constrained library to assess the effects of polymerisation on peptide binding. To enable *in vivo* biodistribution studies a novel DTPA-SA conjugate was synthesised to allow *in vivo* administration of radiolabelled SA-peptide.

The first experiments in this chapter were aimed at optimising assays to determine RGD -peptide binding to plate or cell-bound ligand. A technique for rapid conjugation of biotinylated peptide and purification was optimised and the affinity of the polymeric peptides confirmed in the same assays. The streptavidin-peptide was then derivatised for conjugation to ^{111}In and finally the tetravalent 3.1 and control (scrambled) sequence peptides were tested in the SCID mouse transplantation model.

6.2 Characterisation of RGD peptide

To validate tetramerisation of the peptide *in vitro* it was necessary to use a peptide of the same structure as the synovial homing peptide. For this purpose a novel RGD-containing peptide was used: this peptide was identified from the same phage display library as the synovial-homing phage and hence had the same disulphide-constrained seven amino acid basic structure. This had been done to validate the library and a peptide sequence, CSPRGDHPC (hereafter known as RGD2C), containing the expected RGD motif was identified. Fibronectin is an extracellular matrix protein containing an RGD-domain and is a biological ligand for $\alpha_v\beta_3$ (Ruoslahti 1996) as has been discussed in section 1.2.2. The peptide was first tested for its binding affinity for $\alpha_v\beta_3$: to enable comparison between monomeric and multimeric peptides a competitive binding assay was developed and used in the first instance to confirm activity of the RGD2C peptide.

6.2.1 Optimisation of $\alpha_v\beta_3$ binding to fibronectin in vitro

To assess binding affinity of RGD to $\alpha_v\beta_3$ an ELISA-based assay was developed wherein the RGD peptide would compete with fibronectin for $\alpha_v\beta_3$ binding. Fibronectin is one of the extracellular matrix (ECM) ligands for $\alpha_v\beta_3$ and therefore suitable for use in this assay. As discussed in the introduction, binding of the RGD motif to $\alpha_v\beta_3$ is cation-dependent: the optimal cation conditions for this assay

were unknown and therefore fibronectin binding to immobilised $\alpha_v\beta_3$ was investigated under a number of different cation conditions.

Purified $\alpha_v\beta_3$ was bound to 96-well plates in varying concentrations and incubated with fibronectin in binding buffer containing differing combinations of cations. After washing the plates were incubated with biotin-conjugated anti-fibronectin antibody before incubation with streptavidin-conjugated HRP and developing with TMB. Initial experiments confirmed significant variation in fibronectin binding under the various cation conditions and in a final experiment, the results of which are shown in Figure 6.1, all cation conditions were used in parallel on the same plate. This experiment confirmed that the combination of 0.5 mM $MgCl_2$, 1 mM $MnCl_2$ and 1 mM $CaCl_2$ achieved optimal fibronectin binding. This is consistent with previous data: cation-dependency of the integrin binding to its ligands is well established with the description of cation binding sites within the binding domain of $\alpha_v\beta_3$. Both Mg^{2+} and Mn^{2+} have been shown to enhance binding: the role of Ca^{2+} may be more complicated as a biphasic effect has been shown with inhibition of binding at higher (physiological) concentrations *in vitro* (D'Souza et al. 1994;Hu, Barbas, & Smith 1996;Smith, Piotrowicz, & Mathis 1994). Subsequent experiments were performed with solutions containing divalent cation supplementation with all 3 cations at the concentrations used in this experiment.

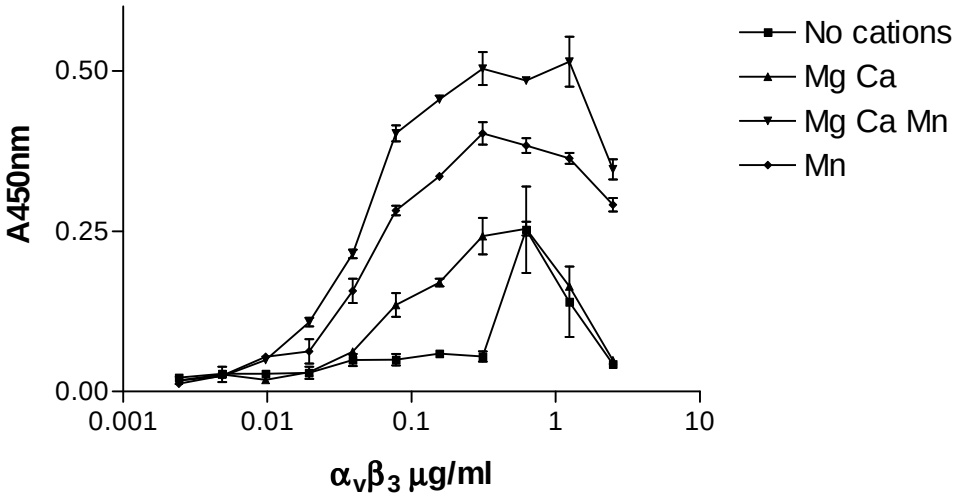

Figure 6.1: **Optimisation of divalent cation conditions for RGD protein/ peptide binding ELISAs.** Duplicate wells of a 96-well plate were coated with reducing concentrations of $\alpha_v\beta_3$. After washing the plate was incubated with 5µg/ml fibronectin, followed by biotinylated anti-fibronectin antibody and finally HRP-conjugated streptavidin. The buffers used in each step were supplemented with cations as indicated. After the final wash the wells were developed with TMB and the absorbance read at 450nm. The results are expressed as mean +/- SD of duplicate wells.

6.2.2 Competition of monovalent peptide with fibronectin in the $\alpha_v\beta_3$ binding assay

In order to confirm that the RGD peptide competes with soluble fibronectin for binding to $\alpha_v\beta_3$ the above assay was adapted for competitive binding. A concentration 0.5 µg/ml $\alpha_v\beta_3$ was used for this and further experiments as it was within the optimum concentration range for fibronectin binding in this assay. $\alpha_v\beta_3$ was bound to the plates overnight following which they were washed and blocked with 5% BSA. After washing again the plates were pre-incubated with varying concentrations of competing peptide before the addition of a fixed concentration

of fibronectin. The plates were washed again and incubated with HRP-conjugated anti-fibronectin antibody. After the final wash the HRP was developed with TMB and absorbance read at 450 nm.

The results are shown in Figure 6.2. There is a clear dose-dependent inhibition of the fibronectin binding with no effect seen with the scrambled peptide sequence. Non-linear regression analysis was performed which gave an EC50 for the RGD peptide in this assay of $1.6x10^{-9}$ M. This experiment confirms that the peptide competes with fibronectin for $\alpha_v\beta_3$ and can completely inhibit binding. This assay was therefore used for further experiments in which competitive binding of monovalent and tetravalent peptides were compared.

6.2.3 Adhesion of $\alpha_v\beta_3$-expressing cells to RGD ligands

In the previous section it was shown that the RGD peptide derived from the peptide phage display library competes with fibronectin for binding to $\alpha_v\beta_3$. However, the immobilised integrin may be in a 'superactivated' form as a purified ligand bound to ELISA plates (John Marshall- personal communication), particularly in the presence of cations, and therefore it could not be assumed that activity was preserved in the more biologically relevant setting of the cell membrane. It was important, therefore, to test the capacity of the peptide to bind the integrin in this more physiological environment. The series of experiments described in the next section were therefore aimed at optimising an assay to test the capacity of the peptides to bind cells expressing $\alpha_v\beta_3$.

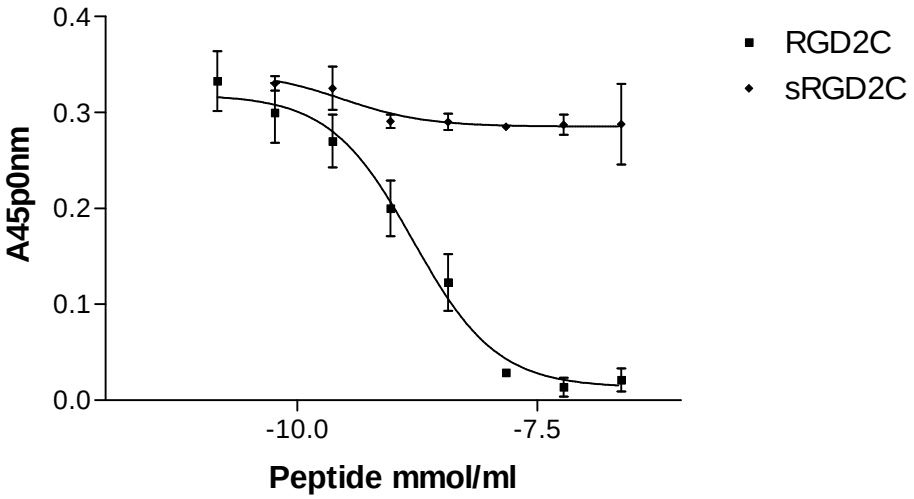

Figure 6.2: **Competitive binding assay of fibronectin with RGD-peptide for fibronectin.** Fibronectin was incubated on an ELISA plate previously coated with $\alpha_v\beta_3$ in the presence of increasing concentration of RGD2C or scrambled peptide. Bound fibronectin was detected with an HRP-conjugated antibody and developed with TMB. Results are mean +/- SD of duplicate wells. There is clear dose-dependent inhibition of fibronectin binding to $\alpha_v\beta_3$.

6.2.4 Characterisation of cell line integrin expression

For the cell binding assays two $\alpha_v\beta_3$-expressing cell lines were used. The MCF7 β3 cell line is a human breast carcinoma cell line that has been stably transfected with the β_3 integrin subunit and hence expresses $\alpha_v\beta_3$ on the cell surface (Pereira et al. 2004). These cells were used to validate the initial assays. However, they do not form xenograft tumours and therefore for later experiments the alternative A375P cell line was used. These are immortalised melanoma cells which express $\alpha_v\beta_3$ in their native form and form tumours when injected into immunodeficient mice. Both cell lines were kind gifts from Dr John Marshall (Cancer Research UK). Prior to use in experiments $\alpha_v\beta_3$ expression was confirmed by FACS. FACS analysis was repeated at regular intervals in both cell lines and expression of $\alpha_v\beta_3$ was confirmed consistently. Representative plots are shown in Figure 6.3.

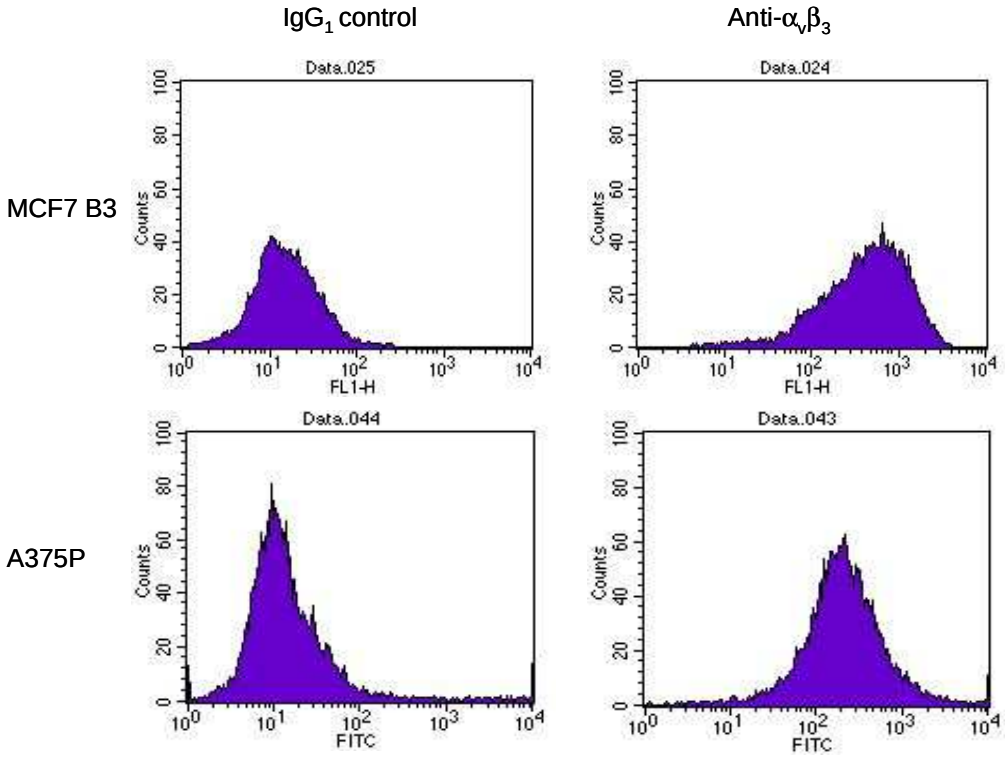

Figure 6.3: **$\alpha_v\beta_3$ expression by MCF7 β_3 and A375P cell lines**. Representative histograms from FACS analysis of MCF7 β3 cells with primary antibodies IgG_1 isotype control (left) and anti-$\alpha_v\beta_3$ (right). The clear shift in fluorescence staining by the secondary antibody confirms expression of the $\alpha_v\beta_3$ dimer by the transfected cells.

6.2.5 Validation of cell adhesion assays: a chromogenic assay produces linear results

p-nitrophenyl-N-acetyl-β-D-glucosaminide (NPAG) is cleaved by the intracellular enzyme b-N-Acetylglucosaminidase to 4-nitrophenol which can be measured by spectrophotometric absorption at 450 nm: this can be utilized to quantify cells in a suspension or adherent to a surface and is thus an excellent means of assessing cell adhesion.

Firstly it was necessary that the NPAG assay worked with the cell lines under investigation and that this could produce an acceptable dose-response curve. To investigate these, doubling dilutions of the cells were prepared after preparation from culture flasks as above. The final re-suspension was made in NPAG buffer as described in the materials and methods as were subsequent dilutions. 50 μl of each dilution was added to a 96 well plate in duplicate. After overnight incubation at 37 ^{0}C and the addition of stop buffer the absorbance was read at 650 nm. The results, shown in Figure 6.4 show a clear dose-response with each of the two cell lines; for subsequent experiments starting concentrations of 10,000 cells per well or 5,000 cells per well were used for the MCF7 β3 and A375P cell lines respectively.

6.2.6 Adhesion of $\alpha_v\beta_3$-expressing cells to fibronectin and vitronectin

To confirm adhesion of the cell lines to their natural ligands the adhesion assay was carried out on plates coated with fibronectin or vitronectin, both of which are ECM ligands for $\alpha_v\beta_3$. Fibronectin was used preferentially as the protein (purified from plasma) was significantly cheaper. For the initial experiments fibronectin or vitronectin were coated to the plates overnight: after washing the plates were blocked before a further wash and addition of cells in 50 μl of serum-free media. Adhesion was allowed to take place for 1 hour at 37 ^{0}C and the plates were then gently washed prior to addition of the NPAG buffer. The reaction was allowed to take place overnight at 37 ^{0}C after which 75 μl of stop buffer was added and absorption read at 450 nm. The results are shown in Figure 6.5: there is clear demonstration of dose-dependent adhesion of the cells to both fibronectin and vitronectin. When visualised under an inverted microscope cell spreading was apparent in adherent cells suggesting activation via the receptor. Thus the assay was shown to be an appropriate means of testing adhesion of these cells to RGD-containing $\alpha_v\beta_3$ ligands: it was therefore used to test for cell adhesion to short RGD-containing peptides as detailed in the next section.

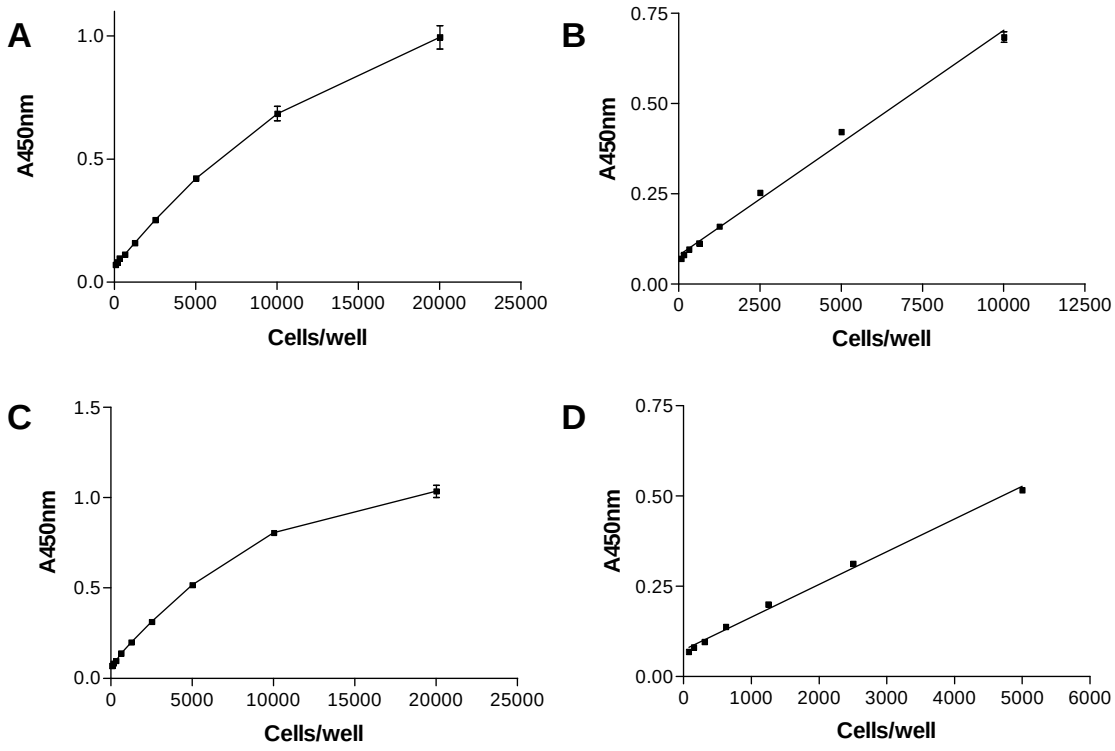

Figure 6.4: **Dose-response of the NPAG colorimetric assay**: Dilutions of cells on 96-well plates were incubated with NPAG/ Triton X-100 substrate buffer overnight at 37 ^{0}C. After the addition of stop buffer absorbance was read at 450 nm. A+C: Results of all cell concentrations used in the experiment for MCF7 B3 (A) and A375P (C). B+D: linear regression analysis of the cell dilutions from the maximum concentration used for adhesion assays. r^2= 0.9916 (B), 0.9945 (D). Results are from quadruplicate wells, mean +/- SD.

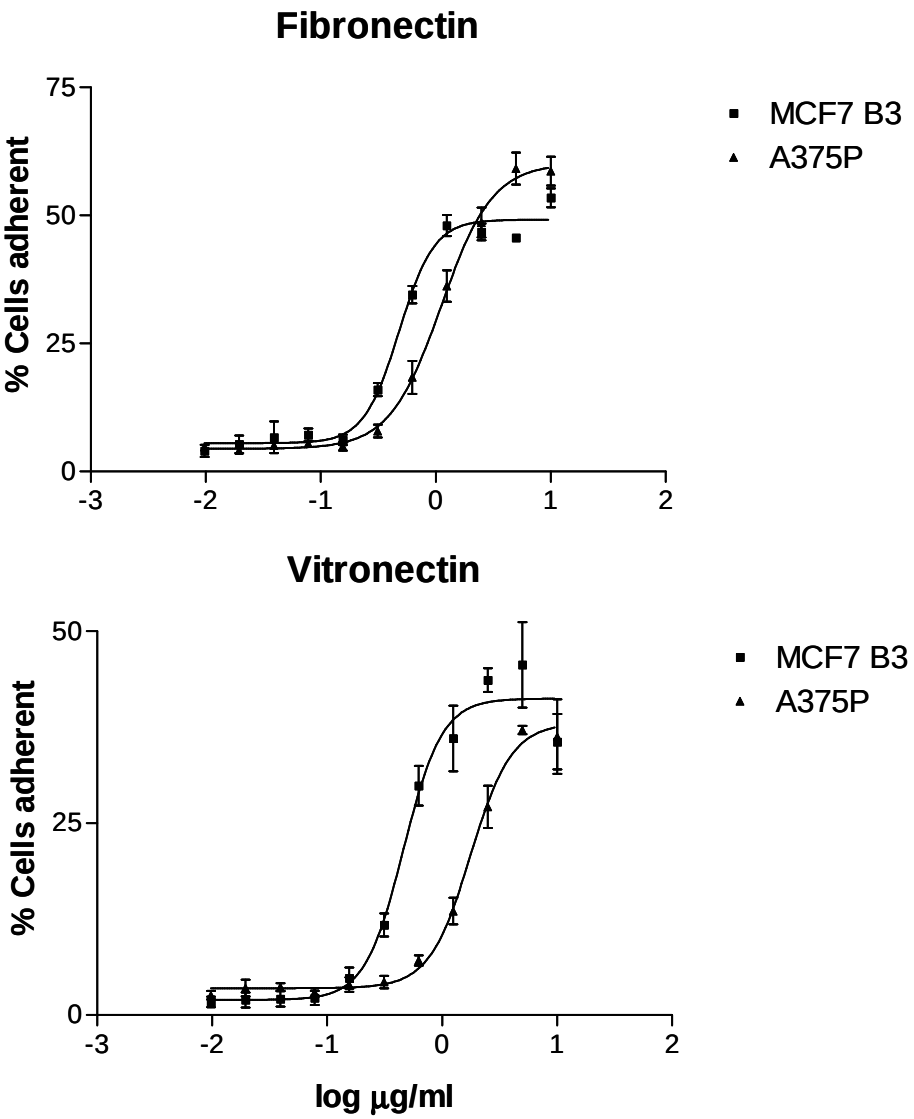

Figure 6.5: **Binding of MCF7 B3 and A375P cell lines to the RGD-motif containing extracellular matrix proteins fibronectin and vitronectin**. 96-well plates were coated with reducing concentrations of protein and incubated with 10^4 (MCF7) or $5x10^3$ (A375P) cells/well for 1 hour at 37 ^{0}C. The plates were washed gently by hand twice in PBS and incubated overnight with NPAG substrate buffer. After addition of stop buffer absorbance was read at 450 nm. Mean of quadruplicate wells +/- SD

6.2.7 Adhesion of $\alpha_v\beta_3$ cells to monomeric peptide

The previous experiment confirmed that the MCF7 β_3 cells adhere to immobilised natural ligands expressing the RGD peptide motif. The next step was to confirm that the cells would bind the monomeric RGD peptide. For this experiment peptides with a 6-carbon aminohexanoic (AHA) acid linker between the biotin tag and the cyclic sequence were used. The biotinylated RGD2C peptide (bRGD2C) was bound to the plate overnight and the adhesion assay carried out as previously. MCF7 β_3 and A375P ells were incubated on the plate in quadruplicate. The results are shown in Figure 6.6. There is a clear dose-response curve with the MCF7 β_3 cells, although the absolute levels were substantially less than those seen with fibronectin or vitronectin. Inspection under an inverted microscope found that whereas cell spreading was seen with fibronectin and vitronectin, no such activation was seen in the peptide-coated plate. Previous reports have demonstrated that although RGD peptide can mediate binding to $\alpha_v\beta_3$, firm adhesion requires domains within the ligand outside the RGD sequence. In this experiment no adhesion was seen of the A375P cells to the RGD2C peptide. The reason for this was unclear; expression of $\alpha_v\beta_3$ had been confirmed by FACS and the A375P cells adhere to both vitronectin and fibronectin. It was possible that the integrin was expressed in an inactive state or that the RGD2C peptide only bound the integrin in its most active conformation. A further possibility is that the peptide/ integrin interaction is insufficient to support adhesion during the washes: A375P cells are larger than MCF7 β3 cells and hence shear forces during washing will be proportionately greater (Lemmon et al. 2005). For *in vivo* experiments it was necessary to use a peptide that was known to bind the A375P cell line and therefore an alternative RGD peptide was used. This peptide, referred to here as cRGD has the structure c(RGDyK): the RGD sequence is followed by a d-tyrosine and a lysine. The peptide is cyclised via an amide bond and the amino side chain of the lysine enables further derivatisation of the peptide linkers and labels. As discussed in the introduction, this peptide sequence has been successfully used in the imaging of $\alpha_v\beta_3$-expressing tumours in animal models in monomeric and

dimeric forms; furthermore internalisation of the peptide has been demonstrated *in vitro* of ^{111}In-DTPA-c(RGDyK) (van Hagen et al. 2000). It was therefore thought appropriate to use this peptide as a 'gold standard' during the validation of the tetrameric constructs.

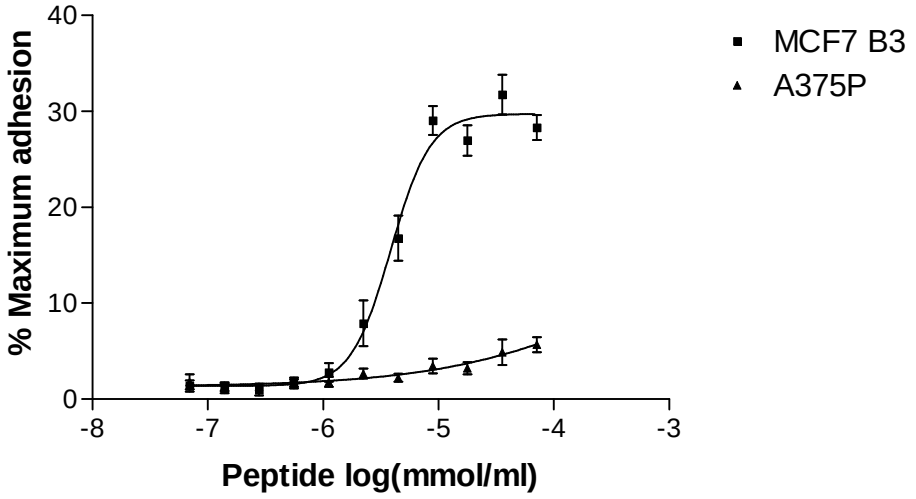

Figure 6.6: **Adhesion of MCF7 β3 and A375P cells to plates coated with RGD2C peptide.** 96-well plates were coated with reducing concentrations of biotinylated RGD2C peptide and incubated with suspensions of MCF7 β3 or A375P cells. Dose-dependent binding is seen with the MCF7 β3 cells whereas none is seen with the A375P cells. Mean +/- SD of quadruplicate wells.

6.2.8 Biotinylation of cyclic RGD peptide

The peptide was biotinylated using sulfo-NHS biotin, a commercially available biotinylation reagent. The molecule consists of a reactive N-hydroxysulfosuccinimide (sulfo NHS) linked to biotin via a six-carbon spacer arm. This spacer is of the same length as the aminohexanoic acid spacer used for the other peptides in this part of the project and the spacer arm was thought likely to provide sufficient separation of the peptide and biotin group. The reagent was conjugated to the peptide in a one-step reaction by incubation of the peptide with a ten-fold molar excess of the biotinylation compound at pH 8.3 for 30 minutes at RT. The reaction was stopped by acidification of the reaction mixture. Prior to the

full-scale reaction it was confirmed that complete biotinylation of the peptide was achieved. Reverse-phase high-performance liquid chromatography (RP-HPLC) was run on the reaction products. The presence of the aromatic tyrosine side-chain in the peptide enables the UV absorption at 280 nm to be monitored: HPLC of the biotinylation reagent found minimal absorption at 280 nm. The HPLC chromatograms are shown in Figure 6.7. The UV absorption at both 220 nm and 280 nm is presented: at 220 nm UV light is absorbed by peptide bonds and so will be absorbed by any peptide and at 280 nm is absorbed by aromatic residues; discrimination between peptide sequences with or without aromatic groups is therefore possible. The first part of the figure shows the trace from the un-conjugated peptide confirming absorbance at 220 and 280 nm. The second trace shows the reaction products. Only one of the 220 nm peaks is associated with a 280 nm peak: as the retention time has shifted from that seen with the unconjugated peptide, this suggests that all of the peptide has reacted. Solvent fractions containing the individual peaks were collected from the HPLC eluate. The peak containing the c(RGDyK) was analysed by MALDI-TOF MS as described in the materials and methods. The results, shown in Figure 6.8, confirm that the reaction product has the same mass as expected, thus confirming biotinylation of the peptide.

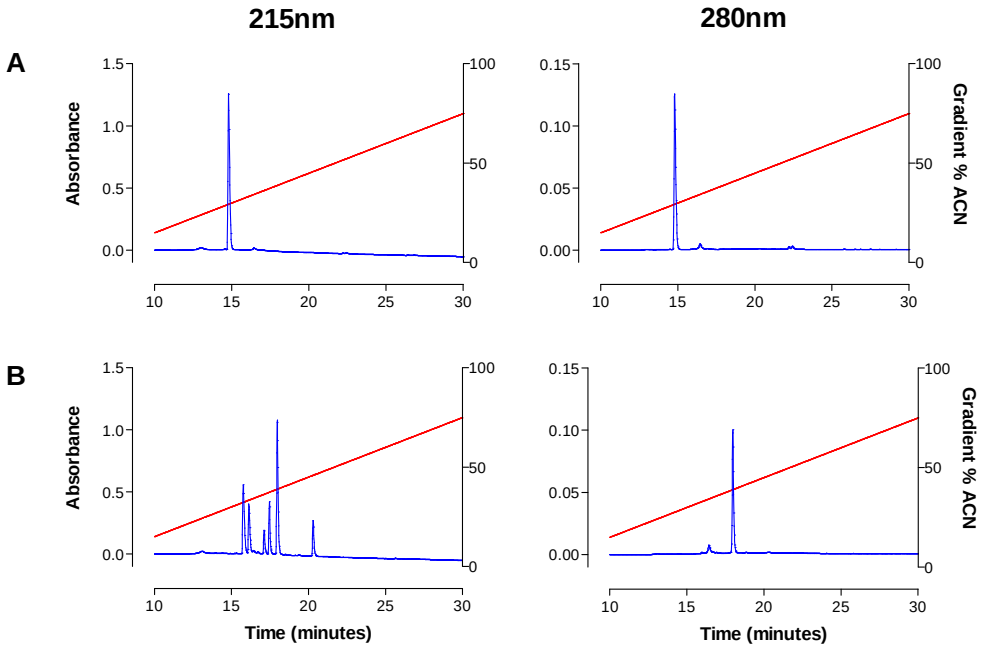

Figure 6.7: **RP-HPLC of c(RGDyk) before (A) and after (B) biotinylation**. Saturation of the peptide with the biotinylation reagent is confirmed by the shift of the retention time of the absorbance peak seen at 280 nm.

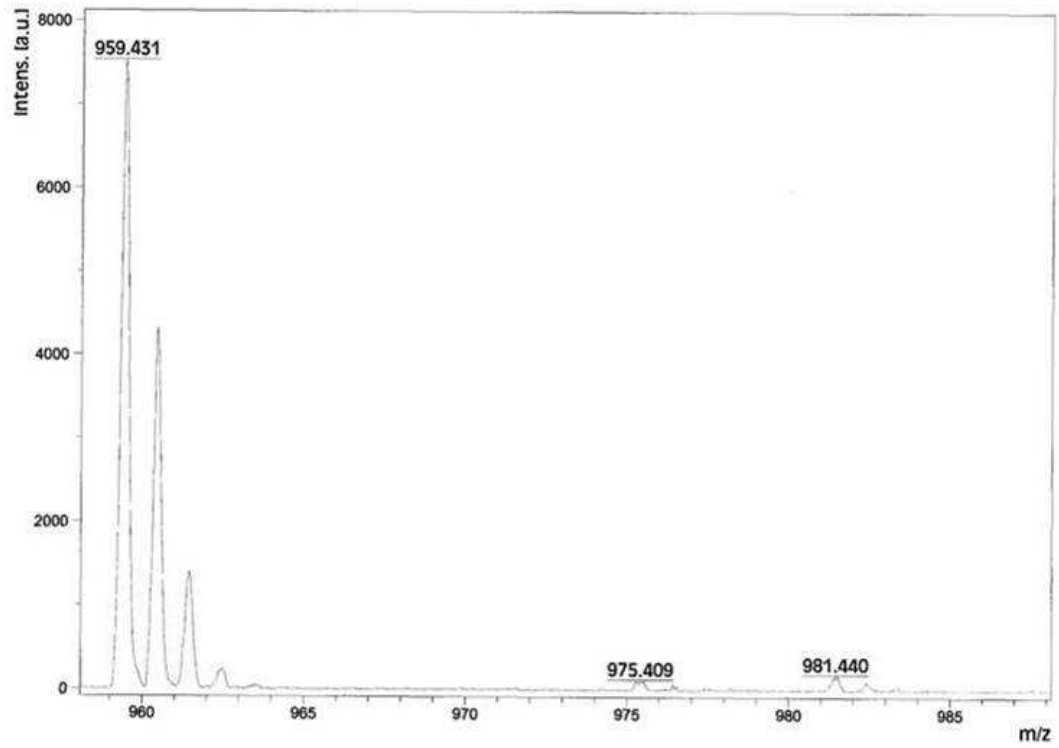

Figure 6.8: **MALDI-TOF mass spectrometry of biotin-LC-c(RGDyK).** The expected molecular weight (960 Da) is confirmed as the major peak.

6.2.9 Comparison of inhibition of fibronectin binding to $\alpha_v\beta_3$ by RGD2C and cRGDyK peptides.

The fibronectin/ $\alpha_v\beta_3$ binding inhibition assay as described in section 6.2.6 was carried out with cRGDyK before and after biotinylation as well as with the biotinylated RGD2C peptide. The assay was performed exactly as previously and the results are shown in Figure 6.9. The IC50 values were similar between the 3 peptides ($1.54x10^{-9}$ M, $8.44x10^{-10}$ M and $1.04x10^{-9}$ M for the RGD2C, cRGDyK and biotinylated cRGDyK peptides respectively, the differences were not significant). This confirms that the cRGDyK peptide binding was unchanged by biotinylation and that both RGD2C and cRGDyK peptides were comparable in this assay. As already discussed, however, behaviour of the peptide in an assay based on immobilised integrin may not necessarily reflect the situation of integrin

expressed on the cell surface and therefore the cell adhesion assays were repeated to address this.

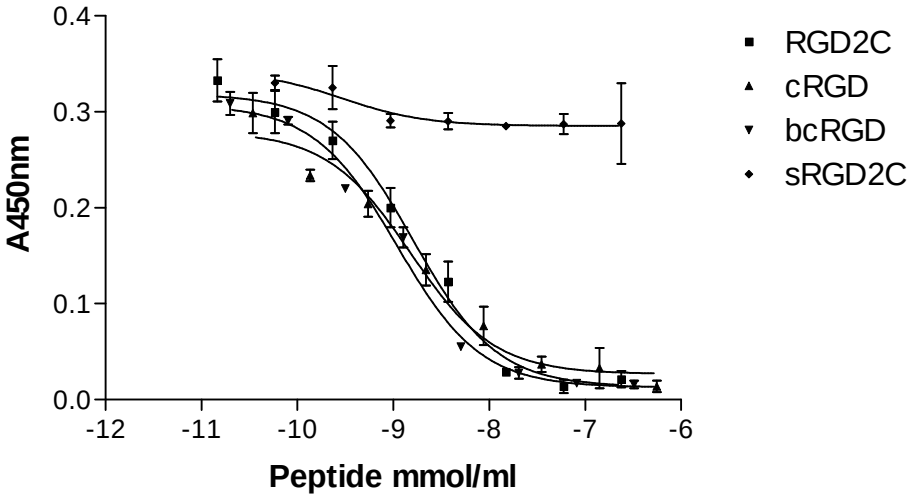

Figure 6.9: **Inhibition of fibronectin binding to immobilised $\alpha_v\beta_3$ by RGD peptides.** RGD2C, cRGD and biotinylated cRGD (bcRGD) were pre-incubated in plates coated with $\alpha_v\beta_3$ prior to the addition of fibronectin. After washing bound fibronectin was detected with HRP-conjugated anti-fibronectin antibody followed by TMB substrate. There is dose dependent inhibition of fibronectin binding with all 3 RGD peptides: no difference is seen before or after biotinylation of the cRGD peptide. Mean of duplicate wells +/- SD.

6.2.10 Adhesion of $\alpha_v\beta_3$ cells to biotin-RGD

The first experiment to assess adhesion of A375P cells to biotin-cRGDyK showed no specific binding: this experiment was performed with an identical protocol to the previous peptide adhesion experiments. At the end of the experiment the plates were washed and incubated with streptavidin-conjugated HRP and developed with TMB in order to determine the presence of biotinylated peptide. This showed that binding of biotin-cRGDyK was minimal (Figure 6.10). To guarantee consistent peptide binding, therefore, 96-well plates pre-coated with streptavidin were used; this would have the added advantage of ensuring availability of the peptide binding site whilst bound to streptavidin. The pre-blocked plates were incubated with saturating concentrations of biotin-cRGDyK, biotin-RGD2C or biotin-

sRGD2C peptides before washing and completion of the adhesion assay as before with both A375P and MCF7 B3 cells. The results are described in section 6.3.2.2.

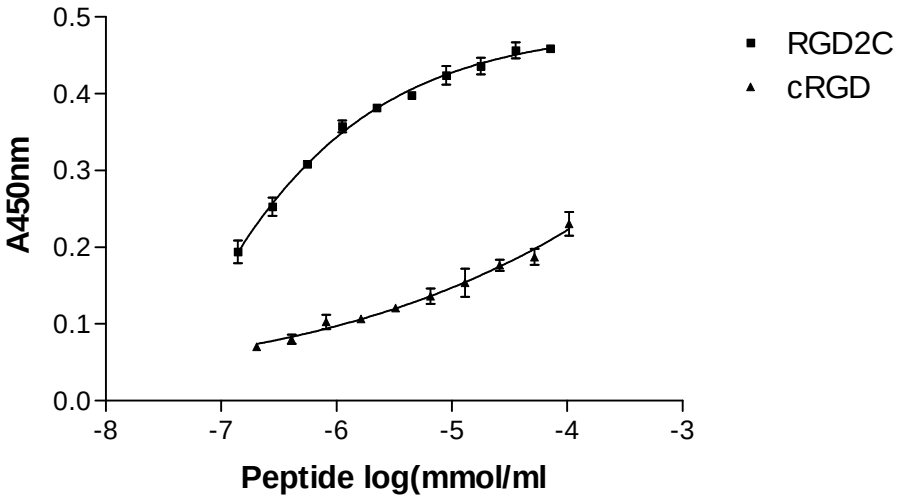

Figure 6.10: Analysis of biotinylated peptide binding to plates. After the RGD-peptide adhesion assay with $\alpha_v\beta_3$-expressing cells found no binding to cRGD peptide, the plates were incubated with HRP-conjugated streptavidin and developed with TMB substrate. Very little biotinylated cRGD peptide was bound to the plates indicating poor binding properties of the peptide. Mean of duplicate wells +/- SD.

6.2.11 Competition assay of monomeric peptide for $\alpha_v\beta_3$ cell adhesion to fibronectin

The adhesion assay was repeated with the intention of showing inhibition of cell binding to fibronectin by the RGD2C peptide. From a series of experiments it was found that inhibition was seen only when the concentration of the fibronectin used to coat the plate was reduced to 0.25 μg/ml. The assay was performed with the MCF7 β3 cells: the wells were pre-incubated for 10 minutes with peptide prior to the addition of the cells; otherwise the procedure was carried out as before. The results are in Figure 6.11. There is dose-dependent inhibition of cell binding by the peptide which is not seen with the control peptide. However, the absolute absorbance readings are low and the error bars (from quadruplicate readings)

wide. It was therefore felt that the reliability of this assay as an assay for inhibitory activity of the peptides would not be optimal.

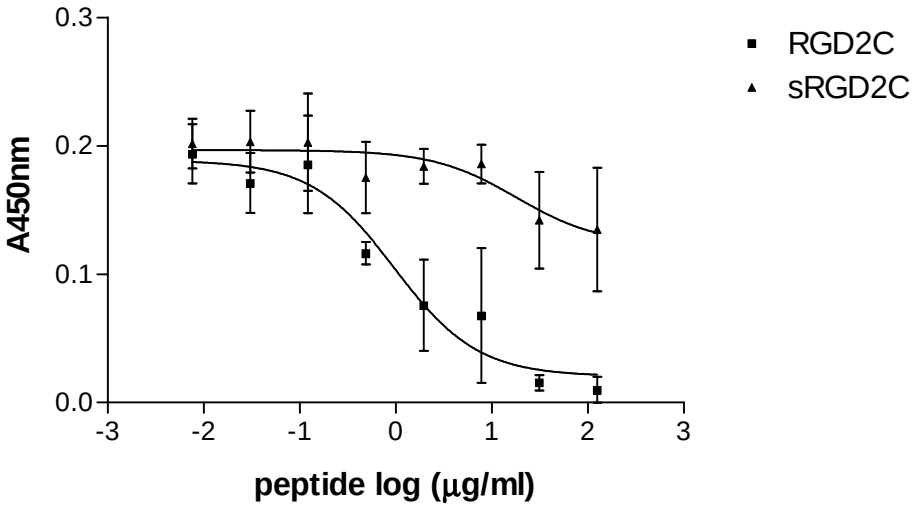

Figure 6.11: **Inhibition of MCF7 B3 cell binding to fibronectin by RGD peptide**. Fibronectin was bound to wells at a concentration of 0.25 μg/ml: after washing the cells were pre-incubated with RGD2C or scrambled RGD2C peptides prior to incubation with MCF7 β_3 cells. The wells were washed twice by hand and bound cells detected with NPAG substrate. Mean of quadruplicate wells +/- SD

6.3 Polymerisation of peptide with streptavidin

As described in the introduction to this chapter, the streptavidin molecule, with its 4 biotin binding sites, is an ideal tool for the rapid tetramerisation of the peptide. A method was therefore developed for the rapid conjugation of biotinylated peptide to streptavidin followed by radiolabelling with ^{111}In and purification.

6.3.1 Saturation of streptavidin binding sites with biotinylated peptide

Streptavidin consists of 4 subunits each with a binding site for biotin: in order to achieve maximum valency, i.e. 4 biotinylated peptides per molecule, streptavidin was incubated with varying concentrations of peptide (in ratios of 4-fold molar excess) in order to assess at which concentrations saturation was achieved. After incubation for 1 hour the solution was diluted and bound to 96-well plates: free biotin binding sites were measured by incubation with biotin-HRP followed by

the addition of the HRP substrate TMB. Results are shown in Figure 6.12. By applying non-linear regression to the streptavidin-alone curve, the derived concentration of free biotin-binding sites for the 4:1 peptide:streptavidin reaction is ~28%. Saturation is effectively achieved with the addition of 8:1 or 16:1 molar ratios of peptide. It was therefore decided to use the 16:1 ratio (i.e. 4-fold excess) of peptide for all future experiments in order to achieve maximum saturation. This would results in the presence of excess free peptide which could interfere with binding studies, and therefore various methods were tested for the purification of tetravalent streptavidin.

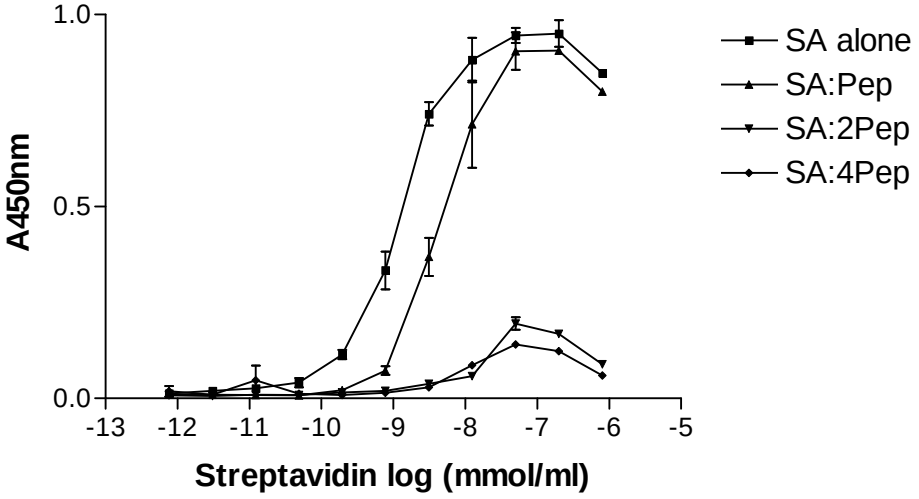

Figure 6.12: **Conjugation of streptavidin to biotinylated peptide.** Streptavidin was incubated with 4:1, 8:1 or 16:1 molar ratios of peptide (Pep/ 2Pep/ 4Pep respectively) for 1 hour at RT. Dilutions of the reaction mixture were then bound to 96 –well plates followed by incubation with biotinylated HRP. The wells were developed with TMB substrate and absorbance read at 450 nm. Mean of duplicate wells +/- SD

6.3.1.1 Purification of tetravalent streptavidin-peptide by size exclusion filtration

Several methods were investigated for the purification of tetravalent SA-peptide from unbound peptide molecules, including dialysis, molecular weight cut-off

filtration and size-exclusion filtration. Of these, size-exclusion filtration was the simplest and most successful: centrifugation of a solution through the embedded resin results in retention of low molecular weight solutes whilst larger molecules emerge in the filtrate. This method would allow rapid purification of the tetravalent streptavidin/ peptide molecule: an additional advantage would be the purification of free radioisotope when the complex was radiolabelled.

The method was tested with an ELISA-based assay. After incubation of streptavidin with biotinylated peptide dilutions of the solution were incubated on ELISA plates with or without prior filtration. The plates were coated overnight and after washing and blocking with BSA were incubated with an anti-streptavidin antibody, streptavidin-conjugated HRP or biotin-conjugated HRP. After a further wash the HRP-treated plates were developed with TMB, whilst the anti-streptavidin Ab-treated plate was incubated with an HRP-conjugated anti-mouse antibody following which TMB could be used to develop the colour. The detection of streptavidin with antibody allows for correction for the amount of streptavidin bound to the plates: by using the unfiltered streptavidin as a reference curve, the bound concentration of filtered streptavidin could be determined and the values for streptavidin and biotin binding adjusted accordingly. Representative results are shown in Figure 6.13. The values have been corrected for variation in the concentration of bound peptide as described. Incubation with biotinylated HRP enables detection of free biotin binding sites on streptavidin: no biotin binding was seen with the streptavidin post-incubation with peptide before or after filtration- this confirms saturation of the molecule and that this is preserved after filtration. Incubation with streptavidin-HRP enables detection of free biotinylated peptide. Whilst some free peptide is detectable, this is around 3% of that present prior to filtration and it was decided that this would be acceptable for further studies.

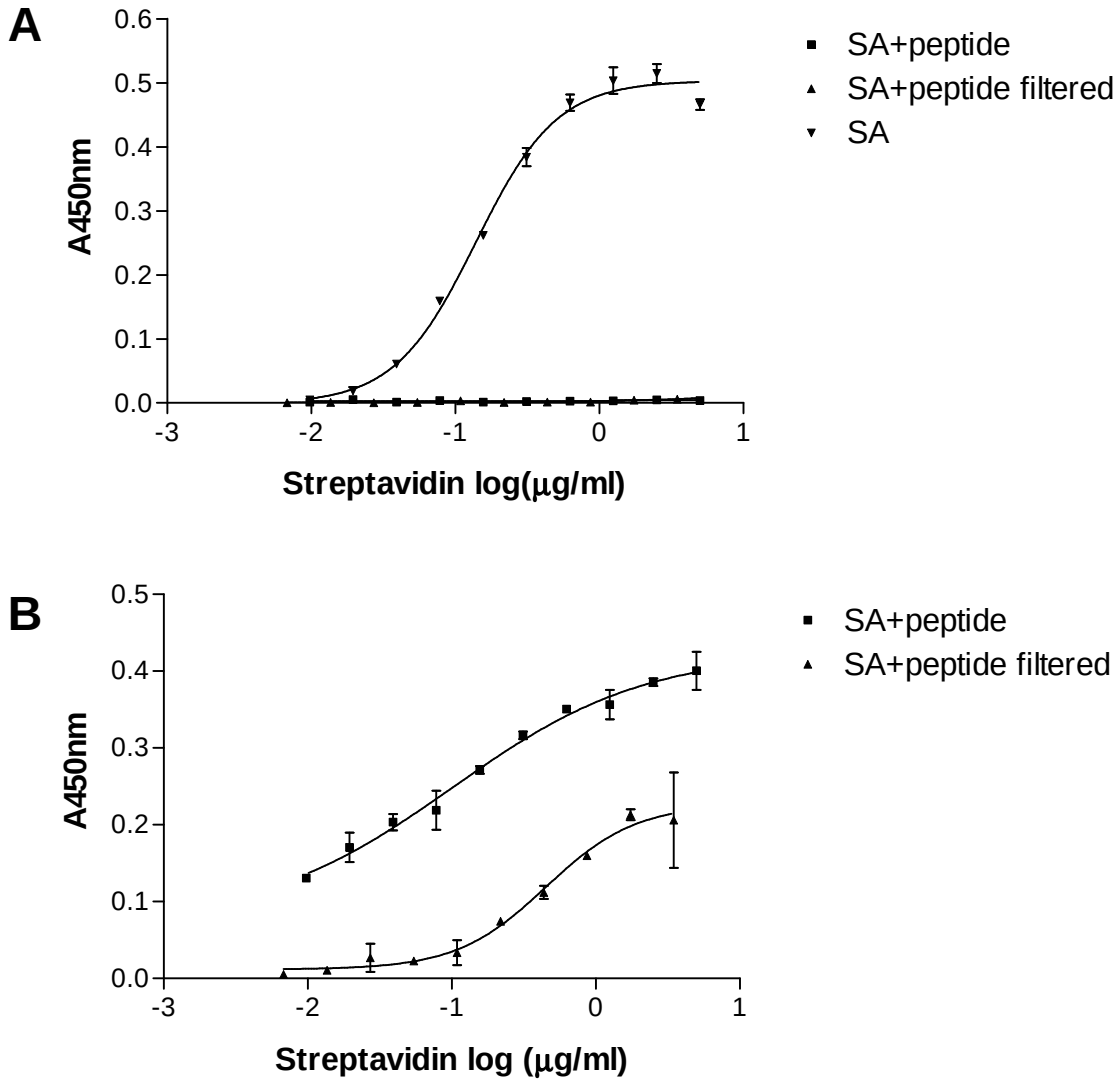

Figure 6.13: **Purification of streptavidin-peptide.** Determination of streptavidin saturation (A) and free peptide concentration (B) after incubation with excess peptide before and after column filtration. After incubation with peptide for 1 hour at RT the reaction mixture was diluted and bound to 96-well plates. Streptavidin concentration was corrected by deriving a standard curve with anti-streptavidin antibody. The wells were incubated with biotinylated HRP to detect free biotin-binding sites (A) or HRP-conjugated streptavidin to detect free biotinylated peptide (B). These results confirm saturation of the streptavidin in this assay: the free biotinylated peptide was ~3% of that seen pre-filtration as determined from non-linear regression analysis. Mean of duplicate wells +/- SD.

6.3.2 Tetrameric peptide binding to $\alpha_v\beta_3$

The biotinylated peptides were designed with the incorporation of a spacer arm: streptavidin has a deep binding pocket for biotin and it has been shown that a short spacer sequence can result in loss of activity of the binding domain of a conjugated peptide (Boturyn et al. 2004). The next stage was therefore to confirm that once conjugated to streptavidin the RGD peptide retained affinity for its receptor. This would also support the prediction that the synovial-homing peptide would retain its affinity for its ligand.

In the first instance, streptavidin was incubated with 1:1 molar ratio of biotinylated peptide (i.e. 1:1 for biotin binding sites). This would enable easy comparison of the RGD2C and scrambled peptide sequences without the need for a further step to quantify streptavidin concentration following column filtration. The plates were coated with $\alpha_v\beta_3$ as for the previous experiments and after blocking were incubated with streptavidin/ peptide. The streptavidin complex was allowed to bind for 1 hour at RT before washing. Streptavidin was detected with an anti-streptavidin antibody followed by HRP-conjugated anti-mouse antibody and developed with TMB.

The results of the first experiment are shown in Figure 6.14**A**. There is obvious dose-dependent binding for streptavidin-conjugated RGD2C to $\alpha_v\beta_3$. There is possibly a low level of binding with the scrambled peptide: however, no inhibition of fibronectin binding to $\alpha_v\beta_3$ was seen in the previous experiments and it is therefore unlikely that the scrambled sequence has activity. The low level of binding seen is most likely to be non-specific, although streptavidin does contain an RGD-mimicking RYD sequence which has been shown to mediate binding to cell membranes (Alon, Bayer, & Wilchek 1990). The assay was later repeated with the cRGDyK peptide (Figure 6.14**B**). Although the assays were not done in parallel, the derived EC50 values were similar: the EC50 for the RGD2C and cRGDyK-streptavidin complexes were $1.6\text{x}10^{-8}$ and $1.08\text{x}10^{-8}$ M respectively, and these were not significantly different.

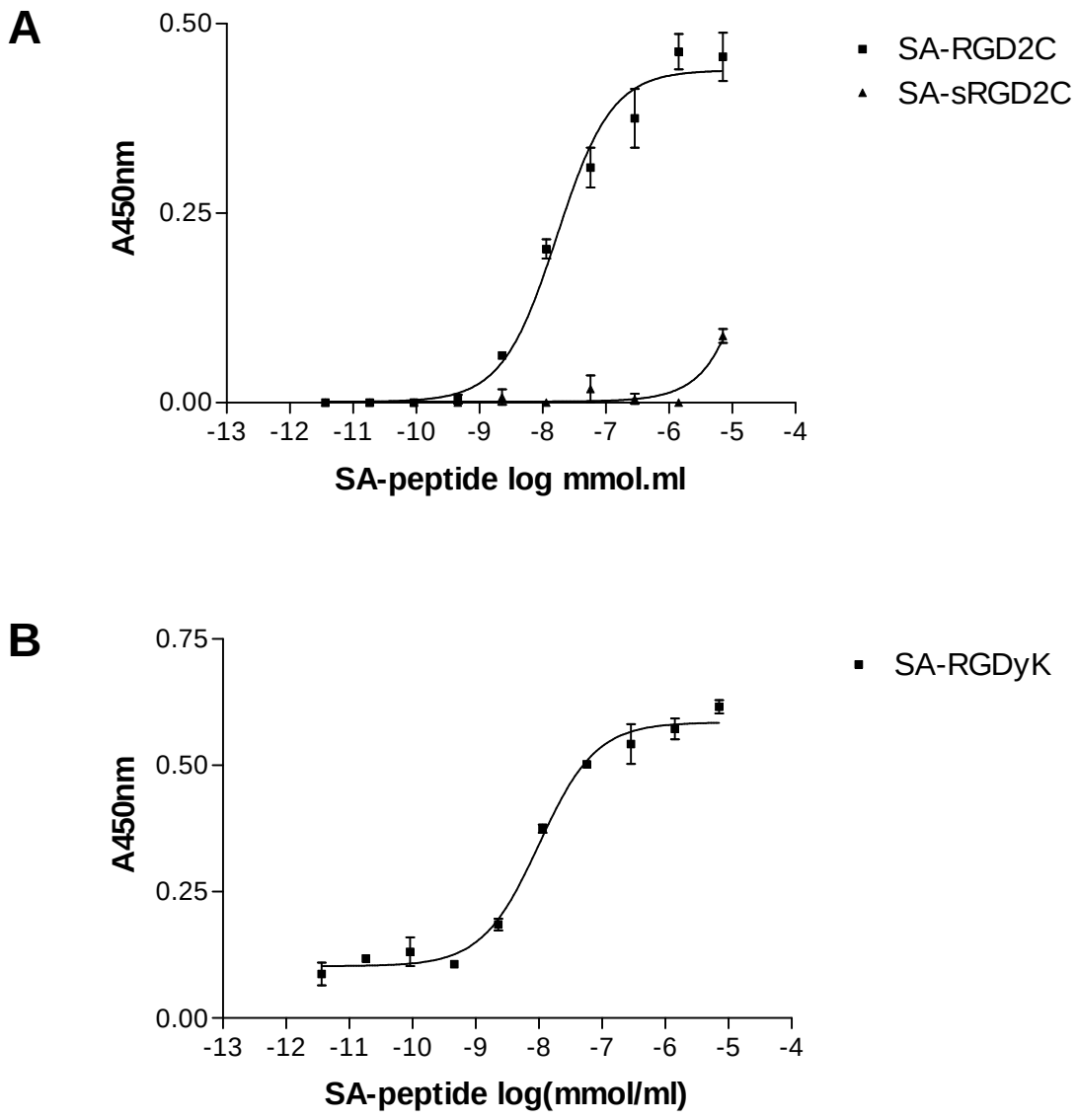

Figure 6.14: **Binding of tetravalent peptides RGD2C and scrambled RGD2C (A) and cRGDyK (B) to immobilised $\alpha_v\beta_3$.** Plates were incubated with dilutions of streptavidin-polymerised peptide: after washing bound streptavidin was detected with anti-streptavidin antibody and developed with TMB substrate. There is dose-dependent binding of both unscrambled peptides to $\alpha_v\beta_3$. Mean of duplicate wells +/- SD.

6.3.2.1 Competition of tetrameric peptide for fibronectin binding to $\alpha_v\beta_3$

The next experiment was to compare the monomeric and tetravalent peptides in the competitive binding assay. This would, firstly, confirm that the spacer arms of the peptides were long enough to enable multimeric binding and, secondly, establish whether this could increase the avidity of the molecule.

The experiment was repeated as with the monomeric peptide. For polymerisation streptavidin was incubated with a 1:1 ratio of peptide (to biotin binding sites) with the same concentration of peptide. The fixed concentration of peptide would enable accurate comparison of the monovalent and tetravalent molecules: the use of a purification step at this stage could introduce error due to the potential inaccuracy introduced by the need to quantify the concentration of purified streptavidin/ peptide. The results are shown in Figure 6.15. There is a small shift of the competitive binding curve to the left with the addition of streptavidin. Analysis by non-linear regression found that the IC50 had halved with the tetravalent peptide, although this was within the margin of error of the experiment.

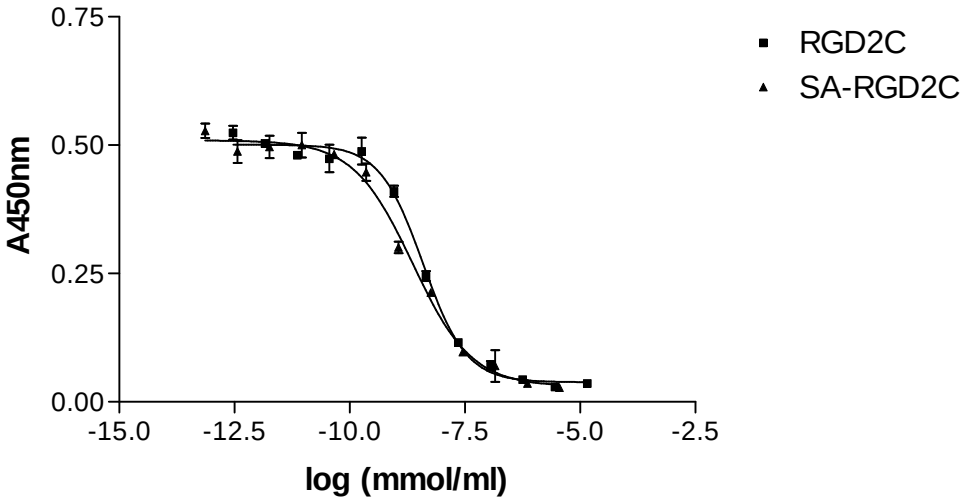

Figure 6.15: Tetravalent peptide inhibition assay. Inhibition of fibronectin binding to $\alpha_v\beta_3$ by monomeric or tetravalent (streptavidin-conjugated) peptide. The competitive binding assay was performed as for previous experiments with monovalent or streptavidin-polymerised peptide. Non-linear regression analysis found the IC50 of the RGD2C and SA-RGD2C inhibitors to be 4.4 $x10^{-9}$ mmol/ml 2.3 $x10^{-9}$ mmol/ml respectively although this difference was not significant. Mean of duplicate wells +/- SD.

6.3.2.2 Adhesion of $\alpha_v\beta_3$ cells to tetravalent peptide

The previous experiment with peptide had shown binding of the MCF7 β3 cell line to the RGD2C peptide; binding was not seen to the A375P cells. Furthermore, binding of the cRGDyK peptide to the plates had been poor and no cell adhesion was seen. These adhesion assays were therefore repeated with plates to which streptavidin was pre-bound in fixed concentrations and pre-blocked. This would enable more uniform and reliable adhesion of the peptides to the plates and also, if binding was seen, confirm that the peptides could support cell adhesion whilst bound to streptavidin.

The plates were incubated with fixed concentrations of biotinylated peptide for 1 hour, washed and incubated with the cells. The adhesion assay was completed as previously. The results are shown in Figure 6.16. In this experiment binding is

seen to both peptides by the A375P cells and, as before, binding only of the MCF7 β3 cells to RGD2C. This observation, that RGD2C does not support A375P cell binding, suggests that the affinity of the RGD peptides differ, with increased cell binding seen to the cRGD peptide. The reason for the differential adhesion to the two cell lines is also unclear. It is likely, as discussed above, that the larger size of the A375P cells results in greater shear forces during the washing steps. It is also possible that there is an additional contribution from differences in the integrin conformation or the number and density of receptors. This could be the subject of future experiments, but at this stage it was sufficient to show that the new biotinylated cRGDyK peptide could support adhesion of both cell lines.

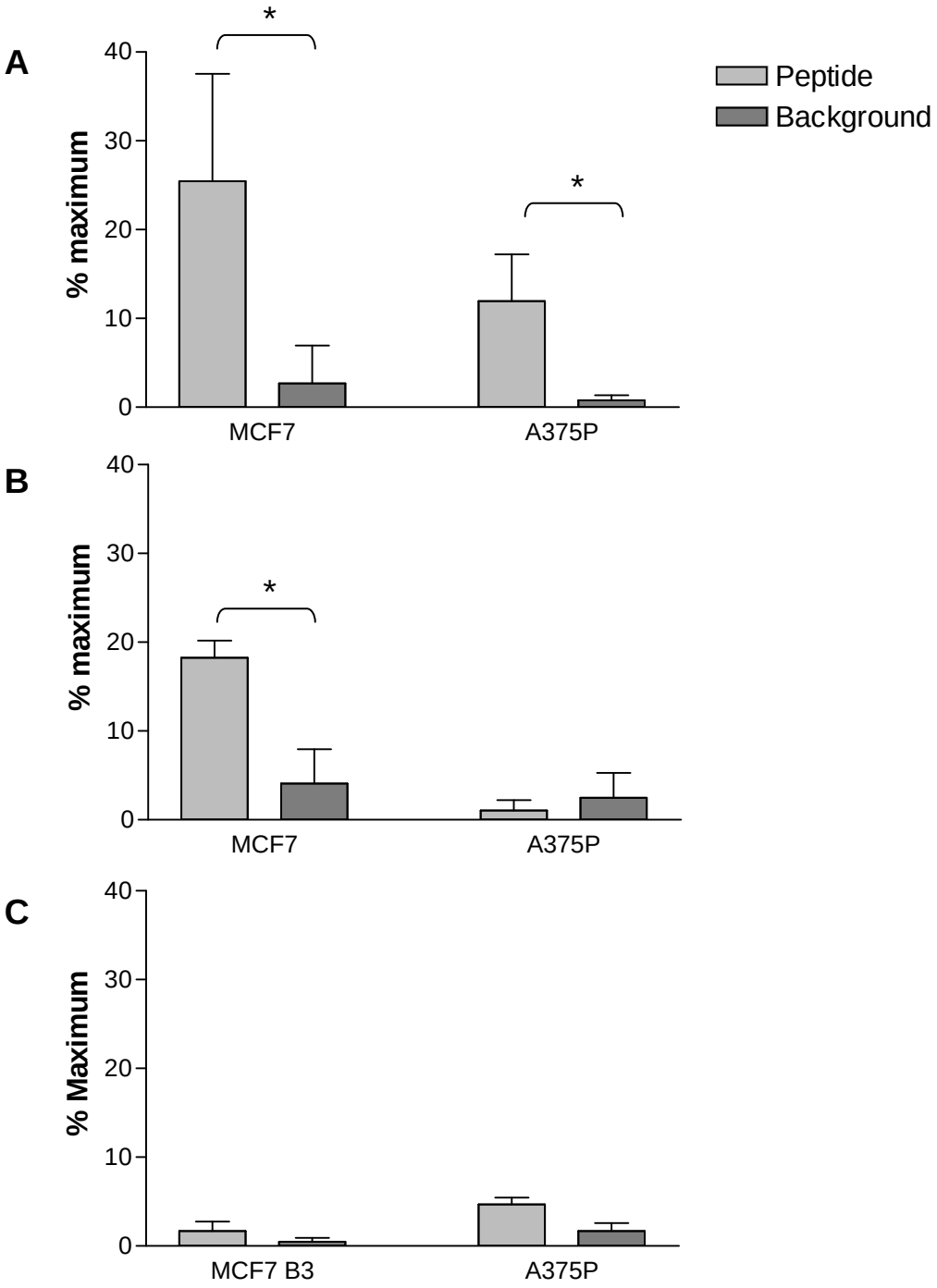

Figure 6.16: **Adhesion of cells to plates coated with streptavidin + biotinylated peptide: A**: cRGD **B**: RGD2C, **C**: sRGD2C. Streptavidin-coated plates were coated with peptide prior to incubation with cells as for the previous adhesion experiments and incubated with cells as previously. There is significantly greater binding of MCF7 β_3 cells to both peptides and of A375P cells to the cRGD peptide only. Mean +/- S.D $^{*}p<0.05$

6.4 Radiolabelling of tetravalent peptide

Radiolabelling provides a sensitive means of quantifying *in vivo* biodistribution. It was therefore decided to devise a means of radiolabelling streptavidin in order to track the tetravalent peptide after injection into transplanted mice. The simplest method for radiolabelling would be conjugation of ^{125}I to tyrosine groups within the protein: it has been shown that a tyrosine residue within the biotin-binding pocket of streptavidin is critical for biotin binding, modification of which with a tyrosine-specific reagent abrogates binding (Gitlin, Bayer, & Wilchek 1990). Modification of lysine, however, only resulted in partial abrogation of biotin binding (Gitlin, Bayer, & Wilchek 1988). Furthermore, ^{111}In is preferable to ^{125}I due to its shorter half life (2.7 vs. 60 days) and is more suitable, if required, for imaging studies. Streptavidin was therefore conjugated to DTPA, a bifunctional chelating agent which allows rapid labelling with ^{111}In. ^{111}In-DTPA has the additional advantage that there is no natural metabolic pathway for excretion from cells: if internalised, therefore, this 'residualising' property would result in longer retention of the radiolabel (Gotthardt et al. 2004).

6.4.1 Conjugation of streptavidin to DTPA

The method used was the same as that for the conjugation of DTPA to antibodies. The conjugated streptavidin was analysed by size-exclusion HPLC, representative results of which are shown in Figure 6.17**A-B**.

It was considered possible that contaminating DTPA or bound DTPA may influence the spectrophotometric absorbance and therefore the concentration was determined by ELISA. A capture method was used whereby anti-streptavidin antibody was bound to the plate prior to incubation with the streptavidin solution. This was then detected with a second (polyclonal) HRP-conjugated anti-streptavidin antibody and developed with TMB substrate. Streptavidin of known concentration was used to produce a standard curve against which the concentration of the streptavidin-DTPA was derived. The derived concentration of streptavidin-DTPA was 1.4 mg/ml

6.4.2 Radiolabelling of DTPA-streptavidin with ^{111}In

DTPA-conjugated streptavidin was labelled with ^{111}In as described in the conjugation protocol. Indium was added to DTPA-SA in acetate buffer pH 6.0 and incubated for 30 minutes. At the end of the incubation period 50 mM EDTA in acetate buffer was added to chelate inbound indium and the radiolabelling efficiency measured ITLC. A 1 µl sample of the conjugation solution was spotted onto a silica gel ITCL strip which was then run with acetate buffer + 50 mM EDTA as solvent. Unbound indium would move with the solvent front whilst indium bound to peptide would stay at the origin. Strips were cut in half allowing activity at the origin and solvent front to be measured in a gamma counter. Labelling efficiency was derived from the ratio of activity at the solvent front to that at the origin. Results from duplicate strips showed that labelling efficiency (i.e. % ^{111}In bound to peptide) was >95%. ^{111}In-labelled streptavidin was also run on SE-HPLC: representative HPLC traces are shown in Figure 6.17**C** and show co-localisation of the 280 nm absorbance and radioactivity peaks at an elution time of ~20 minutes. There is a small secondary peak, likely to represent unbound DTPA: this would be removed with the purification of unbound peptide prior to *in vivo* injection.

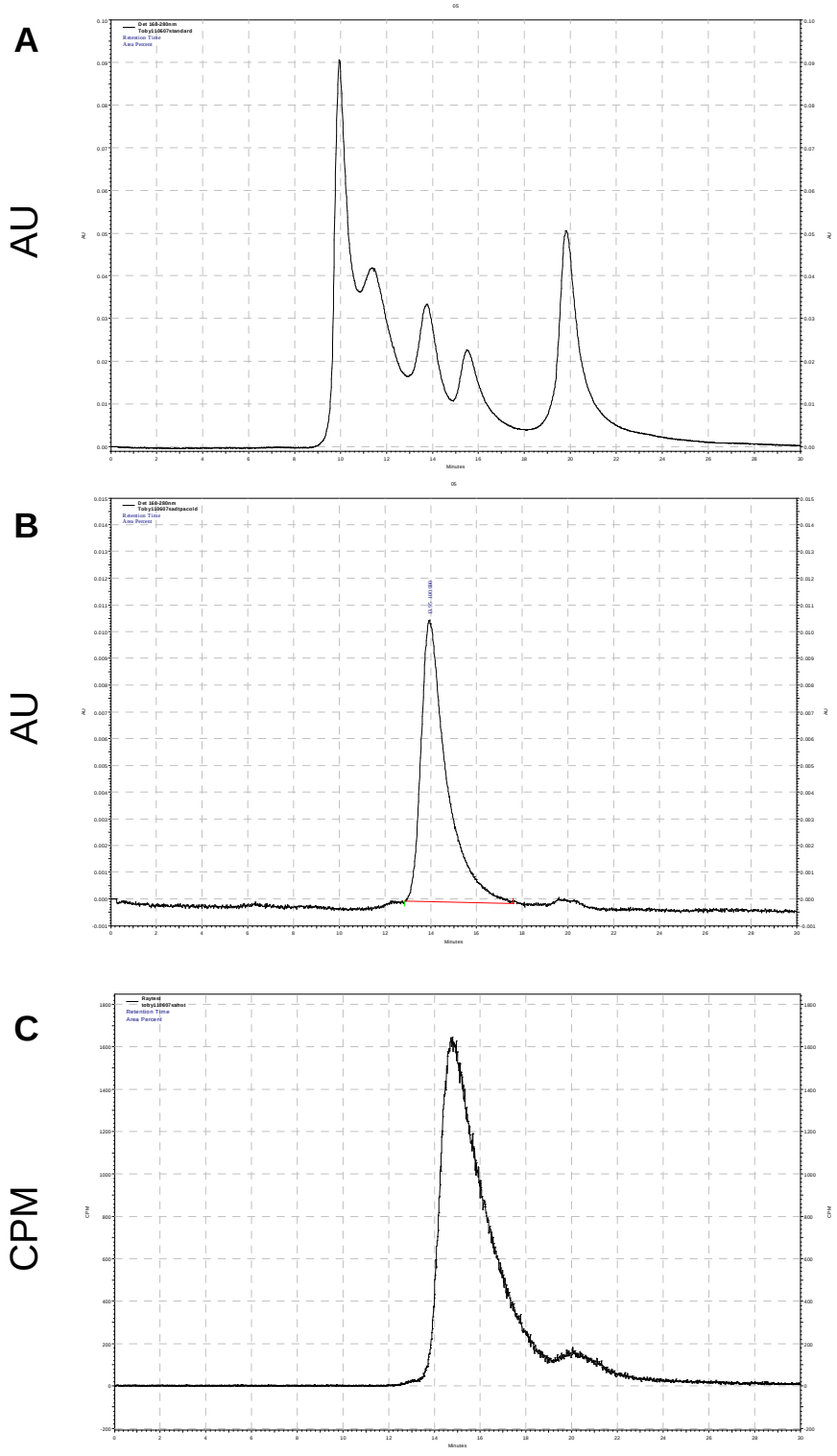

Figure 6.17: **Radiolabelling of streptavidin.** SE-HPLC chromatograms of DTPA-SA. **A**: Standards (molecular weights 670 kDa, 158 kDa, 44 kDa, 17 kDa, 1.35 kDa). **B** UV absorbance peak of cold DTPA-SA **C** Radioactivity peak of ^{111}In-DTPA-SA

6.4.3 Confirmation of biotin binding by DTPA-streptavidin

Having confirmed that DTPA had been successfully conjugated to streptavidin and satisfactory ^{111}In labelling efficiency it was important to ensure that the binding affinity of streptavidin for biotin was unaffected. The streptavidin binding pocket for biotin includes lysine: binding of DTPA to the ε-amino side-chain would be likely to disrupt this, although the probability of these lysine residues being affected is relatively low. The conjugation technique was designed to produce ~1 molecule of DTPA per molecule of protein making this less likely to be a problem: however, each subunit of streptavidin contains seven lysine residues (Argarana et al. 1986) and it is unclear whether local charge and protein folding may render some of these more susceptible to derivatisation. Streptavidin or DTPA-conjugated streptavidin were coated to 96-well plates overnight in doubling dilutions, after which the plates were blocked and incubated with biotinylated HRP for 1 hour. After a further wash TMB was added and, after the colour had developed, absorbance read at 450 nm. In order to correct for the concentration of streptavidin wells on a duplicate plate were incubated with anti-streptavidin antibody followed by an HRP-conjugated anti-mouse antibody with completion of the ELISA as for the other plate. Non-linear regression was then used to correct for the differences in streptavidin concentration on the plates before plotting the biotin-binding curves. The ELISA results are shown in Figure 6.18**A**. The biotin binding is effectively identical before and after DTPA-conjugation: this was confirmed by non-linear regression analysis which found no significant difference between the EC50 of each protein.

As a final experiment to confirm the activity of the tetrameric peptide, inhibition of fibronectin binding by RGD peptide-streptavidin and RGD peptide-DTPA-streptavidin to $\alpha_v\beta_3$ were compared. This assay was carried out as before: in order to ensure direct comparability of the conjugates streptavidin was incubated with a 1:4 molar ratio of peptide, rather than excess, in order to remove potential inaccuracy of quantification post-purification. The results of this experiment are shown in Figure 6.18B and confirm that DTPA conjugation does not affect binding activity of the RGD peptide

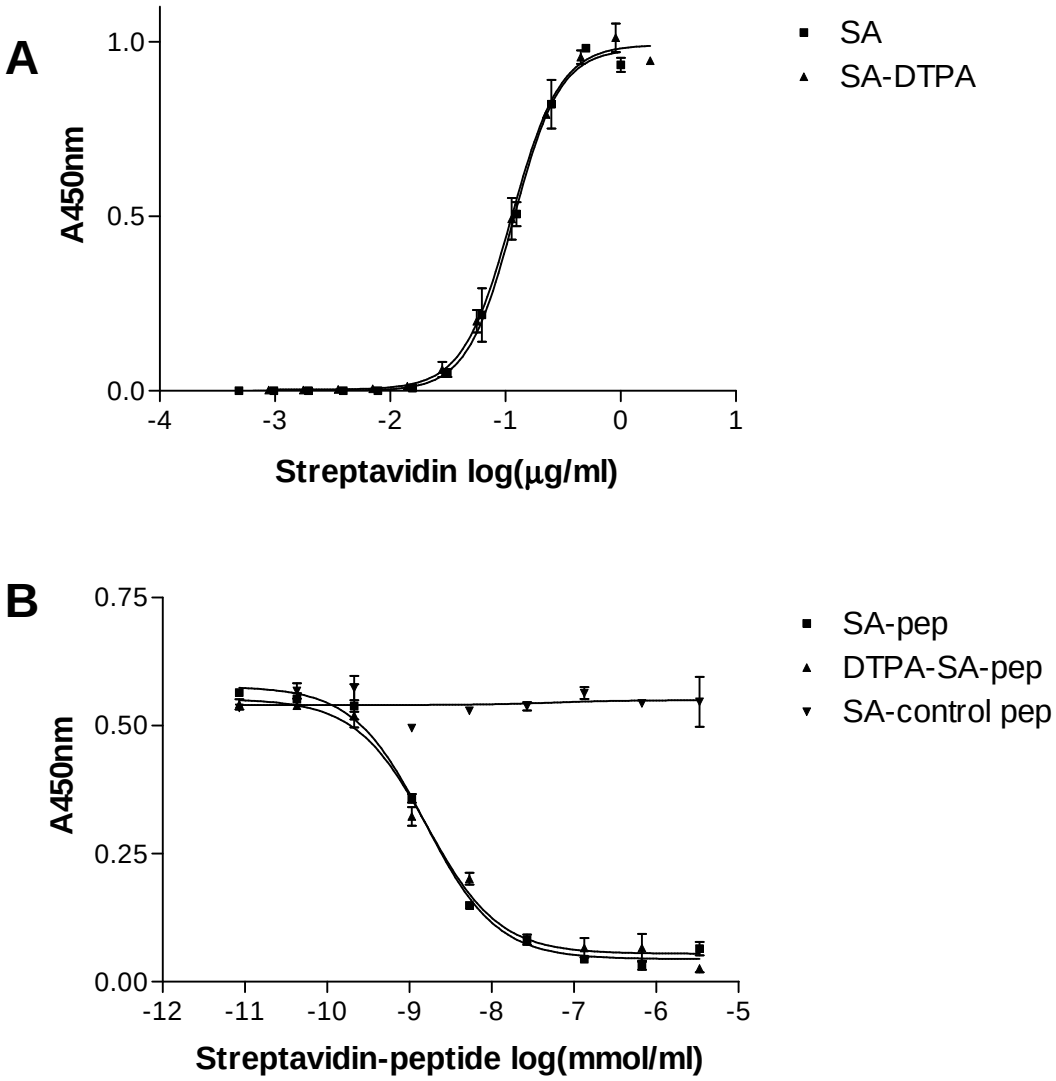

Figure 6.18: **Affinity of streptavidin for biotin and streptavidin-peptide for ligand before and after DTPA conjugation**. **A-** Streptavidin before and after DTPA-conjugation was bound to 96-well plates followed by incubation with biotinylated HRP and developed with TMB substrate. The results were corrected for differences in streptavidin binding by incubation with anti-streptavidin antibody followed by an HRP-conjugated secondary antibody. No significant difference was seen in biotin binding. **B-** Fibronectin/ $\alpha_v\beta_3$ binding inhibition assay with tetrameric peptide bound to DTPA or non-DTPA conjugated streptavidin. No difference was seen between the IC50s. Results of triplicate wells +/- SD.

6.4.4 Radiolabelling of tetrameric peptide-streptavidin with ^{111}In

The use of size-exclusion purification has the advantage that it will remove all low molecular weight impurities in one step, therefore polymerisation of the peptide could be followed by radiolabelling prior to purification.

SA-DTPA was incubated with a 4-fold molar excess of biotinylated peptide for 1 hour at RT at pH 6.0. This was followed by the addition of $^{111}InCl_3$ and a further incubation for 30 minutes. The conjugation reaction was stopped by the addition of 10% by volume 50 mM EDTA after which the reaction solution was purified by size-exclusion spin column filtration as before. Final radiochemical purity was routinely >99%:

6.4.5 Radioligand binding with ^{111}In-SA-cRGD

A number of experiments were performed as detailed in the methods in order to demonstrate binding of RGD peptide- streptavidin to $\alpha_v\beta_3$-expressing cells. No specific binding/ internalisation was seen across a range of concentrations. The absence of specific cell binding with the RGD-conjugated ^{111}In-streptavidin has several possible explanations. Firstly is that the sensitivity of the assay was below the threshold for detection and hence missed a genuine effect. It is difficult to refute this, although other workers have shown substantial levels of binding/ internalisation with radiolabelled RGD-peptides in similar assays. It is also possible that conjugation to streptavidin has altered the kinetics of binding to $\alpha_v\beta_3$: earlier it was seen that A375P and MCF7 β3 cells bound to RGD peptides in an adhesion assay, but in this instance the presentation of the peptide was polymeric and not oligovalent as seen with the streptavidin-peptide. A further consideration is that the larger molecule does not internalise, as is seen with monomeric peptides, and that the complex dissociates from the integrin with the lower concentrations achieved during the washing steps. Finally, it may be that the concentration of the streptavidin-peptide is too low to start with: a level much below the K_d would result in minimal binding. The EC50 observed in the ELISA-based assays was in the nanomolar range, although as already discussed this may be lower than could be seen under these more physiological conditions, with

presentation of integrin on the cell membrane as opposed to immobilised on plastic.

For the purpose of the application of this model for testing the 3.1 peptide, a further possibility needed to be considered. It has already been shown that biotin-binding of the streptavidin was unaffected by DTPA conjugation, but it is theoretically possible that the addition of ^{111}In could abrogate biotin binding. This is unlikely- I have been unable to find any reports of such an effect with DTPA-conjugated proteins- but despite this biotin-binding of ^{111}In-DTPA-streptavidin was tested as follows. ^{111}In-DTPA-streptavidin was incubated with a molar excess of biotinylated HRP for 1 hour at RT, following which the complexed and individual reagents were analysed by SE-HPLC. The chromatograms are shown in Figure 6.19 : there is a clear shift of the retention time to an earlier point after addition of bHRP, confirming binding of ^{111}In-SA to bHRP with the formation of a larger complex: the multiple peaks are due to the formation of complexes of more than two molecules. Although this experiment does not confirm the affinity of the streptavidin for biotin, it does show that biotin binding is retained by the radiolabelled protein.

As a final experiment, ^{111}In-SA-c(RGD) and ^{111}In-SA-sRGD2C were incubated in solution with purified $\alpha_v\beta_3$. After incubation for 1 hour the solutions were analysed by SE-HPLC: the results are shown in Figure 6.20. A small peak is seen after addition of $\alpha_v\beta_3$ to the c(RGD)-SA representing bound tetravalent peptide. Whilst this experiment is insufficient to give an accurate calculation of the K_d, an approximation can be obtained using the data obtained by integrating the peaks to derive the concentration of ^{111}In- SA-peptide unbound and bound to $\alpha_v\beta_3$. The law of mass action equation below was used to estimate the K_d of the tetravalent peptide.

$$K_d = \frac{[\text{ligand}].[\text{receptor}]}{[\text{ligand.receptor}]}$$

Using the figures derived from the radiochromatograms an estimated K_d of $2x10^{-5}$ M is obtained which is several orders of magnitude higher than the IC50 derived from the ELISA-based assays. Although IC50 is only, at best, an estimate of K_d this discrepancy strongly suggests that the affinity of the peptide for receptor differs substantially in solution to that seen when the integrin is immobilised on a plate.

6.4.6 Tumour growth in SCID mice

MCF7 β3 cells do not form tumours *in vivo* and A375P cells were therefore used for these experiments. Cells were injected subcutaneously in Matrigel and experiments were performed when the tumours reached ~0.5 cm. To confirm vascularisation and expression of $\alpha_v\beta_3$ *ex vivo* tumours were snap frozen and stained for murine CD31 and human $\alpha_v\beta_3$. Representative micrographs are shown in Figure 6.21. There is obvious vascularisation throughout the tumours and diffuse expression of $\alpha_v\beta_3$.

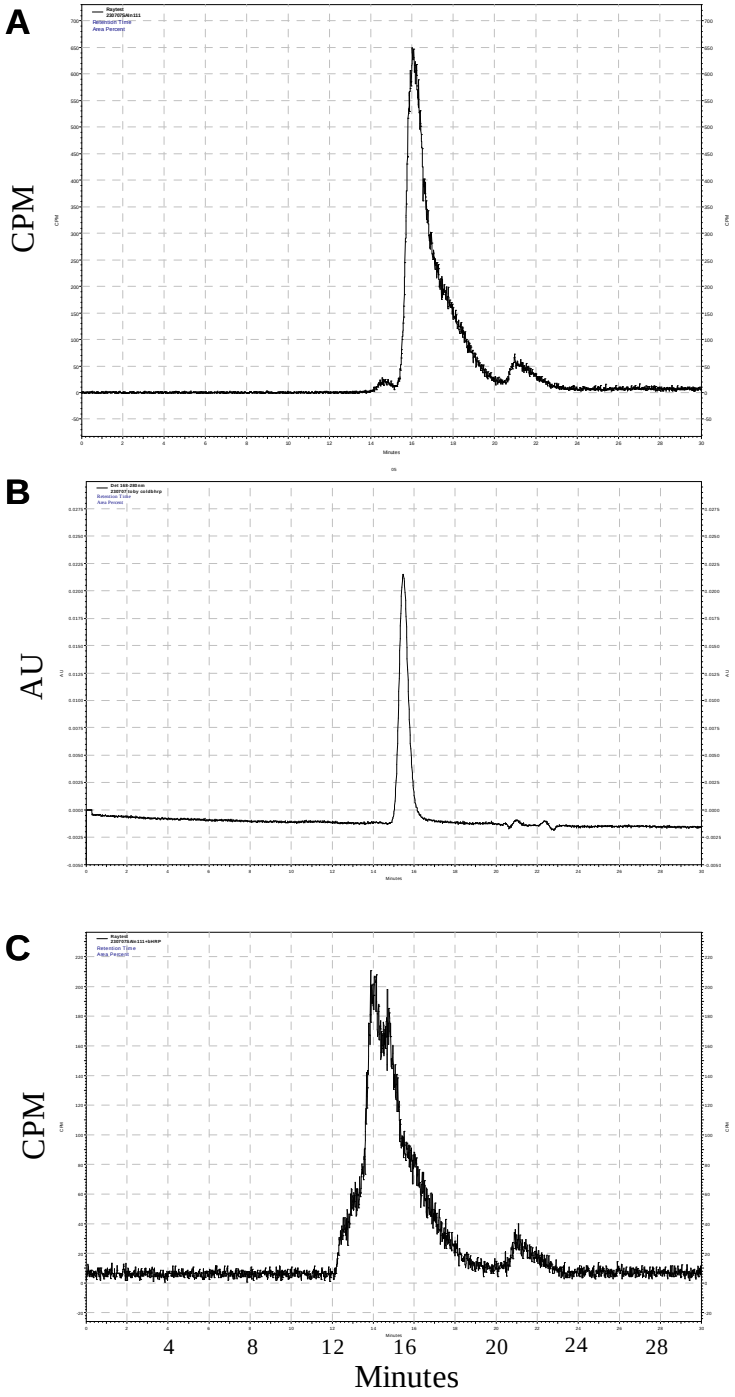

Figure 6.19: **SE-HPLC analysis of ^{111}SA-DTPA +/- biotinylated HRP**. **A** Radiochromatogram of ^{111}In-streptavidin **B** UV absorbance chromatogram of biotinylated HRP **C** Radiochromatogram of ^{111}SA-DTPA after incubation for 1 hour with an excess of biotinylated HRP. The complete shift to an earlier retention time confirms that ^{111}SA-DTPA binds biotin. The presence of a second peak suggests the formation of polymeric products.

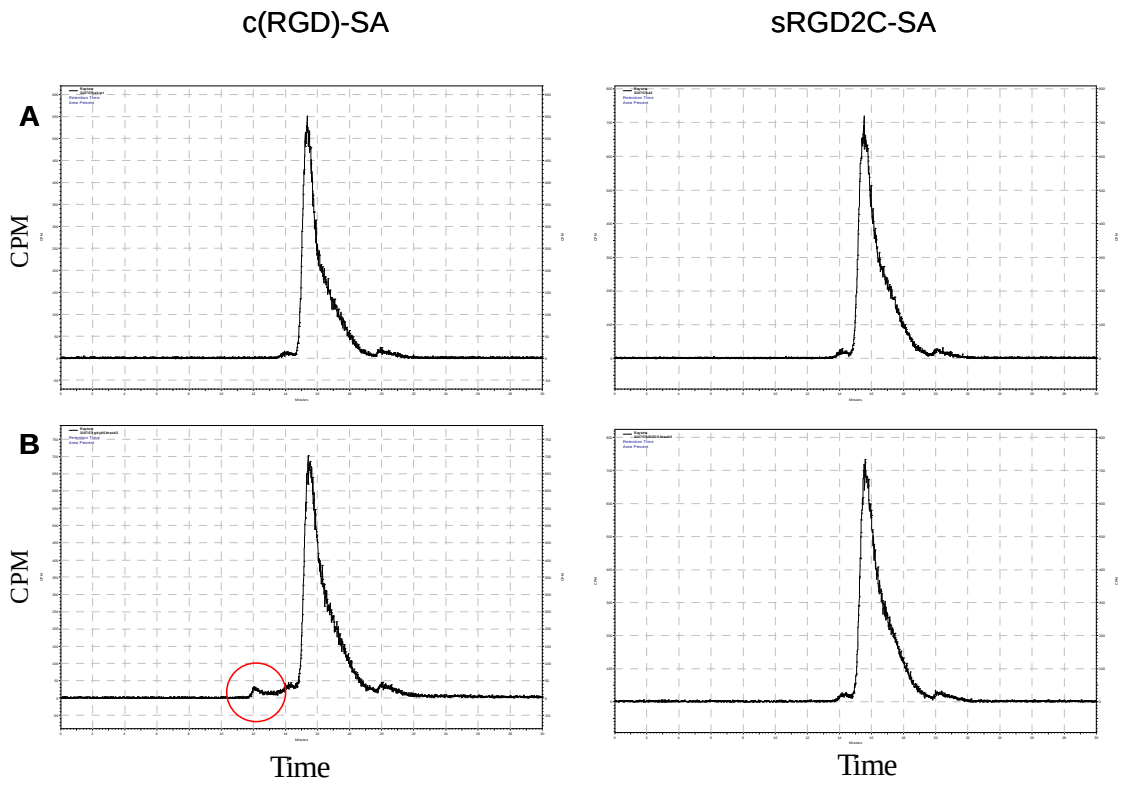

Figure 6.20: Binding of RGD-streptavidin to $\alpha_v\beta_3$ in solution. Radiochromatograms of ^{111}In-conjugated SA-cRGD peptide or the scramble RD2C control incubated in solution with (**B**) or without (**A**) purified $\alpha_v\beta_3$. After 1hour the samples were analysed by SE-HPLC. The appearance of a small (higher molecular weight) peak after incubation with the ^{111}In-SA-cRGD peptide suggests the formation of complexes with $\alpha_v\beta_3$.

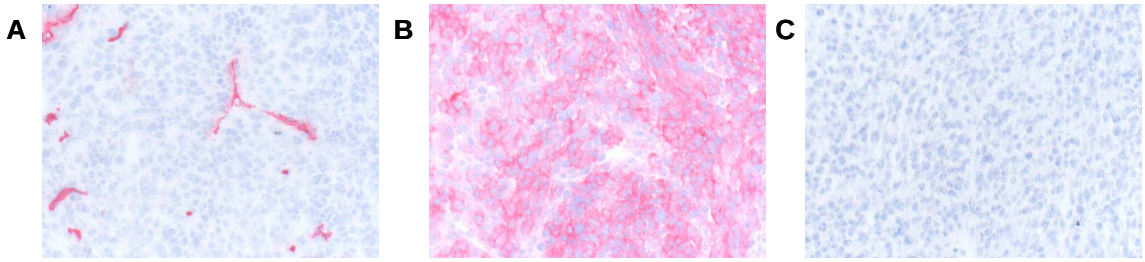

Figure 6.21: **Expression of $\alpha_v\beta_3$ in tumours.** Sections of *ex vivo* A375P tumours were stained for murine CD31 (**A**) $\alpha_v\beta_3$ (**B**) and IgG_1 isotype control (**C**). CD31 staining confirms vascularisation of the tumours whilst there is diffuse staining for $\alpha_v\beta_3$ throughout**.** Original magnification x20

6.4.7 *In vivo* biodistribution of tetravalent RGD peptide

The *in vitro* experiments had shown that, despite convincing binding of the monomeric and polymeric RGD peptides to immobilised $\alpha_v\beta_3$ in ELISA-based assays, binding to cell-expressed integrin was not seen: the possible reasons for this have been discussed. It was therefore unlikely that specific uptake would be seen *in vivo*. It was therefore decided to limit the *in vivo* experiments with the tumour model to a single time point. Mice were injected intravenously with 4 μg (0.6 MBq) of c(RGD)-SA-^{111}In or scrambled control. After 4 hours the animals were killed and the tumours were removed, weighed and the activity counted in a gamma counter. The results are shown in Figure 6.22 and Table 6.1. No significant difference was seen between the peptides. Although the numbers of tumours were small the error bars are small and, in light of the *in vitro* experiments, it was not felt justified to pursue these experiments further.

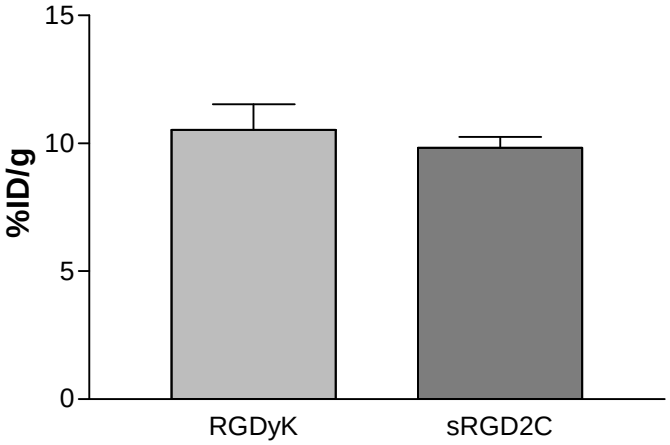

Figure 6.22: **Biodistribution of RGD-streptavidin in A375P tumour-bearing mice.** Mice were injected subcutaneously with A375P cells in Matrigel matrix. When the tumours reached ~0.5 cm the animals were injected intravenously with 4 μg of ^{111}In-labelled c(RGD)-SA or scrambled RGD2C-SA control. After 4 hours the tumours were removed, weighed and the radioactivity counted. n= 5 tumours (c(RGD)-SA), 4 tumours (sRGD2C). No significant difference is seen between the RGD and control peptides. Mean +/- SEM.

	%ID/g	
Tissue	cRGD	RGD2C
Tumour	10.53 ± 1.01	9.83 ± 0.43
Heart	8.01 ± 0.80	9.73 ± 0.58
Lung	10.48 ± 2.91	11.52 ± 0.40
Liver	13.31 ± 2.29	9.78 ± 0.24
Kidney	70.34 ± 11.64	31.5 ± 5.76
Spleen	12.48 ± 1.87	9.10 ± 0.26
Gut	4.30 ± 0.85	4.19 ± 0.07
Muscle	1.06 ± 0.47	2.20 ± 0.15
Blood	18.44 ± 4.84	17.71 ± 3.77

Table 6.1: *In vivo* biodistribution of RGD peptide-streptavidin. SCID mice carrying A375P tumours were injected with ^{111}In-labelled cRGD or sRGD2C-SA. After 4 hours the tumors and murine organs were removed, weighed and radioactivity measured. Mean +/- SEM n=3 animals (cRGD), 2 animals (RGD2C), 2 transplants per animal

6.4.8 *In vivo* biodistribution of tetravalent 3.1 peptide

For the *in vivo* studies with 3.1 peptide DTPA-streptavidin was incubated with saturating concentrations of 3.1 peptide or scrambled control. After incubation for 1 hour the complex was radiolabelled with ^{111}In and purified by spin column filtration. Mice double transplanted with skin and synovium were injected with 0.8 μg (~1 MBq) of ^{111}In-streptavidin-peptide via the tail vein and incubated for 1, 4 or 24 hours prior to sacrifice and excision of the grafts and organs. The tissues were weighed and the activity measured in a gamma counter: the results are shown in Figure 6.23 and Table 6.2. No difference was seen between the 3.1 or scrambled control tetravalent peptides at any of the indicated time points, nor

were there any differences between synovium and skin. The results for blood in the same animals are shown in Figure . The levels seen in the tissues at 4 and 24 hours are similar despite a clear reduction of the levels in circulating blood: this suggests that there is uptake of the tracer into the tissues and that the levels seen are not simply a reflection of the circulating blood pool. Non-specific uptake into the tissue is not unexpected and has been discussed in earlier chapters. Distribution in the murine organs was similar for the two peptides with the exception of kidney where there was significantly higher localisation of the RGD2C-SA. However, the lack of significant differences between the tissues and the test and control peptides suggests that the uptake seen was non-specific. Elimination of the radiolabelled complexes was the same for both peptides as indicated Figure which shows similar circulating levels at all time points. The possibility that the assay has insufficient sensitivity to detect specific uptake cannot be entirely discounted: as discussed in an earlier chapter any specific uptake can be obscured by 'noise' from the non-specific signal. However, it is more likely that significant internalisation by cells would be seen as was shown with anti-E-selectin in chapter 3. Again, such an effect may exist below the detection threshold of this assay: if, however, there is specific binding the inability of this assay to detect it implies that this construct, and those of similar molecular weight, is unlikely to have any advantages as a specific delivery agent. The stability of the ^{111}In-DTPA-SA was not investigated in this study. However, DTPA is frequently used as a bifunctional chelating agent and previous studies have shown that the conjugate has excellent stability in serum.

Full results of the biodistribution of 3.1 peptide-^{111}In-SA are shown in Table 6.2. This appears to show preferential accumulation of the complex in the transplanted tissues (bearing in mind the lower vascularity described in Chapter 3): as no selectivity was shown for transplanted synovium compared to skin, and levels were similar for the scrambled peptide, this effect appears to be non-specific.

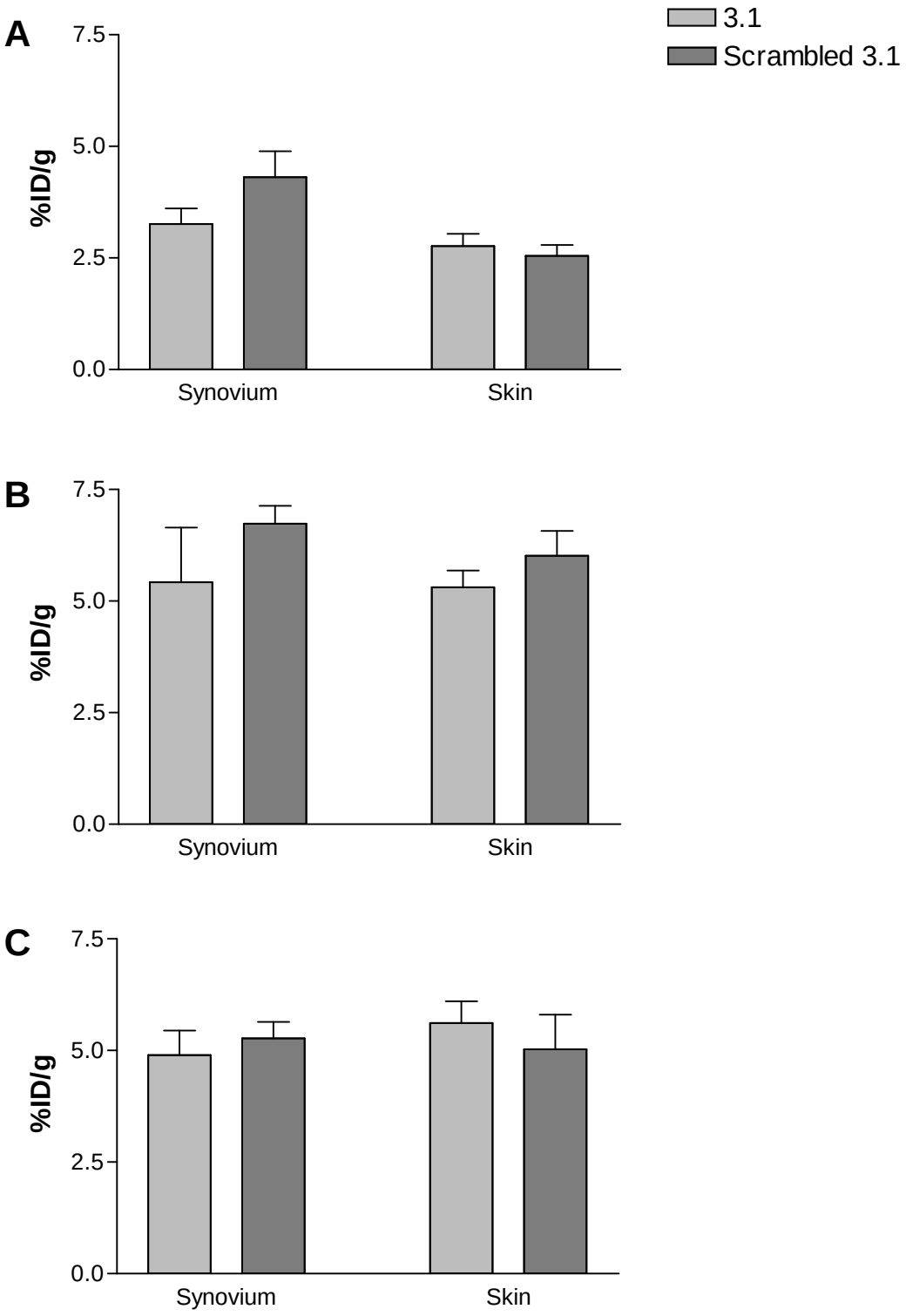
A
B
C
3.1
Scrambled 3.1
%ID/g
7.5
5.0
2.5
0.0
Synovium
Skin

Figure 6.23 (previous page): **Biodistribution of tetravalent SA-peptides.** SCID mice double-transplanted with human skin and synovium were injected intravenously with ^{111}In-3.1-SA or scrambled control. After 1 hour (**A**), 4 hours (**B**) and 24 hours (**C**) the transplants were removed, weighed and the radioactivity measured. No significant differences were seen between the test or control peptides, or between skin and synovium at any of the time points. n= 6 transplants per condition, mean +/- SEM.

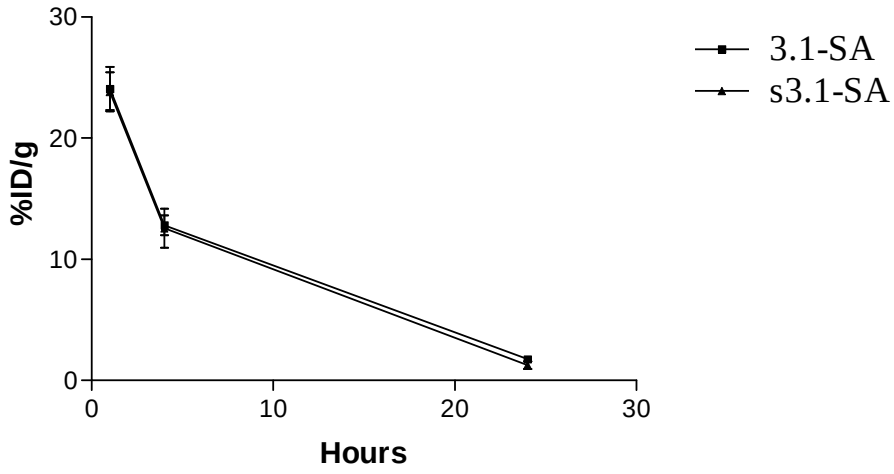

Figure 6.24: Levels of ^{111}In-SA-peptide in the blood of the animals used for the biodistribution experiment. There is no significant difference in the rate of decay between the two tetravalent peptides. Non-linear regression analysis suggested a half-life of around 6 hours. N= 3 mice per condition per time point. Mean +/- SEM.

	%ID/g tissue		
Tissue	1 hour	4 hours	24 hours
Synovium	3.26 ± 0.35	5.42 ± 1.23	4.90 ± 0.55
Skin	2.77 ± 0.28	5.31 ± 0.37	5.61 ± 0.49
Heart	8.09 ± 0.75	5.40 ± 0.13	4.84 ± 1.01
Lung	11.33 ± 1.95	6.91 ± 0.27	3.67 ± 0.46
Liver	6.64 ± 0.66	6.24 ± 0.13	9.43 ± 0.25
Kidney	22.90 ± 3.29	38.25 ± 1.48	74.66 ± 3.37
Spleen	6.33 ± 0.70	8.19 ± 1.06	16.07 ± 2.61
Gut	3.19 ± 1.33	2.95 ± 0.18	2.34 ± 0.17
Muscle	1.48 ± 0.065	3.18 ± 1.07	1.09 ± 0.09
Blood	24.09 ± 1.79	12.81 ± 0.83	1.77 ± 0.19

Table 6.2A: Results of the biodistribution experiment with 3.1-peptide-conjugated ^{111}In-streptavidin. Double-transplanted mice were injected with 0.8μg of the tetravalent peptide and incubated for 1, 4, or 24 hours after which the transplanted tissues were removed for weighing and measurement of radioactivity. Mean +/- SEM. n=3 animals (6 transplants) per condition

	%ID/g tissue		
Tissue	1 hour	4 hours	24 hours
Synovium	4.30 ± 0.58	6.73 ± 0.40	5.27 ± 0.55
Skin	2.55 ± 0.24	6.01 ± 0.56	5.03 ± 0.49
Heart	8.18 ± 0.43	5.25 ± 0.0.30	3.57 ± 1.01
Lung	10.36 ± 0.61	6.94 ± 0.0.43	3.21 ± 0.46
Liver	6.36 ± 0.45	7.44 ± 0.55	9.20 ± 0.25
Kidney	39.37 ± 4.46	85.96 ± 14.96	117.9 ± 3.37
Spleen	7.23 ± 0.58	9.44 ± 1.42	15.41 ± 2.61
Gut	4.63 ± 0.75	3.31 ± 0.18	2.14 ± 0.17
Muscle	1.44 ± 0.09	1.91 ± 0.14	1.26 ± 0.09
Blood	23.82 ± 1.62	12.56 ± 1.61	1.27 ± 0.19

Table 6.2B: Results of the biodistribution experiment with scrambled 3.1-peptide-conjugated ^{111}In-streptavidin. Double-transplanted mice were injected with 0.8μg of the tetravalent peptide and incubated for 1, 4, or 24 hours after which the transplanted tissues were removed for weighing and measurement of radioactivity. Mean +/- SEM. n=3 animals (6 transplants) per condition

6.5 Summary

In this chapter the two issues of peptide size and valency were addressed by producing complexes of peptide bound via biotin to streptavidin. It was possible that the larger molecular weight might limit extravasation into the transplanted tissues, although this would not be certain in light of the earlier data demonstrating increased extravasation of albumin. The increase in valency, it was hoped, would enhance the avidity of the peptide for its tissue receptor with a consequent increases in specific uptake: the strategy of complexing peptide with streptavidin was shown to be highly effective in a previous study in which it was demonstrated that tetramerisation resulted in a 200-fold increase in the EC50 of a P-selectin binding peptide in an adhesion assay (Molenaar et al. 2004). As no *in vitro* assay was available for the synovial-homing 3.1 peptide, RGD peptides of similar structure were used to validate the method *in vitro* and polymerised peptide were shown to be effective in ELISA-based assays of binding to $\alpha_v\beta_3$ directly and in inhibition of fibronectin binding. The streptavidin-bound peptides were also shown to bind $\alpha_v\beta_3$-expressing cells, although this did not result in cell spreading as seen with the natural ECM ligands vitronectin and fibronectin. A method was also developed for the rapid conjugation to streptavidin and subsequent radiolabelling with ^{111}In: the ensuing single-step purification produced a product with minimal contamination with free radioisotope or peptide.

Despite the efficacy of the streptavidin-RGD peptide complexes in ELISA-based assays, binding of the radiolabelled complex was not shown in cell-based radioligand binding assays. The reasons for this are unclear: it was shown that DTPA-conjugation and radiolabelling did not affect biotin binding by streptavidin The remaining possibility, that radiolabelling abrogates binding affinity of bound RGD peptide seems most unlikely, particularly bearing in mind the presence of spacer arms between the biotin and the active peptide moiety. It was therefore unsurprising, although disappointing, that specific homing was not seen in a preliminary *in vivo* experiment. A tempting explanation for this stems from what is already known about the binding kinetics of RGD peptides, and this will be returned to in the final chapter.

In the final section, tetravalent 3.1 and scrambled control-peptide were tested in the SCID mouse transplantation model. As with the monomeric peptides, specific uptake of the complexes in synovium was not seen: the differences in uptake between synovium and skin, and between 3.1 and scrambled control peptides were not significant. Despite this, as has been previously observed, there did appear to be selective accumulation of the peptide complexes in the transplanted tissues, again reflecting earlier observations. This accumulation of large molecules in transplanted tissue suggests similarities with that observed in tumour tissues, known as the enhanced permeability and retention (EPR) effect, and this concept will be discussed in the final chapter.

As discussed at the end of Chapter 5, the large phage particles, measuring around 900 nm in length, are likely to be retained in the intravascular space more so than relatively small molecules or peptides. In the next chapter a method was developedto produce large polyvalent particles and to test whether specific synovial homing could be achieved by this novel approach.

Chapter 7

Peptide polymerisation by conjugation to fluorescent microspheres and investigation of synovial targeting *in vivo*

7.1 Introduction

As already discussed, the presentation of the peptide by phage is multivalent, furthermore phage are large (~900x5 nm). This combination of oligovalency and particle size are likely to be responsible for the differences seen between *in vivo* localisation of the phage. In particular, phage valency could increase binding avidity whilst the large phage size prevents rapid extrusion from the circulation. In an attempt to overcome this issue I developed a novel multimerisation approach using fluorescent microspheres. The use of fluorescent microspheres has been described in a number of applications including as a marker for cell-surface antigens for detection by FACS. It has been shown that microspheres can be more sensitive than some conventionally used fluorescent markers and as such may be particularly suitable for the detection of low-abundance antigens (Bhalgat et al. 1998;Wojchowski & Sytkowski 1986). The most frequent *in vivo* application of fluorescent microspheres is for the determination of regional blood flow: this relies on the trapping of large systemically-administered microspheres in the microcirculation of organs of interest (Deveci & Egginton 1999). There are few reports of the used of specifically-targeted fluorescent microspheres *in vivo.* Kiani *et al* used microspheres coated with an anti-ICAM-1 antibody to target irradiated brain tissue (Kiani et al. 2002): localisation was measured by intravital microscopy of an exposed area of brain tissue. This approach was successful with a highly significant increase in localisation of specifically targeted compared to control microspheres.

The conjugation of peptide to fluorescent microspheres therefore offers a number of advantages. The size of those used in the proceeding experiments (1μm diameter) is similar to that of the phage and hence non-specific extravasation is likely to be minimised. Conjugation of the peptide to the microspheres will produce a polyvalent particle: the use of an intermediate molecule (in the case of this work Neutravidin) allows a simple final conjugation step and a means of easy radiolabelling by the use of ^{111}In-labelled biotin. An added advantage of this approach is that surface coating of the microspheres with Neutravidin will

increase the spacing of the peptides and hence reduce steric hindrance which is a theoretical problem with closely-associated peptide molecules. Success with this approach would also provide information as to the capacity of the peptide to deliver larger particles (such as liposomes) *in vivo*.

In this chapter a novel method was developed for the rapid and predictable labelling of fluorescent microspheres with peptide and ^{111}In. It will be shown that RGD-peptide conjugated microspheres bind αvβ3–expressing cells *in vitro* and that this is dependent on the surface density of peptide. Finally the peptide-coated microspheres are tested in the SCID mouse model.

7.2 Peptide conjugation to microspheres

For these experiments a method was developed for the rapid conjugation of biotinylated peptide to microspheres. This involved coating of fluorescent microspheres with biotin-binding molecules with subsequent confirmation of peptide conjugation and assessment of the microsphere affinity for a ligand *in vitro.* The lack of an *in vitro* assay for the synovial-homing peptide required the use of an alternative RGD-containing peptide as in the previous chapter.

7.2.1 Radiolabelling of DTPA-(biotin)$_2$

Radiolabelling of the microspheres for the *in* vivo experiments was to be achieved by simultaneous incubation of Neutravidin-coated microspheres with biotinylated peptide and the compound diethylenetriaminepentaacetic acid α,ω-bis(biocytinamide) (DTPA-(biotin)$_2$). This molecule contains a DTPA residue conjugated to 2 biotin molecules and is conjugated to ^{111}In using an identical method to that used previously. Previous reports of radiolabelling of DTPA-(biotin)$_2$ have used a method in which the radiolabelled molecule is incubated with streptavidin prior to passing through a size-exclusion column to confirm radiolabelling. This is time consuming compared with ITLC (use of which for ^{111}In-DTPA-(biotin)$_2$ has not been described): the two methods were therefore compared. It was not known whether ^{111}In-DTPA-(biotin)$_2$ would migrate with the acetate solvent (as used for earlier radiolabelling experiments) and ITLC of ^{111}In-DTPA-(biotin)$_2$ before and after incubation with an excess of streptavidin

were compared, as well as the results of spin column filtration. It was shown in the previous chapter that purification of ^{111}In-DTPA-SA from unconjugated ^{111}In was effective using this method. The results are shown in Table 7.1 and Figure 7.1. The RP-HPLC chromatograms show a shift to an earlier retention time of ^{111}In-DTPA-(biotin)$_2$ after incubation with streptavidin suggesting that all detectable ^{111}In is conjugated to DTPA-(biotin)$_2$. This is supported by the ITLC data: here it is seen that the activity remaining at the origin is similar (~99%) before and after incubation of ^{111}In-DTPA-(biotin)$_2$ with streptavidin, and the data from size-exclusion spin column filtration (although) there is a little retention of ^{111}In-DTPA-(biotin)$_2$ by the column. These results confirm that ITLC is effective for the confirmation of radiolabelling of DTPA-(biotin)$_2$ with ^{111}In.

ITLC (% at origin)		Size-exclusion column filtration (% in eluate)
^{111}In-DTPA-(biotin)$_2$	^{111}In-DTPA-(biotin)$_2$+ streptavidin	^{111}In-DTPA-(biotin)$_2$+ streptavidin
99.0%	99.8%	95.2%

Table 7.1: ITLC and size-exclusion column analysis of ^{111}In-DTPA-(biotin)$_2$ with or without incubation with an excess of streptavidin. Almost all of the activity migrated with the solvent front on ITLC, whilst the majority of the activity was eluted thought the size-exclusion spin column resin. These results confirm excellent radiochemical yield (>10 MBq/ μg) and binding efficiency of the labelling reaction.

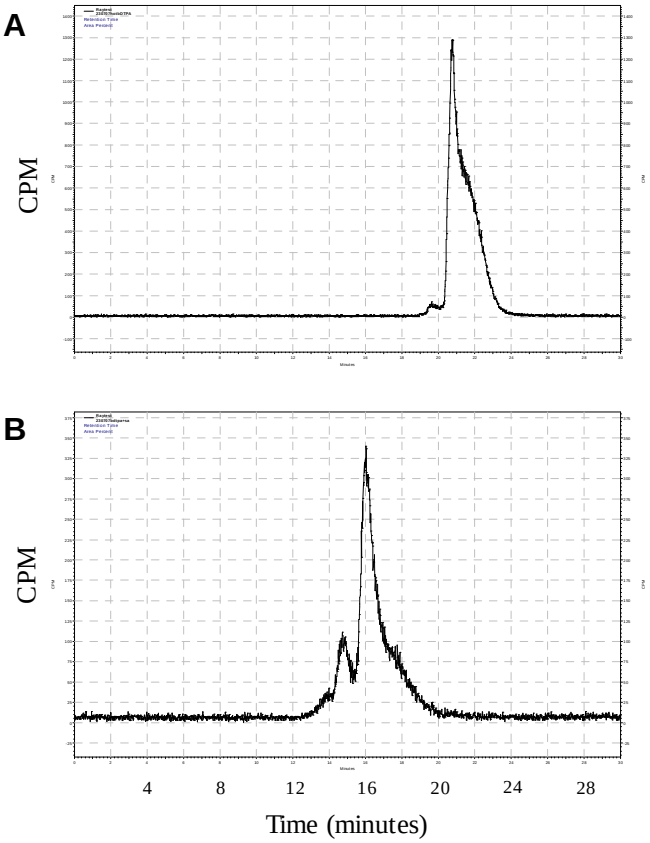

Figure 7.1: ^{111}In labelling of DTPA-(biotin)$_2$. Size-exclusion HPLC chromatograms of ^{111}In-DTPA-(biotin)$_2$ before (**A**) and after (**B**) incubation with an excess of streptavidin. The shift of all detectable activity to an earlier retention time confirms high radiolabelling efficiency with almost 100% of the ^{111}In being associated with DTPA-(biotin)$_2$. The presence of an earlier peak in **B** is due to the formation of streptavidin-biotin multimers.

7.2.2 Confirmation of Neutravidin conjugation to microspheres by competitive radioligand binding assay

Microspheres were coated with Neutravidin as described in Chapter 2: this allows coating of the microspheres with biotinylated peptide by a simple incubation step followed by washes repeated until there was no spectrophotometric detection of free Neutravidin in the wash buffer. Neutravidin is a proprietary de-glycosylated avidin analogue: the lack of glycosylated side chains reduces non-specific binding and the molecule has the added advantage that it lacks the RGD-mimicking RYD sequence of streptavidin. A further advantage is cost, Neutravidin being significantly cheaper than avidin or streptavidin. The first step in the validation process was to confirm the presence of surface Neutravidin by demonstrating competitive inhibition of ^{111}In-DTPA-(biotin)$_2$ by a competitive radioligand binding assay. The results, shown in Figure 7.1A, clearly demonstrate dose-dependent inhibition of ^{111}In-DTPA-(biotin)$_2$ binding by cold DTPA-(biotin)$_2$. These results also allowed the concentration of peptide at which saturation of biotin binding occurred to be determined; this allowed me to ensure that maximal labelling of microspheres with biotin-peptide was achieved. The results were also used to plot a saturation binding curve after subtraction of background binding (fig. 7.1B): although there are a limited number of data points, this allowed an estimate of Bmax (the maximum biotin binding of the microspheres). Correction of this figure for the number of microspheres and the Avagadro constant allows an approximate value to be calculated for the number of biotin binding sites per microsphere of ~80,000.

To confirm that the peptides to be used in the *in vivo* experiment were bound to the microspheres ^{111}In-DTPA-(biotin)$_2$ was incubated with microspheres with or without pre-incubation with a ten-fold excess of 3.1 or scrambled 3.1 peptides. After incubation for an hour the microspheres were washed twice and the radioactivity of the pellets counted. The results are shown in Figure 7.2: there is binding of ^{111}In-DTPA-(biotin)$_2$ to Neutravidin-conjugated microspheres which is

almost completely inhibited by pre-incubation with either peptide; little binding is seen to non-Neutravidin conjugated microspheres.

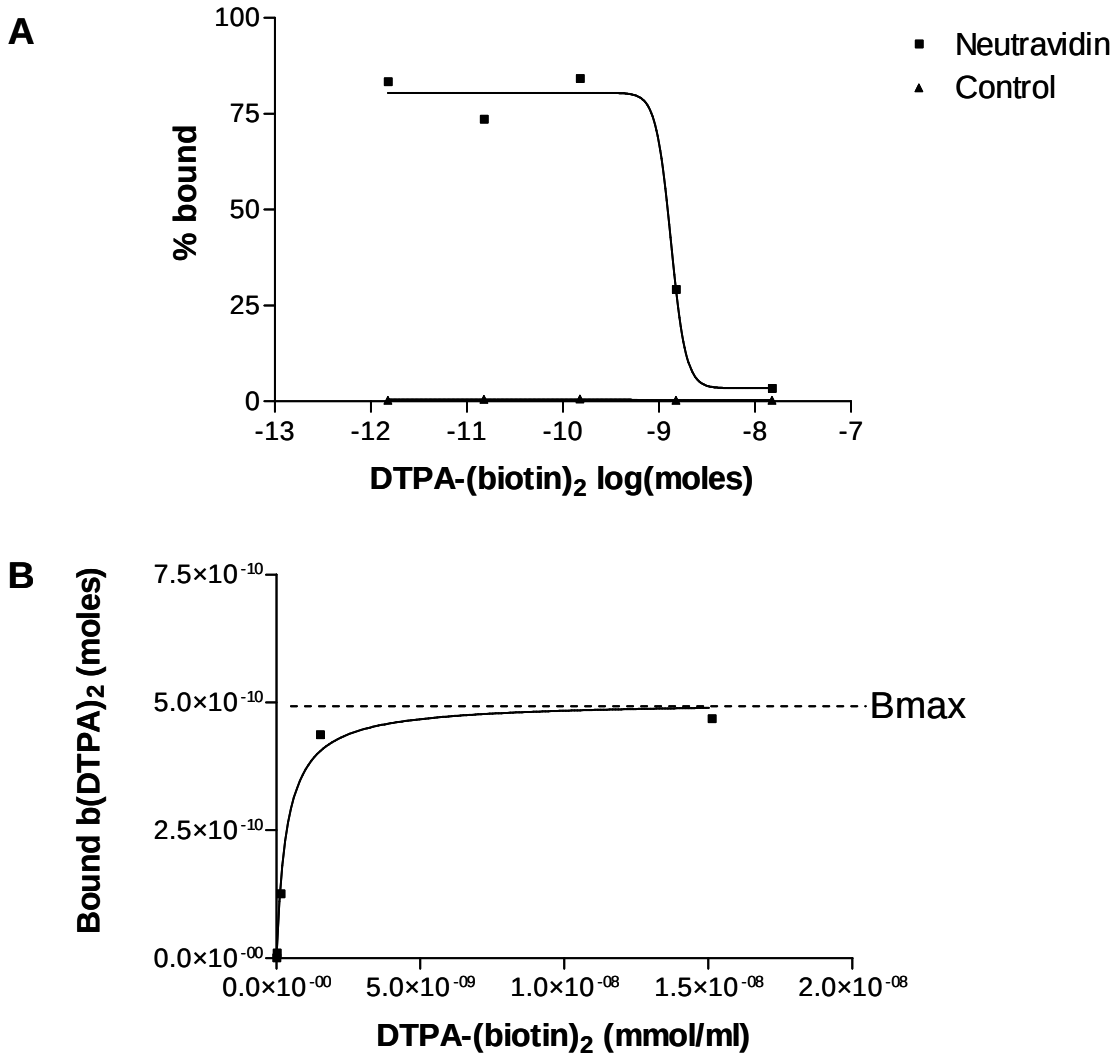

Figure 7.2: Competitive binding assay of ^{111}In-DTPA-(biotin)$_2$. A ^{111}In-DTPA-(biotin)$_2$ was incubated with various concentrations of cold DTPA-(biotin)$_2$ with Neutravidin-conjugated or unlabelled microspheres. There is dose-dependent inhibition of ^{111}In-DTPA-(biotin)$_2$ binding to Neutravidin-microspheres, with no specific binding to unconjugated microspheres thus showing specific binding of biotin. **B** Saturation binding curve from the same data after correction for background binding. The Bmax allows an approximate calculation of the number of biotin binding sites per microsphere of 80,000.

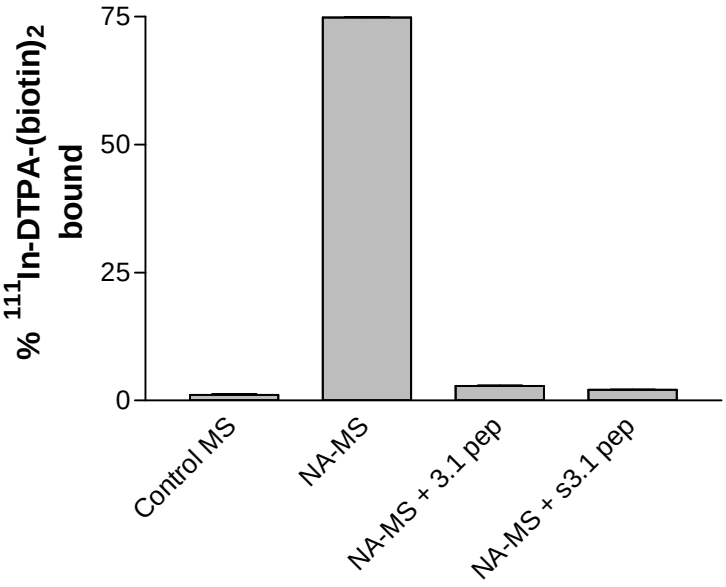

Figure 7.3: ^{111}In-DTPA-(biotin)$_2$ labelling of fluorescent microspheres. Inhibition of ^{111}In-DTPA-(biotin)$_2$ binding to NA-MS by biotinylated 3.1 or scrambled 3.1 peptides. NA-MS were incubated with a sub-saturating concentration of ^{111}In-DTPA-(biotin)$_2$ with or without pre-incubation with peptide; non Neutravidin-conjugated MS were used as a control. There is almost complete inhibition of binding with each peptide. Results of duplicate samples +/- SD

7.3 RGD-microspheres bind $\alpha_v\beta_3$-expressing cells in vitro

As discussed in the previous chapter, it is important to confirm the binding of RGD –coated microspheres to $\alpha_v\beta_3$-expressing cells. In the absence of an *in vitro* assay for the 3.1 peptide the RGD2C peptide, having the same basic seven amino-acid, disulphide constrained structure was used to confirm activity of the peptide binding domain when bound to Neutravidin-microspheres. The potential problems of the fast off-rate of RGD peptides will be mentioned in the final chapter: the polyvalency of this model could increase the avidity of the peptide for ligand.

Microspheres were coated with RGD2C, scrambled RGD2C or biotinylated cRGDyK peptides by incubation with saturating concentrations of peptide followed by 3 washes. The effect of washing on microsphere concentrations was assessed in one experiment by comparing the final microsphere concentration of 6 separate samples and incubated at various microspheres-to-cell ratios: the variability between the samples was within 6% of the mean and this was thought acceptable for further experiments. The reproducibility of the counting technique was checked by counting the microsphere concentrations in the original stock solution: the derived concentration was within 0.5% of the expected concentration, and reproducibility was confirmed by demonstrating deviation from the mean of $\leq$ 0.6% on 5 successive samples. After washing the cells were analysed by FACS analysis: regions of interest were drawn around cells labelled and unlabelled on the dot-plot and the proportion of labelled cells determined. The results are shown in Figure 7.5: a clear difference is seen between binding of the RGD and scrambled peptide-coated microspheres: the FACS plots and histograms suggest that the majority of these cells have only one microsphere attached- on the histogram discrete peaks can be seen representing increasing numbers of microspheres. The relatively low labelling efficiency again is likely to reflect the unfavourable kinetics of RGD peptide interactions with their ligands, however these experiments confirm successful coating of microspheres with the peptide and that this confers specific binding activity.

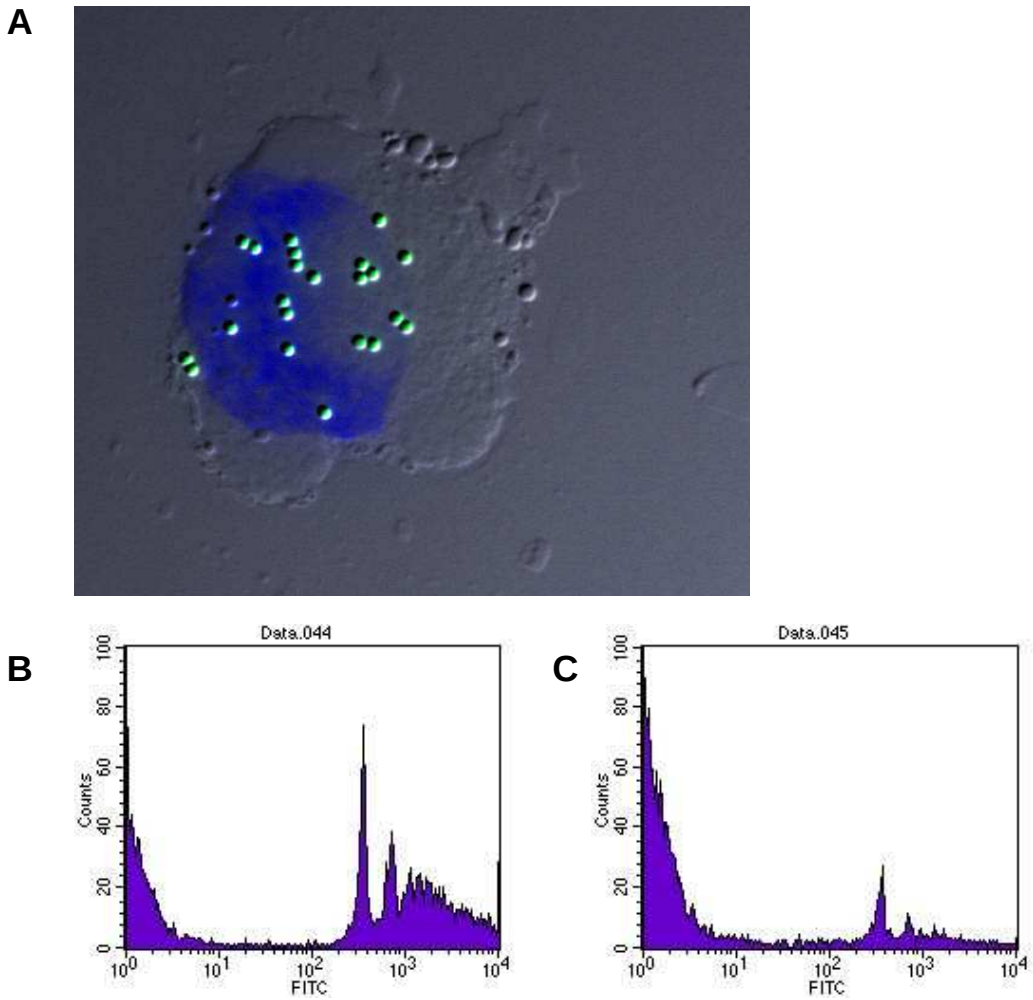

Figure 7.4: Binding of RGD peptide coated microspheres to $\alpha_v\beta_3$-expressing cells. A Micrograph of A375P cell after incubation with RGD2C-conjugated fluorescent microspheres. Double exposure with fluorescent microscopy/ differential interference contrast, original magnification 60x. **B + C** Representative histograms from FACS analysis of A375P cells incubated with fluorescent microspheres conjugated to cRGDyK peptide (**B**) or scrambled RGD2C (**C**).

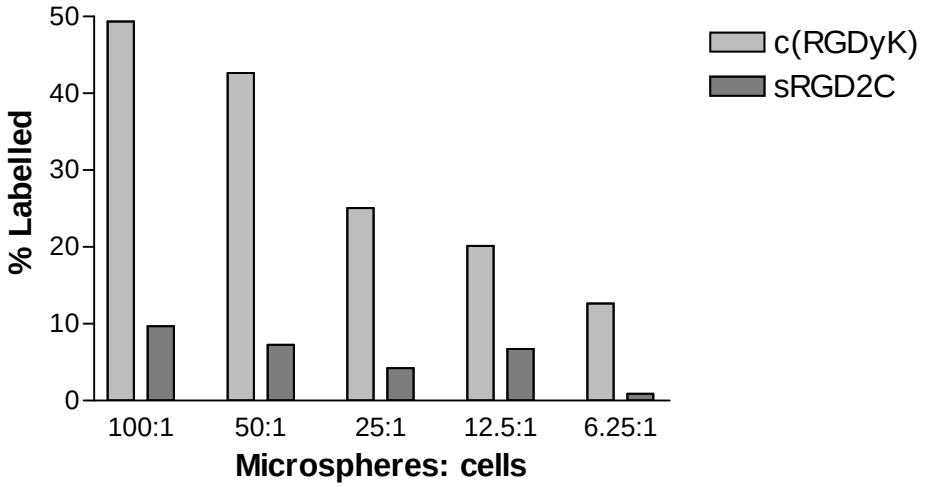

Figure 7.5: Binding of RGD-microspheres to A375P cells. Data from FACS analysis of A375P cells incubated with fluorescent microspheres conjugated to cRGDyK or control peptide. Increased cell labelling was seen for the RGDyK peptide-microspheres at all concentrations, with the best ratio to control seen at a microsphere: cell ratio of 100:1.

7.4 Substitution of peptide with ^{111}In-DTPA-biotin results in a linear increase in specific activity of microspheres

Radiolabelling of the fluorescent microspheres was to be achieved by the substitution of peptide residues with ^{111}In-DTPA-(biotin)$_2$: adding accurate molar ratios of peptide and the radioligand to the microspheres would enable labelling with a known specific activity. A concern was that the bivalent structure of the DTPA-(biotin)$_2$ would complicate the relative binding kinetics of DTPA-(biotin)$_2$ and peptide. In order to investigate the functional effects of the addition of DTPA-(biotin)$_2$ microspheres were incubated with a range of molar ratios of biotinylated cRGDyK and DTPA-(biotin)$_2$. After washing the activity of the microsphere pellet was measured in a gamma counter. The results are shown in Figure 7.6: there is a linear relationship between the ratio of biotinylated peptide to ^{111}In-DTPA-biotin (r^2=0.9968) suggesting that the biotinylated molecules have equal

affinity for the Neutravidin. This linear correlation supports the hypothesis that DTPA-$(biotin)_2$ has similar K_d to biotinylated RGDyK and there is a predictable response to DTPA-$(biotin)_2$ substitution.

This confirms that substitution of peptide with radiolabelled biotin will produce predictable changes in the surface concentration of peptide: having ensured this the next experiment was designed to examine the effect of this substitution on affinity of the microspheres for the ligand.

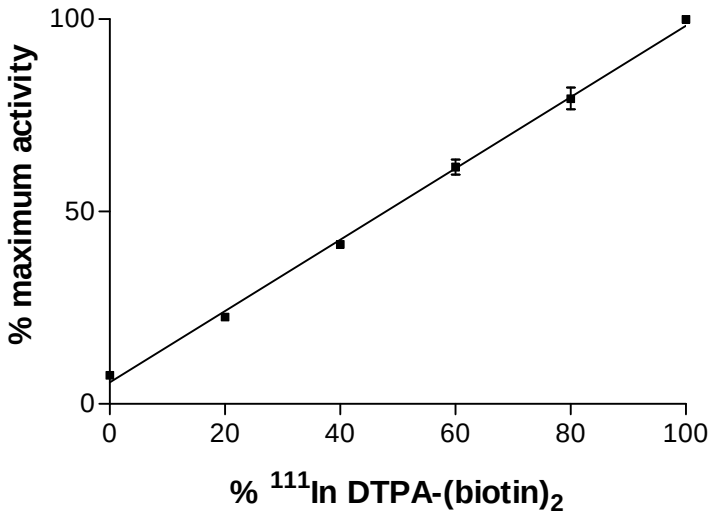

Figure 7.6: Radiolabelling of fluorescent microspheres. Neutravidin-coated microspheres were incubated with varying molar ratios of biotinylated peptide and ^{111}In-DTPA-biotin. After washing the radioactivity of the pellets were measured in a gamma counter. The results confirm a linear correlation between the proportion of ^{111}In-DTPA-biotin and radioactivity of the microsphere pellet. r^2=0.997, mean +/- SD of duplicate samples.

7.5 Substitution of peptide with biotin-DTPA results in linear reduction in binding avidity of microspheres

To test the peptide-conjugated microspheres' avidity *in vivo* they were to be radiolabelled by substitution of active peptide residues with ^{111}In-DTPA-(biotin)$_2$. The disadvantage to this is the possibility that the microspheres' avidity for the ligand would be reduced due to the reduced surface valency. To determine the effect of this substitution on binding affinity of the microspheres, Neutravidin-microsphere suspensions were incubated with varying ratios of biotinylated RGD2C peptide to DTPA-(biotin)$_2$ (non-radiolabelled). After incubation with peptide and washing as in previous experiments the microspheres were incubated with A375P cells at a concentration of 100:1. After incubation with cells for 1 hour the cells were washed and analysed by FACS as before. The results are shown in Figure 7.7. There is a linear relationship between the relative concentration of microsphere surface-bound peptide and the percentage of labelled cells in the FACS analysis. This suggests that the relationship between surface density of peptide and microsphere avidity for the ligand is linear: it therefore likely that substitution of peptide with 20% ^{111}In-DTPA-(biotin)$_2$ would result in minimal loss of microsphere avidity.

Radiolabelling of the microspheres using this method (incubation with an excess of peptide and ^{111}In- DTPA-(biotin)$_2$) would require large activities of ^{111}In. To minimize this I wanted to ensure that the use of reagent concentrations less than the maximum used with cold reagents could still result in optimal ligand binding. It was anticipated that the results from this experiment would reflect those from the saturation binding experiments described in 7.2.2. Neutravidin-MS were incubated with doubling dilutions of biotinylated peptide and incubated with A375P cells as before with subsequent FACS analysis. The results are shown in Figure 7.8: binding avidity is maintained down to a peptide concentration of ~10^{-5} mmol/ml which broadly reflects the results of the saturation binding experiment. These results allowed the reliable use of lower peptide concentrations for MS labelling, and hence lower activity of ^{111}In.

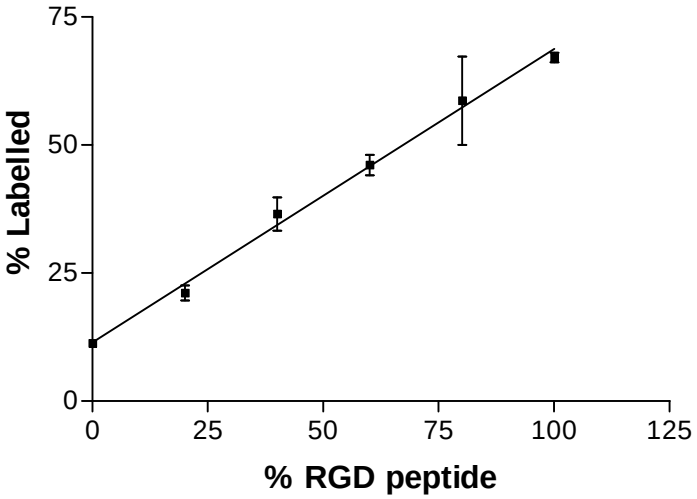

Figure 7.7: Effect of variation of surface peptide density to *in vitro* binding of RGD-microspheres. Neutravidin microspheres were incubated with various ratios of biotinylated cRGDyK peptide to DTPA-$(biotin)_2$ (not radiolabelled). After washing the microspheres were added to cell suspensions at a microsphere: cell ratio of 100:1 and incubated for 1 hour at the end of which the cells were washed and analysed by FACS. There is a linear relationship between the surface concentration of peptide and the proportion of cells labelled. r^2=0.975, mean +/- SD of duplicate samples.

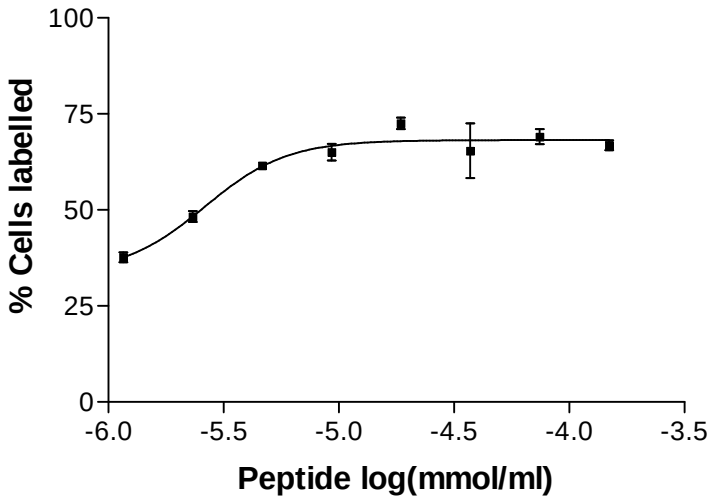

Figure 7.8: Effect of variation of concentration of peptide labelling solution on RGD-microsphere binding *in vitro*. Neutravidin-MS were incubated with doubling dilutions of biotinylated cRGDyK as for previous experiments and washed. MS were then incubated with A375P at a ratio of 100:1 for 1 hour prior to further washing and FACS analysis, with the proportion of labelled cells counted. Mean of 2 samples +/- SD.

7.6 In vivo biodistribution of radiolabelled peptide-microspheres

7.6.1 Homing of RGD-microspheres to A375P tumours

Although the RGD peptide-coated fluorescent microspheres bound $\alpha_v\beta_3$ *in vitro*, the data suggested that only a limited number of microspheres were bound to each cell and, therefore, that the absolute avidity of the microspheres for the ligand remained low. For this reason, and due to time constraints, a limited experiment was performed *in vivo* with A375P tumour-expressing SCID mice. Tumours were allowed to grow to 0.5-1cm in diameter prior to the experiment. Microspheres were incubated with a 4:1 molar ratio of bRGDyK to ^{111}In-DTPA-biotin as before, washed and injected into the mice via the tail vein (total injected activity ~2 MBq). After 15 minutes incubation the mice were killed, the transplants and organs retrieved and the radioactivity measured. The results are shown in Figure 7.9 and Table 7.2. No significant difference was seen between the cRGDyK and

scrambled RGD2C peptide in the tumours: there was rapid clearance of the blood pool with very high uptake seen, as expected, in the liver.

Although no specific uptake was seen between the cRGDyK and control peptide-labelled microspheres, this may not have been unexpected. The tetravalent RGD peptide described in the previous chapter whilst showing consistent avidity for $\alpha_v\beta_3$ was not seen to bind to cells, and as will be discussed in the final chapter this may reflect the binding kinetics of RGD-containing peptides. Furthermore, in the previous sections it was shown that the polyvalent RGD microspheres, whilst showing specific avidity for $\alpha_v\beta_3$-expressing cells, only bound at relatively low levels. Despite this, it was clearly seen that there was a linear relationship between the density of bound peptide and binding. The binding properties of the peptide can not necessarily be extrapolated to that of the 3.1 peptide, and therefore further experiments were performed to determine whether specific uptake could be demonstrated *in vivo* in the synovial transplantation model.

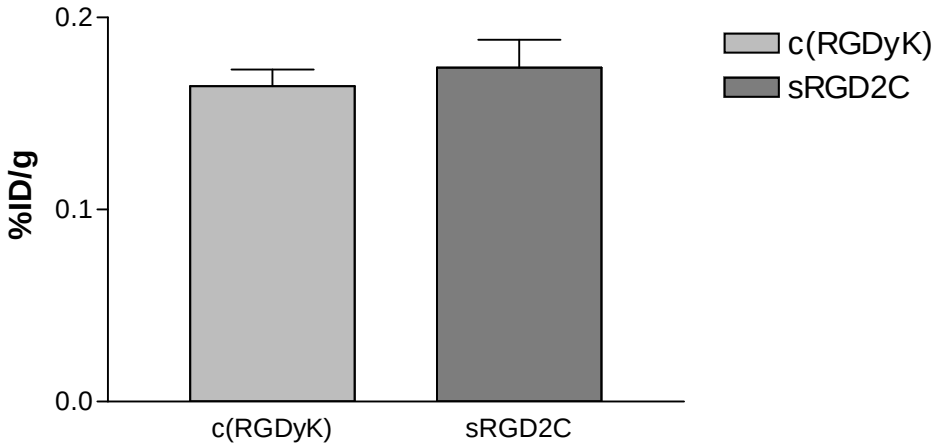

Figure 7.9: *In vivo* biodistribution of RGD-microspheres. SCID mice carrying A375P tumours were injected with ^{111}In-labelled cRGD-coated microspheres. After 15 minutes the tumors and murine organs were removed, weighed and radioactivity measured. This graph shows uptake of the test and control-peptide labelled microspheres in tumour tissue: no significant difference was seen between the peptides. Mean +/- SEM n=3 animals (2 transplants each) per condition

	15 minutes, %ID/g	
Tissue	cRGD	RGD2C
Tumour	0.16 ± 0.01	0.17 ± 0.01
Heart	0.21 ± 0.02	0.26 ± 0.01
Lung	2.72 ± 0.74	1.20 ± 0.73
Liver	97.5 ± 12.9	107.8 ± 11.9
Kidney	0.83 ± 0.03	1.92 ± 0.948
Spleen	19.2 ± 4.9	17.4 ± 4.8
Gut	0.23 ± 0.03	0.47 ± 0.26
Muscle	0.19 ± 0.08	0.14 ± 0.02
Blood	0.87 ± 0.06	1.30 ± 0.15

Table 7.2: *In vivo* biodistribution of RGD-microspheres. SCID mice carrying A375P tumours were injected with ^{111}In-labelled cRGD or sRGD2C-coated microspheres. After 15 minutes the tumors and murine organs were removed, weighed and radioactivity measured. Mean +/- SEM n=3 animals per condition

7.6.2 Homing of synovial-homing peptide-coated microspheres *in vivo*

Fluorescent microspheres were surface-coated with ^{111}In and 3.1 or scrambled-control peptide as described. SCID mice double-transplanted with human synovium and skin were injected intravenously with microsphere suspensions 6 hours after intragraft injection of TNFα and killed at 15 minutes, 1 or 4 hours. Localisation of radioactivity was determined for the transplants and murine tissues (Figure 7.10 and Table 7.3).

Similar tissue uptake was seen to that observed with the RGD peptide experiments. There was rapid clearance of radioactivity from the blood pool with substantial uptake in the reticuloendothelial tissues. No significant differences were observed between the 3.1 or scrambled control peptide-labelled microspheres in uptake to synovium or skin at 15 minutes or 1 hour. At 4 hours there was slightly but significantly greater uptake in the synovium with the scrambled peptide. The reasons for this are unclear: the blood levels at 4 hours were slightly greater with the control peptide and this cannot, therefore be explained by faster clearance of the microspheres. This may results may, possibly, reflect differences in non-specific binding between the 3.1 and scrambled-sequence peptides. These results do not support the specific homing of 3.1peptide-coated microspheres to transplanted human synovium.

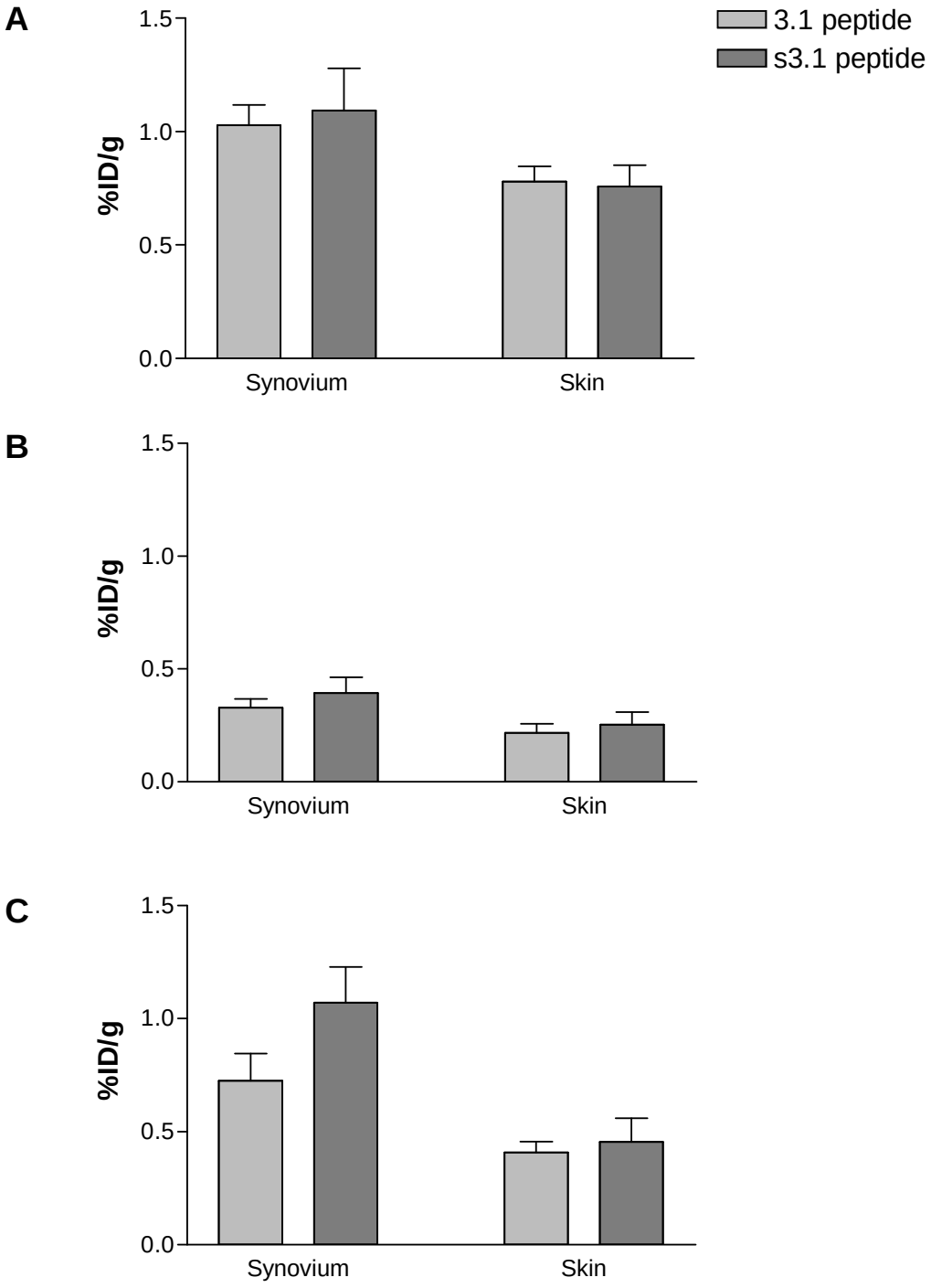

Figure 7.10: *In vivo* biodistribution of 3.1-microspheres. SCID mice double-transplanted with human skin and synovial tissue were injected intravenously with ^{111}In-labelled 3.1 or scrambled 3.1 (s3.1)-coated microspheres. After 15 minutes (**A**), 1 (**B**) or 4 hours (**C**) the transplanted tissues and murine tissue were retrieved, weighed and radioactivity measured. The results for the transplants are shown here: no significant differences were seen at 15 minutes or 1 hour: at 4 hours

uptake of the scrambled peptide-microspheres was significantly greater in synovium than that seen for the 3.1 peptide. Mean +/- SEM n= 6 transplants per condition.

	%ID/g tissue		
Tissue	15 minutes	1 hour	4 hours
Synovium	0.51 ± 0.04	0.33 ± 0.04	0.72 ± 0.12
Skin	0.39 ± 0.03	0.18 ± 0.02	0.41 ± 0.05
Heart	0.52 ± 0.02	0.41 ± 0.04	0.73 ± 0.05
Lung	10.76 ± 1.24	9.31 ± 0.69	11.34 ± 1.74
Liver	66.23 ± 4.93	57.26 ± 1.82	61.23 ± 14.6
Kidney	2.10 ± 0.06	1.56 ± 0.74	5.32 ± 0.68
Spleen	27.62 ± 5.49	20.97 ± 1.75	22.64 ± 0.92
Gut	0.61 ± 0.06	0.32 ± 0.04	0.63 ± 0.12
Muscle	0.25 ± 0.06	0.11 ± 0.01	0.12 ± 0.03
Blood	1.99 ± 0.30	1.44 ± 0.22	1.25 ± 0.03

Table 7.3A: In vivo biodistribution of 3.1 peptide-microspheres. SCID mice double-transplanted with human skin and synovium tumours were injected with ^{111}In-labelled 3.1 or control peptide-coated microspheres. After 15 minutes the tumors and murine organs were removed, weighed and radioactivity measured. Mean +/- SEM. n=3 animals per condition.

	%ID/g tissue		
Tissue	15 minutes	1 hour	4 hours
Synovium	0.55 ± 0.09	0.39 ± 0.07	1.07 ± 0.16
Skin	0.38 ± 0.05	0.25 ± 0.06	0.45 ± 0.10
Heart	0.48 ± 0.04	0.36 ± 0.04	0.70 ± 0.07
Lung	10.29 ± 2.99	7.56 ± 3.70	8.85 ± 0.78
Liver	63.99 ± 5.13	50.09 ± 1.65	68.40 ± 7.87
Kidney	2.34 ± 0.18	1.65 ± 0.78	4.56 ± 0.16
Spleen	29.02 ± 7.46	20.30 ± 2.34	24.11 ± 4.53
Gut	0.63 ± 0.14	0.19 ± 0.04	0.59 ± 0.07
Muscle	0.36 ± 0.19	0.11 ± 0.01	0.15 ± 0.04
Blood	1.39 ± 0.18	1.10 ± 0.10	1.03 ± 0.07

Table 7.4B: In vivo biodistribution of s3.1 peptide-microspheres. SCID mice double-transplanted with human skin and synovium tumours were injected with ^{111}In-labelled 3.1 or control peptide-coated microspheres. After 15 minutes the tumors and murine organs were removed, weighed and radioactivity measured. Mean +/- SEM. n=3 animals per condition.

7.7 Summary

In this chapter a technique was developed for labelling fluorescent microspheres with biotinylated peptide which also allowed co-labelling with ^{111}In thus enabling *in vivo* biodistribution studies.

Firstly, it was shown that pre-coating of the microspheres with Neutravidin, a biotin-binding streptavidin analogue, allowed simple conjugation to both biotinylated ^{111}In and biotinylated peptide in a simple step, with a predictable linear relationship between surface-bound groups and the relative concentrations of biotinylated compounds in solution. Furthermore, it was shown that RGD peptide-coated microspheres bound $\alpha_v\beta_3$ –expressing cells whereas microspheres coated with a control sequence peptide did not. Moreover, it was seen that increasing the surface density of peptide resulted in a linear increase in binding as shown by the results of the FACS experiments and that the maximum binding affinities were achieved with the concentrations used. Despite this, the absolute numbers of microspheres bound to cells appeared to be low suggesting that the absolute avidity of the microspheres under these conditions was relatively low: it was therefore disappointing although not unexpected that no specific binding was seen to $\alpha_v\beta_3$ –expressing A375P tumours *in vivo*.

In the final experiment SCID mice double-transplanted with human skin and synovium were injected intravenously with ~3 MBq ^{111}In-labelled 3.1 or scrambled 3.1 peptide-coated microspheres. For these experiments the grafts were pre-stimulated with TNFα 6 hours prior to administration of the microsphere suspensions. It was decided to adopt this strategy as the phage experiments described in chapter 3 showed that homing of the 3.1 phage clones was selectively upregulated to transplanted human synovium- this was not seen in human skin or with the control phage clone. A potential concern with the use of TNFα is its capacity to enhance endothelial permeability and thus to increase non-specific uptake. It is well established that TNFα increases vessel permeability (Royall et

al. 1989) and this property has been exploited to improve uptake of chemotherapeutic agents by tumour tissue (Lejeune 2002). Despite this, no increase was seen in the control groups in the phage experiments and, therefore, it was hoped that the larger particle size of the microspheres would limit susceptibility to such increases in permeability in this model. However, no significant differences were seen in favour of specific 3.1 peptide-microsphere homing, although, unexpectedly, there were differences in favour of the control peptide at 4 hours. The reason for this is unclear although and this possibly reflects modest differences in non-specific binding. The substantial uptake of polystyrene microspheres by the liver has been previously noted with corresponding rapid elimination from the blood: little difference was noted when 50 nm and 500 nm microspheres were compared (Ogawara et al. 1999) although surface modification of microspheres can markedly limit hepatic uptake (Lode et al. 2001;Ogawara et al. 2001). A further consideration is the effect of the size of the particle in shear force: larger particle size can result in reduced adhesion due to higher shear force, as has been shown *in vitro* in a P-selectin-mediated adhesion model (Shinde et al. 2001). It is possible, therefore, that smaller particle size would increase sensitivity in this model.

Chapter 8
Final discussion and conclusions

As outlined in the Introduction, the aims of the work carried out for this thesis were threefold:

1. To further develop and characterise the synovial-homing phage and the human SCID mouse transplantation model as a platform for the validation of novel targeting agents.
2. To develop monomeric synthetic synovial homing peptides to deliver radioisotope imaging agents specifically to human synovium in *in vivo* biodistribution studies in the SCID mouse chimera model.
3. To develop novel polymeric peptide constructs in order to increase specific affinity and tissue targeting delivery.

The first two of these aims were successful in that a number of novel strategies were developed both for the exploitation of the SCID mouse transplantation model as a platform for the testing of novel agents for the specific delivery of agents for therapy or imaging, and for the polymerisation and radiolabelling of monovalent synthetic peptides. The third component of this thesis, the application of these tools to the testing of the synovial homing peptide, did not ultimately show any specificity of the 3.1 peptide for synovium under the conditions used in these experiments. The major findings of the thesis will be discussed here, along with the strengths and limitations of the techniques used. Finally, some conclusions will be drawn along with suggestions for future work in this area.

8.1 Validation of the synovial homing phage in the SCID mouse transplantation model as a platform for testing *in vivo* localisation of novel targeting agents

The aim of the work in Chapter 3 was, firstly, to confirm the viability of the SCID mouse transplantation model in my hands- this was achieved with similar graft viability to that seen in previous work. Furthermore, the presence of human/ murine anastomoses was confirmed in both transplanted synovium and skin. The specificity of phage 3.1 homing for transplanted human synovium was confirmed by repetition of *in vivo* experiments with 3.1 and the SC1 control phage clones. As had been seen before, specificity of the 3.1 phage was confirmed with

significantly higher numbers of phage clones retrieved from transplanted human synovium compared with skin in mice injected with 3.1 phage, and significantly greater homing seen in these animals compared with those injected with the control phage. These experiments confirm that the presence of the 3.1 peptide sequence confers homing specificity for human synovium compared with human skin and murine kidney.

I also examined the effect of up-regulation of the inflammatory phenotype of the transplanted tissue by intragraft injection of TNFα. Up-regulation of the endothelial inflammatory phenotype was demonstrated by staining for the adhesion molecules ICAM-1 and E-selectin: these are eminently suitable markers of TNFα stimulation in this model- RA synovial tissue is characterized by marked up-regulation in the expression of both (Kriegsmann et al. 1995;Tak et al. 1995) and these are reduced following treatment with anti-TNFα (Smith 1997;Tak et al. 1996) and other agents (Smith et al. 2001;Youssef et al. 1996b). Furthermore, it is well-established that TNFα stimulates ICAM-1 and E-selectin on synovial endothelial cell *in vitro* (To et al. 1996) and, as mentioned, we have previously shown that intragraft injection of TNFα in this model produced up-regulation of ICAM-1 and VCAM-1 expression at 48 hours, although at this time point up-regulation of E-selectin was no longer seen (Wahid et al. 2000). These results are in keeping with the observed expression dynamics of these adhesion molecules following TNFα stimulation (To et al. 1996), but at this time-point it is clear from these results that molecules that are constantly up-regulated under the influence of the pro-inflammatory cytokine environment in RA may be relatively under-expressed in this model. We wanted, therefore, to confirm adhesion molecule up-regulation at an earlier time point and to investigate the effects on graft localisation of the synovium homing phage. In order to assess the effect of TNFα stimulation on the transplanted tissues we assessed the expression of E-selectin and ICAM-1 at 6 hours, at which point both were substantially up-regulated. Previously we found that by 48 hours post-TNFα E-selectin expression was at basal levels whereas ICAM-1 and VCAM-1 up-regulation persisted at 48 hours (Wahid et al. 2000). In this study we showed that both ICAM-1 and E-selectin

were up-regulated in synovial transplants, and E-selectin equally in synovial and skin transplants as early as 6 hours after intragraft injection of TNFα. The observation of up-regulation of ICAM-1 and E-selectin in both human tissues confirms that the enhanced phage homing to synovium in response to TNFα is specific.

In these experiments there was significant up-regulation of CKSTHDRLC (3.1) phage localization at 6 hours in the synovial tissue, with down-regulation to baseline by 18 hours. This suggests that the ligand for the 3.1 phage is up-regulated by TNFα as well as being present under basal conditions in these tissues. Furthermore, no significant differences were seen in the control tissue (skin): this is despite there being a clearly demonstrable pro-inflammatory effect as evidenced by up-regulation of both E-selectin and ICAM-1 expression at 6 hours. The observation that the phage are binding a synovium-specific TNFα–responsive ligand supports the possibility of the presence of a synovial homing-receptor. Although tissue-specific homing receptor/ addressin pairs have not been identified for human synovium there is substantial indirect evidence that such interactions may exist, such as the observation of non-random accumulation of lymphocyte subsets in the inflamed synovium (Pitzalis et al. 1987) and the selective adhesion of lymphocytes isolated from inflamed human synovium to synovial tissue sections (Salmi et al. 1992).

As has been discussed in the introduction, *in vivo* phage display has a number of advantages in the identification of novel tissue-specific ligands. Foremost of these are the selection of phage under physiological conditions and from within the circulation: this will result in the selection of clones expressing peptide sequences which bind ligands expressed in the vascular lumen (most probably by vascular endothelial cells or the extracellular matrix), and that have the affinity to maintain tissue-binding under conditions of shear stress. Immunofluorescence microscopy of tissue sections from *ex vivo* transplants from mice injected with phage showed that phage were confined to the vasculature at the 15 minute time point at which tissues were retrieved for these experiments.

The time course of up-regulation of phage homing to synovium may provide some insight into the nature of the ligand. The relatively short-term time frame, with down-regulation by 18 hours, suggests cell membrane expression (as opposed to extracellular matrix). E-selectin expression peaks *in vitro* after TNFα-stimulation at 4-6 hours, although expression can remain up-regulated for 24-48 hours (To et al. 1996). However, the lack of an increase in homing of the 3.1 phage to skin despite up-regulation of E-selectin expression in our study makes this an unlikely ligand although tissue-specific post-translational modification is possible. Similarly, up-regulation of ICAM-1 expression is seen in both skin and synovium and is therefore less likely to be the target: furthermore the dynamics of ICAM-1 expression as already discussed are not in its favour and lack of binding of the phage to ICAM-1 was confirmed later in this chapter by ELISA. Although TNFα is known to synergise with VEGF in the stimulation of neoangiogenesis, the short time frame of the effect on phage homing effectively rules this out as an explanation for the phenomenon. Our findings therefore raise the possibility that the synovial endothelial ligand may be a novel tissue homing receptor; the observation that phage homing is seen in the resting as well as the inflammatory state suggests that it may have roles in cell recruitment in diseases states as well, possibly, as in routine immunosurveillance. The demonstration that the synovial-homing of the phage is up-regulated by TNFα adds significantly to the potential of the specific peptide sequence as targeting tool. Potentially, reagents bearing this specific sequence would be not only be selective for synovial tissue and but also preferentially accumulate in actively inflamed synovial tissue. This has obvious implications for imaging and tissue-specific delivery of therapeutic molecules for rheumatoid arthritis.

A BLAST search of the peptide sequence produced a striking match with a sequence of the extracellular domain of the α_m (CD11b) integrin subunit, which associates with β_2 (CD18) to form the mac-1 integrin. The matched sequence is outside the I-domain of the sequence and is within the so-called membrane-proximal 'lectin-binding' domain. Mac-1 is the most promiscuous of the

leukocyte integrins and adhesive interactions have been described with a number of endothelial cell-expressed molecules and extracellular matrix proteins including ICAM-1(Diamond et al. 1991), ICAM-2 (Xie et al. 1995), fibrinogen (Lishko et al. 2004) and fibronectin (Lishko, Yakubenko, & Ugarova 2003) as well as non-protein ligands such as glycosaminoglycans (Diamond et al. 1995). Of these, ICAM-1 and fibronectin are attractive candidates in the RA synovium, although our experiments did not show specificity of 3.1 clone phage binding for the purified proteins in an ELISA-based assay.

A number of studies have implicated mac-1 in the pathogenesis of RA: increased cellular expression of mac-1 has been demonstrated in RA synovial tissue when compared with controls (Tak et al. 1995) and mac-1 expression by T-lymphocytes is increased in patients with active RA and this correlates with disease activity (Grober et al. 1993). Furthermore, increased peripheral blood neutrophil expression of mac-1 has also been shown in RA when compared with healthy controls which decreases after prednisolone treatment (Torsteinsdottir et al. 1999). This latter study contrasts with another study in which, although whilst peripheral blood neutrophil expression of CD11b was not raised, it was upregulated in mononuclear cells from synovial fluid (Lopez et al. 1995). In an *in vitro* adhesion assay monocyte adhesion to frozen RA synovial tissue sections was partially inhibited by pre-incubation with an antibody to α_m (Grober et al. 1993). The promiscuity of mac-1 binding is well described and adds weight to the hypothesis that the synovial receptor for the peptide may be a novel ligand. As has already been described, ICAM-1 is up-regulated in the inflamed synovium and is a ligand for mac-1 although the time frame of TNFα-induced upregulation of phage homing are not consistent with its being the synovial receptor for the phage. Fibronectin is also well-established as a mac-1 ligand although our own experiments have not shown any specificity for plasma fibronectin or ICAM-1 *in vitro*. However, the fibronectin gene consists of 50 exons, and alternative splicing results in a number of polypeptide variants of which there are at least 20 in humans (Kornblihtt et al. 1996) with resultant differences in the tissue and plasma forms of the protein. Two alternative splice sites, known as extra domains A and

B (ED-A and ED-B), are only found in tissue forms of fibronectin (Carsons 2001). Expression of ED-B is up-regulated in the vessels of some types of tumour (Nilsson et al. 2001) and in inflamed synovial tissue (Kriegsmann et al. 2004) and it has been exploited as a ligand for specific targeting of neoplastic tissues (Nilsson et al. 2001). Another alternative splice site is between the 14^{th} and 15^{th} type III repeats and is known as III-CS (connecting sequence). The CS-1 peptide sequence is contained within the III-CS, and includes the LDV motif which mediates binding to the integrin $\alpha_4\beta_1$ (Komoriya et al. 1991): staining of rheumatoid synovium with antibodies specific to the CS-1 domain has shown expression at the luminal surface of vascular endothelial cells and on lining layer synoviocytes where they meet the joint cavity; minimal staining was seen in normal synovial tissue (Elices et al. 1994;Muller-Ladner et al. 1997). The CS-1 peptide was found to down-regulate *in vitro* lymphocyte adhesion to rheumatoid synovial tissue sections (Elices et al. 1994). The sequence matched with that of the peptide within the α_m subunit is at positions 660-666 which places it membrane-proximal to the I-domain binding region: regions of the I-domain have been shown to mediate binding of mac-1 to a number of its ligands including ICAM-1 (Ehirchiou et al. 2005). Site-specific mutagenesis studies within the I-domain have found abrogation of ICAM-1 binding although the coincident finding that the I-domain can have a regulatory role over the confirmation of the integrin means that the existence of alternative binding sites cannot be precluded (Ehirchiou et al. 2005). Binding of other mac-1 ligands, such as ic3b, has been shown to persist if the α_m I-domain is deleted from mac-1 (Yalamanchili et al. 2000) and binding to carbohydrate ligands has been mapped to a 'lectin-binding' domain between residues 400-1092 of the α_m subunit (Xia & Ross 1999); experiments with site-specific antibodies to the α_m subunit suggest that lectin binding activity may be in the most membrane-proximal region of the sequence (Thornton et al. 1996). It is therefore possible that the peptide is binding a carbohydrate-based tissue ligand, although the nature of the tissue ligand remains unknown and this is the subject of ongoing work.

8.2 Development of the SCID transplantation model as a tool for imaging transplanted human synovium

In Chapter 4 the SCID mouse transplantation model was further developed as a tool for the pre-clinical assessment of agents for the imaging of inflamed synovium. Although the subsequent work did not produce agents with homing specificity suitable for further assessment in this model, its success with the anti E-selectin antibody has proved its potential for other agents in development. As discussed in detail in the introduction, there is substantial ongoing research into the development of novel agents for the nuclear imaging of inflamed synovial tissue in human subjects. There are strong justifications for the level of investment in such research: as already mentioned there is a clear need for the availability of relatively low cost, sensitive imaging techniques which can identify inflammation and quantify it over time. This would enable earlier diagnosis and sensitive monitoring of response to treatment, both of which are essential in light of the widely accepted paradigm in which early effective treatment of RA is critical to long term outcome. An obvious disadvantage to such research is the availability of patients willing to enrol in these studies which, in combination with the ethical constraints on denying patients optimum treatment, limits the pace at which this research can progress.

The application of animal models to the development of novel imaging agents is hampered by the limited resolution of conventional 2D nuclear imaging techniques: consequently it is often impossible to determine the sensitivity of novel agents prior to clinical trials. However, advances in small animal imaging techniques, particularly SPECT and positron emission tomography (PET) scanning, both of which enable greater spatial resolution, are now enabling quantification of uptake within defined areas with some promising results (Kneilling et al. 2007;Ostendorf et al. 2006). Whilst widespread use of PET is limited by the poor availability and short half-life of positron-emitting isotopes, SPECT uses isotopes already in widespread use such as ^{111}In and ^{99m}Tc. Furthermore, multi-pinhole collimators further increase SPECT sensitivity with

resolution greater than that of PET achievable in small animal imaging systems (King et al. 2002).Although animal models can be used for imaging studies, differences in pathology between animal models and human disease, as well as the presence of species-specific molecular determinants has limited the application of such models to arthritis research. This model, therefore, provides a powerful interface between the development of synovial-targeted imaging agents *in vitro* and clinical trials in human subjects.

E-selectin has many of the properties of an ideal target for the specific imaging of inflamed tissue. It is confined to vascular endothelial tissue where its expression is minimal in the uninflamed state; it is dramatically and rapidly upregulated in synovial inflammation both in RA patients and under the experimental conditions described here and, crucially, binding antibody is internalised upon ligation. This, particularly when exploited with the use of a 'residualising' bifunctional radioisotope chelator such as DTPA, optimises the retention time of the tracer in the tissue and hence will maximise the tissue-to-background ratio.

The NanoSPECT/CT technology used in this project is relatively new and there is no published data reporting its ability to accurately quantify tissue uptake. During the imaging experiments, therefore, the tissue uptake quantified by the SPECT software was correlated with the 'gold standard' of measurement in the gamma counter- this produced good correlation, although not perfect. Partly this will be accountable by the imprecision in exactly delineating the transplanted tissue on the images obtained, particularly as this has to be done in 2D on the maximum intensity projections (MIPs), and also by the difficulty in exactly dissecting all the transplanted tissue from the adherent skin. Despite this it was felt that the correlations were sufficient to determine whether the technique had the sensitivity to detect tissue-specific uptake.

Image quality of the reconstructed CT/SPECT fusion images was excellent with the transplants clearly visible as early as 1 hour after injection of ^{111}In-labelled antibody. The rapid ingress of antibody into the tissue suggests that the vessels of

TNFα-stimulated transplants are hyperpermeable. The vessels of inflamed synovium are known to have increased permeability (Levick 1981) and this is likely to account for the difficulties that have been encountered in developing agents with specific targeting properties that have enhanced uptake over agents, typified by HIg, which rely mainly on non-specific uptake. As was described in the introduction, HIg is an effective imaging agent in RA with superior properties to conventional diphosphate-based imaging (de Bois et al. 1994). Studies with agents directed at specific targets have met with mixed success, and although good synovial uptake is seen with macromolecule-based specific tracers, much or all of this uptake often seems to be due to a non-specific effect. This phenomenon invites comparison with the enhanced permeability and retention (EPR) effect which has been exploited so successfully in the therapy of some cancers. The EPR effect was originally described in the context of tumour tissue where there is vessel hyperpermeability and abnormal lymphatic drainage: it refers to the observed accumulation of macromolecules (typically >45 kDa) with resultant concentrations of several times that seen in normal tissues and plasma (Maeda et al. 2003) (Torchilin & Lukyanov 2003). RA synovium, as previously mentioned, is characterized by florid neoangiogenesis (Paleolog 2002) and shares a number of features with tumour tissue. Firstly, the aforementioned hyperpermeability which is also a feature of tumour vasculature, and this has been associated with more rapid egress of large molecules into the RA joint (Simkin 1979). Secondly, the abnormal vascularisation is associated in some patients with increased vessel tortuosity (Salvador et al. 2006), another feature of neovasularisation in tumour tissue, which further increases the relative tissue vessel density. Finally, a number of vasoactive mediators, notably VEGF are upregulated in the synovium and plasma of patients with RA (Salvador et al. 2006). Analysis of the distribution of the (non-specific) MRI contrast agent gadolinium-DTPA, in which there was rapid diffusion into the joint fluid, confirm that this hyperpermeability is also seen with small molecules (Ostergaard & Klarlund 2001). The conjugation of drugs or radioisotopes to large molecules is therefore a potential strategy for the targeting of inflamed synovium.

Despite these difficulties, radiolabelled E-selectin has been the most successful of the directly targeted agents and has shown superiority in direct comparison with HIg (Jamar et al. 1997) and thus has considerable potential both as an imaging agent and also as a means of targeting drugs or drug delivery vectors to inflamed synovium. E-selectin was thus regarded as an ideal target for the assessment of the imaging model to discriminate specific from non-specific uptake. As expected, there was substantial uptake of the isotype control antibody into the TNFα-stimulated grafts and a clear transplant-to-background contrast was seen at all time points. Despite this, a significant difference was seen between the anti-E-selectin and control antibodies at 4 and 24 hours indicating that there was additional specific uptake of the anti-E-selectin antibody. It should be noted that the 1.2B6 antibody also binds P-selectin with low affinity: P-selectin is also expressed in the vascular endothelium of RA synovial tissue (Johnson et al. 1993)- the increased uptake seen may therefore also represent P-selectin binding to some degree, although this does not detract from our conclusions to this work.

As well as reaffirming the potential of this antibody as a tool for specific delivery to RA tissues (something which could be further pursued in our transplantation model), this also demonstrates the potential of this model for the assessment of novel imaging agents. Crucially, it was shown that specific uptake could be resolved from non-specific uptake: this model could therefore be used to identify specific agents in the pre-clinical setting that may have increased sensitivity over radiotracers which rely on non-specific mechanisms to image inflamed synovial tissue. This is the first time, to our knowledge, that imaging of xenografted non-malignant human tissue has been attempted. Although this project did not produce reagents which were suitable for further imaging experiments, we hope that this system will prove useful in the development of other agents.

There are, of course, limitations to this model, particularly that the synovium is not being imaged in the context of the joint: resolution of synovial tissue uptake from other articular structures is not tested under these conditions. Furthermore there are significant differences in the expression of inflammatory molecules in

fresh and transplanted synovium: in this study TNFα was used to up-regulate E-selectin expression but expression of other target molecules in the transplants would need to be validated prior to experiments with other agents. Despite this it gives a unique platform to image changes over time in the same tissue with evident applications to the testing of novel radiopharmaceutical agents and in particular their capacity to resolve specific from non-specific uptake and consequent potential to image specific molecules. Furthermore, this technology could be applied to other tissues: human lymph node tissue, for instance, has been successfully transplanted into SCID mice in our laboratory (Blades et al. 2002).

8.3 Investigation of tissue specificity of the synovium-homing monomeric peptide *in vitro* and *in vivo*

In Chapter 5 the binding properties of monovalent peptide were examined *in vitro* and *in vivo*. One of the great advantages of *in vivo* phage display is its capacity to identify as yet unknown ligands and this is a powerful approach to the identification of tissue-specific epitopes. However, the lack of a purified ligand molecule for further *in vitro* analysis presents a number of problems, some of which were exemplified by the experiments in this chapter. Staining of tissue sections with fluorescent 3.1 and control peptides did not demonstrate a difference in binding. As discussed previously the different amino acid composition of the control peptide may have conferred a greater degree of non-specific binding which could mask specific binding of the control: previous workers have found that peptide binding can vary significantly with pH reflecting the importance of charge (Sherman et al. 1994). This aside, an essentially linear increase in binding of both peptides was observed with increasing concentration suggesting either a lack of specificity *under these conditions* or lack of sensitivity of the assay to detect specific binding. The methods used in the *in vivo* phage experiments allow very sensitive detection of phage homing to tissues, and this does not provide any information about the receptor density which may be below the detection limit of the *in vitro* assay. The *in vitro* conditions also differ from those *in vivo* and the importance of this is not known: cation conditions, for instance, may be critical as will be discussed later. Furthermore, the identification of tissue-specific peptide-displaying phage by screening from within the vascular compartment does not

preclude the presence of the vascular antigen in the extravascular space: if there were specific binding to cells outside the vasculature this could also mask specific vessel binding. Finally, and perhaps most importantly, is the concept of valency and this will be returned to later.

Several of these difficulties, particularly those due to differences between conditions *in vivo* and *in vitro* were addressed by the *in vivo* biodistribution experiments. For these experiments the peptides were linked, via an aminohexanoic acid spacer, to the bifunctional chelating agents DTPA and HYNIC for the conjugation of ^{111}In and ^{99m}Tc respectively. It was already known that the free synthetic peptide could inhibit specific phage homing when co-administered *in vivo* (Lee et al. 2002), albeit in high doses. In absolute terms, peptide was administered in ~10^6-fold excess to phage: the necessity for this is likely to be largely due to rapid elimination of the peptide from the circulation, although it is also very possible that the monovalent peptide has lower avidity for the tissue receptor than the phage and hence is required in substantial excess to block binding. Initial comparison of peptide-conjugated with free ^{111}In with labelled 3.1 peptide did demonstrate increased transplant localisation but this is most likely to be due non-specific differences in pharmacokinetics. No difference was seen when the ^{111}In-conjugated 3.1 and control peptides were compared *in vivo*, and, additionally, no differences were seen in homing of either peptide to transplanted human skin or synovium.

These experiments were repeated with ^{99m}Tc-conjugated 3.1 peptide with the same results: extension of the incubation time to 4 hours did not identify synovial-specific homing and the results were similar with variation of the co-ligand chemistry. Despite these results, there did appear to be relatively high uptake in the transplants compared with the murine organs. Once again, these results, this time in tissues not pre-stimulated with TNFα, suggest that there is hyperpermeability within the vasculature and that this is seen in both transplanted skin and synovium. This hypothesis was confirmed in the subsequent experiments examining tissue localisation of the albumin-binding dye Evans Blue. These

results were not unexpected in the synovium, although the reasons for the observed hyperpermeability in the transplanted skin tissue is less clear. We have shown that anastomoses are formed between the human and murine circulations in transplanted tissues and it is likely that this neoangiogenic vasculature is hyperpermeable. Furthermore, the presence of pro-angiogenic mediators such as VEGF may further contribute to this effect (Dvorak et al. 1995). Expression of angiogenic mediators has not been specifically examined in transplants in this model but may form an interesting basis for further work.

Whether the 3.1 peptide is internalised upon ligation of its tissue receptor is unknown: the success of approaches to the radiolabelling of regulatory peptides for imaging is partly reliant on the fact that internalisation of the complex is an important pathway of peptide inactivation. This, in combination with the use of residualising radiotracers, will contribute to the effective tumour-to-background ratios that are achieved with these agents. In the case of peptides which bind the receptors for the naturally occurring peptides, it has been shown that agonists are more likely to induce internalisation than antagonists and this, therefore, is a critical factor in determining peptide structure for the development of novel radiotracers (Cescato et al. 2006;Mantey et al. 1993). Thus it might seem, perhaps, that the odds are somewhat stacked against the relative success of peptides selected by peptide phage display. However, the relatively weak binding of small peptides makes them less likely to have the binding energy to displace water molecules at sites other than the binding site of a target molecule, and hence phage-displayed peptides, as opposed to antibodies, are more likely to target a binding site (George, Lee, & Pitzalis 2003). Even accounting for this, it seems intuitively more likely that selection of peptide from a randomly-generated library would be most likely to result in the identification of antagonist sequences. Despite this, there are reports of peptides identified by phage display being phage internalised upon receptor ligation, either from direct evidence (Laakkonen et al. 2004) or indirectly from the observed efficacy of conjugation to pro-apoptotic peptide sequences which are only cytotoxic upon internalisation (Kolonin et al. 2004). It is possible that more sophisticated methods of phage selection can result

in the identification of more peptides which are internalised, such as pre-screening with positive selection *in vitro* prior to *in vivo* biopanning (Laakkonen et al. 2004).

The findings from the work presented in this chapter suggested a two-fold approach to these problems: both of these- size and valency- were addressed in the following chapter.

8.4 Development of a tetravalent radiolabelled peptide molecule and investigation of *in vivo* synovial targeting

In chapter 6 a method was developed for the polymerisation and testing of tetravalent peptides by conjugation to streptavidin: this also enabled the radiolabelling of the construct for testing of *in* vivo biodistribution. As discussed in the introduction to the chapter, polyvalent interactions are ubiquitous in biological systems (Mammen, Choi, & Whitesides 1998): increased valency results in increased binding affinity and this can be used as a regulatory mechanism, for instance as described for integrin clustering in the cell adhesion cascade. Increasing the valency of peptides has been shown, for example, to enhance cellular uptake of vectors carrying short peptide 'protein transduction domains' (Sung, Poon, & Gariepy 2006) and to increase antigenicity of peptide in the form of multiple antigen peptides (MAPs) (Tam 1996): surface density of peptides conjugated to microspheres has been correlated with valency (Iannone & Consler 2006). Even a modest increases in valency, by the conjugation of biotinylated peptides to streptavidin, was shown to increase the inhibitory EC50 of a P-selectin binding peptide 200-fold (Molenaar et al. 2002).

Naturally occurring RGD peptide interactions take place in the context of multivalent presentation: the construction of molecules containing polyvalent RGD sites could therefore increase the binding avidity of the relatively weakly binding monomeric peptides. Increasing the valency of a molecule will allow it to potentially bind multiple receptors simultaneously thus decreasing the off-rate with resultant increase in apparent avidity. As will be discussed below, increases

in avidity seen when a multivalent molecule may not be large enough to bind two receptors are likely to be due to an increase in the effective local concentration of ligand with resultant increase in the on-rate (Liu 2006). Using a strategy in which multiple cyclic RGD peptide sequences were conjugated onto a decapeptide backbone it was shown that a molecule expressing 4 RGD domains had enhanced inhibitory activity compared to a monovalent peptide in cell adhesion inhibition assay, with around a 50-fold lower IC50 (Boturyn et al. 2004;Garanger et al. 2006;Garanger et al. 2005). When these peptide constructs were conjugated to fluorescent dyes it could be shown that the CHO cells internalized the peptide, an effect not seen with a control peptide (Boturyn et al. 2004). Internalisation was also seen when biotinylated multivalent RGD molecules were conjugated to streptavidin, demonstrating intracellular delivery of large conjugated molecules. The concentrations used in this experiment (10 μM) were ten-fold higher than the maximum achieved in our experiments and this may explain why we did not show cell uptake in the radioligand binding assay. In a separate approach, Kok *et al* showed that conjugation of multiple copies of a cyclic RGD peptide to an irrelevant human immunoglobulin resulted in a molecule that inhibited $\alpha_v\beta_3$-dependent cell binding to vitronectin in an adhesion assay, and had significantly lower IC50 than monomeric peptide for inhibition of the multivalent protein to cells in a radioligand binding assay (Kok et al. 2002). Dimeric RGD compounds have been tested for tumour homing *in vivo*. Two radiolabelled compounds, ^{64}Cu-DOTA-E[c(RGDfK)] and ^{64}Cu-DOTA-E[c(RGDyK)], were tested in a human breast carcinoma xenograft model: both showed specific tumour uptake with the peptide containing the tyrosine substitution having slightly more favourable pharmacokinetics with improved tumour-to-blood and tumour-to-liver ratios (Chen et al. 2004a). An investigation of monomeric, dimeric and tetrameric cy5.5-RGD peptides found and decrease in IC50 with increases in valency in an echistatin /$\alpha_v\beta_3$ radioligand binding assay (Cheng et al. 2005). When used for near-infrared fluorescence imaging in a tumour model the dimer was had significantly higher uptake than the monomer, with the tetramer showing a non-significant improvement over the dimer. In another study the tetrameric peptide $[cRGDfK)_2]_2$ conjugated to ^{111}In via DOTA had increased affinity for $\alpha_v\beta_3$ *in vitro*

and significantly enhanced tumour uptake *in vivo* compared with the dimer and monomer at 2.7,5.61 and 7.32 %ID/g respectively (Dijkgraaf et al. 2007a).

Linker length has been shown to be critical in the design of peptides linked to functional groups, and at least two groups have reported their observations of this as applied to RGD peptides. Preliminary results with multivalent RGD peptides, synthesised on a short peptide backbone, in a vitronectin/ $\alpha_v\beta_3$ competitive binding assay showed that varying spacer length affected IC50, although not predictably so, with the IC50 rising or falling with increasing spacer length with bi- or tetravalent peptides respectively (Thumshirn et al. 2003). That an effect of spacer arm length could also be seen with varying spacer arm length of a hydrophilic, but not a lipophilic, spacer was also seen with a monomeric peptide demonstrates the relevance of the choice of spacer itself. The effect of the spacer arm length on behaviour of a biotinylated monovalent RGD peptide has been demonstrated when conjugated to streptavidin (Boturyn et al. 2004): cell adhesion to these peptides was only seen when the spacer arm consisted of 6 or more carbon atoms, emphasizing the importance of exceeding a minimum distance between the biotin and active binding domain of such molecules when conjugated to streptavidin. In another solid-phase adhesion assay, RGD peptides bound to a poly(methyl methacrylate) surface were found to require a minimum spacer length of >6 carbon residues in order to enable cell binding (Kantlehner et al. 2000)- this corresponds to an absolute distance of around 3.5 nm between the ligand and the surface. These results, and results from another study showing reduced activity of a peptide-linked multivalent RGD construct compared to constructs with lower valency but longer spacer groups (Garanger et al. 2006), suggest that steric hindrance may be an important factor in the design of these molecules. A further important consideration in the choice of linker is the effect of charge on biodistribution- linker variation can have a significant impact in this regard (Dijkgraaf et al. 2007b).

Investigations into the binding kinetics of RGD-containing peptide fragments and natural RGD-containing ligands have provided interesting insights into the

mechanisms of RGD/ integrin interactions. Vitronectin and an RGD-containing vitronectin peptide fragment were compared a binding assay in which purified $\alpha_v\beta_3$ was immobilized on plates. Binding of ^{125}I-vitronectin to immobilized integrin was found to be effectively non-dissociable when challenged with competing non-labelled vitronectin, and dissociated only when incubated with high concentrations of GRGDSPK peptide. The 15-amino acid residue peptide fragment also bound specifically but was dissociable with small concentrations of competing GRGDSPK peptide (Orlando & Cheresh 1991). These observations suggested that a second stabilizing event occurred after initial RGD ligation and that this was not seen with the peptide fragment: this implies that a complementary domain within vitronectin is responsible for this phenomenon. Similar results were seen in a cell adhesion assay: binding to immobilized vitronectin could be inhibited in a dose-dependent fashion when co-incubated with GRGDSPK peptide, but displacement was only seen with high concentrations of peptide if this was added after the initial adhesion had been allowed to take place. This mechanism involved is likely to be due to conformational change within the integrin structure as these observations were the same if the cells were pre-treated with cytochalasin B, which inhibits cytoskeletal actin polymerization, but stabilization was inhibited when immobilized integrin was treated with gluteraldehyde, which cross-links free amino groups within the protein (Orlando & Cheresh 1991). These findings were supported in a later study in which fibrinogen (another RGD-containing protein) and RGD peptide binding to $\alpha_{IIB}\beta_3$ incorporated into lipid bilayers was monitored in real time (Muller et al. 1993). Once again rapid and stable association of fibrinogen with the integrin was seen which was non-dissociable. In contrast, binding of the GRGDSPC peptide was rapid but washing resulted in fast dissociation, this process was so fast that the off-rate could not be resolved within the resolution of the technique. This biphasic interaction with RGD ligands was further characterized more recently. Using an ELISA-based assay, where soluble $\alpha_v\beta_3$ was incubated on vitronectin-coated plates in the presence of increasing concentrations of the cyclic peptide c(RGDfV) (Legler et al. 2001). It was found that at low (sub-nanomolar) concentrations the RGD peptide ‘superactivated’ the integrin with increasing

binding of $\alpha_v\beta_3$ to vitronectin, whereas at higher concentrations it had an inhibitory effect due to integrin binding. It is well-established that RGD ligation of cell-surface receptors can results in internalisation: increasing the valency of a fluorochrome-conjugated peptide-linked RGD group resulted in increased internalisation by $\alpha_v\beta_3$-expressing cells compared with a monovalent peptide (Boturyn et al. 2004). In a separate study a cy5.5-conjugated peptide was shown to be effectively internalised by cells expressing $\alpha_v\beta_3$, an effect not seen with a negative control cell line or in the presence of competing peptide (Chen, Conti, & Moats 2004). In a further study it was shown that although a monomeric RGD peptide could inhibit $\alpha_v\beta_3$-dependent cell adhesion, internalisation of the peptide occurred through $\alpha_v\beta_3$-independent fluid-phase endocytosis (Castel et al. 2001).

As we did not have an *in vitro* assay for the synovial homing peptide, RGD peptides were used to validate the tetravalent peptide technique *in vitro.* The peptide used initially, RGD2C, was derived from the same phage display library as the 3.1 peptide and hence had the same basic peptide structure. Some of the experiments, including the *in* vivo experiment, were conducted with a different peptide (cRGDyK). This peptide had a smaller primary amino acid sequence consisting of 5 residues cyclised by an amino-bond, whereas the RGD2C and 3.1 peptides have seven amino acids flanked by cysteine residues, between which a disulphide bind cyclises the peptide. It is unlikely that these small differences between the peptide structures would be of significance as the linkers separating the biotin from the peptide were the same. In the experiment reported here streptavidin-conjugated RGD peptides were effective in direct $\alpha_v\beta_3$ binding assays, in competitive binding assays with fibronectin and in cell adhesion assays. These results suggest the RGD activity is retained after streptavidin conjugation in these peptides which have 6-carbon spacers between the biotin and RGD groups. Conjugation to DTPA did not affect biotin biding and this was retained after radiolabelling. Thus, a method was developed for the rapid production of radiolabelled multimeric peptide constructs. Binding of the radiolabelled tetramers was not, however, seen to $\alpha_v\beta_3$ cells *in vitro* or *in vivo*. The concentrations used in the *in vitro* experiments were lower than those used in several of papers quoted

above, and it may be that in our system higher concentrations would have been required, particularly bearing in mind the kinetics of RGD binding discussed above. There are clear differences between the multimerisation techniques discussed: the use of small peptide backbones will result in a higher local concentration of RGD groups, whereas the relative size of streptavidin will result in lower local availability of these groups with implications for binding kinetics. It has been shown previously that the binding properties of purified and cell-bound receptors can differ substantially (Sherman et al. 1994) and it is possible that the plate-bound integrin, particularly in the this cation environment, is present in a 'superactivated' form. As discussed above, the rapid binding kinetics of RGD peptides may prohibit binding under these conditions: this was therefore not seen as an impediment to proceeding with 3.1 peptide experiments as the binding kinetics may be very different. The phage work had shown that the peptide was effective in an oligovalent form and was capable of supporting the binding of large phage particles under physiological conditions.

The stability of the peptide after conjugation to streptavidin was not examined as this would have been technically difficult, but it is conceivable that proteolytic breakdown could reduce the binding affinity of the streptavidin/ peptide conjugates. It is very possible, however that the conjugation enhances peptide stability- it has previously been shown that peptide conjugation to dendrimers results in increased stability (Bracci et al. 2003).

The *in vivo* experiments with the tetrameric peptide did not show any significant differences in homing to skin or synovium of either test or control peptides at any of the 3 time-points. As has been discussed, it is probable that the peptide group was available and that the construct was stable *in vivo* and these results are likely, therefore, to show a genuine lack of specificity for synovium. Previous experiments have shown that the transplanted tissues are hyperpermeable to macromolecules (albumin) and the molecular weight of the streptavidin-peptide tetramers (~75,000 Da) is similar to that of albumin (~60,000 Da). It is possible that this is limiting the sensitivity of the model to determine specific uptake,

although after 24 hours (around 4 half-lives) specificity was still not seen. A further limitation is the valency; the tetrameric molecule caries four peptide groups but the structure is probably limiting the number of groups available to a surface-bound epitope to two. The phage express 5 copies of peptide at one end and the physiological valency is therefore probably greater than that seen with this molecule. For the final part of this work a method was developed for the production of polyvalent particles by conjugation of the peptide to fluorescent microspheres

8.5 Polymerisation of peptide by conjugation to fluorescent microspheres and investigation of synovial targeting *in vivo*

In Chapter 7 a novel method was described for the surface labelling of fluorescent microspheres with peptide with or without co-labelling with a radioisotope. Binding of the peptide to Neutravidin-coated microspheres was confirmed by the demonstration of the blockade of biotin binding, and the RGD-microspheres were shown to bind $\alpha_v\beta_3$-expressing cells *in vitro*. Furthermore, it was shown that surface density of the peptide could be varied and this variation in valency had a linear relationship with cell binding. A limited *in vivo* experiment with RGD-coated microspheres in A375P tumour carrying mice did not demonstrate specific uptake. Although specific binding had been shown *in vitro* the absolute numbers of microspheres binding to cells is likely to have been small, suggesting that the avidity of the microspheres for RGD-binding integrins is low. It is very likely, under conditions of flow, that binding of microspheres was limited. The experiment was therefore repeated with 3.1 or scrambled-control coated microspheres in the SCID mice double-transplanted with human skin and synovium. Again, no specific uptake was seen at any time point. The particles are polyvalent and therefore, under these conditions, it is unlikely that low valency is the problem. However, the 1μm microspheres are subject to significant shear stresses under flow conditions and the size of the particles is such that these will be somewhat greater to that experienced by phage. A further consideration is the rapid clearance of the microspheres from the circulation seen in this and other work. Despite these observations, other workers have shown specific binding of

antibody-coated fluorescent microspheres in a model of brain inflammation (Kiani et al. 2002) and hence there is likely to be bioavailability of the microspheres to the transplanted tissues. The absence of specific homing was seen despite pre-stimulation of the transplants with TNFα: pre-stimulation was shown to specifically up-regulate 3.1 phage binding to transplanted synovium at 6 hours in Chapter 3. The large size of the microspheres was anticipated to limit non-specific extravasation; although TNFα can increase vessel permeability no increase of control phage homing was seen after TNFα stimulation. These findings therefore add weight to the possibility that the 3.1 peptide, in this form, does not confer homing specificity to conjugated molecules or microparticles. The stability of the peptide has been discussed: in Chapter 5 the stability of the HYNIC-conjugated (acetylated) peptide was shown to be reasonable at 1 hour, although there was significant loss of the label at 4 hours. Although the stability of the peptide in its tetrameric or microsphere-conjugated from was not tested, previously quoted work suggests that peptide conjugated to large particles is likely to have increased resistance to proteolytic digestion in serum. Furthermore, the rapid clearance of the microspheres from the circulation maximises the potential sensitivity of this assay at early time points.

Although no specific uptake was seen *in vivo*, this fluorescent microsphere technique, as shown with the RGD peptide-based assays, represents a potentially powerful assay for the detection of peptide-binding epitopes on cells *in vitro*. Several groups have reported the use of microspheres for the *in vitro* detection of cell-surface epitopes and it has been shown that this technique can successfully detect epitopes present at low density (Wojchowski & Sytkowski 1986). Here it was shown that their use can be extended to small peptides: this technique may therefore prove invaluable for the detection of cell-surface ligands *in vitro*: it is hoped that endothelial cell-lines will be screened for the expression of 3.1 peptide-binding epitopes.

8.6 Conclusions and future work

To summarise, a number of approaches have been used to investigate the homing capacity of the 3.1 peptide. Both the monovalent peptide and multivalent constructs were investigated: I was unable to demonstrate specificity for transplanted synovium under any of these conditions. The limitations of the model and the various approaches have been discussed: however, the data presented in this thesis suggest that the peptide is unlikely to have potential as a mediator of specific delivery to human synovium.

Despite this, several positive conclusions can be drawn. A number of novel techniques have been developed which, it is hoped, will prove useful to the investigation of specific peptide homing in other circumstances. The radiolabelled streptavidin-peptide tetramers described in Chapter 6 are a simple-to-use yet potentially powerful tool for the screening of potential homing peptides *in vivo* and the fluorescent microsphere techniques described here may have particular value for the investigation of cell-surface ligand expression *in vitro.* Furthermore, the SCID mouse model has been further characterised as a tool for the investigation of specific targeting strategies and a novel technique for the investigation of imaging agents was described in Chapter 4.

It is, of course, disappointing that the *in vivo* peptide experiments were not more successful. So how can the convincing data from the phage experiments, in which the peptide-expressing phage were consistently shown to home specifically to human synovium, and the negative data from the peptide experiments be reconciled? Of course, the reasons for this may be methodological and the potential problems in this respect have been discussed at length. However, that multiple approaches to the question provided negative results provide an increasingly convincing body of evidence that the peptide on its own has limited, if any, specificity. This therefore raised the question of whether the peptide, fused to the phage PIII surface protein is *necessary* but not *sufficient* for specific homing. The sequence similarity between the peptide and a membrane-proximal domain of the mac-1 integrin is compelling, but, as this sequence is not within the

I-domain, it may represent a complementary biding sequence. There is one report in the literature of binding specificity of peptide-expressing phage, selected for binding affinity to bone marrow endothelial cells, in which the specificity was ultimately found to be conferred not by the expressed peptide but by a domain of the PIII protein (Clement et al. 2003;Finger et al. 2002). It could therefore be hypothesised that a region of the PIII protein, acting as a mimotope for a synovial ligand, requires a synergistic interaction involving the expressed peptide. This hypothesis is also supported by the difficulty which we have encountered in our lab in attempts to isolate the synovial ligand by affinity chromatography using peptide-coated resin-containing columns. This raises the obvious question of whether this hypothesis can be tested: work in which leucocyte binding to frozen synovial tissue sections can be partially inhibited by antibodies to mac-1 has already been discussed (Grober et al. 1993) and it would be interesting to test the peptide as an inhibitor of cell binding under the same conditions.

Despite the negative results reported in this thesis, the original phage work still provides convincing evidence for the presence of a synovial-specific molecule, available to circulating phage, which may be suitable for exploitation as a specific target. Work is currently underway in our laboratory to screen synovial tissue in the same model with antibody-based phage libraries and it is very possible that the very different *in vivo* pharmacokinetics of these larger molecules may enable greater success with this approach. As was shown in Chapter 4 and as has been shown in human imaging studies, antibodies to E-selectin, which although not specific are highly selective for inflamed tissue, have considerable potential as imaging agents and, possibly as tools for the delivery of therapeutic agents. Work in pre-clinical models has also produced promising results with a number of other potential targets and these were discussed earlier.

Finally, the place of targeted therapies in the context of recent advances in RA therapeutics could perhaps be questioned. As has already been discussed, the advent of biological therapies has heralded a significant step forward in RA treatment, and anti-TNFα treatment is now firmly established as treatment for

DMARD non-responders. However, a significant proportion of patients do not respond to these agents. Furthermore, a large number of other targets are at various stages of investigation: so far the only other target for which therapy has been approved and recommended for routine use in the UK is CD20. Head-to-head studies with anti-TNFα therapies have not been done and it is therefore likely to become the second-line biologic for those who have failed anti-TNFα. The (apparent) exponential increase in biologic agents is going to make informed treatment choice virtually impossible, as the trials to define which patients will respond to which treatment are likely to take years, if not decades. The medium-term direction of therapeutics in this respect is therefore unclear, and it is likely that non-responders will simply be rotated through various biologic alternatives. Another possibility is the combination of these agents, but recent data have suggested significantly increased toxicity with the combinations that have been trialled (Genovese et al. 2004;Weinblatt et al. 2007;Weinblatt et al. 2006): specific targeting of biologics, as well as conventional DMARDs, may well still have an important role in the increasingly complex management of rheumatoid arthritis.

Appendix A: the amino acids and their abbreviations

One-letter code	Amino acid	Three-letter code
A	Alanine	Ala
C	Cysteine	Cys
D	Aspartic acid	Asp
E	Glutamic acid	Glu
F	Phenylalanine	Phe
G	Glycine	Gly
H	Histidine	His
I	Isoleucine	Ile
K	Lysine	Lys
L	Leucine	Leu
M	Methionine	Met
N	Asparagine	Asn
P	Proline	Pro
Q	Glutamine	Gln
R	Arginine	Arg
S	Serine	Ser
T	Threonine	Thr
V	Valine	Val
W	Tryptophan	Trp
Y	Tyrosine	Tyr

Appendix B: Phage-derived peptides used in this project

Peptide name	Sequence
3.1 (synovial homing peptide)	CKSTHDRLC
s3.1 (scrambled 3.1)	CLTKRSHDC
RGD2C	CSPRGDHPC
sRGD2C (scrambled RGD2C)	CDPRPHSGC
SC7 (streptavidin-binding sequence)	CGRYDHPQC

Appendix C: publications arising from this thesis

Garrood T, Blades M, Haskard D, Mather S, Pitzalis C. A novel model for the pre-clinical imaging of inflamed human synovial vasculature. Under review

Garrood T, Pitzalis C. Targeting the inflamed synovium: the quest for specificity. Arthritis Rheum 2006; 54 (4): 1055-60

Garrood T, Lee L, Pitzalis C. Molecular mechanisms of cell recruitment to inflammatory sites: general and tissue specific pathways. Rheumatology (Oxford) 2006; 45 (3): 250-60

References

Abitorabi, M. A., Mackay, C. R., Jerome, E. H., Osorio, O., Butcher, E. C., & Erle, D. J. 1996, Differential expression of homing molecules on recirculating lymphocytes from sheep gut, peripheral, and lung lymph, *J.Immunol.*, 156(9):pp. 3111-3117.

Abitorabi, M. A., Pachynski, R. K., Ferrando, R. E., Tidswell, M., & Erle, D. J. 1997, Presentation of integrins on leukocyte microvilli: a role for the extracellular domain in determining membrane localization, *J.Cell Biol.*, 139(2):pp. 563-571.

Adriaansen, J., Vervoordeldonk, M. J., & Tak, P. P. 2006, Gene therapy as a therapeutic approach for the treatment of rheumatoid arthritis: innovative vectors and therapeutic genes, *Rheumatology (Oxford)*, 45(6):pp. 656-668.

Aird, W. C. 2003, Endothelial cell heterogeneity, *Crit Care Med.*, 31(4 Suppl):p. S221-S230.

Akahoshi, T., Endo, H., Kondo, H., Kashiwazaki, S., Kasahara, T., Mukaida, N., Harada, A., & Matsushima, K. 1994, Essential involvement of interleukin-8 in neutrophil recruitment in rabbits with acute experimental arthritis induced by lipopolysaccharide and interleukin-1, *Lymphokine Cytokine Res.*, 13(2):pp. 113-116.

Ali, S., Palmer, A. C., Banerjee, B., Fritchley, S. J., & Kirby, J. A. 2000, Examination of the function of RANTES, MIP-1alpha, and MIP-1beta following interaction with heparin-like glycosaminoglycans, *J.Biol.Chem.*, 275(16):pp. 11721-11727.

Alon, R., Bayer, E. A., & Wilchek, M. 1990, Streptavidin contains an RYD sequence which mimics the RGD receptor domain of fibronectin, *Biochem.Biophys.Res.Commun.*, 170(3):pp. 1236-1241.

Alon, R., Kassner, P. D., Carr, M. W., Finger, E. B., Hemler, M. E., & Springer, T. A. 1995, The integrin VLA-4 supports tethering and rolling in flow on VCAM-1, *J.Cell Biol.*, 128(6):pp. 1243-1253.

Andresen, T. L., Jensen, S. S., & Jorgensen, K. 2005, Advanced strategies in liposomal cancer therapy: problems and prospects of active and tumor specific drug release, *Prog.Lipid Res.*, 44(1):pp. 68-97.

Appelboom, T., Emery, P., Tant, L., Dumarey, N., & Schoutens, A. 2003, Evaluation of technetium-99m-ciprofloxacin (Infecton) for detecting sites of inflammation in arthritis, *Rheumatology.*42(10):pp. 1179-82.

Arap, W., Haedicke, W., Bernasconi, M., Kain, R., Rajotte, D., Krajewski, S., Ellerby, H. M., Bredesen, D. E., Pasqualini, R., & Ruoslahti, E. 2002a, Targeting the prostate for destruction through a vascular address, *Proceedings of the National Academy of Sciences of the United States of America.*99(3):pp. 1527-31.

Arap, W., Kolonin, M. G., Trepel, M., Lahdenranta, J., Cardo-Vila, M., Giordano, R. J., Mintz, P. J., Ardelt, P. U., Yao, V. J., Vidal, C. I., Chen, L., Flamm, A., Valtanen, H., Weavind, L. M., Hicks, M. E., Pollock, R. E., Botz, G. H., Bucana, C. D., Koivunen, E., Cahill, D., Troncoso, P., Baggerly, K. A., Pentz, R. D., Do, K. A., Logothetis, C. J., & Pasqualini, R. 2002b, Steps toward mapping the human vasculature by phage display, *Nat.Med.*, 8(2):pp. 121-127.

Arap, W., Pasqualini, R., & Ruoslahti, E. 1998, Cancer treatment by targeted drug delivery to tumor vasculature in a mouse model, *Science*, 279(5349):pp. 377-380.

Arbones, M. L., Ord, D. C., Ley, K., Ratech, H., Maynard-Curry, C., Otten, G., Capon, D. J., & Tedder, T. F. 1994, Lymphocyte homing and leukocyte rolling and migration are impaired in L-selectin-deficient mice, *Immunity.*, 1(4):pp. 247-260.

Argarana, C. E., Kuntz, I. D., Birken, S., Axel, R., & Cantor, C. R. 1986, Molecular cloning and nucleotide sequence of the streptavidin gene, *Nucleic Acids Res.*, 14(4):pp. 1871-1882.

Arnett, F. C., Edworthy, S. M., Bloch, D. A., McShane, D. J., Fries, J. F., Cooper, N. S., Healey, L. A., Kaplan, S. R., Liang, M. H., Luthra, H. S., & . 1988, The American Rheumatism Association 1987 revised criteria for the classification of rheumatoid arthritis, *Arthritis Rheum.*, 31(3):pp. 315-324.

Arroyo, A. G., Taverna, D., Whittaker, C. A., Strauch, U. G., Bader, B. L., Rayburn, H., Crowley, D., Parker, C. M., & Hynes, R. O. 2000, In vivo roles of integrins during leukocyte development and traffic: insights from the analysis of mice chimeric for alpha 5, alpha v, and alpha 4 integrins, *J.Immunol.*, 165(8):pp. 4667-4675.

Arzu, G. E., Aras, G., Kucuk, O., Atay, G., Tutak, I., Ataman, S., Soylu, A., & Ibis, E. 2003, Comparison of Tc-99m HIG and three-phase Tc-99m MDP bone scintigraphy for evaluating the efficacy of Yttrium-90 silicate radionuclide synovectomy, *Clin.Nucl.Med.*, 28(4):pp. 277-285.

Aumailley, M., Gurrath, M., Muller, G., Calvete, J., Timpl, R., & Kessler, H. 1991, Arg-Gly-Asp constrained within cyclic pentapeptides. Strong and selective inhibitors of cell adhesion to vitronectin and laminin fragment P1, *FEBS Lett.*, 291(1):pp. 50-54.

Backhaus, M., Burmester, G. R., Sandrock, D., Loreck, D., Hess, D., Scholz, A., Blind, S., Hamm, B., & Bollow, M. 2002, Prospective two year follow up study comparing novel and conventional imaging procedures in patients with arthritic finger joints, *Ann.Rheum.Dis.*, 61(10):pp. 895-904.

Backhaus, M., Kamradt, T., Sandrock, D., Loreck, D., Fritz, J., Wolf, K. J., Raber, H., Hamm, B., Burmester, G. R., & Bollow, M. 1999, Arthritis of the finger joints: a comprehensive approach comparing conventional radiography,

scintigraphy, ultrasound, and contrast-enhanced magnetic resonance imaging, *Arthritis & Rheumatism.*, 42(6):pp. 1232-1245.

Baekkevold, E. S., Yamanaka, T., Palframan, R. T., Carlsen, H. S., Reinholt, F. P., von Andrian, U. H., Brandtzaeg, P., & Haraldsen, G. 2001, The CCR7 ligand elc (CCL19) is transcytosed in high endothelial venules and mediates T cell recruitment, *J.Exp.Med.*, 193(9):pp. 1105-1112.

Baeten, D., Demetter, P., Cuvelier, C., Van den, B. F., Kruithof, E., Van Damme, N., Verbruggen, G., Mielants, H., Veys, E. M., & De Keyser, F. 2000, Comparative study of the synovial histology in rheumatoid arthritis, spondyloarthropathy, and osteoarthritis: influence of disease duration and activity, *Ann.Rheum.Dis.*, 59(12):pp. 945-953.

Bakker, A. C., van De Loo, F. A., Joosten, L. A., Bennink, M. B., Arntz, O. J., Dmitriev, I. P., Kashentsera, E. A., Curiel, D. T., & van den Berg, W. B. 2001, A tropism-modified adenoviral vector increased the effectiveness of gene therapy for arthritis, *Gene Therapy.*8(23):pp. 1785-93.

Ballara, S., Taylor, P. C., Reusch, P., Marme, D., Feldmann, M., Maini, R. N., & Paleolog, E. M. 2001, Raised serum vascular endothelial growth factor levels are associated with destructive change in inflammatory arthritis, *Arthritis & Rheumatism.*44(9): pp. 2055-64.

Barrera, P., Oyen, W. J., Boerman, O. C., & van Riel, P. L. 2003, Scintigraphic detection of tumour necrosis factor in patients with rheumatoid arthritis, *Annals of the Rheumatic Diseases.*, 62(9):pp. 825-828.

Barrera, P., van der Laken, C. J., Boerman, O. C., Oyen, W. J., van de Ven, M. T., van Lent, P. L., van de Putte, L. B., & Corstens, F. H. 2000, Radiolabelled interleukin-1 receptor antagonist for detection of synovitis in patients with rheumatoid arthritis, *Rheumatology.*, 39(8):pp. 870-874.

Bathon, J. M., Martin, R. W., Fleischmann, R. M., Tesser, J. R., Schiff, M. H., Keystone, E. C., Genovese, M. C., Wasko, M. C., Moreland, L. W., Weaver, A. L., Markenson, J., & Finck, B. K. 2000, A comparison of etanercept and methotrexate in patients with early rheumatoid arthritis, *N.Engl.J Med.*, 343(22):pp. 1586-1593.

Beckers, C., Ribbens, C., Andre, B., Marcelis, S., Kaye, O., Mathy, L., Kaiser, M. J., Hustinx, R., Foidart, J., & Malaise, M. G. 2004, Assessment of disease activity in rheumatoid arthritis with (18)F-FDG PET, *J Nucl.Med.*, 45(6):pp. 956-964.

Berg, E. L., McEvoy, L. M., Berlin, C., Bargatze, R. F., & Butcher, E. C. 1993, L-selectin-mediated lymphocyte rolling on MAdCAM-1, *Nature,* 366(6456):pp. 695-698.

Berg, E. L., Yoshino, T., Rott, L. S., Robinson, M. K., Warnock, R. A., Kishimoto, T. K., Picker, L. J., & Butcher, E. C. 1991, The cutaneous lymphocyte

antigen is a skin lymphocyte homing receptor for the vascular lectin endothelial cell-leukocyte adhesion molecule 1, *Journal of Experimental Medicine.*, 174(6):pp. 1461-1466.

Berger, J. R. & Koralnik, I. J. 2005, Progressive multifocal leukoencephalopathy and natalizumab--unforeseen consequences, *N.Engl.J.Med.*, 353(4):pp. 414-416.

Bergstrom, U., Book, C., Lindroth, Y., Marsal, L., Saxne, T., & Jacobsson, L. 1999, Lower disease activity and disability in Swedish patients with rheumatoid arthritis in 1995 compared with 1978, *Scand.J Rheumatol.*, 28(3):pp. 160-165.

Berlin, C., Berg, E. L., Briskin, M. J., Andrew, D. P., Kilshaw, P. J., Holzmann, B., Weissman, I. L., Hamann, A., & Butcher, E. C. 1993, Alpha 4 beta 7 integrin mediates lymphocyte binding to the mucosal vascular addressin MAdCAM-1, *Cell*, 74(1):pp. 185-195.

Berna, L., Torres, G., Diez, C., Estorch, M., Martinez-Duncker, D., & Carrio, I. 1992, Technetium-99m human polyclonal immunoglobulin G studies and conventional bone scans to detect active joint inflammation in chronic rheumatoid arthritis, *Eur.J Nucl.Med.*, 19(3):pp. 173-176.

Bevilacqua, M. P., Pober, J. S., Mendrick, D. L., Cotran, R. S., & Gimbrone, M. A., Jr. 1987, Identification of an inducible endothelial-leukocyte adhesion molecule, *Proc.Natl.Acad.Sci.U.S.A*, 84(24):pp. 9238-9242.

Bhalgat, M. K., Haugland, R. P., Pollack, J. S., Swan, S., & Haugland, R. P. 1998, Green- and red-fluorescent nanospheres for the detection of cell surface receptors by flow cytometry, *J Immunol.Methods*, 219(1-2):pp. 57-68.

Binstadt, B. A., Patel, P. R., Alencar, H., Nigrovic, P. A., Lee, D. M., Mahmood, U., Weissleder, R., Mathis, D., & Benoist, C. 2006, Particularities of the vasculature can promote the organ specificity of autoimmune attack, *Nat.Immunol.*, 7(3):pp. 284-292.

Blades, M. C., Manzo, A., Ingegnoli, F., Taylor, P. R., Panayi, G. S., Irjala, H., Jalkanen, S., Haskard, D. O., Perretti, M., & Pitzalis, C. 2002, Stromal cell-derived factor 1 (CXCL12) induces human cell migration into human lymph nodes transplanted into SCID mice, *J.Immunol.*, 168(9):pp. 4308-4317.

Boerman, O. C., Oyen, W. J., Storm, G., Corvo, M. L., van, B. L., van der Meer, J. W., & Corstens, F. H. 1997, Technetium-99m labelled liposomes to image experimental arthritis, *Annals of the Rheumatic Diseases.*56(6):pp. 369-73.

Boers, M., Kostense, P. J., Verhoeven, A. C., & van der, L. S. 2001, Inflammation and damage in an individual joint predict further damage in that joint in patients with early rheumatoid arthritis, *Arthritis Rheum.*, 44(10):pp. 2242-2246.

Boers, M., Verhoeven, A. C., Markusse, H. M., van de Laar, M. A., Westhovens, R., van Denderen, J. C., van Zeben, D., Dijkmans, B. A., Peeters, A. J., Jacobs, P., van den Brink, H. R., Schouten, H. J., van der Heijde, D. M., Boonen, A., & van

der, L. S. 1997, Randomised comparison of combined step-down prednisolone, methotrexate and sulphasalazine with sulphasalazine alone in early rheumatoid arthritis, *Lancet*, 350(9074):pp. 309-318.

Bogdanowich-Knipp, S. J., Chakrabarti, S., Williams, T. D., Dillman, R. K., & Siahaan, T. J. 1999, Solution stability of linear vs. cyclic RGD peptides, *J Pept.Res.*, 53(5):pp. 530-541.

Borges, E., Pendl, G., Eytner, R., Steegmaier, M., Zollner, O., & Vestweber, D. 1997, The binding of T cell-expressed P-selectin glycoprotein ligand-1 to E- and P-selectin is differentially regulated, *J.Biol.Chem.*, 272(45):pp. 28786-28792.

Borsum, T., Hagen, I., Henriksen, T., & Carlander, B. 1982, Alterations in the protein composition and surface structure of human endothelial cells during growth in primary culture, *Atherosclerosis*, 44(3):pp. 367-378.

Bosma, G. C., Custer, R. P., & Bosma, M. J. 1983, A severe combined immunodeficiency mutation in the mouse, *Nature*, 301(5900):pp. 527-530.

Boturyn, D., Coll, J. L., Garanger, E., Favrot, M. C., & Dumy, P. 2004, Template assembled cyclopeptides as multimeric system for integrin targeting and endocytosis, *J Am Chem.Soc.*, 126(18):pp. 5730-5739.

Bracci, L., Falciani, C., Lelli, B., Lozzi, L., Runci, Y., Pini, A., De Montis, M. G., Tagliamonte, A., & Neri, P. 2003, Synthetic peptides in the form of dendrimers become resistant to protease activity, *J Biol.Chem.*, 278(47):pp. 46590-46595.

Breeman, W. A., Kwekkeboom, D. J., Kooij, P. P., Bakker, W. H., Hofland, L. J., Visser, T. J., Ensing, G. J., Lamberts, S. W., & Krenning, E. P. 1995, Effect of dose and specific activity on tissue distribution of indium-111-pentetreotide in rats, *J.Nucl.Med.*, 36(4):pp. 623-627.

Brentano, F., Schorr, O., Gay, R. E., Gay, S., & Kyburz, D. 2005, RNA released from necrotic synovial fluid cells activates rheumatoid arthritis synovial fibroblasts via Toll-like receptor 3, *Arthritis Rheum.*, 52(9):pp. 2656-2665.

Bresnihan, B. & Cobby, M. 2003, Clinical and radiological effects of anakinra in patients with rheumatoid arthritis, *Rheumatology (Oxford)*, 42 Suppl 2:p. ii22-ii28.

Brinckerhoff, C. E. & Harris, E. D., Jr. 1981, Survival of rheumatoid synovium implanted into nude mice, *Am.J.Pathol.*, 103(3):pp. 411-419.

Brooks, P. C., Stromblad, S., Klemke, R., Visscher, D., Sarkar, F. H., & Cheresh, D. A. 1995, Antiintegrin alpha v beta 3 blocks human breast cancer growth and angiogenesis in human skin, *J Clin.Invest*, 96(4):pp. 1815-1822.

Brower, A. C. 1990, Use of the radiograph to measure the course of rheumatoid arthritis. The gold standard versus fool's gold, *Arthritis Rheum.*, 33(3):pp. 316-324.

Brown, A. K., Conaghan, P. G., Karim, Z., Quinn, M. A., Ikeda, K., Peterfy, C. G., Hensor, E., Wakefield, R. J., O'Connor, P. J., & Emery, P. 2008, An explanation for the apparent dissociation between clinical remission and continued structural deterioration in rheumatoid arthritis, *Arthritis Rheum.*, 58(10):pp. 2958-2967.

Brown, A. K., Quinn, M. A., Karim, Z., Conaghan, P. G., Peterfy, C. G., Hensor, E., Wakefield, R. J., O'Connor, P. J., & Emery, P. 2006, Presence of significant synovitis in rheumatoid arthritis patients with disease-modifying antirheumatic drug-induced clinical remission: Evidence from an imaging study may explain structural progression, *Arthritis Rheum.*, 54(12):pp. 3761-3773.

Bruehl, R. E., Moore, K. L., Lorant, D. E., Borregaard, N., Zimmerman, G. A., McEver, R. P., & Bainton, D. F. 1997, Leukocyte activation induces surface redistribution of P-selectin glycoprotein ligand-1, *J.Leukoc.Biol.*, 61(4):pp. 489-499.

Bruehl, R. E., Springer, T. A., & Bainton, D. F. 1996, Quantitation of L-selectin distribution on human leukocyte microvilli by immunogold labelling and electron microscopy, *J.Histochem.Cytochem.*, 44(8):pp. 835-844.

Butler, S. R., Lam, R. W., & Fisher, D. A. 1984, Iodination of thyroliberin by use of Iodogen, *Clin.Chem.*, 30(4):pp. 547-548.

Campbell, D. J. & Butcher, E. C. 2002, Rapid acquisition of tissue-specific homing phenotypes by CD4(+) T cells activated in cutaneous or mucosal lymphoid tissues, *J.Exp.Med.*, 195(1):pp. 135-141.

Campbell, J. J., Haraldsen, G., Pan, J., Rottman, J., Qin, S., Ponath, P., Andrew, D. P., Warnke, R., Ruffing, N., Kassam, N., Wu, L., & Butcher, E. C. 1999, The chemokine receptor CCR4 in vascular recognition by cutaneous but not intestinal memory T cells, *Nature*, 400(6746):pp. 776-780.

Campbell, J. J., Hedrick, J., Zlotnik, A., Siani, M. A., Thompson, D. A., & Butcher, E. C. 1998, Chemokines and the arrest of lymphocytes rolling under flow conditions, *Science*, 279(5349):pp. 381-384.

Campbell, J. J., Murphy, K. E., Kunkel, E. J., Brightling, C. E., Soler, D., Shen, Z., Boisvert, J., Greenberg, H. B., Vierra, M. A., Goodman, S. B., Genovese, M. C., Wardlaw, A. J., Butcher, E. C., & Wu, L. 2001, CCR7 expression and memory T cell diversity in humans, *J.Immunol.*, 166(2):pp. 877-884.

Campbell, J. J., O'Connell, D. J., & Wurbel, M. A. 2007, Cutting Edge: Chemokine receptor CCR4 is necessary for antigen-driven cutaneous accumulation of CD4 T cells under physiological conditions, *Journal of Immunology.*178(6):pp. 3358-62.

Campbell, J. J., Qin, S., Bacon, K. B., MacKay, C. R., & Butcher, E. C. 1996, Biology of chemokine and classical chemoattractant receptors: differential

requirements for adhesion-triggering versus chemotactic responses in lymphoid cells, *J.Cell Biol.*, 134(1):pp. 255-266.

Capell, H. 2002, Longterm maintenance therapy with disease modifying antirheumatic drugs, *J.Rheumatol.Suppl*, 66:pp. 38-43.

Carsons, S. 2001, Extra domain-positive fibronectins in arthritis: wolf in sheep's clothing?, *Rheumatology (Oxford)*, 40(7):pp. 721-723.

Carter, R. A. & Wicks, I. P. 2001, Vascular cell adhesion molecule 1 (CD106): a multifaceted regulator of joint inflammation. [Review] [133 refs], *Arthritis & Rheumatism.*44(5):pp.985-94.

Castel, S., Pagan, R., Mitjans, F., Piulats, J., Goodman, S., Jonczyk, A., Huber, F., Vilaro, S., & Reina, M. 2001, RGD peptides and monoclonal antibodies, antagonists of alpha(v)-integrin, enter the cells by independent endocytic pathways, *Lab Invest*, 81(12):pp. 1615-1626.

Cescato, R., Schulz, S., Waser, B., Eltschinger, V., Rivier, J. E., Wester, H. J., Culler, M., Ginj, M., Liu, Q., Schonbrunn, A., & Reubi, J. C. 2006, Internalization of sst2, sst3, and sst5 receptors: effects of somatostatin agonists and antagonists, *J.Nucl.Med.*, 47(3):pp. 502-511.

Champagne, B., Tremblay, P., Cantin, A., & St Pierre, Y. 1998, Proteolytic cleavage of ICAM-1 by human neutrophil elastase, *J.Immunol.*, 161(11):pp. 6398-6405.

Chang, C. H., Sharkey, R. M., Rossi, E. A., Karacay, H., McBride, W., Hansen, H. J., Chatal, J. F., Barbet, J., & Goldenberg, D. M. 2002, Molecular advances in pretargeting radioimunotherapy with bispecific antibodies, *Mol.Cancer Ther.*, 1(7):pp. 553-563.

Chen, X., Conti, P. S., & Moats, R. A. 2004, In vivo near-infrared fluorescence imaging of integrin alphavbeta3 in brain tumor xenografts, *Cancer Res.*, 64(21):pp. 8009-8014.

Chen, X., Liu, S., Hou, Y., Tohme, M., Park, R., Bading, J. R., & Conti, P. S. 2004a, MicroPET imaging of breast cancer alphav-integrin expression with 64Cu-labelled dimeric RGD peptides, *Mol.Imaging Biol.*, 6(5):pp. 350-359.

Chen, X., Park, R., Shahinian, A. H., Bading, J. R., & Conti, P. S. 2004b, Pharmacokinetics and tumor retention of 125I-labelled RGD peptide are improved by PEGylation, *Nucl.Med.Biol.*, 31(1):pp. 11-19.

Chen, X., Plasencia, C., Hou, Y., & Neamati, N. 2005, Synthesis and biological evaluation of dimeric RGD peptide-paclitaxel conjugate as a model for integrin-targeted drug delivery, *J Med.Chem.*, 48(4):pp. 1098-1106.

Cheng, Z., Wu, Y., Xiong, Z., Gambhir, S. S., & Chen, X. 2000, Near-infrared fluorescent RGD peptides for optical imaging of integrin alphavbeta3 expression in living mice, *Bioconjugate Chemistry.*16(6):pp. 1433-41

Choi, H. K., Hernan, M. A., Seeger, J. D., Robins, J. M., & Wolfe, F. 2002, Methotrexate and mortality in patients with rheumatoid arthritis: a prospective study, *Lancet*, 359(9313):pp. 1173-1177.

Chong, B. F., Murphy, J. E., Kupper, T. S., & Fuhlbrigge, R. C. 2004, E-selectin, thymus- and activation-regulated chemokine/CCL17, and intercellular adhesion molecule-1 are constitutively coexpressed in dermal microvessels: a foundation for a cutaneous immunosurveillance system, *J.Immunol.*, 172(3):pp. 1575-1581.

Choy, E. H., Hazleman, B., Smith, M., Moss, K., Lisi, L., Scott, D. G., Patel, J., Sopwith, M., & Isenberg, D. A. 2002, Efficacy of a novel PEGylated humanized anti-TNF fragment (CDP870) in patients with rheumatoid arthritis: a phase II double-blinded, randomized, dose-escalating trial, *Rheumatology.*41(10):pp. 1133-7.

Choy, E. H. & Panayi, G. S. 2001, Cytokine pathways and joint inflammation in rheumatoid arthritis, *N.Engl.J.Med.*, 344(12):pp. 907-916.

Cimmino, M. A., Innocenti, S., Livrone, F., Magnaguagno, F., Silvestri, E., & Garlaschi, G. 2003, Dynamic gadolinium-enhanced magnetic resonance imaging of the wrist in patients with rheumatoid arthritis can discriminate active from inactive disease, *Arthritis & Rheumatism.*, 48(5):pp. 1207-1213.

Cinamon, G., Shinder, V., & Alon, R. 2001, Shear forces promote lymphocyte migration across vascular endothelium bearing apical chemokines, *Nat.Immunol.*, 2(6):pp. 515-522.

Clark, E. R. & Clark, E. L. 1935, Observations on changes in blood vascular endothelium in the living animal, *Am.J.Anat.*, 57:pp. 385-438.

Clement, G., Bisoffi, M., Finger, A. N., Wetterwald, A., Thalmann, G. N., & Cecchini, M. G. 2003, Peptabodies as tools to test ligands isolated from phage-displayed peptide libraries, *J Immunol.Methods*, 276(1-2):pp. 135-141.

Cloutier, S. M., Couty, S., Terskikh, A., Marguerat, L., Crivelli, V., Pugnieres, M., Mani, J. C., Leisinger, H. J., Mach, J. P., & Deperthes, D. 2000, Streptabody, a high avidity molecule made by tetramerization of in vivo biotinylated, phage display-selected scFv fragments on streptavidin, *Mol.Immunol.*, 37(17):pp. 1067-1077.

Cohen, S. B., Emery, P., Greenwald, M. W., Dougados, M., Furie, R. A., Genovese, M. C., Keystone, E. C., Loveless, J. E., Burmester, G. R., Cravets, M. W., Hessey, E. W., Shaw, T., Totoritis, M. C., & REFLEX Trial Group 2006, Rituximab for rheumatoid arthritis refractory to anti-tumor necrosis factor therapy: Results of a multicenter, randomized, double-blind, placebo-controlled,

phase III trial evaluating primary efficacy and safety at twenty-four weeks, *Arthritis & Rheumatism.*54(9):pp. 2793-806.

Conti, F., Priori, R., Chimenti, M. S., Coari, G., Annovazzi, A., Valesini, G., & Signore, A. 2005, Successful treatment with intraarticular infliximab for resistant knee monarthritis in a patient with spondylarthropathy: a role for scintigraphy with 99mTc-infliximab, *Arthritis & Rheumatism.*52(4):pp. 1224-6.

Cooper, M. S., Sabbah, E., & Mather, S. J. 2006, Conjugation of chelating agents to proteins and radiolabelling with trivalent metallic isotopes, *Nat.Protocols*, 1(1):pp. 314-317.

Cooper, N. J. 2000, Economic burden of rheumatoid arthritis: a systematic review, *Rheumatology (Oxford)*, 39(1):pp. 28-33.

Crockett-Torabi, E. 1998, Selectins and mechanisms of signal transduction, *J.Leukoc.Biol.*, 63(1):pp. 1-14.

Curtis, J. R., Patkar, N., Xie, A., Martin, C., Allison, J. J., Saag, M., Shatin, D., & Saag, K. G. 2007, Risk of serious bacterial infections among rheumatoid arthritis patients exposed to tumor necrosis factor alpha antagonists, *Arthritis Rheum*, 56(4):pp. 1125-1133.

D'Ambrosio, D., Albanesi, C., Lang, R., Girolomoni, G., Sinigaglia, F., & Laudanna, C. 2002, Quantitative differences in chemokine receptor engagement generate diversity in integrin-dependent lymphocyte adhesion, *J.Immunol.*, 169(5):pp. 2303-2312.

D'Souza, S. E., Haas, T. A., Piotrowicz, R. S., Byers-Ward, V., McGrath, D. E., Soule, H. R., Cierniewski, C., Plow, E. F., & Smith, J. W. 1994, Ligand and cation binding are dual functions of a discrete segment of the integrin beta 3 subunit: cation displacement is involved in ligand binding, *Cell*, 79(4):pp. 659-667.

Dams, E. T., Oyen, W. J., Boerman, O. C., Storm, G., Laverman, P., Kok, P. J., Buijs, W. C., Bakker, H., van der Meer, J. W., & Corstens, F. H. 2000, 99mTc-PEG liposomes for the scintigraphic detection of infection and inflammation: clinical evaluation, *J Nucl.Med.*, 41(4):pp. 622-630.

Danen, E. H. & Sonnenberg, A. 2003, Integrins in regulation of tissue development and function, *J.Pathol.*, 200(4):pp. 471-480.

Dangerfield, J., Larbi, K. Y., Huang, M. T., Dewar, A., & Nourshargh, S. 2002a, PECAM-1 (CD31) homophilic interaction up-regulates alpha6beta1 on transmigrated neutrophils in vivo and plays a functional role in the ability of alpha6 integrins to mediate leukocyte migration through the perivascular basement membrane, *J.Exp.Med.*, 196(9):pp. 1201-1211.

Dangerfield, J., Larbi, K. Y., Huang, M. T., Dewar, A., & Nourshargh, S. 2002b, PECAM-1 (CD31) homophilic interaction up-regulates alpha6beta1 on

transmigrated neutrophils in vivo and plays a functional role in the ability of alpha6 integrins to mediate leukocyte migration through the perivascular basement membrane, *J.Exp.Med.*, 196(9):pp. 1201-1211.

De Bandt, M., Ben Mahdi, M. H., Ollivier, V., Grossin, M., Dupuis, M., Gaudry, M., Bohlen, P., Lipson, K. E., Rice, A., Wu, Y., Gougerot-Pocidalo, M. A., & Pasquier, C. 2003, Blockade of vascular endothelial growth factor receptor I (VEGF-RI), but not VEGF-RII, suppresses joint destruction in the K/BxN model of rheumatoid arthritis, *Journal of Immunology.*171(9):pp. 4853-9.

de Bois, M. H., Arndt, J. W., van, d., V, Pauwels, E. K., & Breedveld, F. C. 1994, Joint scintigraphy for quantification of synovitis with 99mTc-labelled human immunoglobulin G compared to late phase scintigraphy with 99mTc-labelled diphosphonate, *Br.J Rheumatol.*, 33(1):pp. 67-73.

de Bono, D. P. & Green, C. 1984, The adhesion of different cell types to cultured vascular endothelium: effects of culture density and age, *Br.J Exp.Pathol*, 65(1):pp. 145-154.

De Fougerolles, A. R., Stacker, S. A., Schwarting, R., & Springer, T. A. 1991, Characterization of ICAM-2 and evidence for a third counter-receptor for LFA-1, *J.Exp.Med.*, 174(1):pp. 253-267.

de Silva, M., Hazleman, B. L., Thomas, D. P., & Wraight, P. 1979, Liposomes in arthritis: a new approach, *Lancet*, 1(8130):pp. 1320-1322.

Decristoforo, C., Faintuch-Linkowski, B., Rey, A., von, G. E., Rupprich, M., Hernandez-Gonzales, I., Rodrigo, T., & Haubner, R. 2006, [99mTc]HYNIC-RGD for imaging integrin alphavbeta3 expression, *Nucl.Med.Biol.*, 33(8):pp. 945-952.

Decristoforo, C. & Mather, S. J. 1999a, Preparation, 99mTc-labelling, and in vitro characterization of HYNIC and N3S modified RC-160 and [Tyr3]octreotide, *Bioconjug.Chem.*, 10(3):pp. 431-438.

Decristoforo, C. & Mather, S. J. 1999b, 99m-Technetium-labelled peptide-HYNIC conjugates: effects of lipophilicity and stability on biodistribution, *Nucl.Med.Biol.*, 26(4):pp. 389-396.

DeGrendele, H. C., Estess, P., & Siegelman, M. H. 1997, Requirement for CD44 in activated T cell extravasation into an inflammatory site, *Science*, 278(5338):pp. 672-675.

Dennissen, M. A., Jenniskens, G. J., Pieffers, M., Versteeg, E. M., Petitou, M., Veerkamp, J. H., & van Kuppevelt, T. H. 2002, Large, tissue-regulated domain diversity of heparan sulfates demonstrated by phage display antibodies, *J Biol.Chem.*, 277(13):pp. 10982-10986.

Desmetz, C., Lin, Y. L., Mettling, C., Portales, P., Noel, D., Clot, J., Jorgensen, C., & Corbeau, P. 2007, Cell surface CCR5 density determines the intensity of T

cell migration towards rheumatoid arthritis synoviocytes, *Clinical Immunology.*123(2):pp. 148-54.

Deveci, D. & Egginton, S. 1999, Development of the fluorescent microsphere technique for quantifying regional blood flow in small mammals, *Exp.Physiol*, 84(4):pp. 615-630.

Devlin, J. J., Panganiban, L. C., & Devlin, P. E. 1990, Random peptide libraries: a source of specific protein binding molecules, *Science*, 249(4967):pp. 404-406.

Diamond, M. S., Alon, R., Parkos, C. A., Quinn, M. T., & Springer, T. A. 1995, Heparin is an adhesive ligand for the leukocyte integrin Mac-1 (CD11b/CD1), *J Cell Biol.*, 130(6):pp. 1473-1482.

Diamond, M. S., Staunton, D. E., Marlin, S. D., & Springer, T. A. 1991, Binding of the integrin Mac-1 (CD11b/CD18) to the third immunoglobulin-like domain of ICAM-1 (CD54) and its regulation by glycosylation, *Cell*, 65(6):pp. 961-971.

Dijkgraaf, I., Kruijtzer, J. A., Liu, S., Soede, A. C., Oyen, W. J., Corstens, F. H., Liskamp, R. M., & Boerman, O. C. 2007a, Improved targeting of the alpha(v)beta (3) integrin by multimerisation of RGD peptides, *Eur.J Nucl.Med.Mol.Imaging*, 34(2):pp. 267-273.

Dijkgraaf, I., Liu, S., Kruijtzer, J. A., Soede, A. C., Oyen, W. J., Liskamp, R. M., Corstens, F. H., & Boerman, O. C. 2007b, Effects of linker variation on the in vitro and in vivo characteristics of an (111)In-labelled RGD peptide, *Nucl.Med.Biol.*, 34(1):pp. 29-35.

Dohn, U. M., Ejbjerg, B. J., Court-Payen, Hasselquist, M., Narvestad, E., Szkudlarek, M., Moller, J. M., Thomsen, H. S., & Ostergaard, M. 2006, Are bone erosions detected by magnetic resonance imaging and ultrasonography true erosions? A comparison with computed tomography in rheumatoid arthritis metacarpophalangeal joints, *Arthritis Res.Ther.*, 8(4):p. R110.

Drossaers-Bakker, K. W., de Buck, M., van Zeben, D., Zwinderman, A. H., Breedveld, F. C., & Hazes, J. M. 1999, Long-term course and outcome of functional capacity in rheumatoid arthritis: the effect of disease activity and radiologic damage over time, *Arthritis Rheum.*, 42(9):pp. 1854-1860.

Dudda, J. C. & Martin, S. F. 2004, Tissue targeting of T cells by DCs and microenvironments, *Trends Immunol.*, 25(8):pp. 417-421.

Dudda, J. C., Simon, J. C., & Martin, S. 2004, Dendritic cell immunization route determines CD8+ T cell trafficking to inflamed skin: role for tissue microenvironment and dendritic cells in establishment of T cell-homing subsets, *J.Immunol.*, 172(2):pp. 857-863.

Duke, O., Panayi, G. S., Janossy, G., & Poulter, L. W. 1982b, An immunohistological analysis of lymphocyte subpopulations and their

microenvironment in the synovial membranes of patients with rheumatoid arthritis using monoclonal antibodies, *Clin.Exp.Immunol.*, 49(1):pp. 22-30.

Duke, O., Panayi, G. S., Janossy, G., & Poulter, L. W. 1982a, An immunohistological analysis of lymphocyte subpopulations and their microenvironment in the synovial membranes of patients with rheumatoid arthritis using monoclonal antibodies, *Clin.Exp.Immunol.*, 49(1):pp. 22-30.

Dulin, N. O., Sorokin, A., Reed, E., Elliott, S., Kehrl, J. H., & Dunn, M. J. 1999, RGS3 inhibits G protein-mediated signaling via translocation to the membrane and binding to Galpha11, *Mol.Cell Biol.*, 19(1):pp. 714-723.

Dvorak, H. F., Brown, L. F., Detmar, M., & Dvorak, A. M. 1995, Vascular permeability factor/vascular endothelial growth factor, microvascular hyperpermeability, and angiogenesis, *Am.J Pathol.*, 146(5):pp. 1029-1039.

Edwards, J. C. 2000, Fibroblast biology. Development and differentiation of synovial fibroblasts in arthritis, *Arthritis Res.*, 2(5):pp. 344-347.

Edwards, S. W. & Hallett, M. B. 1997, Seeing the wood for the trees: the forgotten role of neutrophils in rheumatoid arthritis, *Immunol.Today*, 18(7):pp. 320-324.

Ehirchiou, D., Xiong, Y. M., Li, Y., Brew, S., & Zhang, L. 2005, Dual function for a unique site within the beta2I domain of integrin alphaMbeta2, *J Biol.Chem.*, 280(9):pp. 8324-8331.

Ejbjerg, B. J., Vestergaard, A., Jacobsen, S., Thomsen, H., & Ostergaard, M. 2006, Conventional radiography requires a MRI-estimated bone volume loss of 20% to 30% to allow certain detection of bone erosions in rheumatoid arthritis metacarpophalangeal joints, *Arthritis Res.Ther.*, 8(3):p. R59.

Eliceiri, B. P. & Cheresh, D. A. 1999, The role of alphav integrins during angiogenesis: insights into potential mechanisms of action and clinical development, *J Clin.Invest*, 103(9):pp. 1227-1230.

Elices, M. J., Tsai, V., Strahl, D., Goel, A. S., Tollefson, V., Arrhenius, T., Wayner, E. A., Gaeta, F. C., Fikes, J. D., & Firestein, G. S. 1994, Expression and functional significance of alternatively spliced CS1 fibronectin in rheumatoid arthritis microvasculature, *J.Clin.Invest*, 93(1):pp. 405-416.

Ellegala, D. B., Leong-Poi, H., Carpenter, J. E., Klibanov, A. L., Kaul, S., Shaffrey, M. E., Sklenar, J., & Lindner, J. R. 2003, Imaging tumor angiogenesis with contrast ultrasound and microbubbles targeted to alpha(v)beta3, *Circulation.*108(3):pp. 336-41.

Ellerby, H. M., Arap, W., Ellerby, L. M., Kain, R., Andrusiak, R., Rio, G. D., Krajewski, S., Lombardo, C. R., Rao, R., Ruoslahti, E., Bredesen, D. E., & Pasqualini, R. 1999, Anti-cancer activity of targeted pro-apoptotic peptides, *Nat.Med.*, 5(9):pp. 1032-1038.

Elzinga, E. H., van der Laken, C. J., Comans, E. F., Lammertsma, A. A., Dijkmans, B. A., & Voskuyl, A. E. 2007, 2-Deoxy-2-[F-18]fluoro-D-glucose joint uptake on positron emission tomography images: rheumatoid arthritis versus osteoarthritis, *Molecular Imaging & Biology.*9(6):pp. 357-60

Emery, P., Fleischmann, R., Filipowicz-Sosnowska, A., Schechtman, J., Szczepanski, L., Kavanaugh, A., Racewicz, A. J., van Vollenhoven, R. F., Li, N. F., Agarwal, S., Hessey, E. W., Shaw, T. M., & DANCER Study Group 2006, The efficacy and safety of rituximab in patients with active rheumatoid arthritis despite methotrexate treatment: results of a phase IIB randomized, double-blind, placebo-controlled, dose-ranging trial.[see comment], *Arthritis & Rheumatism.*54(5):pp. 1390-400.

Endo, H., Akahoshi, T., Nishimura, A., Tonegawa, M., Takagishi, K., Kashiwazaki, S., Matsushima, K., & Kondo, H. 1994, Experimental arthritis induced by continuous infusion of IL-8 into rabbit knee joints, *Clin.Exp.Immunol.*, 96(1):pp. 31-35.

Engelhardt, B. & Wolburg, H. 2004, Mini-review: Transendothelial migration of leukocytes: through the front door or around the side of the house?, *Eur.J.Immunol.*, 34(11):pp. 2955-2963.

Epstein, W. V. 1996, Expectation bias in rheumatoid arthritis clinical trials. The anti-CD4 monoclonal antibody experience, *Arthritis Rheum.*, 39(11):pp. 1773-1780.

Essler, M. & Ruoslahti, E. 2002, Molecular specialization of breast vasculature: a breast-homing phage-displayed peptide binds to aminopeptidase P in breast vasculature, *Proceedings of the National Academy of Sciences of the United States of America.*, 99(4):pp. 2252-2257.

Fairburn, K., Kunaver, M., Wilkinson, L. S., Cambridge, G., Haskard, D., & Edwards, J. C. 1993, Intercellular adhesion molecules in normal synovium, *Br.J Rheumatol.*, 32(4):pp. 302-306.

Farragher, T. M., Lunt, M., Bunn, D. K., Silman, A. J., & Symmons, D. P. M. 2007, Early functional disability predicts both all-cause and cardiovascular mortality in people with inflammatory polyarthritis: Results from the Norfolk Arthritis Register, *Annals of the Rheumatic Diseases.Vol.66(4)()(pp 486-492), 2007.*(4):pp. 486-492.

Fava, R. A., Olsen, N. J., Spencer-Green, G., Yeo, K. T., Yeo, T. K., Berse, B., Jackman, R. W., Senger, D. R., Dvorak, H. F., & Brown, L. F. 1994, Vascular permeability factor/endothelial growth factor (VPF/VEGF): accumulation and expression in human synovial fluids and rheumatoid synovial tissue, *J.Exp.Med.*, 180(1):pp. 341-346.

Feldmann, M. & Maini, R. N. 2001, Anti-TNF alpha therapy of rheumatoid arthritis: what have we learned?, *Annu.Rev.Immunol.*, 19:pp. 163-196.

Fiehn, C., Muller-Ladner, U., Gay, S., Krienke, S., Freudenberg-Konrad, S., Funk, J., Ho, A. D., Sinn, H., & Wunder, A. 2004a, Albumin-coupled methotrexate (MTX-HSA) is a new anti-arthritic drug which acts synergistically to MTX, *Rheumatology (Oxford)*, 43(9):pp. 1097-1105.

Fiehn, C., Neumann, E., Wunder, A., Krienke, S., Gay, S., & Muller-Ladner, U. 2004b, Methotrexate (MTX) and albumin coupled with MTX (MTX-HSA) suppress synovial fibroblast invasion and cartilage degradation in vivo, *Ann.Rheum.Dis.*, 63(7):pp. 884-886.

Finckh, A., Ciurea, A., Brulhart, L., Kyburz, D., Moller, B., Dehler, S., Revaz, S., Dudler, J., Gabay, C., & Physicians of the Swiss Clinical Quality Management Program for Rheumatoid Arthritis 2007, B cell depletion may be more effective than switching to an alternative anti-tumor necrosis factor agent in rheumatoid arthritis patients with inadequate response to anti-tumor necrosis factor agents, *Arthritis & Rheumatism.*56(5):pp. 1417-23.

Finger, A. N., Bisoffi, M., Wetterwald, A., Gautschi, E., Hohenfeld, U., Klima, I., Stadler, B. M., Mazzucchelli, L., Thalmann, G. N., & Cecchini, M. G. 2002, Scavenger receptor block as strategy for the identification of bone marrow homing phages by panning in vivo random peptide phage displayed libraries, *J Immunol.Methods*, 264(1-2):pp. 173-186.

Firestein, G. S. 1998, "Rheumatoid synovitis and pannus," in *Rheumatology*, Second edn, J. A. Klippel & P. A. Dieppe, eds., Mosby, p. 13.1-13.24.

Fischer, C., Thiele, H. G., & Hamann, A. 1993, Lymphocyte-endothelial interactions in inflamed synovia: involvement of several adhesion molecules and integrin epitopes, *Scandinavian Journal of Immunology.*38(2):pp. 158-66.

FitzGerald, O., Soden, M., Yanni, G., Robinson, R., & Bresnihan, B. 1991, Morphometric analysis of blood vessels in synovial membranes obtained from clinically affected and unaffected knee joints of patients with rheumatoid arthritis, *Ann.Rheum.Dis.*, 50(11):pp. 792-796.

Forster, R., Schubel, A., Breitfeld, D., Kremmer, E., Renner-Muller, I., Wolf, E., & Lipp, M. 1999, CCR7 coordinates the primary immune response by establishing functional microenvironments in secondary lymphoid organs, *Cell*, 99(1):pp. 23-33.

Foxman, E. F., Campbell, J. J., & Butcher, E. C. 1997, Multistep navigation and the combinatorial control of leukocyte chemotaxis, *J.Cell Biol.*, 139(5):pp. 1349-1360.

Foxman, E. F., Kunkel, E. J., & Butcher, E. C. 1999, Integrating conflicting chemotactic signals. The role of memory in leukocyte navigation, *J.Cell Biol.*, 147(3):pp. 577-588.

Franklin, J., Lunt, M., Bunn, D., Symmons, D., & Silman, A. 2007, Influence of inflammatory polyarthritis on cancer incidence and survival: results from a community-based prospective study, *Arthritis Rheum.*, 56(3):pp. 790-798.

Freedman, F. B. & Johnson, J. A. 1969, Equilibrium and kinetic properties of the Evans blue-albumin system, *Am.J.Physiol*, 216(3):pp. 675-681.

Fuhlbrigge, R. C., Kieffer, J. D., Armerding, D., & Kupper, T. S. 1997, Cutaneous lymphocyte antigen is a specialized form of PSGL-1 expressed on skin-homing T cells, *Nature*, 389(6654):pp. 978-981.

Fulop, G. M. & Phillips, R. A. 1990, The scid mutation in mice causes a general defect in DNA repair, *Nature*, 347(6292):pp. 479-482.

Gabriel, M., Decristoforo, C., Donnemiller, E., Ulmer, H., Watfah, R. C., Mather, S. J., & Moncayo, R. 2003, An intrapatient comparison of 99mTc-EDDA/HYNIC-TOC with 111In-DTPA-octreotide for diagnosis of somatostatin receptor-expressing tumors, *J.Nucl.Med.*, 44(5):pp. 708-716.

Gabriel, S. E. 2001, The epidemiology of rheumatoid arthritis, *Rheum.Dis.Clin.North Am.*, 27(2):pp. 269-281.

Gabriel, S. E., Crowson, C. S., & O'Fallon, W. M. 1999, Mortality in rheumatoid arthritis: have we made an impact in 4 decades?, *J Rheumatol.*, 26(12):pp. 2529-2533.

Gahmberg, C. G., Tolvanen, M., & Kotovuori, P. 1997, Leukocyte adhesion--structure and function of human leukocyte beta2-integrins and their cellular ligands. [Review] [226 refs], *European Journal of Biochemistry.*245(2):pp. 215-32.

Galkina, E., Florey, O., Zarbock, A., Smith, B. R., Preece, G., Lawrence, M. B., Haskard, D. O., & Ager, A. 2007, T lymphocyte rolling and recruitment into peripheral lymph nodes is regulated by a saturable density of L-selectin (CD62L), *European Journal of Immunology.*37(5):pp. 1243-53.

Ganpule, G., Knorr, R., Miller, J. M., Carron, C. P., & Dustin, M. L. 1997, Low affinity of cell surface lymphocyte function-associated antigen-1 (LFA-1) generates selectivity for cell-cell interactions, *J.Immunol.*, 159(6):pp. 2685-2692.

Garanger, E., Boturyn, D., Coll, J. L., Favrot, M. C., & Dumy, P. 2006, Multivalent RGD synthetic peptides as potent alphaVbeta3 integrin ligands, *Org.Biomol.Chem.*, 4(10):pp. 1958-1965.

Garanger, E., Boturyn, D., Jin, Z., Dumy, P., Favrot, M. C., & Coll, J. L. 2005, New multifunctional molecular conjugate vector for targeting, imaging, and therapy of tumors, *Mol.Ther.*, 12(6):pp. 1168-1175.

Garrood, T. & Scott, D. L. 2001, Combination therapy with disease modifying anti-rheumatic drugs in rheumatoid arthritis, *BioDrugs.*, 15(8):pp. 543-561.

Geijtenbeek, T. B., Krooshoop, D. J., Bleijs, D. A., van Vliet, S. J., van Duijnhoven, G. C., Grabovsky, V., Alon, R., Figdor, C. G., & Van, K. Y. 2000, DC-SIGN-ICAM-2 interaction mediates dendritic cell trafficking, *Nat.Immunol.*, 1(4):pp. 353-357.

Genovese, M. C., Becker, J. C., Schiff, M., Luggen, M., Sherrer, Y., Kremer, J., Birbara, C., Box, J., Natarajan, K., Nuamah, I., Li, T., Aranda, R., Hagerty, D. T., & Dougados, M. 2005, Abatacept for rheumatoid arthritis refractory to tumor necrosis factor alpha inhibition, *N.Engl.J Med*, 353(11):pp. 1114-1123.

Genovese, M. C., Cohen, S., Moreland, L., Lium, D., Robbins, S., Newmark, R., & Bekker, P. 2004, Combination therapy with etanercept and anakinra in the treatment of patients with rheumatoid arthritis who have been treated unsuccessfully with methotrexate, *Arthritis Rheum.*, 50(5):pp. 1412-1419.

George, A. J., Lee, L., & Pitzalis, C. 2003, Isolating ligands specific for human vasculature using in vivo phage selection, *Trends Biotechnol.*, 21(5):pp. 199-203.

Gerlag, D. M., Borges, E., Tak, P. P., Ellerby, H. M., Bredesen, D. E., Pasqualini, R., Ruoslahti, E., & Firestein, G. S. 2001, Suppression of murine collagen-induced arthritis by targeted apoptosis of synovial neovasculature, *Arthritis Research.*, 3(6):pp. 357-361.

Gershman, B., Hoppin, J., Schramm, N., Lackas, C., & Norenberg, J. 2007, Evaluation of the quantification capabilities of a NanoSPECT/CT as a function of angular sampling, counting statistics, reconstruction parameters and the dynamic range of measured activity, *Society of Nuclear Medicine Annual Meeting Abstracts*, 48(MeetingAbstracts_2):pp. 433P-433a.

Gerszten, R. E., Garcia-Zepeda, E. A., Lim, Y. C., Yoshida, M., Ding, H. A., Gimbrone, M. A., Jr., Luster, A. D., Luscinskas, F. W., & Rosenzweig, A. 1999, MCP-1 and IL-8 trigger firm adhesion of monocytes to vascular endothelium under flow conditions, *Nature*, 398(6729):pp. 718-723.

Giebel, L. B., Cass, R. T., Milligan, D. L., Young, D. C., Arze, R., & Johnson, C. R. 1995, Screening of cyclic peptide phage libraries identifies ligands that bind streptavidin with high affinities, *Biochemistry*, 34(47):pp. 15430-15435.

Girard, J. P. & Springer, T. A. 1995, High endothelial venules (HEVs): specialized endothelium for lymphocyte migration, *Immunol.Today*, 16(9):pp. 449-457.

Gitlin, G., Bayer, E. A., & Wilchek, M. 1988, Studies on the biotin-binding site of streptavidin. Tryptophan residues involved in the active site, *Biochem.J.*, 256(1):pp. 279-282.

Gitlin, G., Bayer, E. A., & Wilchek, M. 1990, Studies on the biotin-binding sites of avidin and streptavidin. Tyrosine residues are involved in the binding site, *Biochem.J.*, 269(2):pp. 527-530.

Godfrey, H. P., Ilardi, C., Engber, W., & Graziano, F. M. 1984, Quantitation of human synovial mast cells in rheumatoid arthritis and other rheumatic diseases, *Arthritis Rheum.*, 27(8):pp. 852-856.

Goekoop-Ruiterman, Y. P., de Vries-Bouwstra, J. K., Allaart, C. F., van, Z. D., Kerstens, P. J., Hazes, J. M., Zwinderman, A. H., Ronday, H. K., Han, K. H., Westedt, M. L., Gerards, A. H., van Groenendael, J. H., Lems, W. F., van Krugten, M. V., Breedveld, F. C., & Dijkmans, B. A. 2005, Clinical and radiographic outcomes of four different treatment strategies in patients with early rheumatoid arthritis (the BeSt study): a randomized, controlled trial, *Arthritis Rheum.*, 52(11):pp. 3381-3390.

Goekoop-Ruiterman, Y. P., Vries-Bouwstra, J. K., Allaart, C. F., van Zeben, D., Kerstens, P. J., Hazes, J. M., Zwinderman, A. H., Peeters, A. J., Jonge-Bok, J. M., Mallee, C., de Beus, W. M., de Sonnaville, P. B., Ewals, J. A., Breedveld, F. C., & Dijkmans, B. A. 2007, Comparison of treatment strategies in early rheumatoid arthritis: a randomized trial.[see comment], *Annals of Internal Medicine.*146(6):pp. 406-15.

Goerres, G. W., Forster, A., Uebelhart, D., Seifert, B., Treyer, V., Michel, B., von Schulthess, G. K., & Kaim, A. H. 2006, F-18 FDG whole-body PET for the assessment of disease activity in patients with rheumatoid arthritis, *Clin.Nucl.Med.*, 31(7):pp. 386-390.

Goger, B., Halden, Y., Rek, A., Mosl, R., Pye, D., Gallagher, J., & Kungl, A. J. 2002, Different affinities of glycosaminoglycan oligosaccharides for monomeric and dimeric interleukin-8: a model for chemokine regulation at inflammatory sites, *Biochemistry*, 41(5):pp. 1640-1646.

Goldenberg, D. M., Sharkey, R. M., Paganelli, G., Barbet, J., & Chatal, J. F. 2006, Antibody pretargeting advances cancer radioimmunodetection and radioimmunotherapy, *J Clin.Oncol.*, 24(5):pp. 823-834.

Gordon, D. A. & Hastings, D. E. 1998, "Rheumatoid arthritis: clinical features of early, progressive and late disease.," in *Rheumatology*, 2 edn, J. H. Klippel & P. Dieppe, eds., Mosby, p. 3.1-3.14.

Gordon, K. B., Papp, K. A., Hamilton, T. K., Walicke, P. A., Dummer, W., Li, N., Bresnahan, B. W., & Menter, A. 2003, Efalizumab for patients with moderate to severe plaque psoriasis: a randomized controlled trial, *JAMA*, 290(23):pp. 3073-3080.

Gotthardt, M., Boermann, O. C., Behr, T. M., Behe, M. P., & Oyen, W. J. 2004, Development and clinical application of peptide-based radiopharmaceuticals, *Curr.Pharm Des*, 10(24):pp. 2951-2963.

Gowans, J. L. & Knight, E. J. 1964, The route of re-circulation of lymphocytes in the rat, *Proc.R.Soc.Lond B Biol.Sci.*, 159:pp. 257-282.

Grabovsky, V., Feigelson, S., Chen, C., Bleijs, D. A., Peled, A., Cinamon, G., Baleux, F., Arenzana-Seisdedos, F., Lapidot, T., van Kooyk, Y., Lobb, R. R., & Alon, R. 2000, Subsecond induction of alpha4 integrin clustering by immobilized chemokines stimulates leukocyte tethering and rolling on endothelial vascular cell adhesion molecule 1 under flow conditions, *J.Exp.Med.*, 192(4):pp. 495-506.

Gretz, J. E., Norbury, C. C., Anderson, A. O., Proudfoot, A. E., & Shaw, S. 2000, Lymph-borne chemokines and other low molecular weight molecules reach high endothelial venules via specialized conduits while a functional barrier limits access to the lymphocyte microenvironments in lymph node cortex, *J.Exp.Med.*, 192(10):pp. 1425-1440.

Grisar, J., Aletaha, D., Steiner, C. W., Kapral, T., Steiner, S., Saemann, M., Schwarzinger, I., Buranyi, B., Steiner, G., & Smolen, J. S. 2007, Endothelial progenitor cells in active rheumatoid arthritis: effects of tumour necrosis factor and glucocorticoid therapy, *Annals of the Rheumatic Diseases.*66(10):pp. 1284-8.

Grober, J. S., Bowen, B. L., Ebling, H., Athey, B., Thompson, C. B., Fox, D. A., & Stoolman, L. M. 1993, Monocyte-endothelial adhesion in chronic rheumatoid arthritis. In situ detection of selectin and integrin-dependent interactions.[see comment], *Journal of Clinical Investigation.*91(6):pp. 2609-19.

Grosios, K., Wood, J., Esser, R., Raychaudhuri, A., & Dawson, J. 2004, Angiogenesis inhibition by the novel VEGF receptor tyrosine kinase inhibitor, PTK787/ZK222584, causes significant anti-arthritic effects in models of rheumatoid arthritis, *Inflammation Research.*53(4):pp. 133-42.

Gunn, M. D., Tangemann, K., Tam, C., Cyster, J. G., Rosen, S. D., & Williams, L. T. 1998, A chemokine expressed in lymphoid high endothelial venules promotes the adhesion and chemotaxis of naive T lymphocytes, *Proc.Natl.Acad.Sci.U.S.A*, 95(1):pp. 258-263.

Gurrath, M., Muller, G., Kessler, H., Aumailley, M., & Timpl, R. 1992, Conformation/activity studies of rationally designed potent anti-adhesive RGD peptides, *Eur.J Biochem.*, 210(3):pp. 911-921.

Hamann, A., Andrew, D. P., Jablonski-Westrich, D., Holzmann, B., & Butcher, E. C. 1994, Role of alpha 4-integrins in lymphocyte homing to mucosal tissues in vivo, *J.Immunol.*, 152(7):pp. 3282-3293.

Hamm, C. W. 2003, Anti-integrin therapy. [Review] [32 refs], *Annual Review of Medicine.*54:pp. 425-35.

Han, S. W., Kim, G. W., Seo, J. S., Kim, S. J., Sa, K. H., Park, J. Y., Lee, J., Kim, S. Y., Goronzy, J. J., Weyand, C. M., & Kang, Y. M. 2004, VEGF gene polymorphisms and susceptibility to rheumatoid arthritis, *Rheumatology.*43(9):pp. 1173-7.

Han, W., Ding, P., Xu, M., Wang, L., Rui, M., Shi, S., Liu, Y., Zheng, Y., Chen, Y., Yang, T., & Ma, D. 2003, Identification of eight genes encoding chemokine-like factor superfamily members 1-8 (CKLFSF1-8) by in silico cloning and experimental validation, *Genomics*, 81(6):pp. 609-617.

Hansch, A., Frey, O., Hilger, I., Sauner, D., Haas, M., Schmidt, D., Kurrat, C., Gajda, M., Malich, A., Brauer, R., & Kaiser, W. A. 2004, Diagnosis of arthritis using near-infrared fluorochrome Cy5.5, *Invest Radiol.*, 39(10):pp. 626-632.

Hapke, S., Kessler, H., Arroyo, d. P., Benge, A., Schmitt, M., Lengyel, E., & Reuning, U. 2001, Integrin alpha(v)beta(3)/vitronectin interaction affects expression of the urokinase system in human ovarian cancer cells, *J.Biol.Chem.*, 276(28):pp. 26340-26348.

Harada, M., Mitsuyama, K., Yoshida, H., Sakisaka, S., Taniguchi, E., Kawaguchi, T., Ariyoshi, M., Saiki, T., Sakamoto, M., Nagata, K., Sata, M., Matsuo, K., & Tanikawa, K. 1998, Vascular endothelial growth factor in patients with rheumatoid arthritis, *Scandinavian Journal of Rheumatology.*27(5):pp. 377-80.

Haringman, J. J., Gerlag, D. M., Smeets, T. J., Baeten, D., Van den, B. F., Bresnihan, B., Breedveld, F. C., Dinant, H. J., Legay, F., Gram, H., Loetscher, P., Schmouder, R., Woodworth, T., & Tak, P. P. 2006a, A randomized controlled trial with an anti-CCL2 (anti-monocyte chemotactic protein 1) monoclonal antibody in patients with rheumatoid arthritis, *Arthritis & Rheumatism.*54(8):pp. 2387-92.

Haringman, J. J., Kraan, M. C., Smeets, T. J., Zwinderman, K. H., & Tak, P. P. 2003, Chemokine blockade and chronic inflammatory disease: proof of concept in patients with rheumatoid arthritis, *Ann.Rheum.Dis.*, 62(8):pp. 715-721.

Haringman, J. J., Ludikhuize, J., & Tak, P. P. 2004, Chemokines in joint disease: the key to inflammation?. [Review] [123 refs], *Annals of the Rheumatic Diseases.*63(10):pp. 1186-94.

Haringman, J. J., Smeets, T. J., Reinders-Blankert, P., & Tak, P. P. 2006b, Chemokine and chemokine receptor expression in paired peripheral blood mononuclear cells and synovial tissue of patients with rheumatoid arthritis, osteoarthritis, and reactive arthritis, *Annals of the Rheumatic Diseases.*65(3):pp. 294-300.

Harris, J. M. & Chess, R. B. 2003, Effect of PEGylation on pharmaceuticals, *Nature Reviews Drug Discovery*, 2:pp. 214-221.

Haubner, R., Wester, H. J., Burkhart, F., Senekowitsch-Schmidtke, R., Weber, W., Goodman, S. L., Kessler, H., & Schwaiger, M. 2001, Glycosylated RGD-containing peptides: tracer for tumor targeting and angiogenesis imaging with improved biokinetics, *J Nucl.Med.*, 42(2):pp. 326-336.

Haubner, R., Wester, H. J., Reuning, U., Senekowitsch-Schmidtke, R., Diefenbach, B., Kessler, H., Stocklin, G., & Schwaiger, M. 1999, Radiolabelled alpha(v)beta3 integrin antagonists: a new class of tracers for tumor targeting, *Journal of Nuclear Medicine.*40(6):pp. 1061-71.

Hautanen, A., Gailit, J., Mann, D. M., & Ruoslahti, E. 1989, Effects of modifications of the RGD sequence and its context on recognition by the fibronectin receptor, *J Biol.Chem.*, 264(3):pp. 1437-1442.

Hemmerich, S., Bistrup, A., Singer, M. S., van Zante, A., Lee, J. K., Tsay, D., Peters, M., Carminati, J. L., Brennan, T. J., Carver-Moore, K., Leviten, M., Fuentes, M. E., Ruddle, N. H., & Rosen, S. D. 2001, Sulfation of L-selectin ligands by an HEV-restricted sulfotransferase regulates lymphocyte homing to lymph nodes, *Immunity.*, 15(2):pp. 237-247.

Hench, P. S., Kendall, E. C., Slocumb, C. H., & Polley, H. F. 1950, Effects of cortisone acetate and pituitary ACTH on rheumatoid arthritis, rheumatic fever and certain other conditions, *Arch.Med.Interna*, 85(4):pp. 545-666.

Henderson, B. & Pettipher, E. R. 1989, Arthritogenic actions of recombinant IL-1 and tumour necrosis factor alpha in the rabbit: evidence for synergistic interactions between cytokines in vivo, *Clin.Exp.Immunol.*, 75(2):pp. 306-310.

Heppeler, A., Froidevaux, S., Eberle, A. N., & Maecke, H. R. 2000, Receptor targeting for tumor localisation and therapy with radiopeptides, *Curr.Med.Chem.*, 7(9):pp. 971-994.

Hidalgo, A., Peired, A. J., Wild, M. K., Vestweber, D., & Frenette, P. S. 2007, Complete identification of E-selectin ligands on neutrophils reveals distinct functions of PSGL-1, ESL-1, and CD44, *Immunity.*26(4):pp. 477-89.

Hillyer, P., Mordelet, E., Flynn, G., & Male, D. 2003, Chemokines, chemokine receptors and adhesion molecules on different human endothelia: discriminating the tissue-specific functions that affect leucocyte migration, *Clinical & Experimental Immunology.*134(3):pp. 431-41.

Hirata, T., Merrill-Skoloff, G., Aab, M., Yang, J., Furie, B. C., & Furie, B. 2000, P-Selectin glycoprotein ligand 1 (PSGL-1) is a physiological ligand for E-selectin in mediating T helper 1 lymphocyte migration, *J.Exp.Med.*, 192(11):pp. 1669-1676.

Hirohata, S. & Sakakibara, J. 1999, Angioneogenesis as a possible elusive triggering factor in rheumatoid arthritis, *Lancet*, 353(9161):p. 1331.

Hjelmstrom, P. 2001, Lymphoid neogenesis: de novo formation of lymphoid tissue in chronic inflammation through expression of homing chemokines, *J.Leukoc.Biol.*, 69(3):pp. 331-339.

Holig, P., Bach, M., Volkel, T., Nahde, T., Hoffmann, S., Muller, R., & Kontermann, R. E. 2004, Novel RGD lipopeptides for the targeting of liposomes

to integrin-expressing endothelial and melanoma cells, *Protein Eng Des Sel*, 17(5):pp. 433-441.

Homey, B., Alenius, H., Muller, A., Soto, H., Bowman, E. P., Yuan, W., McEvoy, L., Lauerma, A. I., Assmann, T., Bunemann, E., Lehto, M., Wolff, H., Yen, D., Marxhausen, H., To, W., Sedgwick, J., Ruzicka, T., Lehmann, P., & Zlotnik, A. 2002, CCL27-CCR10 interactions regulate T cell-mediated skin inflammation, *Nat.Med.*, 8(2):pp. 157-165.

Hu, D. D., Barbas, C. F., & Smith, J. W. 1996, An allosteric Ca2+ binding site on the beta3-integrins that regulates the dissociation rate for RGD ligands, *J Biol.Chem.*, 271(36):pp. 21745-21751.

Hubbard, A. K. & Rothlein, R. 2000, Intercellular adhesion molecule-1 (ICAM-1) expression and cell signaling cascades. [Review] [62 refs], *Free Radical Biology & Medicine.*28(9):pp. 1379-86.

Huber, L. C., Distler, O., Tarner, I., Gay, R. E., Gay, S., & Pap, T. 2006, Synovial fibroblasts: key players in rheumatoid arthritis. [Review] [100 refs], *Rheumatology.*45(6):pp. 669-75.

Humphries, J. D., Byron, A., & Humphries, M. J. 2006, Integrin ligands at a glance, *J Cell Sci*, 119(Pt 19):pp. 3901-3903.

Hurwitz, H., Fehrenbacher, L., Novotny, W., Cartwright, T., Hainsworth, J., Heim, W., Berlin, J., Baron, A., Griffing, S., Holmgren, E., Ferrara, N., Fyfe, G., Rogers, B., Ross, R., & Kabbinavar, F. 2004, Bevacizumab plus irinotecan, fluorouracil, and leucovorin for metastatic colorectal cancer, *N.Engl.J.Med.*, 350(23):pp. 2335-2342.

Iannone, M. A. & Consler, T. G. 2006, Effect of microsphere binding site density on the apparent affinity of an interaction partner, *Cytometry A*, 69(5):pp. 374-383.

Irvine, S., Munro, R., & Porter, D. 1999, Early referral, diagnosis, and treatment of rheumatoid arthritis: evidence for changing medical practice, *Ann.Rheum.Dis.*, 58(8):pp. 510-513.

Issekutz, A. C., Nakazato, S., & Issekutz, T. B. 2003, Differential roles of VLA-4(CD49d/CD29) and LFA-1(CD11a/CD18) integrins and E- and P-selectin during developing and established active or adoptively transferred adjuvant arthritis in the rat, *Immunol.Cell Biol.*, 81(5):pp. 397-408.

Iwata, M., Hirakiyama, A., Eshima, Y., Kagechika, H., Kato, C., & Song, S. Y. 2004, Retinoic acid imprints gut-homing specificity on T cells, *Immunity.*, 21(4):pp. 527-538.

Jackson, J. R., Minton, J. A., Ho, M. L., Wei, N., & Winkler, J. D. 1997, Expression of vascular endothelial growth factor in synovial fibroblasts is induced by hypoxia and interleukin 1beta, *Journal of Rheumatology.*24(7):pp. 1253-9.

Jacobsson, L. T., Turesson, C., Nilsson, J. A., Petersson, I. F., Lindqvist, E., Saxne, T., & Geborek, P. 2007, Treatment with TNF blockers and mortality risk in patients with rheumatoid arthritis, *Ann.Rheum.Dis.*, 66(5):pp. 670-675.

Jalkanen, S., Steere, A. C., Fox, R. I., & Butcher, E. C. 1986, A distinct endothelial cell recognition system that controls lymphocyte traffic into inflamed synovium, *Science*, 233(4763):pp. 556-558.

Jamar, F., Chapman, P. T., Manicourt, D. H., Glass, D. M., Haskard, D. O., & Peters, A. M. 1997, A comparison between 111In-anti-E-selectin mAb and 99Tcm-labelled human non-specific immunoglobulin in radionuclide imaging of rheumatoid arthritis, *Br.J.Radiol.*, 70(833):pp. 473-481.

Jamar, F., Houssiau, F. A., Devogelaer, J. P., Chapman, P. T., Haskard, D. O., Beaujean, V., Beckers, C., Manicourt, D. H., & Peters, A. M. 2002, Scintigraphy using a technetium 99m-labelled anti-E-selectin Fab fragment in rheumatoid arthritis, *Rheumatology.*, 41(1):pp. 53-61.

Jansen, L. M., van der Horst-Bruinsma IE, van, S. D., Bezemer, P. D., & Dijkmans, B. A. 2001, Predictors of radiographic joint damage in patients with early rheumatoid arthritis, *Ann.Rheum.Dis.*, 60(10):pp. 924-927.

Janssen, A. P., Schiffelers, R. M., ten Hagen, T. L., Koning, G. A., Schraa, A. J., Kok, R. J., Storm, G., & Molema, G. 2003, Peptide-targeted PEG-liposomes in anti-angiogenic therapy, *Int.J.Pharm.*, 254(1):pp. 55-58.

Jimenez-Boj, E., Nobauer-Huhmann, I., Hanslik-Schnabel, B., Dorotka, R., Wanivenhaus, A. H., Kainberger, F., Trattnig, S., Axmann, R., Tsuji, W., Hermann, S., Smolen, J., & Schett, G. 2007, Bone erosions and bone marrow edema as defined by magnetic resonance imaging reflect true bone marrow inflammation in rheumatoid arthritis, *Arthritis Rheum*, 56(4):pp. 1118-1124.

Johansson-Lindbom, B., Svensson, M., Wurbel, M. A., Malissen, B., Marquez, G., & Agace, W. 2003, Selective generation of gut tropic T cells in gut-associated lymphoid tissue (GALT): requirement for GALT dendritic cells and adjuvant, *J.Exp.Med.*, 198(6):pp. 963-969.

Johnson, B. A., Haines, G. K., Harlow, L. A., & Koch, A. E. 1993, Adhesion molecule expression in human synovial tissue, *Arthritis Rheum.*, 36(2):pp. 137-146.

Jois, R. N., Masding, A., Somerville, M., Gaffney, K., & Scott, D. G. 2007, Rituximab therapy in patients with resistant rheumatoid arthritis: real-life experience, *Rheumatology.*46(6):pp. 980-2.

Jones, J. L. & Walker, R. A. 1999, Integrins: a role as cell signalling molecules, *Mol.Pathol.*, 52(4):pp. 208-213.

Jorgensen, C., Couret, I., Canovas, F., Bologna, C., Brochier, J., Reme, T., Lipsky, P., & Sany, J. 1996, Mononuclear cell retention in rheumatoid synovial

tissue engrafted in severe combined immunodeficient (SCID) mice is up-regulated by tumour necrosis factor-alpha (TNF-alpha) and mediated through intercellular adhesion molecule-1 (ICAM-1), *Clin.Exp.Immunol.*, 106(1):pp. 20-25.

Jung, U., Norman, K. E., Scharffetter-Kochanek, K., Beaudet, A. L., & Ley, K. 1998, Transit time of leukocytes rolling through venules controls cytokine-induced inflammatory cell recruitment in vivo, *J.Clin.Invest*, 102(8):pp. 1526-1533.

Kadono, T., Venturi, G. M., Steeber, D. A., & Tedder, T. F. 2002, Leukocyte rolling velocities and migration are optimized by cooperative L-selectin and intercellular adhesion molecule-1 functions, *J.Immunol.*, 169(8):pp. 4542-4550.

Kantlehner, M., Schaffner, P., Finsinger, D., Meyer, J., Jonczyk, A., Diefenbach, B., Nies, B., Holzemann, G., Goodman, S. L., & Kessler, H. 2000, Surface coating with cyclic RGD peptides stimulates osteoblast adhesion and proliferation as well as bone formation, *Chembiochem.*, 1(2):pp. 107-114.

Kaplan, R. A., Curd, J. G., Deheer, D. H., Carson, D. A., Pangburn, M. K., Muller-Eberhard, H. J., & Vaughan, J. H. 1980, Metabolism of C4 and factor B in rheumatoid arthritis. Relation to rheumatoid factor, *Arthritis Rheum.*, 23(8):pp. 911-920.

Kavanaugh, A. F., Davis, L. S., Jain, R. I., Nichols, L. A., Norris, S. H., & Lipsky, P. E. 1996, A phase I/II open label study of the safety and efficacy of an anti-ICAM-1 (intercellular adhesion molecule-1; CD54) monoclonal antibody in early rheumatoid arthritis, *J.Rheumatol.*, 23(8):pp. 1338-1344.

Kaya, M., Tuna, H., Fatih, F. M., Tuna, F., Seren, G., & Necmi, Y. O. 2004, (99m)Tc-dextran scintigraphy to detect disease activity in patients with rheumatoid arthritis, *Nucl Med Commun.*, 25(6):pp. 597-601.

Keffer, J., Probert, L., Cazlaris, H., Georgopoulos, S., Kaslaris, E., Kioussis, D., & Kollias, G. 1991, Transgenic mice expressing human tumour necrosis factor: a predictive genetic model of arthritis, *EMBO J*, 10(13):pp. 4025-4031.

Kehoe, J. W. & Kay, B. K. 2005, Filamentous phage display in the new millennium, *Chem.Rev.*, 105(11):pp. 4056-4072.

Kelleher, D., Murphy, A., Hall, N., Omary, M. B., Kearns, G., Long, A., & Casey, E. B. 1995, Expression of CD44 on rheumatoid synovial fluid lymphocytes, *Ann.Rheum.Dis.*, 54(7):pp. 566-570.

Keystone, E. C., Kavanaugh, A. F., Sharp, J. T., Tannenbaum, H., Hua, Y., Teoh, L. S., Fischkoff, S. A., & Chartash, E. K. 2004, Radiographic, clinical, and functional outcomes of treatment with adalimumab (a human anti-tumor necrosis factor monoclonal antibody) in patients with active rheumatoid arthritis receiving concomitant methotrexate therapy: a randomized, placebo-controlled, 52-week trial, *Arthritis Rheum.*, 50(5):pp. 1400-1411.

Kiani, M. F., Yuan, H., Chen, X., Smith, L., Gaber, M. W., & Goetz, D. J. 2002, Targeting microparticles to select tissue via radiation-induced upregulation of endothelial cell adhesion molecules, *Pharm Res.*, 19(9):pp. 1317-1322.

Kikuta, A. & Rosen, S. D. 1994, Localization of ligands for L-selectin in mouse peripheral lymph node high endothelial cells by colloidal gold conjugates, *Blood*, 84(11):pp. 3766-3775.

Kim, C. H., Rott, L., Kunkel, E. J., Genovese, M. C., Andrew, D. P., Wu, L., & Butcher, E. C. 2001, Rules of chemokine receptor association with T cell polarization in vivo, *J.Clin.Invest*, 108(9):pp. 1331-1339.

King, M. A., Pretorius, P. H., Farncombe, T., & Beekman, F. J. 2002, Introduction to the physics of molecular imaging with radioactive tracers in small animals, *J.Cell Biochem.Suppl*, 39:pp. 221-230.

King, R. C., Surfraz, M. B., Biagini, S. C., Blower, P. J., & Mather, S. J. 2007, How do HYNIC-conjugated peptides bind technetium? Insights from LC-MS and stability studies, *Dalton Trans.*(43):pp. 4998-5007.

Kinne, R. W., Becker, W., Simon, G., Paganelli, G., Palombo-Kinne, E., Wolski, A., Bloch, S., Schwarz, A., Wolf, F., & Emmrich, F. 1993, Joint uptake and body distribution of a technetium-99m-labelled anti-rat-CD4 monoclonal antibody in rat adjuvant arthritis, *J.Nucl.Med.*, 34(1):pp. 92-98.

Kinne, R. W., Stuhlmuller, B., Palombo-Kinne, E., & Burmester, G. R. 2006, "The role of macrophages in rheumatoid arthritis," in *Rheumatoid Arthritis*, 2 edn, G. S. Firestein, G. Panayi, & F. A. Wollheim, eds., Oxford University Press, pp. 55-75.

Kirwan, J. R. 2004, The synovium in rheumatoid arthritis: evidence for (at least) two pathologies, *Arthritis Rheum.*, 50(1):pp. 1-4.

Kitayama, J., Carr, M. W., Roth, S. J., Buccola, J., & Springer, T. A. 1997, Contrasting responses to multiple chemotactic stimuli in transendothelial migration: heterologous desensitization in neutrophils and augmentation of migration in eosinophils, *J.Immunol.*, 158(5):pp. 2340-2349.

Klareskog, L., Stolt, P., Lundberg, K., Kallberg, H., Bengtsson, C., Grunewald, J., Ronnelid, J., Harris, H. E., Ulfgren, A. K., Rantapaa-Dahlqvist, S., Eklund, A., Padyukov, L., & Alfredsson, L. 2006, A new model for an etiology of rheumatoid arthritis: smoking may trigger HLA-DR (shared epitope)-restricted immune reactions to autoantigens modified by citrullination, *Arthritis Rheum.*, 54(1):pp. 38-46.

Klarlund, M., Ostergaard, M., Jensen, K. E., Madsen, J. L., Skjodt, H., & Lorenzen, I. 2000, Magnetic resonance imaging, radiography, and scintigraphy of the finger joints: one year follow up of patients with early arthritis. The TIRA Group, *Ann.Rheum.Dis.*, 59(7):pp. 521-528.

Klimiuk, P. A., Sierakowski, S., Latosiewicz, R., Cylwik, J. P., Cylwik, B., Skowronski, J., & Chwiecko, J. 2002, Soluble adhesion molecules (ICAM-1, VCAM-1, and E-selectin) and vascular endothelial growth factor (VEGF) in patients with distinct variants of rheumatoid synovitis, *Ann.Rheum.Dis.*, 61(9):pp. 804-809.

Kneilling, M., Hultner, L., Pichler, B. J., Mailhammer, R., Morawietz, L., Solomon, S., Eichner, M., Sabatino, J., Biedermann, T., Krenn, V., Weber, W. A., Illges, H., Haubner, R., & Rocken, M. 2007, Targeted mast cell silencing protects against joint destruction and angiogenesis in experimental arthritis in mice, *Arthritis Rheum.*, 56(6):pp. 1806-1816.

Koch, A. E., Halloran, M. M., Haskell, C. J., Shah, M. R., & Polverini, P. J. 1995a, Angiogenesis mediated by soluble forms of E-selectin and vascular cell adhesion molecule-1.[see comment], *Nature.*376(6540):pp. 517-9.

Koch, A. E., Kunkel, S. L., Burrows, J. C., Evanoff, H. L., Haines, G. K., Pope, R. M., & Strieter, R. M. 1991, Synovial tissue macrophage as a source of the chemotactic cytokine IL-8, *J Immunol.*, 147(7):pp. 2187-2195.

Koch, A. E., Kunkel, S. L., Shah, M. R., Hosaka, S., Halloran, M. M., Haines, G. K., Burdick, M. D., Pope, R. M., & Strieter, R. M. 1995b, Growth-related gene product alpha. A chemotactic cytokine for neutrophils in rheumatoid arthritis, *J Immunol.*, 155(7):pp. 3660-3666.

Koivunen, E., Wang, B., & Ruoslahti, E. 1995, Phage libraries displaying cyclic peptides with different ring sizes: ligand specificities of the RGD-directed integrins, *Biotechnology (N.Y.)*, 13(3):pp. 265-270.

Kok, R. J., Schraa, A. J., Bos, E. J., Moorlag, H. E., Asgeirsdottir, S. A., Everts, M., Meijer, D. K., & Molema, G. 2002, Preparation and functional evaluation of RGD-modified proteins as alpha(v)beta(3) integrin directed therapeutics, *Bioconjug.Chem.*, 13(1):pp. 128-135.

Kolonin, M. G., Saha, P. K., Chan, L., Pasqualini, R., & Arap, W. 2004, Reversal of obesity by targeted ablation of adipose tissue.[see comment], *Nature Medicine.*10(6):pp. 625-32.

Komoriya, A., Green, L. J., Mervic, M., Yamada, S. S., Yamada, K. M., & Humphries, M. J. 1991, The minimal essential sequence for a major cell type-specific adhesion site (CS1) within the alternatively spliced type III connecting segment domain of fibronectin is leucine-aspartic acid-valine, *J Biol.Chem.*, 266(23):pp. 15075-15079.

Koning, G. A., Schiffelers, R. M., Wauben, M. H., Kok, R. J., Mastrobattista, E., Molema, G., ten Hagen, T. L., & Storm, G. 2006, Targeting of angiogenic endothelial cells at sites of inflammation by dexamethasone phosphate-containing RGD peptide liposomes inhibits experimental arthritis, *Arthritis Rheum.*, 54(4):pp. 1198-1208.

Kornblihtt, A. R., Pesce, C. G., Alonso, C. R., Cramer, P., Srebrow, A., Werbajh, S., & Muro, A. F. 1996, The fibronectin gene as a model for splicing and transcription studies, *FASEB J*, 10(2):pp. 248-257.

Kotzin, B. L. & Kappler, J. 1998, Targeting the T cell receptor in rheumatoid arthritis, *Arthritis Rheum.*, 41(11):pp. 1906-1910.

Kraan, M. C., Versendaal, H., Jonker, M., Bresnihan, B., Post, W. J., Hart, B. A., Breedveld, F. C., & Tak, P. P. 1998, Asymptomatic synovitis precedes clinically manifest arthritis, *Arthritis Rheum.*, 41(8):pp. 1481-1488.

Krag, D. N., Shukla, G. S., Shen, G. P., Pero, S., Ashikaga, T., Fuller, S., Weaver, D. L., Burdette-Radoux, S., & Thomas, C. 2006, Selection of tumor-binding ligands in cancer patients with phage display libraries, *Cancer Res.*, 66(15):pp. 7724-7733.

Kremer, J. M., Westhovens, R., Leon, M., Di, G. E., Alten, R., Steinfeld, S., Russell, A., Dougados, M., Emery, P., Nuamah, I. F., Williams, G. R., Becker, J. C., Hagerty, D. T., & Moreland, L. W. 2003, Treatment of rheumatoid arthritis by selective inhibition of T-cell activation with fusion protein CTLA4Ig, *N.Engl.J Med.*, 349(20):pp. 1907-1915.

Krenning, E. P., Bakker, W. H., Kooij, P. P., Breeman, W. A., Oei, H. Y., de Jong, M., Reubi, J. C., Visser, T. J., Bruns, C., Kwekkeboom, D. J., & . 1992, Somatostatin receptor scintigraphy with indium-111-DTPA-D-Phe-1-octreotide in man: metabolism, dosimetry and comparison with iodine-123-Tyr-3-octreotide, *J.Nucl.Med.*, 33(5):pp. 652-658.

Kriegsmann, J., Berndt, A., Hansen, T., Borsi, L., Zardi, L., Brauer, R., Petrow, P. K., Otto, M., Kirkpatrick, C. J., Gay, S., & Kosmehl, H. 2004, Expression of fibronectin splice variants and oncofetal glycosylated fibronectin in the synovial membranes of patients with rheumatoid arthritis and osteoarthritis, *Rheum.Int.*, 24(1):pp. 25-33.

Kriegsmann, J., Keyszer, G. M., Geiler, T., Lagoo, A. S., Lagoo-Deenadayalan, S., Gay, R. E., & Gay, S. 1995, Expression of E-selectin messenger RNA and protein in rheumatoid arthritis, *Arthritis Rheum.*, 38(6):pp. 750-754.

Kunkel, E. J., Campbell, J. J., Haraldsen, G., Pan, J., Boisvert, J., Roberts, A. I., Ebert, E. C., Vierra, M. A., Goodman, S. B., Genovese, M. C., Wardlaw, A. J., Greenberg, H. B., Parker, C. M., Butcher, E. C., Andrew, D. P., & Agace, W. W. 2000, Lymphocyte CC chemokine receptor 9 and epithelial thymus-expressed chemokine (TECK) expression distinguish the small intestinal immune compartment: Epithelial expression of tissue-specific chemokines as an organizing principle in regional immunity, *J.Exp.Med.*, 192(5):pp. 761-768.

Laakkonen, P., Akerman, M. E., Biliran, H., Yang, M., Ferrer, F., Karpanen, T., Hoffman, R. M., & Ruoslahti, E. 2004, Antitumor activity of a homing peptide

that targets tumor lymphatics and tumor cells, *Proc.Natl.Acad.Sci.U.S.A*, 101(25):pp. 9381-9386.

Lacolley, P., Poitevin, P., Koen, R., & Levy, B. I. 1998, Different effects of calcium antagonists on fluid filtration of large arteries and albumin permeability in spontaneously hypertensive rats, *J.Hypertens.*, 16(3):pp. 349-355.

Ladner, R. C., Sato, A. K., Gorzelany, J., & de, S. M. 2004, Phage display-derived peptides as therapeutic alternatives to antibodies, *Drug Discov.Today*, 9(12):pp. 525-529.

Lally, F., Smith, E., Filer, A., Stone, M. A., Shaw, J. S., Nash, G. B., Buckley, C. D., & Rainger, G. E. 2005, A novel mechanism of neutrophil recruitment in a coculture model of the rheumatoid synovium, *Arthritis & Rheumatism.*52(11):pp. 3460-9.

Lanchbury, J. S. 1992, The HLA association with rheumatoid arthritis, *Clin.Exp.Rheumatol.*, 10(3):pp. 301-304.

Landewe, R. B., Boers, M., Verhoeven, A. C., Westhovens, R., van de Laar, M. A., Markusse, H. M., van Denderen, J. C., Westedt, M. L., Peeters, A. J., Dijkmans, B. A., Jacobs, P., Boonen, A., van der Heijde, D. M., & van der, L. S. 2002, COBRA combination therapy in patients with early rheumatoid arthritis: long-term structural benefits of a brief intervention, *Arthritis Rheum.*, 46(2):pp. 347-356.

Larsen, A., Dale, K., & Eek, M. 1977, Radiographic evaluation of rheumatoid arthritis and related conditions by standard reference films, *Acta Radiol.Diagn.(Stockh),* 18(4):pp. 481-491.

Lasky, H. P., Bauer, K., & Pope, R. M. 1988, Increased helper inducer and decreased suppressor inducer phenotypes in the rheumatoid joint, *Arthritis Rheum.*, 31(1):pp. 52-59.

Latour, F., Zabraniecki, L., Dromer, C., Brouchet, A., Durroux, R., & Fournie, B. 2001, Does vascular endothelial growth factor in the rheumatoid synovium predict joint destruction? A clinical, radiological, and pathological study in 12 patients monitored for 10 years, *Joint, Bone, Spine: Revue du Rhumatisme.*68(6):pp. 493-8.

Laudanna, C., Kim, J. Y., Constantin, G., & Butcher, E. 2002, Rapid leukocyte integrin activation by chemokines. [Review] [65 refs], *Immunological Reviews.*186:pp. 37-46.

Lee, L., Buckley, C., Blades, M. C., Panayi, G., George, A. J., & Pitzalis, C. 2002, Identification of synovium-specific homing peptides by in vivo phage display selection, *Arthritis Rheum.*, 46(8):pp. 2109-2120.

Lee, S. K., Bridges, S. L., Jr., Kirkham, P. M., Koopman, W. J., & Schroeder, H. W., Jr. 1994, Evidence of antigen receptor-influenced oligoclonal B lymphocyte

expansion in the synovium of a patient with longstanding rheumatoid arthritis, *J Clin.Invest*, 93(1):pp. 361-370.

Lee, S. S., Joo, Y. S., Kim, W. U., Min, D. J., Min, J. K., Park, S. H., Cho, C. S., & Kim, H. Y. 2001, Vascular endothelial growth factor levels in the serum and synovial fluid of patients with rheumatoid arthritis, *Clin.Exp.Rheumatol.*, 19(3):pp. 321-324.

Legler, D. F., Wiedle, G., Ross, F. P., & Imhof, B. A. 2001, Superactivation of integrin alphavbeta3 by low antagonist concentrations, *J Cell Sci*, 114(Pt 8):pp. 1545-1553.

Lehmann, J. C., Jablonski-Westrich, D., Haubold, U., Gutierrez-Ramos, J. C., Springer, T., & Hamann, A. 2003, Overlapping and selective roles of endothelial intercellular adhesion molecule-1 (ICAM-1) and ICAM-2 in lymphocyte trafficking, *Journal of Immunology.*171(5):pp. 2588-93.

Lejeune, F. J. 2002, Clinical use of TNF revisited: improving penetration of anti-cancer agents by increasing vascular permeability, *J.Clin.Invest*, 110(4):pp. 433-435.

Lemmon, C. A., Sniadecki, N. J., Ruiz, S. A., Tan, J. L., Romer, L. H., & Chen, C. S. 2005, Shear force at the cell-matrix interface: enhanced analysis for microfabricated post array detectors, *Mech.Chem.Biosyst.*, 2(1):pp. 1-16.

Levick, J. R. 1981, Permeability of rheumatoid and normal human synovium to specific plasma proteins, *Arthritis Rheum.*, 24(12):pp. 1550-1560.

Ley, K. 2003, Arrest chemokines, *Microcirculation.*, 10(3-4):pp. 289-295.

Ley, K. & Kansas, G. S. 2004, Selectins in T-cell recruitment to non-lymphoid tissues and sites of inflammation, *Nat.Rev.Immunol.*, 4(5):pp. 325-335.

Li, Z. 1999, The alphaMbeta2 integrin and its role in neutrophil function, *Cell Res.*, 9(3):pp. 171-178.

Lindqvist, E., Jonsson, K., Saxne, T., & Eberhardt, K. 2003, Course of radiographic damage over 10 years in a cohort with early rheumatoid arthritis, *Ann.Rheum.Dis.*, 62(7):pp. 611-616.

Lipsky, P. E., van der Heijde, D. M., St Clair, E. W., Furst, D. E., Breedveld, F. C., Kalden, J. R., Smolen, J. S., Weisman, M., Emery, P., Feldmann, M., Harriman, G. R., & Maini, R. N. 2000, Infliximab and methotrexate in the treatment of rheumatoid arthritis. Anti-Tumor Necrosis Factor Trial in Rheumatoid Arthritis with Concomitant Therapy Study Group, *N.Engl.J Med.*, 343(22):pp. 1594-1602.

Lishko, V. K., Podolnikova, N. P., Yakubenko, V. P., Yakovlev, S., Medved, L., Yadav, S. P., & Ugarova, T. P. 2004, Multiple binding sites in fibrinogen for integrin alphaMbeta2 (Mac-1), *J Biol.Chem.*, 279(43):pp. 44897-44906.

Lishko, V. K., Yakubenko, V. P., & Ugarova, T. P. 2003, The interplay between integrins alphaMbeta2 and alpha5beta1 during cell migration to fibronectin, *Experimental Cell Research.*283(1):pp. 116-26.

Liu, S. 2006, Radiolabelled multimeric cyclic RGD peptides as integrin alphavbeta3 targeted radiotracers for tumor imaging, *Mol.Pharm*, 3(5):pp. 472-487.

Liu, S. & Edwards, D. S. 2001, Bifunctional chelators for therapeutic lanthanide radiopharmaceuticals, *Bioconjug.Chem.*, 12(1):pp. 7-34.

Liu, S., Edwards, D. S., & Barrett, J. A. 1997, 99mTc labelling of highly potent small peptides, *Bioconjug.Chem.*, 8(5):pp. 621-636.

Lode, J., Fichtner, I., Kreuter, J., Berndt, A., Diederichs, J. E., & Reszka, R. 2001, Influence of surface-modifying surfactants on the pharmacokinetic behavior of 14C-poly (methylmethacrylate) nanoparticles in experimental tumor models, *Pharm.Res.*, 18(11):pp. 1613-1619.

Loetscher, P. & Clark-Lewis, I. 2001, Agonistic and antagonistic activities of chemokines, *J.Leukoc.Biol.*, 69(6):pp. 881-884.

Loetscher, P. & Moser, B. 2002, Homing chemokines in rheumatoid arthritis, *Arthritis Res.*, 4(4):pp. 233-236.

Lopez, S., Halbwachs-Mecarelli, L., Ravaud, P., Bessou, G., Dougados, M., & Porteu, F. 1995, Neutrophil expression of tumour necrosis factor receptors (TNF-R) and of activation markers (CD11b, CD43, CD63) in rheumatoid arthritis, *Clinical & Experimental Immunology.*101(1):pp. 25-32.

Lowe, J. B. 2002, Glycosylation in the control of selectin counter-receptor structure and function, *Immunol.Rev.*, 186:pp. 19-36.

MacDougall, J. R., Croy, B. A., Chapeau, C., & Clark, D. A. 1990, Demonstration of a splenic cytotoxic effector cell in mice of genotype SCID/SCID.BG/BG, *Cell Immunol.*, 130(1):pp. 106-117.

MacGregor, A. J., Snieder, H., Rigby, A. S., Koskenvuo, M., Kaprio, J., Aho, K., & Silman, A. J. 2000, Characterizing the quantitative genetic contribution to rheumatoid arthritis using data from twins, *Arthritis Rheum.*, 43(1):pp. 30-37.

Mackay, C. R. 1993, Homing of naive, memory and effector lymphocytes, *Curr.Opin.Immunol.*, 5(3):pp. 423-427.

Maeda, H., Fang, J., Inutsuka, T., & Kitamoto, Y. 2003, Vascular permeability enhancement in solid tumor: various factors, mechanisms involved and its implications, *Int.Immunopharmacol.*, 3(3):pp. 319-328.

Maini, R. N., Breedveld, F. C., Kalden, J. R., Smolen, J. S., Furst, D., Weisman, M. H., St Clair, E. W., Keenan, G. F., van der, H. D., Marsters, P. A., & Lipsky,

P. E. 2004, Sustained improvement over two years in physical function, structural damage, and signs and symptoms among patients with rheumatoid arthritis treated with infliximab and methotrexate, *Arthritis Rheum.*, 50(4):pp. 1051-1065.

Mammen, M., Choi, S., & Whitesides, G. M. 1998, Polyvalent interactions in biological systems: implications for desing and use of multivalent ligands and inhibitors, *Agnew.Chem.Int.Ed.*, 37:pp. 2754-2794.

Mantey, S., Frucht, H., Coy, D. H., & Jensen, R. T. 1993, Characterization of bombesin receptors using a novel, potent, radiolabelled antagonist that distinguishes bombesin receptor subtypes, *Mol.Pharmacol.*, 43(5):pp. 762-774.

Manzo, A., Paoletti, S., Carulli, M., Blades, M. C., Barone, F., Yanni, G., FitzGerald, O., Bresnihan, B., Caporali, R., Montecucco, C., Uguccioni, M., & Pitzalis, C. 2005, Systematic microanatomical analysis of CXCL13 and CCL21 in situ production and progressive lymphoid organization in rheumatoid synovitis, *Eur.J.Immunol.*, 35(5):pp. 1347-1359.

Marsden, P. & Sutcliffe-Goulden, J. 2000, Principles and technology of PET scanning, *Nucl.Med.Commun.*, 21(3):pp. 221-224.

Marshall, D. & Haskard, D. O. 2002, Clinical overview of leukocyte adhesion and migration: where are we now?. [Review] [78 refs], *Seminars in Immunology.*, 14(2):pp. 133-140.

Marttila-Ichihara, F., Smith, D. J., Stolen, C., Yegutkin, G. G., Elima, K., Mercier, N., Kiviranta, R., Pihlavisto, M., Alaranta, S., Pentikainen, U., Pentikainen, O., Fulop, F., Jalkanen, S., & Salmi, M. 2006, Vascular amine oxidases are needed for leukocyte extravasation into inflamed joints in vivo, *Arthritis Rheum.*, 54(9):pp. 2852-2862.

McIntosh, E. 1996, The cost of rheumatoid arthritis, *Br.J.Rheumatol.*, 35(8):pp. 781-790.

McLafferty, M. A., Kent, R. B., Ladner, R. C., & Markland, W. 1993, M13 bacteriophage displaying disulfide-constrained microproteins, *Gene*, 128(1):pp. 29-36.

McQueen, F. M., Benton, N., Crabbe, J., Robinson, E., Yeoman, S., McLean, L., & Stewart, N. 2001, What is the fate of erosions in early rheumatoid arthritis? Tracking individual lesions using x rays and magnetic resonance imaging over the first two years of disease, *Annals of the Rheumatic Diseases.*, 60(9):pp. 859-868.

McQueen, F. M., Benton, N., Perry, D., Crabbe, J., Robinson, E., Yeoman, S., McLean, L., & Stewart, N. 2003, Bone edema scored on magnetic resonance imaging scans of the dominant carpus at presentation predicts radiographic joint damage of the hands and feet six years later in patients with rheumatoid arthritis, *Arthritis & Rheumatism.*, 48(7):pp. 1814-1827.

McQueen, F. M., Stewart, N., Crabbe, J., Robinson, E., Yeoman, S., Tan, P. L., & McLean, L. 1999, Magnetic resonance imaging of the wrist in early rheumatoid arthritis reveals progression of erosions despite clinical improvement, *Ann.Rheum.Dis.*, 58(3):pp. 156-163.

Meisetschlager, G., Poethko, T., Stahl, A., Wolf, I., Scheidhauer, K., Schottelius, M., Herz, M., Wester, H. J., & Schwaiger, M. 2006, Gluc-Lys([18F]FP)-TOCA PET in patients with SSTR-positive tumors: biodistribution and diagnostic evaluation compared with [111In]DTPA-octreotide, *J.Nucl.Med.*, 47(4):pp. 566-573.

Metselaar, J. M., van den Berg, W. B., Holthuysen, A. E., Wauben, M. H., Storm, G., & van Lent, P. L. 2004, Liposomal targeting of glucocorticoids to synovial lining cells strongly increases therapeutic benefit in collagen type II arthritis, *Annals of the Rheumatic Diseases*.63(4):pp. 348-53.

Metselaar, J. M., Wauben, M. H., Wagenaar-Hilbers, J. P., Boerman, O. C., & Storm, G. 2003, Complete remission of experimental arthritis by joint targeting of glucocorticoids with long-circulating liposomes, *Arthritis & Rheumatism.*, 48(7):pp. 2059-2066.

Middleton, J., Americh, L., Gayon, R., Julien, D., Aguilar, L., Amalric, F., & Girard, J. P. 2004, Endothelial cell phenotypes in the rheumatoid synovium: activated, angiogenic, apoptotic and leaky. [Review] [148 refs], *Arthritis Research & Therapy*.6(2):pp. 60-72.

Middleton, J., Neil, S., Wintle, J., Clark-Lewis, I., Moore, H., Lam, C., Auer, M., Hub, E., & Rot, A. 1997, Transcytosis and surface presentation of IL-8 by venular endothelial cells, *Cell*, 91(3):pp. 385-395.

Middleton, J., Patterson, A. M., Gardner, L., Schmutz, C., & Ashton, B. A. 2002, Leukocyte extravasation: chemokine transport and presentation by the endothelium. [Review] [107 refs], *Blood.*, 100(12):pp. 3853-3860.

Mikecz, K., Dennis, K., Shi, M., & Kim, J. H. 1999, Modulation of hyaluronan receptor (CD44) function in vivo in a murine model of rheumatoid arthritis, *Arthritis Rheum.*, 42(4):pp. 659-668.

Mochizuki, T., Tsukamoto, E., Kuge, Y., Kanegae, K., Zhao, S., Hikosaka, K., Hosokawa, M., Kohanawa, M., & Tamaki, N. 2001, FDG uptake and glucose transporter subtype expressions in experimental tumor and inflammation models, *J Nucl.Med.*, 42(10):pp. 1551-1555.

Mohamadzadeh, M., DeGrendele, H., Arizpe, H., Estess, P., & Siegelman, M. 1998, Proinflammatory stimuli regulate endothelial hyaluronan expression and CD44/HA-dependent primary adhesion, *J.Clin.Invest*, 101(1):pp. 97-108.

Molenaar, E. T., Voskuyl, A. E., Dinant, H. J., Bezemer, P. D., Boers, M., & Dijkmans, B. A. 2004, Progression of radiologic damage in patients with rheumatoid arthritis in clinical remission, *Arthritis Rheum.*, 50(1):pp. 36-42.

Molenaar, T. J., Appeldoorn, C. C., de Haas, S. A., Michon, I. N., Bonnefoy, A., Hoylaerts, M. F., Pannekoek, H., van Berkel, T. J., Kuiper, J., & Biessen, E. A. 2002, Specific inhibition of P-selectin-mediated cell adhesion by phage display-derived peptide antagonists, *Blood*, 100(10):pp. 3570-3577.

Mora, J. R., Bono, M. R., Manjunath, N., Weninger, W., Cavanagh, L. L., Rosemblatt, M., & von Andrian, U. H. 2003, Selective imprinting of gut-homing T cells by Peyer's patch dendritic cells, *Nature*, 424(6944):pp. 88-93.

Mora, J. R., Cheng, G., Picarella, D., Briskin, M., Buchanan, N., & von Andrian, U. H. 2005a, Reciprocal and dynamic control of CD8 T cell homing by dendritic cells from skin- and gut-associated lymphoid tissues, *J.Exp.Med.*, 201(2):pp. 303-316.

Mora, J. R., Cheng, G., Picarella, D., Briskin, M., Buchanan, N., & von Andrian, U. H. 2005b, Reciprocal and dynamic control of CD8 T cell homing by dendritic cells from skin- and gut-associated lymphoid tissues, *J.Exp.Med.*, 201(2):pp. 303-316.

Morales, J., Homey, B., Vicari, A. P., Hudak, S., Oldham, E., Hedrick, J., Orozco, R., Copeland, N. G., Jenkins, N. A., McEvoy, L. M., & Zlotnik, A. 1999, CTACK, a skin-associated chemokine that preferentially attracts skin-homing memory T cells, *Proc.Natl.Acad.Sci.U.S.A*, 96(25):pp. 14470-14475.

Moser, B., Wolf, M., Walz, A., & Loetscher, P. 2004, Chemokines: multiple levels of leukocyte migration control. [Review] [81 refs], *Trends in Immunology.*25(2):pp. 75-84.

Mosier, D. E., Stell, K. L., Gulizia, R. J., Torbett, B. E., & Gilmore, G. L. 1993, Homozygous scid/scid;beige/beige mice have low levels of spontaneous or neonatal T cell-induced B cell generation, *J.Exp.Med.*, 177(1):pp. 191-194.

Mottonen, T. T., Hannonen, P., Toivanen, J., Rekonen, A., & Oka, M. 1988, Value of joint scintigraphy in the prediction of erosiveness in early rheumatoid arthritis, *Ann.Rheum.Dis.*, 47(3):pp. 183-189.

Mulder, W. J., Strijkers, G. J., Habets, J. W., Bleeker, E. J., van der Schaft, D. W., Storm, G., Koning, G. A., Griffioen, A. W., & Nicolay, K. 2005, MR molecular imaging and fluorescence microscopy for identification of activated tumor endothelium using a bimodal lipidic nanoparticle, *FASEB Journal.*(14):pp. 2008-2010.

Muller, B., Zerwes, H. G., Tangemann, K., Peter, J., & Engel, J. 1993, Two-step binding mechanism of fibrinogen to alpha IIb beta 3 integrin reconstituted into planar lipid bilayers, *J Biol.Chem.*, 268(9):pp. 6800-6808.

Muller-Ladner, U., Elices, M. J., Kriegsmann, J. B., Strahl, D., Gay, R. E., Firestein, G. S., & Gay, S. 1997, Alternatively spliced CS-1 fibronectin isoform and its receptor VLA-4 in rheumatoid arthritis synovium, *Journal of Rheumatology.*24(10):pp. 1873-80.

Muller-Ladner, U., Kriegsmann, J., Franklin, B. N., Matsumoto, S., Geiler, T., Gay, R. E., & Gay, S. 1996, Synovial fibroblasts of patients with rheumatoid arthritis attach to and invade normal human cartilage when engrafted into SCID mice, *Am.J.Pathol.*, 149(5):pp. 1607-1615.

Muro, S., Cui, X., Gajewski, C., Murciano, J. C., Muzykantov, V. R., & Koval, M. 2003, Slow intracellular trafficking of catalase nanoparticles targeted to ICAM-1 protects endothelial cells from oxidative stress, *Am J Physiol Cell Physiol*, 285(5):p. C1339-C1347.

Muzykantov, V. R., Christofidou-Solomidou, M., Balyasnikova, I., Harshaw, D. W., Schultz, L., Fisher, A. B., & Albelda, S. M. 1999, Streptavidin facilitates internalization and pulmonary targeting of an anti-endothelial cell antibody (platelet-endothelial cell adhesion molecule 1): a strategy for vascular immunotargeting of drugs, *Proc.Natl.Acad.Sci U.S.A*, 96(5):pp. 2379-2384.

Nagashima, M., Tanaka, H., Takahashi, H., Tachihara, A., Tanaka, K., Ishiwata, T., Asano, G., & Yoshino, S. 2002, Study of the mechanism involved in angiogenesis and synovial cell proliferation in human synovial tissues of patients with rheumatoid arthritis using SCID mice, *Laboratory Investigation.*82(8):pp. 981-8.

Nagashima, M., Wauke, K., Hirano, D., Ishigami, S., Aono, H., Takai, M., Sasano, M., & Yoshino, S. 2000, Effects of combinations of anti-rheumatic drugs on the production of vascular endothelial growth factor and basic fibroblast growth factor in cultured synoviocytes and patients with rheumatoid arthritis, *Rheumatology.*39(11):pp. 1255-62.

Nagashima, M., Yoshino, S., Ishiwata, T., & Asano, G. 1995, Role of vascular endothelial growth factor in angiogenesis of rheumatoid arthritis, *Journal of Rheumatology.*22(9):pp. 1624-30.

Nakahara, H., Song, J., Sugimoto, M., Hagihara, K., Kishimoto, T., Yoshizaki, K., & Nishimoto, N. 2003, Anti-interleukin-6 receptor antibody therapy reduces vascular endothelial growth factor production in rheumatoid arthritis.[see comment], *Arthritis & Rheumatism.*48(6):pp. 1521-9.

Nandakumar, K. S., Svensson, L., & Holmdahl, R. 2003, Collagen type II-specific monoclonal antibody-induced arthritis in mice: description of the disease and the influence of age, sex, and genes, *Am.J Pathol.*, 163(5):pp. 1827-1837.

Naor, D. & Nedvetzki, S. 2003, CD44 in rheumatoid arthritis. [Review] [72 refs], *Arthritis Research & Therapy.*5(3):pp. 105-15.

Nassonov, E. L., Samsonov, M. Y., Chichasova, N. V., Nikiphorova, E. L., Tilz, G. P., Demel, U., Widner, B., & Fuchs, D. 2000, Soluble adhesion molecules in rheumatoid arthritis, *Rheumatology (Oxford)*, 39(7):pp. 808-810.

Newman, P. J. 1997, The biology of PECAM-1, *J.Clin.Invest*, 99(1):pp. 3-8.

Nielen, M. M., van, S. D., Reesink, H. W., van de Stadt, R. J., van der Horst-Bruinsma IE, de Koning, M. H., Habibuw, M. R., Vandenbroucke, J. P., & Dijkmans, B. A. 2004, Specific autoantibodies precede the symptoms of rheumatoid arthritis: a study of serial measurements in blood donors, *Arthritis Rheum.*, 50(2):pp. 380-386.

Nieto, M., Frade, J. M., Sancho, D., Mellado, M., Martinez, A., & Sanchez-Madrid, F. 1997, Polarization of chemokine receptors to the leading edge during lymphocyte chemotaxis, *J.Exp.Med.*, 186(1):pp. 153-158.

Nikkari, L., Haapasalmi, K., Aho, H., Torvinen, A., Sheppard, D., Larjava, H., & Heino, J. 1995, Localization of the alpha v subfamily of integrins and their putative ligands in synovial lining cell layer, *J Rheumatol.*, 22(1):pp. 16-23.

Nilsson, F., Kosmehl, H., Zardi, L., & Neri, D. 2001, Targeted delivery of tissue factor to the ED-B domain of fibronectin, a marker of angiogenesis, mediates the infarction of solid tumors in mice, *Cancer Res.*, 61(2):pp. 711-716.

Nishida, M., Springhorn, J. P., Kelly, R. A., & Smith, T. W. 1993, Cell-cell signaling between adult rat ventricular myocytes and cardiac microvascular endothelial cells in heterotypic primary culture, *J.Clin.Invest*, 91(5):pp. 1934-1941.

Nishimoto, N., Yoshizaki, K., Miyasaka, N., Yamamoto, K., Kawai, S., Takeuchi, T., Hashimoto, J., Azuma, J., & Kishimoto, T. 2004, Treatment of rheumatoid arthritis with humanized anti-interleukin-6 receptor antibody: a multicenter, double-blind, placebo-controlled trial, *Arthritis Rheum.*, 50(6):pp. 1761-1769.

Nishimura, K., Sugiyama, D., Kogata, Y., Tsuji, G., Nakazawa, T., Kawano, S., Saigo, K., Morinobu, A., Koshiba, M., Kuntz, K. M., Kamae, I., & Kumagai, S. 2007, Meta-analysis: diagnostic accuracy of anti-cyclic citrullinated peptide antibody and rheumatoid factor for rheumatoid arthritis.[see comment]. [Review] [115 refs], *Annals of Internal Medicine.*146(11):pp. 797-808.

Norii, M., Yamamura, M., Iwahashi, M., Ueno, A., Yamana, J., & Makino, H. 2006, Selective recruitment of CXCR3+ and CCR5+ CCR4+ T cells into synovial tissue in patients with rheumatoid arthritis, *Acta Medica Okayama.*60(3):pp. 149-57.

O'Doherty, M. J. 2000, PET in oncology I--lung, breast, soft tissue sarcoma, *Nucl.Med.Commun.*, 21(3):pp. 224-229.

Ogawara, K., Furumoto, K., Takakura, Y., Hashida, M., Higaki, K., & Kimura, T. 2001, Surface hydrophobicity of particles is not necessarily the most important

determinant in their in vivo disposition after intravenous administration in rats, *J Control Release*, 77(3):pp. 191-198.

Ogawara, K., Yoshida, M., Higaki, K., Kimura, T., Shiraishi, K., Nishikawa, M., Takakura, Y., & Hashida, M. 1999, Hepatic uptake of polystyrene microspheres in rats: effect of particle size on intrahepatic distribution, *J Control Release*, 59(1):pp. 15-22.

Oh, I. Y., Yoon, C. H., Hur, J., Kim, J. H., Kim, T. Y., Lee, C. S., Park, K. W., Chae, I. H., Oh, B. H., Park, Y. B., & Kim, H. S. 2007, Involvement of E-selectin in recruitment of endothelial progenitor cells and angiogenesis in ischemic muscle, *Blood.*110(12):pp. 3891-9.

Oliver, J. E., Worthington, J., & Silman, A. J. 2006, Genetic epidemiology of rheumatoid arthritis, *Curr.Opin.Rheumatol.*, 18(2):pp. 141-146.

Oliver, S. J., Banquerigo, M. L., & Brahn, E. 1994, Suppression of collagen-induced arthritis using an angiogenesis inhibitor, AGM-1470, and a microtubule stabilizer, taxol, *Cell Immunol.*, 157(1):pp. 291-299.

Ollier, W. E. & MacGregor, A. 1995, Genetic epidemiology of rheumatoid disease, *Br.Med.Bull.*, 51(2):pp. 267-285.

Orlando, R. A. & Cheresh, D. A. 1991, Arginine-glycine-aspartic acid binding leading to molecular stabilization between integrin alpha v beta 3 and its ligand, *J Biol.Chem.*, 266(29):pp. 19543-19550.

Ostendorf, B., Scherer, A., Wirrwar, A., Hoppin, J. W., Lackas, C., Schramm, N. U., Cohnen, M., Modder, U., van den Berg, W. B., Muller, H. W., Schneider, M., & Joosten, L. A. 2006, High-resolution multipinhole single-photon-emission computed tomography in experimental and human arthritis, *Arthritis Rheum.*, 54(4):pp. 1096-1104.

Ostergaard, M., Hansen, M., Stoltenberg, M., Gideon, P., Klarlund, M., Jensen, K. E., & Lorenzen, I. 1999, Magnetic resonance imaging-determined synovial membrane volume as a marker of disease activity and a predictor of progressive joint destruction in the wrists of patients with rheumatoid arthritis, *Arthritis Rheum.*, 42(5):pp. 918-929.

Ostergaard, M. & Klarlund, M. 2001, Importance of timing of post-contrast MRI in rheumatoid arthritis: what happens during the first 60 minutes after IV gadolinium-DTPA?, *Ann.Rheum.Dis.*, 60(11):pp. 1050-1054.

Ostergaard, M. & Szkudlarek, M. 2003, Imaging in rheumatoid arthritis--why MRI and ultrasonography can no longer be ignored. [Review] [114 refs], *Scandinavian Journal of Rheumatology.*, 32(2):pp. 63-73.

Paleolog, E. M. 2002, Angiogenesis in rheumatoid arthritis, *Arthritis Res.*, 4 Suppl 3:p. S81-S90.

Paleolog, E. M., Hunt, M., Elliott, M. J., Feldmann, M., Maini, R. N., & Woody, J. N. 1996, Deactivation of vascular endothelium by monoclonal anti-tumor necrosis factor alpha antibody in rheumatoid arthritis.[see comment], *Arthritis & Rheumatism.*39(7):pp. 1082-91.

Paleolog, E. M., Young, S., Stark, A. C., McCloskey, R. V., Feldmann, M., & Maini, R. N. 1998, Modulation of angiogenic vascular endothelial growth factor by tumor necrosis factor alpha and interleukin-1 in rheumatoid arthritis, *Arthritis & Rheumatism.*41(7):pp. 1258-65.

Palosaari, K., Vuotila, J., Takalo, R., Jartti, A., Niemela, R. K., Karjalainen, A., Haapea, M., Soini, I., Tervonen, O., & Hakala, M. 2006, Bone oedema predicts erosive progression on wrist MRI in early RA--a 2-yr observational MRI and NC scintigraphy study, *Rheumatology.*45(12):pp. 1542-8.

Pap, T., Aupperle, K. R., Gay, S., Firestein, G. S., & Gay, R. E. 2001, Invasiveness of synovial fibroblasts is regulated by p53 in the SCID mouse in vivo model of cartilage invasion, *Arthritis Rheum.*, 44(3):pp. 676-681.

Pap, T. & Distler, O. 2005, Linking angiogenesis to bone destruction in arthritis, *Arthritis Rheum.*, 52(5):pp. 1346-1348.

Pap, T., Shigeyama, Y., Kuchen, S., Fernihough, J. K., Simmen, B., Gay, R. E., Billingham, M., & Gay, S. 2000, Differential expression pattern of membrane-type matrix metalloproteinases in rheumatoid arthritis, *Arthritis Rheum.*, 43(6):pp. 1226-1232.

Pasqualini, R., Koivunen, E., Kain, R., Lahdenranta, J., Sakamoto, M., Stryhn, A., Ashmun, R. A., Shapiro, L. H., Arap, W., & Ruoslahti, E. 2000, Aminopeptidase N is a receptor for tumor-homing peptides and a target for inhibiting angiogenesis, *Cancer Res.*, 60(3):pp. 722-727.

Patel, D. D., Koopmann, W., Imai, T., Whichard, L. P., Yoshie, O., & Krangel, M. S. 2001, Chemokines have diverse abilities to form solid phase gradients, *Clin.Immunol.*, 99(1):pp. 43-52.

Patel, K. D., Cuvelier, S. L., & Wiehler, S. 2002, Selectins: critical mediators of leukocyte recruitment. [Review] [82 refs], *Seminars in Immunology.*, 14(2):pp. 73-81.

Pereira, J. J., Meyer, T., Docherty, S. E., Reid, H. H., Marshall, J., Thompson, E. W., Rossjohn, J., & Price, J. T. 2004, Bimolecular interaction of insulin-like growth factor (IGF) binding protein-2 with alphavbeta3 negatively modulates IGF-I-mediated migration and tumor growth, *Cancer Res.*, 64(3):pp. 977-984.

Perlman, H., Georganas, C., Pagliari, L. J., Koch, A. E., Haines, K., III, & Pope, R. M. 2000, Bcl-2 expression in synovial fibroblasts is essential for maintaining mitochondrial homeostasis and cell viability, *J Immunol.*, 164(10):pp. 5227-5235.

Pfaff, M., Tangemann, K., Muller, B., Gurrath, M., Muller, G., Kessler, H., Timpl, R., & Engel, J. 1994, Selective recognition of cyclic RGD peptides of NMR defined conformation by alpha IIb beta 3, alpha V beta 3, and alpha 5 beta 1 integrins, *J Biol.Chem.*, 269(32):pp. 20233-20238.

Picker, L. J., Michie, S. A., Rott, L. S., & Butcher, E. C. 1990, A unique phenotype of skin-associated lymphocytes in humans. Preferential expression of the HECA-452 epitope by benign and malignant T cells at cutaneous sites, *Am.J.Pathol.*, 136(5):pp. 1053-1068.

Picker, L. J., Treer, J. R., Ferguson-Darnell, B., Collins, P. A., Bergstresser, P. R., & Terstappen, L. W. 1993a, Control of lymphocyte recirculation in man. II. Differential regulation of the cutaneous lymphocyte-associated antigen, a tissue-selective homing receptor for skin-homing T cells, *J.Immunol.*, 150(3):pp. 1122-1136.

Picker, L. J., Treer, J. R., Ferguson-Darnell, B., Collins, P. A., Buck, D., & Terstappen, L. W. 1993b, Control of lymphocyte recirculation in man. I. Differential regulation of the peripheral lymph node homing receptor L-selectin on T cells during the virgin to memory cell transition, *J.Immunol.*, 150(3):pp. 1105-1121.

Pierschbacher, M. D. & Ruoslahti, E. 1984a, Cell attachment activity of fibronectin can be duplicated by small synthetic fragments of the molecule, *Nature*, 309(5963):pp. 30-33.

Pierschbacher, M. D. & Ruoslahti, E. 1984b, Variants of the cell recognition site of fibronectin that retain attachment-promoting activity, *Proc.Natl.Acad.Sci U.S.A*, 81(19):pp. 5985-5988.

Pierschbacher, M. D. & Ruoslahti, E. 1987, Influence of stereochemistry of the sequence Arg-Gly-Asp-Xaa on binding specificity in cell adhesion, *J Biol.Chem.*, 262(36):pp. 17294-17298.

Pincus, T., Ferraccioli, G., Sokka, T., Larsen, A., Rau, R., Kushner, I., & Wolfe, F. 2002, Evidence from clinical trials and long-term observational studies that disease-modifying anti-rheumatic drugs slow radiographic progression in rheumatoid arthritis: updating a 1983 review, *Rheumatology (Oxford)*, 41(12):pp. 1346-1356.

Pincus, T., Sokka, T., & Kautiainen, H. 2005, Patients seen for standard rheumatoid arthritis care have significantly better articular, radiographic, laboratory, and functional status in 2000 than in 1985, *Arthritis Rheum.*, 52(4):pp. 1009-1019.

Pitzalis, C., Cauli, A., Pipitone, N., Smith, C., Barker, J., Marchesoni, A., Yanni, G., & Panayi, G. S. 1996, Cutaneous lymphocyte antigen-positive T lymphocytes preferentially migrate to the skin but not to the joint in psoriatic arthritis, *Arthritis Rheum.*, 39(1):pp. 137-145.

Pitzalis, C., Kingsley, G., Murphy, J., & Panayi, G. 1987, Abnormal distribution of the helper-inducer and suppressor-inducer T-lymphocyte subsets in the rheumatoid joint, *Clin.Immunol.Immunopathol.*, 45(2):pp. 252-258.

Pless, J. 1992, From somatostatin to Sandostatin: history and chemistry, *Metabolism*, 41(9 Suppl 2):pp. 5-6.

Polisson, R. P., Schoenberg, O. I., Fischman, A., Rubin, R., Simon, L. S., Rosenthal, D., & Palmer, W. E. 1995, Use of magnetic resonance imaging and positron emission tomography in the assessment of synovial volume and glucose metabolism in patients with rheumatoid arthritis, *Arthritis & Rheumatism.*38(6):pp. 819-25.

Ponta, H., Sherman, L., & Herrlich, P. A. 2003, CD44: from adhesion molecules to signalling regulators, *Nat.Rev.Mol.Cell Biol.*, 4(1):pp. 33-45.

Postigo, A. A., Garcia-Vicuna, R., az-Gonzalez, F., Arroyo, A. G., De Landazuri, M. O., Chi-Rosso, G., Lobb, R. R., Laffon, A., & Sanchez-Madrid, F. 1992, Increased binding of synovial T lymphocytes from rheumatoid arthritis to endothelial-leukocyte adhesion molecule-1 (ELAM-1) and vascular cell adhesion molecule-1 (VCAM-1), *Journal of Clinical Investigation.*89(5):pp. 1445-52.

Proudfoot, A. E., Handel, T. M., Johnson, Z., Lau, E. K., LiWang, P., Clark-Lewis, I., Borlat, F., Wells, T. N., & Kosco-Vilbois, M. H. 2003, Glycosaminoglycan binding and oligomerization are essential for the in vivo activity of certain chemokines, *Proceedings of the National Academy of Sciences of the United States of America.*100(4):pp. 1885-90.

Proudman, S. M., Cleland, L. G., Fusco, M., & Mayrhofer, G. 1999, Accessible xenografts of human synovium in the subcutaneous tissues of the ears of SCID mice, *Immunol.Cell Biol.*, 77(2):pp. 109-120.

Proudman, S. M., Cleland, L. G., & Mayrhofer, G. 1999, Effects of tumor necrosis factor-alpha, interleukin 1beta, and activated peripheral blood mononuclear cells on the expression of adhesion molecules and recruitment of leukocytes in rheumatoid synovial xenografts in SCID mice, *Journal of Rheumatology.*26(9):pp. 1877-89.

Qvistgaard, E., Rogind, H., Torp-Pedersen, S., Terslev, L., nneskiold-Samsoe, B., & Bliddal, H. 2001, Quantitative ultrasonography in rheumatoid arthritis: evaluation of inflammation by Doppler technique, *Ann.Rheum.Dis.*, 60(7):pp. 690-693.

Rajotte, D., Arap, W., Hagedorn, M., Koivunen, E., Pasqualini, R., & Ruoslahti, E. 1998, Molecular heterogeneity of the vascular endothelium revealed by in vivo phage display, *J.Clin.Invest*, 102(2):pp. 430-437.

Rajotte, D. & Ruoslahti, E. 1999, Membrane dipeptidase is the receptor for a lung-targeting peptide identified by in vivo phage display, *J.Biol.Chem.*, 274(17):pp. 11593-11598.

Richards, P. J., Williams, A. S., Goodfellow, R. M., & Williams, B. D. 1999, Liposomal clodronate eliminates synovial macrophages, reduces inflammation and ameliorates joint destruction in antigen-induced arthritis, *Rheumatology (Oxford)*, 38(9):pp. 818-825.

Rinaldi, N., Schwarz-Eywill, M., Weis, D., Leppelmann-Jansen, P., Lukoschek, M., Keilholz, U., & Barth, T. F. 1997a, Increased expression of integrins on fibroblast-like synoviocytes from rheumatoid arthritis in vitro correlates with enhanced binding to extracellular matrix proteins, *Ann.Rheum.Dis.*, 56(1):pp. 45-51.

Rinaldi, N., Weis, D., Brado, B., Schwarz-Eywill, M., Lukoschek, M., Pezzutto, A., Keilholz, U., & Barth, T. F. 1997b, Differential expression and functional behaviour of the alpha v and beta 3 integrin subunits in cytokine stimulated fibroblast-like cells derived from synovial tissue of rheumatoid arthritis and osteoarthritis in vitro, *Ann.Rheum.Dis.*, 56(12):pp. 729-736.

Rodi, D. J. & Makowski, L. 1999, Phage-display technology--finding a needle in a vast molecular haystack. [Review] [64 refs], *Current Opinion in Biotechnology.*, 10(1):pp. 87-93.

Rollins, B. J. 1997, Chemokines, *Blood*, 90(3):pp. 909-928.

Rooney, M., Condell, D., Quinlan, W., Daly, L., Whelan, A., Feighery, C., & Bresnihan, B. 1988, Analysis of the histologic variation of synovitis in rheumatoid arthritis, *Arthritis Rheum.*, 31(8):pp. 956-963.

Rosen, S. D. 2004, Ligands for L-selectin: homing, inflammation, and beyond, *Annu.Rev.Immunol.*, 22:pp. 129-156.

Rossi, D. & Zlotnik, A. 2000, The biology of chemokines and their receptors, *Annu.Rev.Immunol.*, 18:pp. 217-242.

Royall, J. A., Berkow, R. L., Beckman, J. S., Cunningham, M. K., Matalon, S., & Freeman, B. A. 1989, Tumor necrosis factor and interleukin 1 alpha increase vascular endothelial permeability, *Am.J Physiol*, 257(6 Pt 1):p. L399-L410.

Ruger, B., Giurea, A., Wanivenhaus, A. H., Zehetgruber, H., Hollemann, D., Yanagida, G., Groger, M., Petzelbauer, P., Smolen, J. S., Hoecker, P., & Fischer, M. B. 2004, Endothelial precursor cells in the synovial tissue of patients with rheumatoid arthritis and osteoarthritis, *Arthritis Rheum.*, 50(7):pp. 2157-2166.

Ruggeri, Z. M. & Ware, J. 1993, von Willebrand factor, *FASEB J.*, 7(2):pp. 308-316.

Ruoslahti, E. 1996, RGD and other recognition sequences for integrins, *Annu.Rev.Cell Dev.Biol.*, 12:pp. 697-715.

Rusckowski, M., Fogarasi, M., Virzi, F., & Hnatowich, D. J. 1995, Influence of endogenous biotin on the biodistribution of labelled biotin derivatives in mice, *Nucl.Med.Commun.*, 16(1):pp. 38-46.

Sallusto, F., Lenig, D., Forster, R., Lipp, M., & Lanzavecchia, A. 1999, Two subsets of memory T lymphocytes with distinct homing potentials and effector functions, *Nature*, 401(6754):pp. 708-712.

Salmi, M., Andrew, D. P., Butcher, E. C., & Jalkanen, S. 1995, Dual binding capacity of mucosal immunoblasts to mucosal and synovial endothelium in humans: dissection of the molecular mechanisms, *J.Exp.Med.*, 181(1):pp. 137-149.

Salmi, M., Granfors, K., Leirisalo-Repo, M., Hamalainen, M., MacDermott, R., Leino, R., Havia, T., & Jalkanen, S. 1992, Selective endothelial binding of interleukin-2-dependent human T-cell lines derived from different tissues, *Proc.Natl.Acad.Sci.U.S.A*, 89(23):pp. 11436-11440.

Salmi, M. & Jalkanen, S. 2001, Human leukocyte subpopulations from inflamed gut bind to joint vasculature using distinct sets of adhesion molecules, *J.Immunol.*, 166(7):pp. 4650-4657.

Salmi, M., Rajala, P., & Jalkanen, S. 1997, Homing of mucosal leukocytes to joints. Distinct endothelial ligands in synovium mediate leukocyte-subtype specific adhesion, *J.Clin.Invest*, 99(9):pp. 2165-2172.

Salmi, M., Tohka, S., Berg, E. L., Butcher, E. C., & Jalkanen, S. 1997, Vascular adhesion protein 1 (VAP-1) mediates lymphocyte subtype-specific, selectin-independent recognition of vascular endothelium in human lymph nodes, *J.Exp.Med.*, 186(4):pp. 589-600.

Salvador, G., Sanmarti, R., Gil-Torregrosa, B., Garcia-Peiro, A., Rodriguez-Cros, J. R., & Canete, J. D. 2006, Synovial vascular patterns and angiogenic factors expression in synovial tissue and serum of patients with rheumatoid arthritis, *Rheumatology (Oxford)*, 45(8):pp. 966-971.

Santamaria Babi, L. F., Picker, L. J., Perez Soler, M. T., Drzimalla, K., Flohr, P., Blaser, K., & Hauser, C. 1995, Circulating allergen-reactive T cells from patients with atopic dermatitis and allergic contact dermatitis express the skin-selective homing receptor, the cutaneous lymphocyte-associated antigen, *J.Exp.Med.*, 181(5):pp. 1935-1940.

Santiago, B., Baleux, F., Palao, G., Gutierrez-Canas, I., Ramirez, J. C., renzana-Seisdedos, F., & Pablos, J. L. 2006, CXCL12 is displayed by rheumatoid endothelial cells through its basic amino-terminal motif on heparan sulfate proteoglycans, *Arthritis Res.Ther.*, 8(2):p. R43.

Sarraj, B., Ludanyi, K., Glant, T. T., Finnegan, A., & Mikecz, K. 2006, Expression of CD44 and L-selectin in the innate immune system is required for severe joint inflammation in the proteoglycan-induced murine model of rheumatoid arthritis, *Journal of Immunology.*177(3):pp. 1932-40.

Schaerli, P., Ebert, L., Willimann, K., Blaser, A., Roos, R. S., Loetscher, P., & Moser, B. 2004, A skin-selective homing mechanism for human immune surveillance T cells, *J.Exp.Med.*, 199(9):pp. 1265-1275.

Schechter, B., Silberman, R., Arnon, R., & Wilchek, M. 1990, Tissue distribution of avidin and streptavidin injected to mice. Effect of avidin carbohydrate, streptavidin truncation and exogenous biotin, *Eur.J Biochem.*, 189(2):pp. 327-331.

Scott, D. L. 2000, Prognostic factors in early rheumatoid arthritis, *Rheumatology (Oxford)*, 39 Suppl 1:pp. 24-29.

Scott, D. L., Coulton, B. L., & Popert, A. J. 1986, Long term progression of joint damage in rheumatoid arthritis, *Ann.Rheum.Dis.*, 45(5):pp. 373-378.

Scott, D. L. & Kingsley, G. H. 2006, Tumor necrosis factor inhibitors for rheumatoid arthritis, *N.Engl.J Med.*, 355(7):pp. 704-712.

Scott, D. L., Pugner, K., Kaarela, K., Doyle, D. V., Woolf, A., Holmes, J., & Hieke, K. 2000, The links between joint damage and disability in rheumatoid arthritis, *Rheumatology.(Oxford)*, 39(2):pp. 122-132.

Scott, D. L., Symmons, D. P., Coulton, B. L., & Popert, A. J. 1987, Long-term outcome of treating rheumatoid arthritis: results after 20 years, *Lancet.*1(8542):pp. 1108-11.

Shamri, R., Grabovsky, V., Gauguet, J. M., Feigelson, S., Manevich, E., Kolanus, W., Robinson, M. K., Staunton, D. E., von Andrian, U. H., & Alon, R. 2005, Lymphocyte arrest requires instantaneous induction of an extended LFA-1 conformation mediated by endothelium-bound chemokines, *Nat.Immunol.*, 6(5):pp. 497-506.

Sharp, J. T., Bluhm, G. B., Brook, A., Brower, A. C., Corbett, M., Decker, J. L., Genant, H. K., Gofton, J. P., Goodman, N., Larsen, A., & . 1985, Reproducibility of multiple-observer scoring of radiologic abnormalities in the hands and wrists of patients with rheumatoid arthritis, *Arthritis Rheum*, 28(1):pp. 16-24.

Sherman, M. A., Runnels, H. A., Moore, J. C., Stern, L. J., & Jensen, P. E. 1994, Membrane interactions influence the peptide binding behavior of DR1, *J Exp.Med*, 179(1):pp. 229-234.

Shimizu, Y. & Mobley, J. L. 1993, Distinct divalent cation requirements for integrin-mediated CD4+ T lymphocyte adhesion to ICAM-1, fibronectin, VCAM-1, and invasin, *J Immunol.*, 151(8):pp. 4106-4115.

Shinde, P., V, Campbell, C. J., Yun, Y. H., Slack, S. M., & Goetz, D. J. 2001, Particle diameter influences adhesion under flow, *Biophys.J*, 80(4):pp. 1733-1743.

Shyjan, A. M., Bertagnolli, M., Kenney, C. J., & Briskin, M. J. 1996, Human mucosal addressin cell adhesion molecule-1 (MAdCAM-1) demonstrates structural and functional similarities to the alpha 4 beta 7-integrin binding domains of murine MAdCAM-1, but extreme divergence of mucin-like sequences, *J.Immunol.*, 156(8):pp. 2851-2857.

Siewert, C., Menning, A., Dudda, J., Siegmund, K., Lauer, U., Floess, S., Campbell, D. J., Hamann, A., & Huehn, J. 2007, Induction of organ-selective CD4+ regulatory T cell homing, *European Journal of Immunology.*37(4):pp. 978-89.

Silverman, M. D., Haas, C. S., Rad, A. M., Arbab, A. S., & Koch, A. E. 2007, The role of vascular cell adhesion molecule 1/ very late activation antigen 4 in endothelial progenitor cell recruitment to rheumatoid arthritis synovium, *Arthritis Rheum.*, 56(6):pp. 1817-1826.

Simkin, P. A. 1979, Synovial permeability in rheumatoid arthritis, *Arthritis Rheum.*, 22(7):pp. 689-696.

Smith, J. W., Piotrowicz, R. S., & Mathis, D. 1994, A mechanism for divalent cation regulation of beta 3-integrins, *J Biol.Chem.*, 269(2):pp. 960-967.

Smith, M. D. 1997, Decrease in cell adhesion molecules by treatment with anti-tumor necrosis factor alpha monoclonal antibody.[comment], *Arthritis & Rheumatism.*40(4):pp. 789-90.

Smith, M. D., Slavotinek, J., Au, V., Weedon, H., Parker, A., Coleman, M., Roberts-Thomson, P. J., & Ahern, M. J. 2001, Successful treatment of rheumatoid arthritis is associated with a reduction in synovial membrane cytokines and cell adhesion molecule expression, *Rheumatology.*40(9):pp. 965-77.

Sone, H., Kawakami, Y., Sakauchi, M., Nakamura, Y., Takahashi, A., Shimano, H., Okuda, Y., Segawa, T., Suzuki, H., & Yamada, N. 2001, Neutralization of vascular endothelial growth factor prevents collagen-induced arthritis and ameliorates established disease in mice, *Biochem.Biophys.Res.Commun.*, 281(2):pp. 562-568.

Sperandio, M., Smith, M. L., Forlow, S. B., Olson, T. S., Xia, L., McEver, R. P., & Ley, K. 2003, P-selectin glycoprotein ligand-1 mediates L-selectin-dependent leukocyte rolling in venules, *J.Exp.Med.*, 197(10):pp. 1355-1363.

Springer, T. A. 1994, Traffic signals for lymphocyte recirculation and leukocyte emigration: the multistep paradigm, *Cell*, 76(2):pp. 301-314.

Staton, T. L., Habtezion, A., Winslow, M. M., Sato, T., Love, P. E., & Butcher, E. C. 2006, CD8+ recent thymic emigrants home to and efficiently repopulate the

small intestine epithelium.[erratum appears in Nat Immunol. 2006 Jun;7(6):672], *Nature Immunology.*7(5):pp. 482-8.

Stehle, G., Wunder, A., Sinn, H., Schrenk, H. H., Schutt, S., Frei, E., Hartung, G., Maier-Borst, W., & Heene, D. L. 1997, Pharmacokinetics of methotrexate-albumin conjugates in tumor-bearing rats, *Anticancer Drugs*, 8(9):pp. 835-844.

Stein, C. M. & Pincus, T. 1999, Placebo-controlled studies in rheumatoid arthritis: ethical issues, *Lancet*, 353(9150):pp. 400-403.

Stein, J. V., Cheng, G., Stockton, B. M., Fors, B. P., Butcher, E. C., & von Andrian, U. H. 1999, L-selectin-mediated leukocyte adhesion in vivo: microvillous distribution determines tethering efficiency, but not rolling velocity, *J.Exp.Med.*, 189(1):pp. 37-50.

Stevens, C. R., Blake, D. R., Merry, P., Revell, P. A., & Levick, J. R. 1991a, A comparative study by morphometry of the microvasculature in normal and rheumatoid synovium, *Arthritis Rheum.*, 34(12):pp. 1508-1513.

Stevens, C. R., Williams, R. B., Farrell, A. J., & Blake, D. R. 1991b, Hypoxia and inflammatory synovitis: observations and speculation, *Ann.Rheum.Dis.*, 50(2):pp. 124-132.

Storgard, C. M., Stupack, D. G., Jonczyk, A., Goodman, S. L., Fox, R. I., & Cheresh, D. A. 1999, Decreased angiogenesis and arthritic disease in rabbits treated with an alphavbeta3 antagonist, *J.Clin.Invest*, 103(1):pp. 47-54.

Strand, V., Cohen, S., Schiff, M., Weaver, A., Fleischmann, R., Cannon, G., Fox, R., Moreland, L., Olsen, N., Furst, D., Caldwell, J., Kaine, J., Sharp, J., Hurley, F., & Loew-Friedrich, I. 1999, Treatment of active rheumatoid arthritis with leflunomide compared with placebo and methotrexate. Leflunomide Rheumatoid Arthritis Investigators Group, *Arch.Intern.Med*, 159(21):pp. 2542-2550.

Strunk, J., Bundke, E., & Lange, U. 2006, Anti-TNF-alpha antibody Infliximab and glucocorticoids reduce serum vascular endothelial growth factor levels in patients with rheumatoid arthritis: a pilot study, *Rheumatology International.*26(3):pp. 252-6.

Su, Z. F., He, J., Rusckowski, M., & Hnatowich, D. J. 2003, In vitro cell studies of technetium-99m labelled RGD-HYNIC peptide, a comparison of tricine and EDDA as co-ligands, *Nuclear Medicine & Biology.*, 30(2):pp. 141-149.

Su, Z. F., Liu, G., Gupta, S., Zhu, Z., Rusckowski, M., & Hnatowich, D. J. 2002, In vitro and in vivo evaluation of a Technetium-99m-labelled cyclic RGD peptide as a specific marker of alpha(V)beta(3) integrin for tumor imaging.[see comment], *Bioconjugate Chemistry.*, 13(3):pp. 561-570.

Sung, M., Poon, G. M., & Gariepy, J. 2006, The importance of valency in enhancing the import and cell routing potential of protein transduction domain-containing molecules, *Biochim.Biophys.Acta*, 1758(3):pp. 355-363.

Szekanecz, Z. & Koch, A. E. 2007, Macrophages and their products in rheumatoid arthritis, *Curr.Opin.Rheumatol.*, 19(3):pp. 289-295.

Szkudlarek, M., Klarlund, M., Narvestad, E., Court-Payen, Strandberg, C., Jensen, K. E., Thomsen, H. S., & Ostergaard, M. 2006, Ultrasonography of the metacarpophalangeal and proximal interphalangeal joints in rheumatoid arthritis: a comparison with magnetic resonance imaging, conventional radiography and clinical examination, *Arthritis Res.Ther.*, 8(2):p. R52.

Tak, P. P., Taylor, P. C., Breedveld, F. C., Smeets, T. J., Daha, M. R., Kluin, P. M., Meinders, A. E., & Maini, R. N. 1996, Decrease in cellularity and expression of adhesion molecules by anti-tumor necrosis factor alpha monoclonal antibody treatment in patients with rheumatoid arthritis.[see comment], *Arthritis Rheum*, 39(7):pp. 1077-1081.

Tak, P. P., Thurkow, E. W., Daha, M. R., Kluin, P. M., Smeets, T. J., Meinders, A. E., & Breedveld, F. C. 1995, Expression of adhesion molecules in early rheumatoid synovial tissue, *Clin.Immunol.Immunopathol.*, 77(3):pp. 236-242.

Tam, J. P. 1996, Recent advances in multiple antigen peptides, *J.Immunol.Methods*, 196(1):pp. 17-32.

Tarner, I. H., Harle, P., Muller-Ladner, U., Gay, R. E., & Gay, S. 2005, The different stages of synovitis: acute vs chronic, early vs late and non-erosive vs erosive, *Best Pract.Res.Clin.Rheumatol.*, 19(1):pp. 19-35.

Taylor, P. C., Chu, C. Q., Plater-Zyberk, C., & Maini, R. N. 1996, Transfer of type II collagen-induced arthritis from DBA/1 to severe combined immunodeficiency mice can be prevented by blockade of Mac-1, *Immunology*, 88(2):pp. 315-321.

Taylor, P. C., Steuer, A., Gruber, J., Cosgrove, D. O., Blomley, M. J., Marsters, P. A., Wagner, C. L., McClinton, C., & Maini, R. N. 2004, Comparison of ultrasonographic assessment of synovitis and joint vascularity with radiographic evaluation in a randomized, placebo-controlled study of infliximab therapy in early rheumatoid arthritis, *Arthritis Rheum.*, 50(4):pp. 1107-1116.

Tedder, T. F., Steeber, D. A., & Pizcueta, P. 1995, L-selectin-deficient mice have impaired leukocyte recruitment into inflammatory sites, *J.Exp.Med.*, 181(6):pp. 2259-2264.

Thornton, B. P., Vetvicka, V., Pitman, M., Goldman, R. C., & Ross, G. D. 1996, Analysis of the sugar specificity and molecular location of the beta-glucan-binding lectin site of complement receptor type 3 (CD11b/CD18), *J Immunol.*, 156(3):pp. 1235-1246.

Thumshirn, G., Hersel, U., Goodman, S. L., & Kessler, H. 2003, Multimeric cyclic RGD peptides as potential tools for tumor targeting: solid-phase peptide synthesis and chemoselective oxime ligation, *Chemistry*, 9(12):pp. 2717-2725.

To, S. S., Newman, P. M., Hyland, V. J., Robinson, B. G., & Schrieber, L. 1996, Regulation of adhesion molecule expression by human synovial microvascular endothelial cells in vitro, *Arthritis & Rheumatism.*39(3):pp. 467-77.

Torchilin, V. P. 2005, Recent advances with liposomes as pharmaceutical carriers, *Nat.Rev.Drug Discov.*, 4(2):pp. 145-160.

Torchilin, V. P. & Lukyanov, A. N. 2003, Peptide and protein drug delivery to and into tumors: challenges and solutions, *Drug Discov.Today*, 8(6):pp. 259-266.

Torsteinsdottir, I., Arvidson, N. G., Hallgren, R., & Hakansson, L. 1999, Enhanced expression of integrins and CD66b on peripheral blood neutrophils and eosinophils in patients with rheumatoid arthritis, and the effect of glucocorticoids, *Scandinavian Journal of Immunology.*50(4):pp. 433-9.

Tu, L., Chen, A., Delahunty, M. D., Moore, K. L., Watson, S. R., McEver, R. P., & Tedder, T. F. 1996, L-selectin binds to P-selectin glycoprotein ligand-1 on leukocytes: interactions between the lectin, epidermal growth factor, and consensus repeat domains of the selectins determine ligand binding specificity, *J.Immunol.*, 157(9):pp. 3995-4004.

Turesson, C., Jacobsson, L. T., Sturfelt, G., Matteson, E. L., Mathsson, L., & Ronnelid, J. 2007, Rheumatoid factor and antibodies to cyclic citrullinated peptides are associated with severe extra-articular manifestations in rheumatoid arthritis, *Ann.Rheum.Dis.*, 66(1):pp. 59-64.

Turesson, C., McClelland, R. L., Christianson, T. J., & Matteson, E. L. 2006, Multiple extra-articular manifestations are associated with poor survival in patients with rheumatoid arthritis, *Ann.Rheum.Dis.*, 65(11):pp. 1533-1534.

Turesson, C., O'Fallon, W. M., Crowson, C. S., Gabriel, S. E., & Matteson, E. L. 2002, Occurrence of extraarticular disease manifestations is associated with excess mortality in a community based cohort of patients with rheumatoid arthritis, *Journal of Rheumatology.*29(1):pp. 62-7.

Turesson, C., O'Fallon, W. M., Crowson, C. S., Gabriel, S. E., & Matteson, E. L. 2003, Extra-articular disease manifestations in rheumatoid arthritis: incidence trends and risk factors over 46 years, *Ann.Rheum.Dis.*, 62(8):pp. 722-727.

Turk, M. J., Breur, G. J., Widmer, W. R., Paulos, C. M., Xu, L. C., Grote, L. A., & Low, P. S. 2002, Folate-targeted imaging of activated macrophages in rats with adjuvant-induced arthritis, *Arthritis Rheum.*, 46(7):pp. 1947-1955.

van Buul, J. D. & Hordijk, P. L. 2004, Signaling in leukocyte transendothelial migration, *Arterioscler.Thromb.Vasc.Biol.*, 24(5):pp. 824-833.

van der Flier, A. & Sonnenberg, A. 2001, Function and interactions of integrins. [Review] [198 refs], *Cell & Tissue Research.*305(3):pp. 285-98.

Van der Heijden, J. W., Dijkmans, B. A., Scheper, R. J., & Jansen, G. 2007, Drug Insight: resistance to methotrexate and other disease-modifying antirheumatic drugs--from bench to bedside, *Nat.Clin.Pract.Rheumatol.*, 3(1):pp. 26-34.

van der Laken, C. J., Elzinga, E. H., Kropholler, M. A., Molthoff, C. F. M., Van der Heijden, J. W., Maruyama, K., Boellaard, R., Dijkmans, B. A., Lammertsma, A. A., & Voskuyl, A. E. 2008, Noninvasie imaging of receptors in rheumatoid synovitis using 11C-(R)-PK1195 and positron emission tomography, *Arthritis & Rheumatism.*, 58(11):pp. 3350-3355.

van Gaalen, F. A., Toes, R. E., Ditzel, H. J., Schaller, M., Breedveld, F. C., Verweij, C. L., & Huizinga, T. W. 2004, Association of autoantibodies to glucose-6-phosphate isomerase with extraarticular complications in rheumatoid arthritis, *Arthritis & Rheumatism.*50(2):pp. 395-9.

van Hagen, P. M., Breeman, W. A., Bernard, H. F., Schaar, M., Mooij, C. M., Srinivasan, A., Schmidt, M. A., Krenning, E. P., & de Jong, M. 2000, Evaluation of a radiolabelled cyclic DTPA-RGD analogue for tumour imaging and radionuclide therapy, *Int.J.Cancer*, 90(4):pp. 186-198.

Veber, D. F. & Freidinger, R. M. 1985, The design of metabolically stable peptide analogues, *Trend in Neurosciences*, 8:pp. 392-396.

von Asmuth, E. J., Smeets, E. F., Ginsel, L. A., Onderwater, J. J., Leeuwenberg, J. F., & Buurman, W. A. 1992, Evidence for endocytosis of E-selectin in human endothelial cells, *Eur.J Immunol.*, 22(10):pp. 2519-2526.

Vos, K., Thurlings, R. M., Wijbrandts, C. A., van Schaardenburg, D., Gerlag, D. M., & Tak, P. P. 2007, Early effects of rituximab on the synovial cell infiltrate in patients with rheumatoid arthritis, *Arthritis & Rheumatism.*56(3):pp. 772-8.

Wagner, N., Lohler, J., Kunkel, E. J., Ley, K., Leung, E., Krissansen, G., Rajewsky, K., & Muller, W. 1996, Critical role for beta7 integrins in formation of the gut-associated lymphoid tissue, *Nature*, 382(6589):pp. 366-370.

Wahid, S., Blades, M. C., De Lord, D., Brown, I., Blake, G., Yanni, G., Haskard, D. O., Panayi, G. S., & Pitzalis, C. 2000, Tumour necrosis factor-alpha (TNF-alpha) enhances lymphocyte migration into rheumatoid synovial tissue transplanted into severe combined immunodeficient (SCID) mice [In Process Citation], *Clin.Exp.Immunol.*, 122(1):pp. 133-142.

Wakefield, R. J., Gibbon, W. W., Conaghan, P. G., O'Connor, P., McGonagle, D., Pease, C., Green, M. J., Veale, D. J., Isaacs, J. D., & Emery, P. 2000, The value of sonography in the detection of bone erosions in patients with rheumatoid arthritis: a comparison with conventional radiography, *Arthritis Rheum.*, 43(12):pp. 2762-2770.

Walcheck, B., Moore, K. L., McEver, R. P., & Kishimoto, T. K. 1996, Neutrophil-neutrophil interactions under hydrodynamic shear stress involve L-

selectin and PSGL-1. A mechanism that amplifies initial leukocyte accumulation on P-selectin in vitro, *J.Clin.Invest*, 98(5):pp. 1081-1087.

Walsh, D. A., Wade, M., Mapp, P. I., & Blake, D. R. 1998, Focally regulated endothelial proliferation and cell death in human synovium, *American Journal of Pathology*, 152(3):pp. 691-702.

Walther, M., Harms, H., Krenn, V., Radke, S., Faehndrich, T. P., & Gohlke, F. 2001, Correlation of power Doppler sonography with vascularity of the synovial tissue of the knee joint in patients with osteoarthritis and rheumatoid arthritis, *Arthritis Rheum.*, 44(2):pp. 331-338.

Wang, L., Fuster, M., Sriramarao, P., & Esko, J. D. 2005, Endothelial heparan sulfate deficiency impairs L-selectin- and chemokine-mediated neutrophil trafficking during inflammatory responses.[see comment], *Nature Immunology*.6(9)pp. :902-10.

Wassenberg, S., Rau, R., Steinfeld, P., & Zeidler, H. 2005, Very low-dose prednisolone in early rheumatoid arthritis retards radiographic progression over two years: a multicenter, double-blind, placebo-controlled trial, *Arthritis Rheum.*, 52(11):pp. 3371-3380.

Watts, G. M., Beurskens, F. J., Martin-Padura, I., Ballantyne, C. M., Klickstein, L. B., Brenner, M. B., & Lee, D. M. 2005, Manifestations of inflammatory arthritis are critically dependent on LFA-1, *Journal of Immunology*.174(6):pp. 3668-75.

Weber, C., Kitayama, J., & Springer, T. A. 1996, Differential regulation of beta 1 and beta 2 integrin avidity by chemoattractants in eosinophils, *Proc.Natl.Acad.Sci.U.S.A*, 93(20):pp. 10939-10944.

Weber, P. C., Ohlendorf, D. H., Wendoloski, J. J., & Salemme, F. R. 1989, Structural origins of high-affinity biotin binding to streptavidin, *Science*, 243(4887):pp. 85-88.

Weber, P. C., Pantoliano, M. W., & Thompson, L. D. 1992, Crystal structure and ligand-binding studies of a screened peptide complexed with streptavidin, *Biochemistry*, 31(39):pp. 9350-9354.

Weinblatt, M., Combe, B., Covucci, A., Aranda, R., Becker, J. C., & Keystone, E. 2006, Safety of the selective costimulation modulator abatacept in rheumatoid arthritis patients receiving background biologic and nonbiologic disease-modifying antirheumatic drugs: A one-year randomized, placebo-controlled study, *Arthritis Rheum.*, 54(9):pp. 2807-2816.

Weinblatt, M., Schiff, M., Goldman, A., Kremer, J., Luggen, M., Li, T., Chen, D., & Becker, J. C. 2007, Selective costimulation modulation using abatacept in patients with active rheumatoid arthritis while receiving etanercept: a randomised clinical trial, *Ann.Rheum.Dis.*, 66(2):pp. 228-234.

Weinblatt, M. E., Kaplan, H., Germain, B. F., Block, S., Solomon, S. D., Merriman, R. C., Wolfe, F., Wall, B., Anderson, L., Gall, E., & . 1994, Methotrexate in rheumatoid arthritis. A five-year prospective multicenter study, *Arthritis Rheum.*, 37(10):pp. 1492-1498.

Weinblatt, M. E., Reda, D., Henderson, W., Giobbie-Hurder, A., Williams, D., Diani, A., & Docsa, S. 1999, Sulfasalazine treatment for rheumatoid arthritis: a metaanalysis of 15 randomized trials, *J Rheumatol.*, 26(10):pp. 2123-2130.

Welsing, P. M., Fransen, J., & van Riel, P. L. 2005, Is the disease course of rheumatoid arthritis becoming milder? Time trends since 1985 in an inception cohort of early rheumatoid arthritis, *Arthritis Rheum.*, 52(9):pp. 2616-2624.

Wessels, J. A., Kooloos, W. M., De Jonge, R., Vries-Bouwstra, J. K., Allaart, C. F., Linssen, A., Collee, G., De Sonnaville, P., Lindemans, J., Huizinga, T. W., & Guchelaar, H. J. 2006, Relationship between genetic variants in the adenosine pathway and outcome of methotrexate treatment in patients with recent-onset rheumatoid arthritis.[see comment], *Arthritis & Rheumatism.*54(9):pp. 2830-9.

Weyand, C. M. & Goronzy, J. J. 2003, Ectopic germinal center formation in rheumatoid synovitis, *Ann.N.Y.Acad.Sci*, 987:pp. 140-149.

Weyand, C. M., Schmidt, D., Wagner, U., & Goronzy, J. J. 1998, The influence of sex on the phenotype of rheumatoid arthritis, *Arthritis Rheum.*, 41(5):pp. 817-822.

Wiewrodt, R., Thomas, A. P., Cipelletti, L., Christofidou-Solomidou, M., Weitz, D. A., Feinstein, S. I., Schaffer, D., Albelda, S. M., Koval, M., & Muzykantov, V. R. 2002, Size-dependent intracellular immunotargeting of therapeutic cargoes into endothelial cells, *Blood.*99(3):pp. 912-22.

Wilder, R. L. 2002, Integrin alpha V beta 3 as a target for treatment of rheumatoid arthritis and related rheumatic diseases, *Ann.Rheum.Dis.*, 61 Suppl 2:p. ii96-ii99.

Wiles, N., Symmons, D. P., Harrison, B., Barrett, E., Barrett, J. H., Scott, D. G., & Silman, A. J. 1999, Estimating the incidence of rheumatoid arthritis: trying to hit a moving target?, *Arthritis Rheum.*, 42(7):pp. 1339-1346.

Williams, A., Goodfellow, R., Topley, N., Amos, N., & Williams, B. 2000, The suppression of rat collagen-induced arthritis and inhibition of macrophage derived mediator release by liposomal methotrexate formulations, *Inflamm.Res.*, 49(4):pp. 155-161.

Williams, A. S., Camilleri, J. P., & Williams, B. D. 1994, Suppression of adjuvant-induced arthritis by liposomally conjugated methotrexate in the rat, *Br.J Rheumatol.*, 33(6):pp. 530-533.

Wipke, B. T., Wang, Z., Nagengast, W., Reichert, D. E., & Allen, P. M. 2004, Staging the initiation of autoantibody-induced arthritis: a critical role for immune complexes, *J.Immunol.*, 172(12):pp. 7694-7702.

Wojchowski, D. M. & Sytkowski, A. J. 1986, Detection of low-density cell-surface molecules using biotinylated fluorescent microspheres, *Biochim.Biophys.Acta*, 857(1):pp. 61-67.

Wolfe, F. & Michaud, K. 2007, Biologic treatment of rheumatoid arthritis and the risk of malignancy: analyses from a large US observational study, *Arthritis & Rheumatism.*56(9):pp. 2886-95.

Wolff, B., Burns, A. R., Middleton, J., & Rot, A. 1998, Endothelial cell "memory" of inflammatory stimulation: human venular endothelial cells store interleukin 8 in Weibel-Palade bodies, *J.Exp.Med.*, 188(9):pp. 1757-1762.

Woolley, D. E. 2003, The mast cell in inflammatory arthritis, *N.Engl.J Med.*, 348(17):pp. 1709-1711.

Wunder, A., Muller-Ladner, U., Stelzer, E. H., Funk, J., Neumann, E., Stehle, G., Pap, T., Sinn, H., Gay, S., & Fiehn, C. 2003, Albumin-based drug delivery as novel therapeutic approach for rheumatoid arthritis, *J.Immunol.*, 170(9):pp. 4793-4801.

Xia, Y. & Ross, G. D. 1999, Generation of recombinant fragments of CD11b expressing the functional beta-glucan-binding lectin site of CR3 (CD11b/CD18), *J Immunol.*, 162(12):pp. 7285-7293.

Xie, J., Li, R., Kotovuori, P., Vermot-Desroches, C., Wijdenes, J., Arnaout, M. A., Nortamo, P., & Gahmberg, C. G. 1995, Intercellular adhesion molecule-2 (CD102) binds to the leukocyte integrin CD11b/CD18 through the A domain, *J Immunol.*, 155(7):pp. 3619-3628.

Xiong, J. P., Stehle, T., Zhang, R., Joachimiak, A., Frech, M., Goodman, S. L., & Arnaout, M. A. 2002, Crystal structure of the extracellular segment of integrin alpha Vbeta3 in complex with an Arg-Gly-Asp ligand, *Science*, 296(5565):pp. 151-155.

Yadav, R., Larbi, K. Y., Young, R. E., & Nourshargh, S. 2003, Migration of leukocytes through the vessel wall and beyond, *Thromb.Haemost.*, 90(4):pp. 598-606.

Yakubenko, V. P., Lishko, V. K., Lam, S. C., & Ugarova, T. P. 2002, A molecular basis for integrin alphaMbeta 2 ligand binding promiscuity, *J Biol.Chem.*, 277(50):pp. 48635-48642.

Yalamanchili, P., Lu, C., Oxvig, C., & Springer, T. A. 2000, Folding and function of I domain-deleted Mac-1 and lymphocyte function-associated antigen-1, *J Biol.Chem.*, 275(29):pp. 21877-21882.

Yan, H. C., DeLisser, H. M., Pilewski, J. M., Barone, K. M., Szklut, P. J., Chang, X. J., Ahern, T. J., Langer-Safer, P., & Albelda, S. M. 1994, Leukocyte recruitment into human skin transplanted onto severe combined immunodeficient

mice induced by TNF-alpha is dependent on E-selectin, *J.Immunol.*, 152(6):pp. 3053-3063.

Yan, H. C., Juhasz, I., Pilewski, J., Murphy, G. F., Herlyn, M., & Albelda, S. M. 1993, Human/severe combined immunodeficient mouse chimeras. An experimental in vivo model system to study the regulation of human endothelial cell-leukocyte adhesion molecules, *J.Clin.Invest*, 91(3):pp. 986-996.

Young, A., Koduri, G., Batley, M., Kulinskaya, E., Gough, A., Norton, S., & Dixey, J. 2007, Mortality in rheumatoid arthritis. Increased in the early course of disease, in ischaemic heart disease and in pulmonary fibrosis, *Rheumatology.Vol.46(2)()(pp 350-357), 2007.*(2):pp. 350-357.

Youssef, P. P., Cormack, J., Evill, C. A., Peter, D. T., Roberts-Thomson, P. J., Ahern, M. J., & Smith, M. D. 1996a, Neutrophil trafficking into inflamed joints in patients with rheumatoid arthritis, and the effects of methylprednisolone, *Arthritis Rheum.*, 39(2):pp. 216-225.

Youssef, P. P., Triantafillou, S., Parker, A., Coleman, M., Roberts-Thomson, P. J., Ahern, M. J., & Smith, M. D. 1996b, Effects of pulse methylprednisolone on cell adhesion molecules in the synovial membrane in rheumatoid arthritis. Reduced E-selectin and intercellular adhesion molecule 1 expression, *Arthritis Rheum.*, 39(12):pp. 1970-1979.

Zendman, A. J., van Venrooij, W. J., & Pruijn, G. J. 2006, Use and significance of anti-CCP autoantibodies in rheumatoid arthritis. [Review], *Rheumatology.*45(1):pp. 20-5.

Zlotnik, A. & Yoshie, O. 2000, Chemokines: a new classification system and their role in immunity, *Immunity.*, 12(2):pp. 121-127.

Zurita, A. J., Troncoso, P., Cardo-Vila, M., Logothetis, C. J., Pasqualini, R., & Arap, W. 2004, Combinatorial screenings in patients: the interleukin-11 receptor alpha as a candidate target in the progression of human prostate cancer, *Cancer Res.*, 64(2):pp. 435-439.